Data Report:
Background document for the Workshop on the Regional Environmental Management Plan for the Area of the Northern Mid-Atlantic Ridge

Evora, Portugal
25-29 November, 2019

Jesse Cleary, Sarah DeLand, Elisabetta Menini, Sena McCrory, Khaira Ismail, Patrick N. Halpin
Marine Geospatial Ecology Lab, Duke University

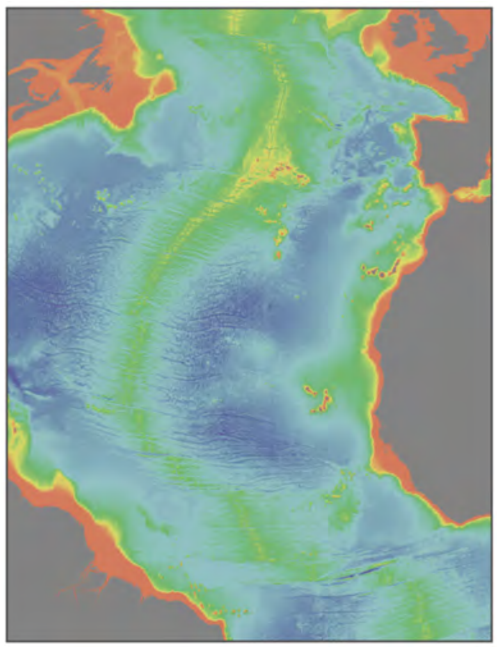

Supported by

European Commission

This work was supported by the Atlantic REMP project, funded under Service Contract EASME/EMFF/2017/1.3.1.1 - SI2.775068 to the European Commission.

Introduction

The Atlantic REMP project is an initiative funded by the EU to work with the secretariat of the International Seabed Authority to support its efforts to facilitate the development of a draft Regional Environmental Management Plan for the Area in the North Atlantic. The Plan will focus on the polymetallic sulphide deposits of the Mid-Atlantic Ridge. This data report, together with a Regional Environmental Assessment, has been produced by the Atlantic REMP project to provide information for two workshops that will be convened by the ISA secretariat with support from the Atlantic REMP project. The first workshop took place in Évora, Portugal in November 2019, which will be followed by the second workshop in St Petersburg, Russian Federation in June 2020.

The area to be included in the draft REMP will be discussed in the above-noted ISA workshops and will not necessarily coincide with the area covered by this data report.

The project is executed by a consortium of scientists and scientific organisations:

Seascape Consultants Ltd, UK
Deep Seas Environmental Solutions Ltd, UK
Instituto do Mar (University of the Azores), Portugal
Institute for Advanced Sustainability Studies, Germany
Duke University Marine Geospatial Ecology Lab, USA
Environmental Resources Management Ltd, UK
Jose Angel Alvarez Perez, Universidade do Vale do Itajaí – UNIVALI, Brazil
Alexander Turra, Universidade de São Paulo, Brazil

Important Notice:

Information contained in this publication comprises general statements based on scientific research. The Atlantic REMP project advises the reader to note that such information may be incomplete or unable to be used in any specific situation. No reliance or actions must therefore be made on that information without seeking prior expert professional, scientific and technical advice. Additionally, some data sets used herein require permission from the data providers for use.

Citation:

Cleary, J., S. DeLand, E. Menini, S. McCrory, K. Ismail, P.N. Halpin (2019) "Data Report: Workshop on the Regional Environmental Management Plan for the Area of the Northern Mid-Atlantic Ridge", 137 pp. Atlantic REMP Project.

Digital versions of individual maps herein are also available online:
https://duke.box.com/s/wvrx2gonzpy6i4ybs74xxtet13yq5ixk

Table of Contents

Figures

1 Context

The Marine Geospatial Ecology Lab at Duke University, with support from Seascape Consultants/Atlantic REMP Project (sponsored by the European Commission) and in conjunction with international partners, has identified and mapped a large number of datasets and analyses pertaining to the northern Mid-Atlantic Ridge and surrounding ocean areas. These datasets and supporting references have been compiled into this data report, an annotated catalog of available spatial data and selected publications to brief workshop participants and aid with data discovery.

This data report accompanies a Regional Environmental Assessment that provides "an aggregation and synthesis of existing information relating to the northern MAR, including geomorphology, physical characteristics and biological communities, as well a description of the current mining areas, mining process and ecosystem features (regional biodiversity, temporal variability, trophic relationships, ecosystem functioning, connectivity, resilience and recovery)."

This data report will be provided to experts at the "Workshop on the Regional Environmental Management Plan for the Area of the Northern Mid-Atlantic Ridge" (Evora, Portugal from 25-29 November, 2019) convened by the International Seabed Authority Secretariat, in collaboration with Atlantic REMP Project and the Government of Portugal.

The datasets described herein will be available on-site at the Evora workshop supported by live GIS and mapping capabilities. Workshop participants will be able to request simple map overlays and analyses be performed at the workshop that will aid in their discussions. The results of the mapping work performed at the workshop will be included in the subsequent ISA Workshop Report.

1.1 Geographical area to be addressed in this report

The Mid-Atlantic Ridge (MAR) extends right from the Arctic Ocean to beyond South Africa. For the purposes of this report on the Northern Mid-Atlantic Ridge, data were collected or generated for areas between 57°N and 9°S and basin-wide in an east/west direction. The area to be included in the draft REMP will be discussed in the ISA meetings and will not necessarily coincide with the area covered by this data report.

EEZ Data Source - VLIZ v10, http://www.marineregions.org/eez.php
ECS Data Source - http://continentalshelf.org/onestopdatashop/6350.aspx
Plate Boundary Data Source - https://ig.utexas.edu/marine-and-tectonics/plates-project/

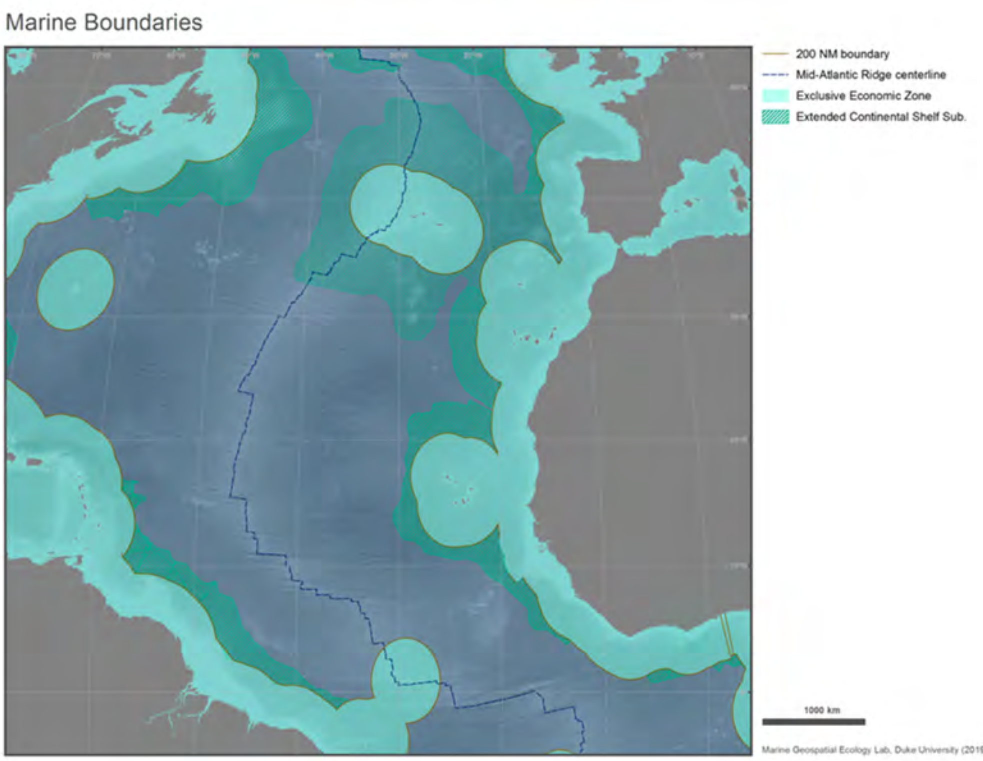

Figure 1.1-1 Data collection scope and boundary context

2 Environmental Data

2.1 Bathymetry and Slope (GEBCO)

GEBCO's gridded bathymetric data set, the GEBCO_2019 grid, is a global terrain model for ocean and land at 15 arc-second intervals. The GEBCO_2019 Grid is the latest global bathymetric product released by the General Bathymetric Chart of the Oceans (GEBCO) and has been developed through the Nippon Foundation-GEBCO Seabed 2030 Project.

The GEBCO_2019 product provides global coverage, spanning 89° 59' 52.5''N, 179° 59' 52.5''W to 89° 59' 52.5''S, 179° 59' 52.5''E on a 15 arc-second grid. It consists of 86400 rows x 43200 columns, giving 3,732,480,000 data points. The data values are pixel-centre registered i.e. they refer to elevations at the centre of grid cells.

Slope and slope acceleration were derived from GEBCO bathymetry with ArcGIS 10.6.1.

Source:
https://www.gebco.net/data_and_products/gridded_bathymetry_data/gebco_2019/gebco_2019_info.html

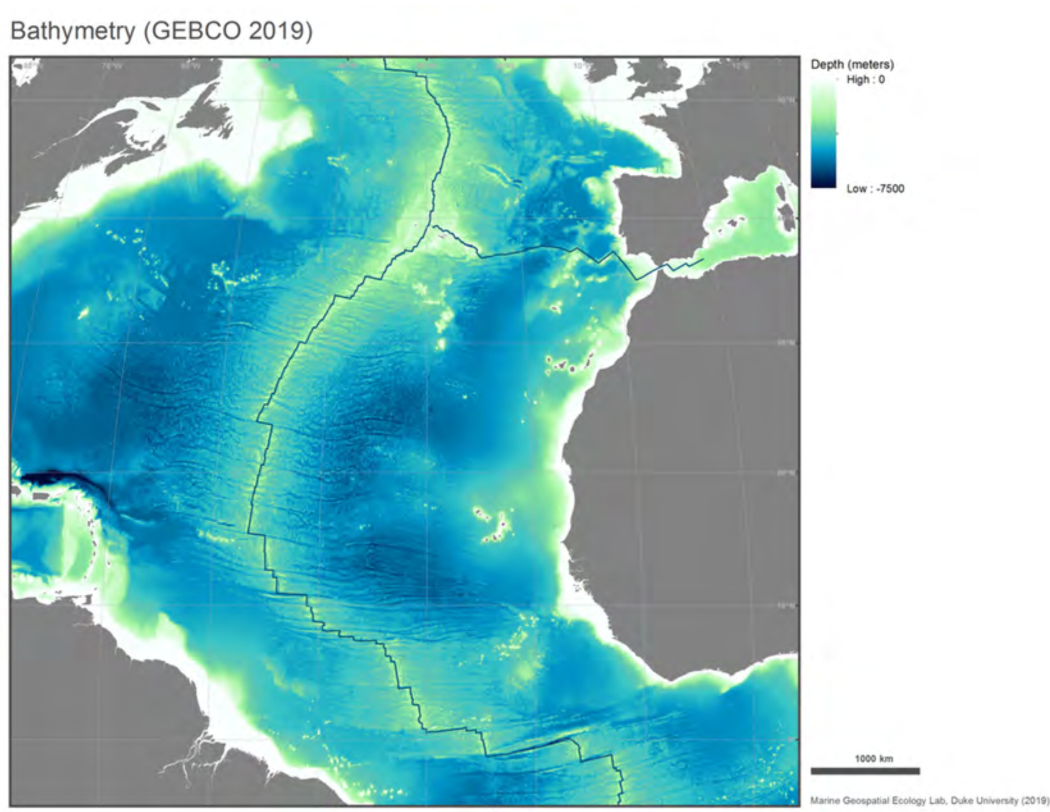

Figure 2.1-1 Bathymetry

Seafloor Slope (from GEBCO 2019)

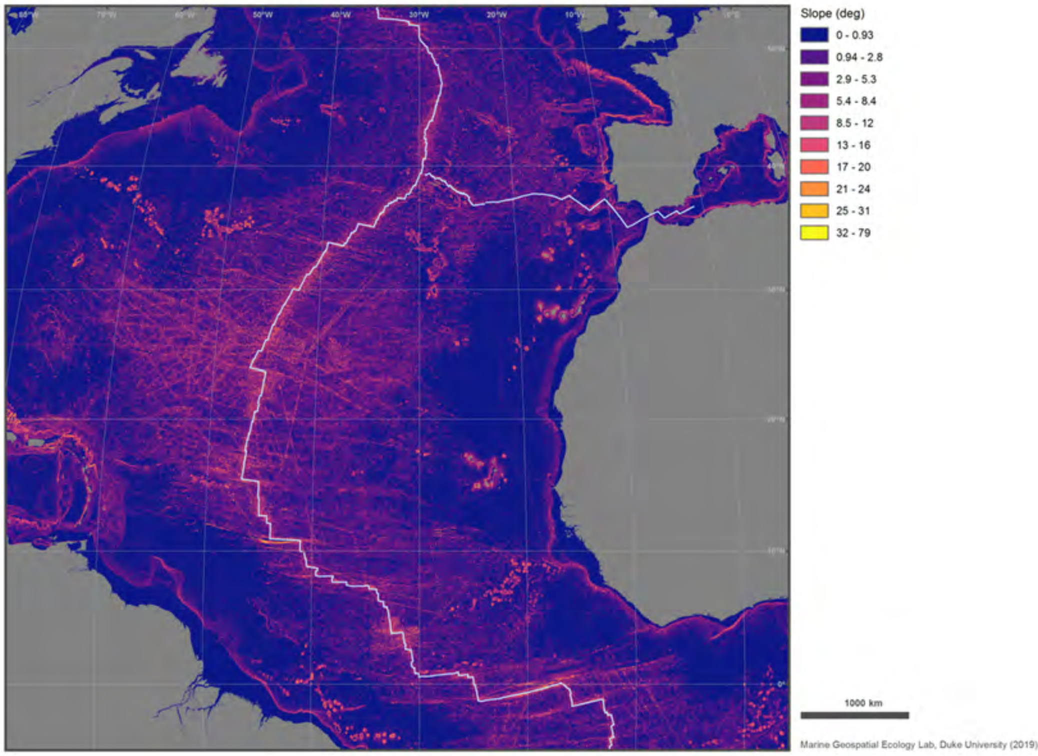

Figure 2.1-2 Seafloor slope

Acceleration of Seafloor Slope (from GEBCO 2019)

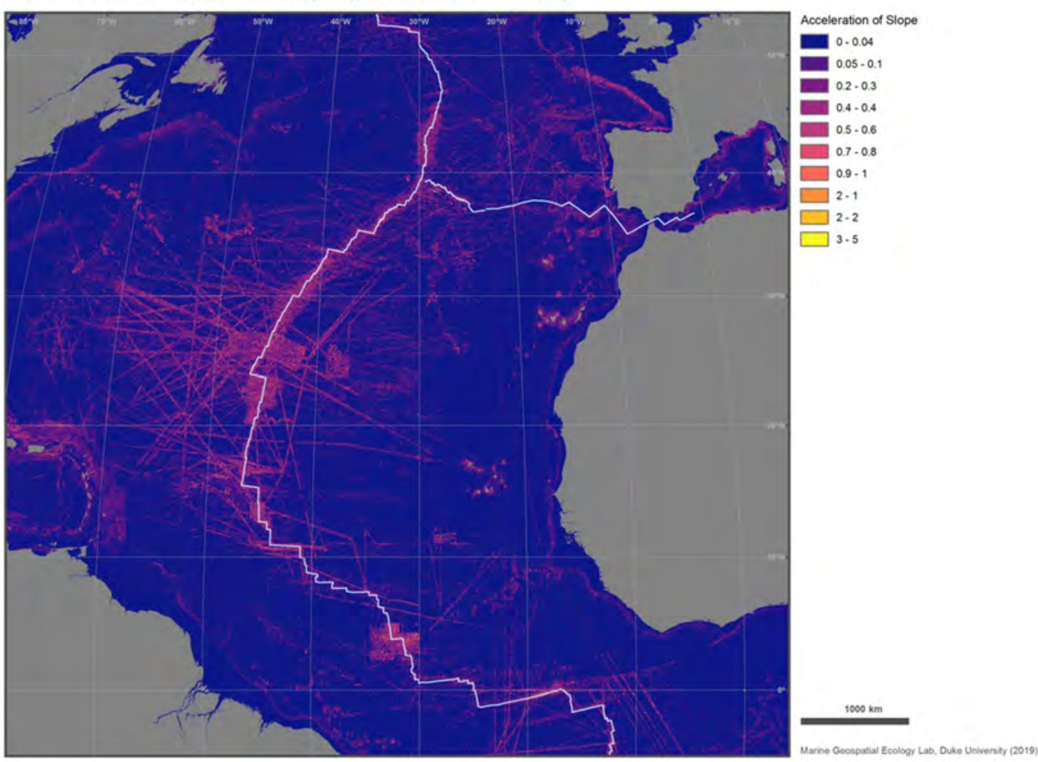

Figure 2.1-3 Seafloor slope acceleration

2.2 Seafloor Geomorphic Features

Abstract (Harris et al. 2014):
"We present the first digital seafloor geomorphic features map (GSFM) of the global ocean. The GSFM includes 131,192 separate polygons in 29 geomorphic feature categories, used here to assess differences between passive and active continental margins as well as between 8 major ocean regions (the Arctic, Indian, North Atlantic, North Pacific, South Atlantic, South Pacific and the Southern Oceans and the Mediterranean and Black Seas). The GSFM provides quantitative assessments of differences between passive and active margins: continental shelf width of passive margins (88 km) is nearly three times that of active margins (31 km); the average width of active slopes (36 km) is less than the average width of passive margin slopes (46 km); active margin slopes contain an area of 3.4 million km2 where the gradient exceeds 5°, compared with 1.3 million km2 on passive margin slopes; the continental rise covers 27 million km2 adjacent to passive margins and less than 2.3 million km2 adjacent to active margins. Examples of specific applications of the GSFM are presented to show that: 1) larger rift valley segments are generally associated with slow-spreading rates and smaller rift valley segments are associated with fast spreading; 2) polar submarine canyons are twice the average size of non-polar canyons and abyssal polar regions exhibit lower seafloor roughness than non-polar regions, expressed as spatially extensive fan, rise and abyssal plain sediment deposits — all of which are attributed here to the effects of continental glaciations; and 3) recognition of seamounts as a separate category of feature from ridges results in a lower estimate of seamount number compared with estimates of previous workers."

Reference:
Harris PT, Macmillan-Lawler M, Rupp J, Baker EK (2014), Geomorphology of the oceans. Marine Geology. doi: 10.1016/j.margeo.2014.01.011

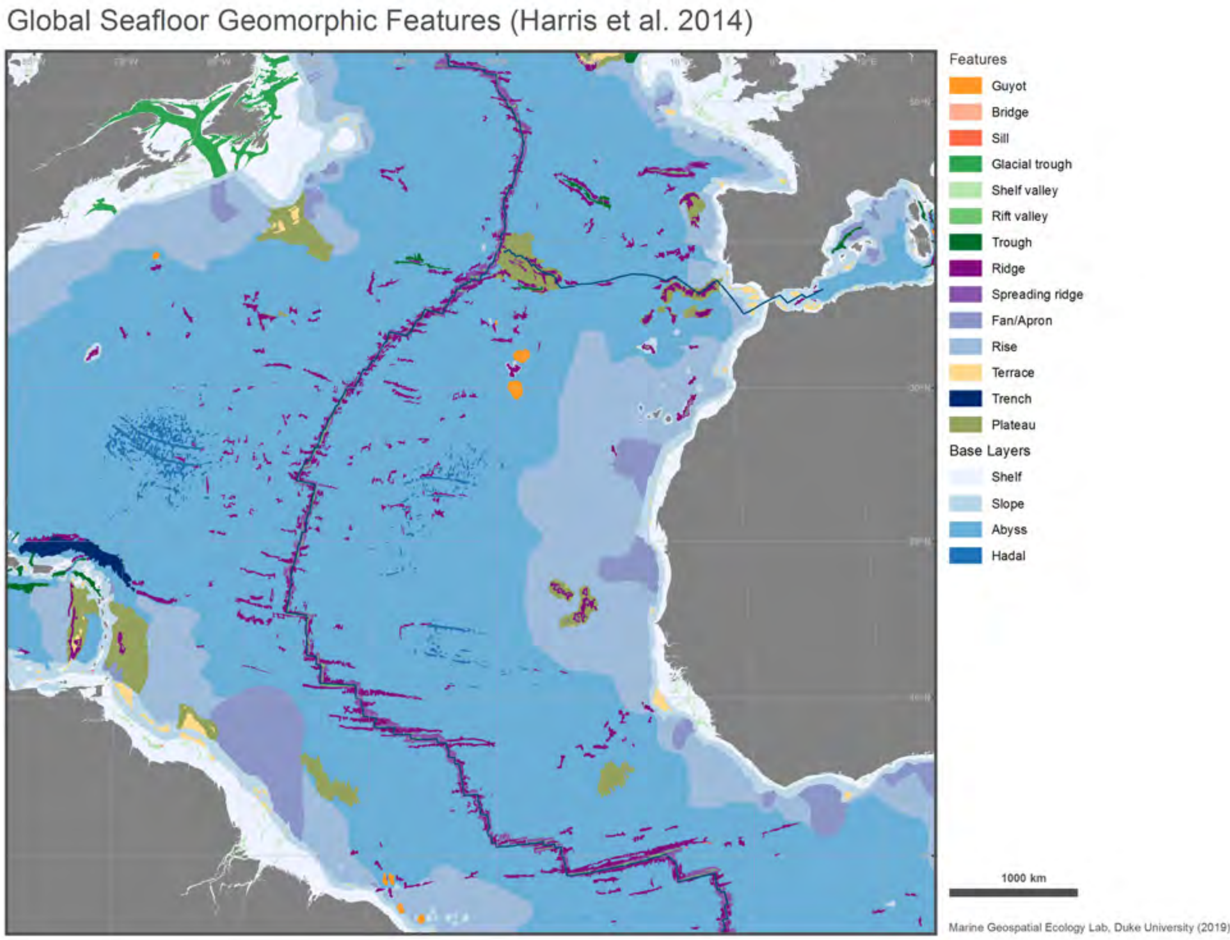

Figure 2.2-1 Seafloor geomorphic features

2.3 InterRidge Vents Database

"The InterRidge Global Database of Active Submarine Hydrothermal Vent Fields, hereafter referred to as the InterRidge Vents Database, is available online as the authoritative source for locations of hydrothermal vent fields worldwide (linked to InterRidge homepage: http://www.interridge.org). The InterRidge Vents Database was developed to provide a comprehensive list of active submarine hydrothermal vent fields for use in academic research and education."

Source: http://vents-data.interridge.org/, database version 3.4

Reference:
Beaulieu, S. E., E. T. Baker, C. R. German, and A. Maffei (2013), An authoritative global database for active submarine hydrothermal vent fields, Geochem. Geophys. Geosys., 14, 4892–4905, doi:10.1002/2013GC004998.

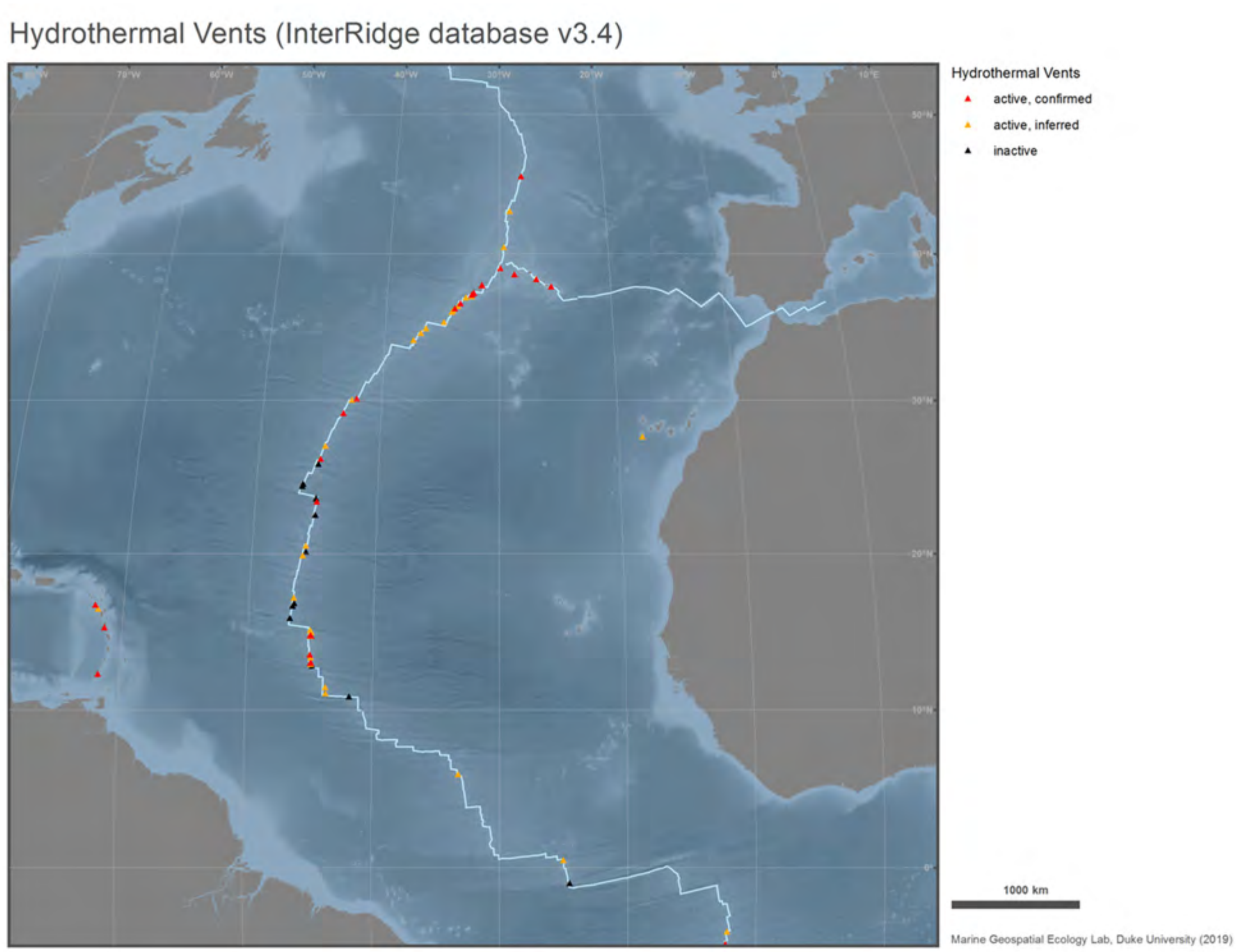

Figure 2.3-1 Mid-Atlantic Ridge hydrothermal vents

Hydrothermal Vent Locations

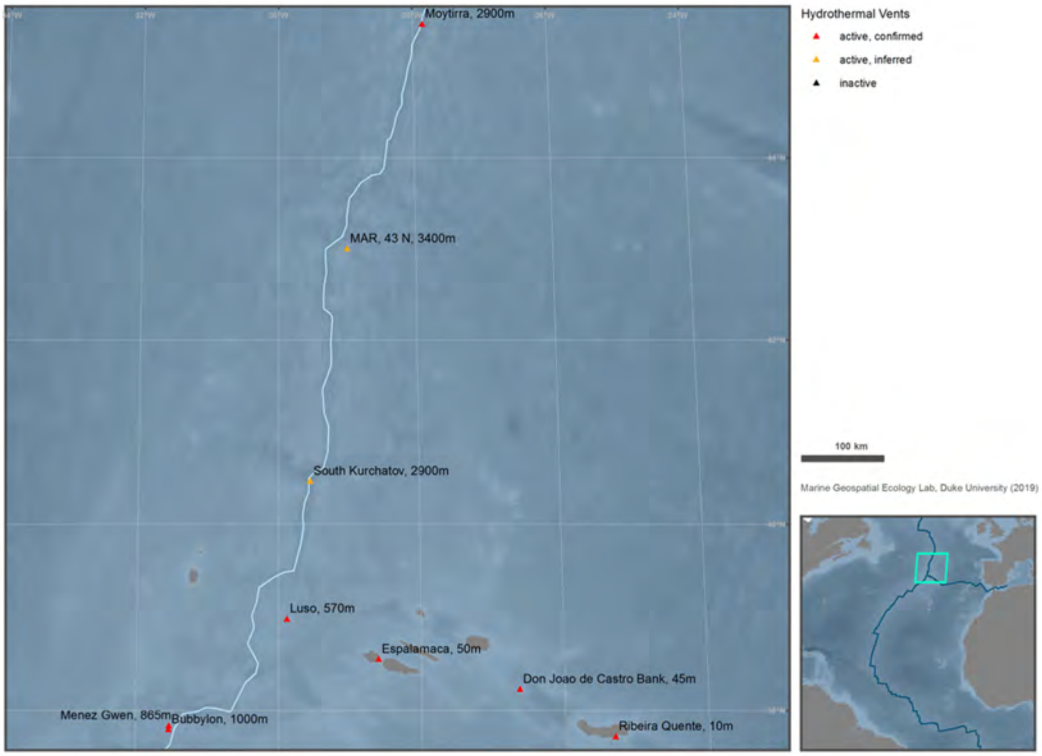

Hydrothermal Vent Locations

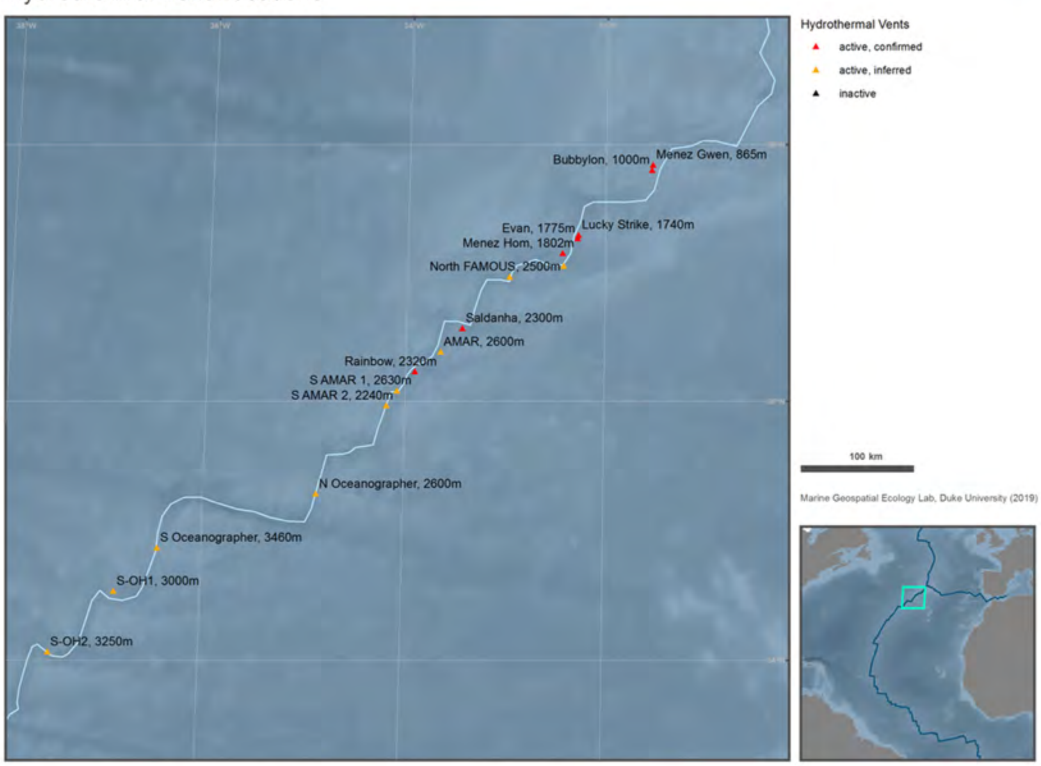

Hydrothermal Vent Locations

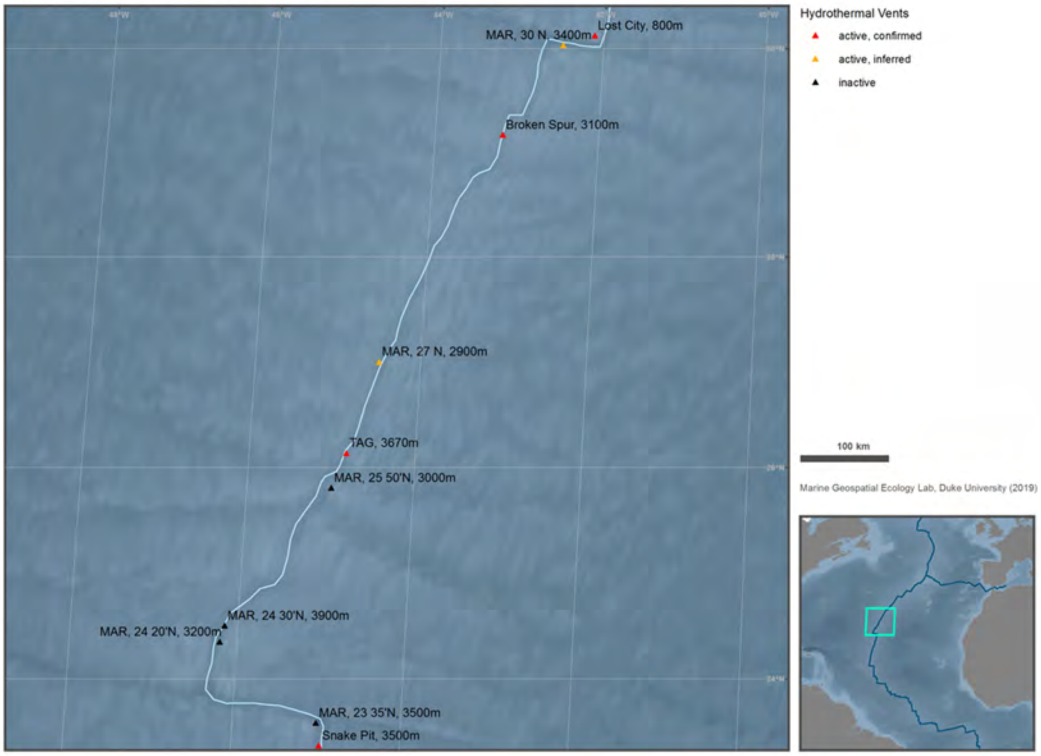

Hydrothermal Vent Locations

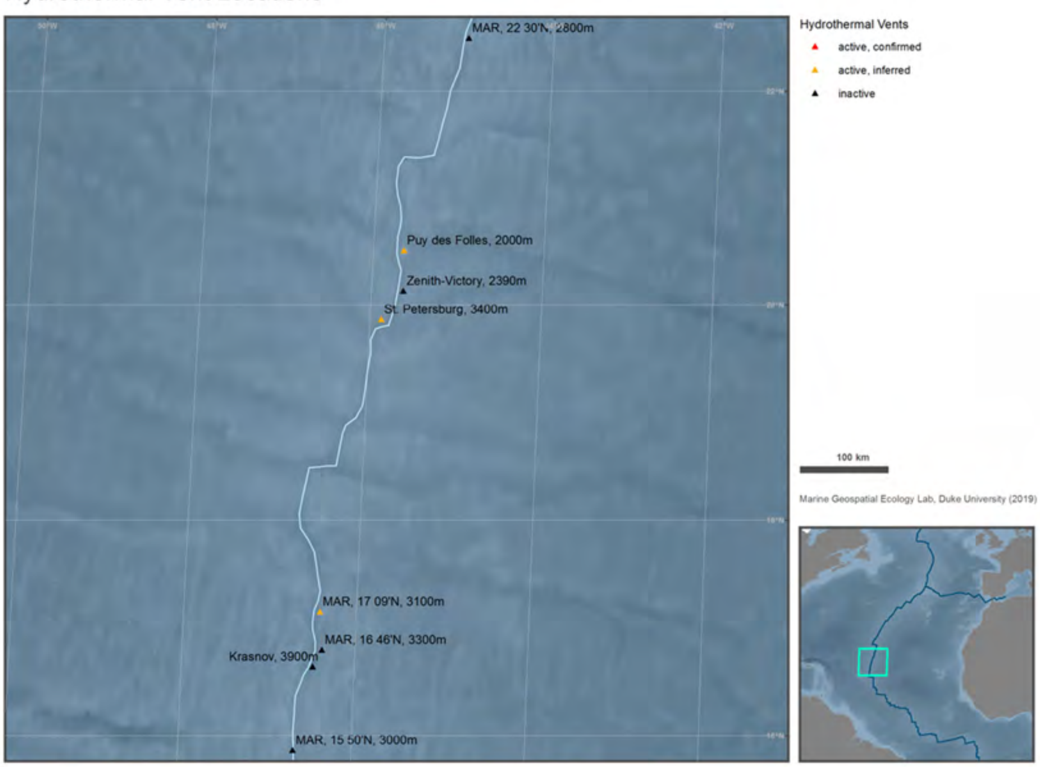

Hydrothermal Vent Locations

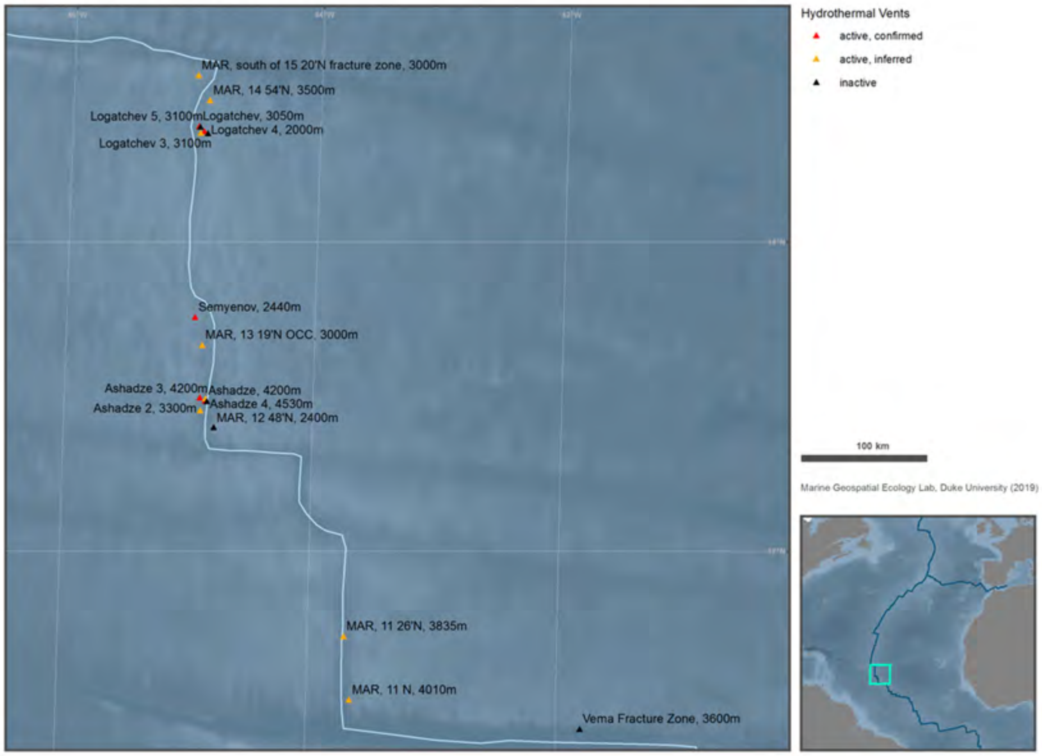

Hydrothermal Vent Locations

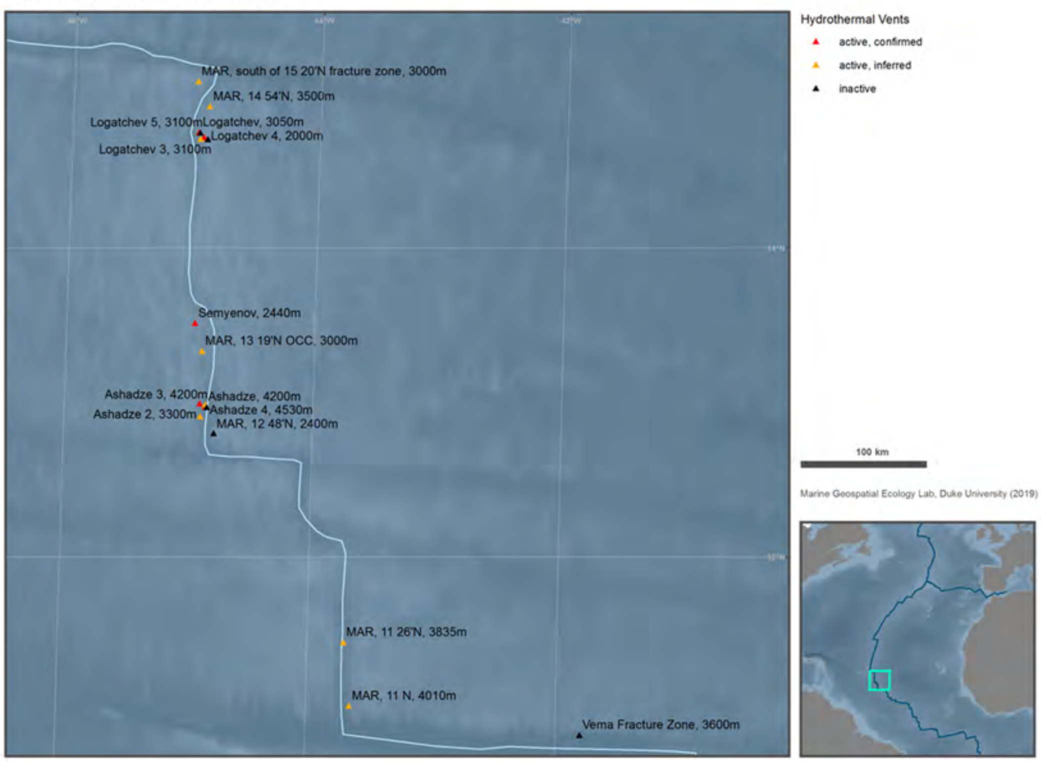

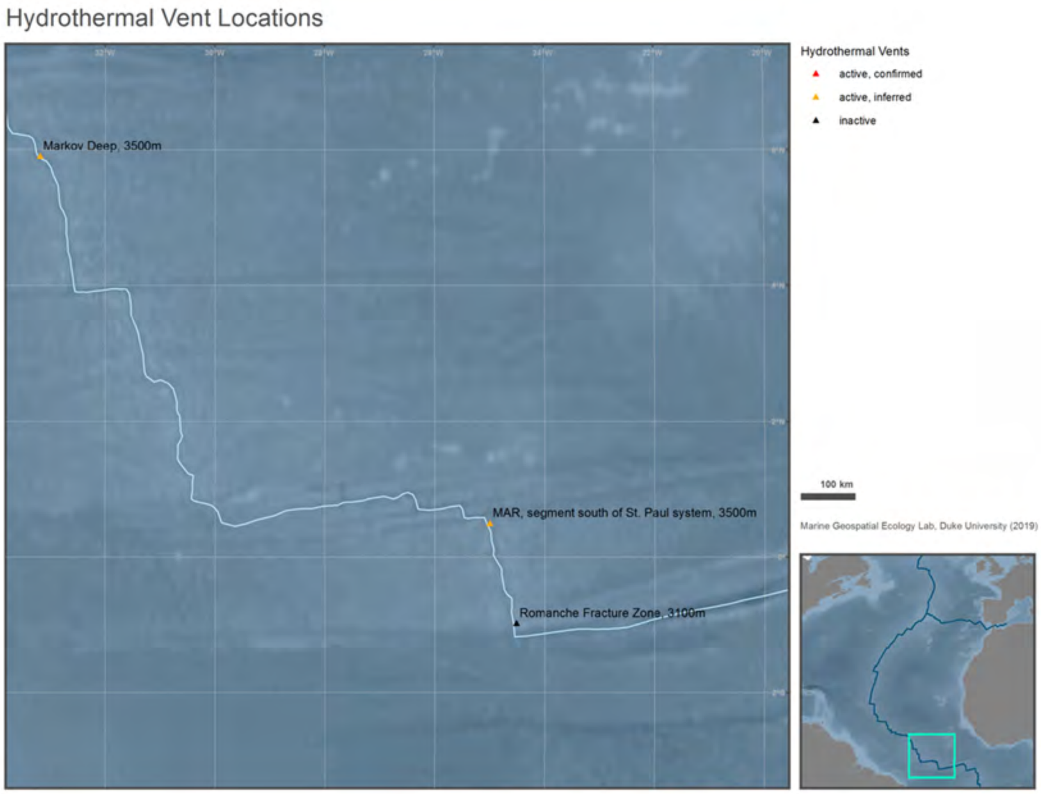

Figure 2.3-2 Hydrothermal vent names, depth and status

2.4 Fracture Zones

Included in this archive are shapefiles of Undersea Feature Names and their geometries for geospatial applications. These data were generated by the General Bathymetric Chart of the Oceans (GEBCO) Gazetteer of Undersea Feature Names.

Source: https://www.gebco.net/data_and_products/undersea_feature_names/

Reference: IHO-IOC GEBCO Gazetteer of Undersea Feature Names, www.gebco.net

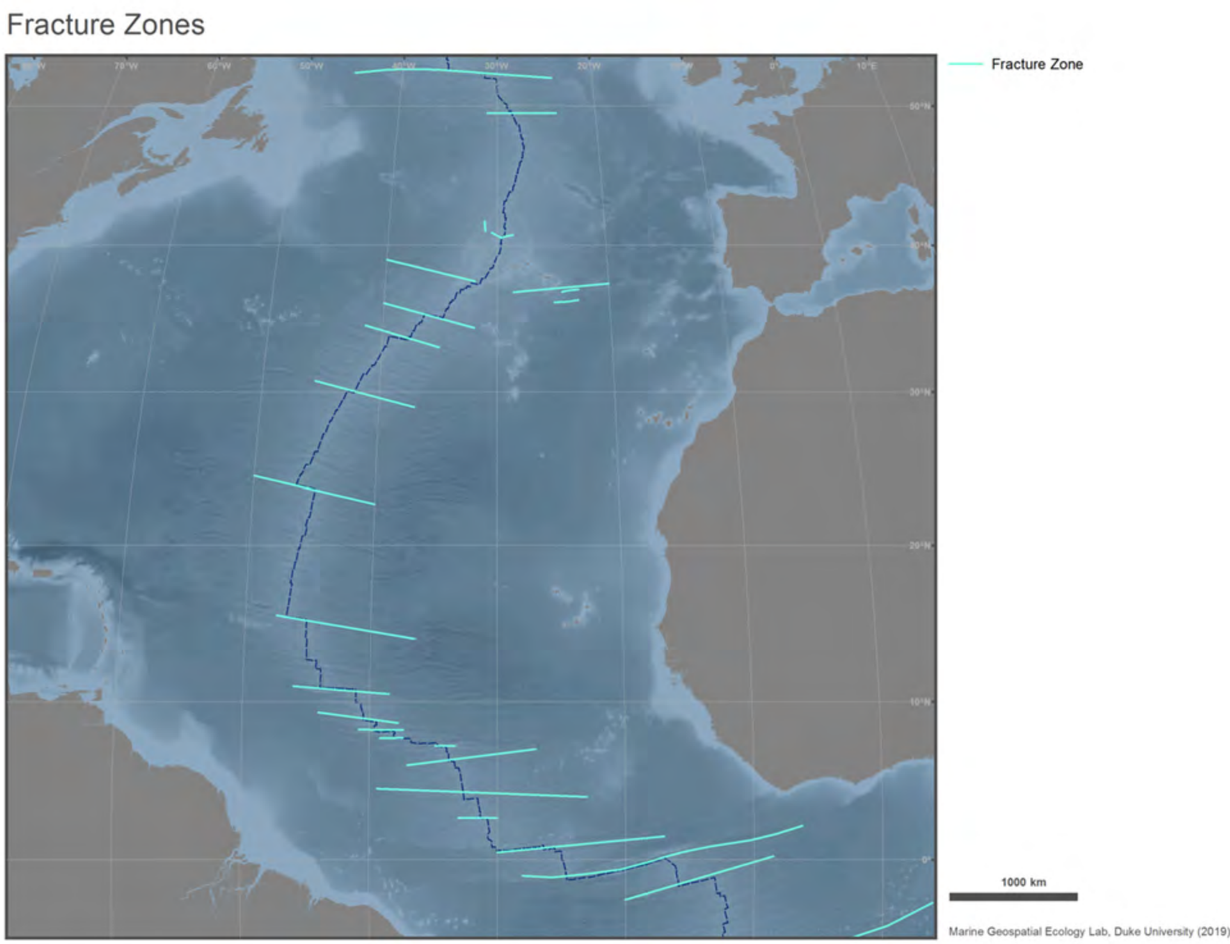

Figure 2.4-1 Fracture zones

2.5 Global Distribution of Seamounts

Abstract (Yesson et al. 2011):
“Seamounts and knolls are ‘undersea mountains’, the former rising more than 1000 m from the seafloor. These features provide important habitats for aquatic predators, demersal deep-sea fish and benthic invertebrates. However most seamounts have not been surveyed and their numbers and locations are not well known. Previous efforts to locate and quantify seamounts have used relatively coarse bathymetry grids. Here we use global bathymetric data at 30 arc-second resolution to identify seamounts and knolls. We identify 33,452 seamounts and 138,412 knolls, representing the largest global set of identified seamounts and knolls to date. We compare estimated seamount numbers, locations, and depths with validation sets of seamount data from New Zealand and Azores. This comparison indicates the method we apply finds 94% of seamounts, but may overestimate seamount numbers along ridges and in areas where faulting and seafloor spreading creates highly complex topography. The seamounts and knolls identified herein are significantly geographically biased towards areas surveyed with ship-based soundings. As only 6.5% of the ocean floor has been surveyed with soundings it is likely that new seamounts will be uncovered as surveying improves. Seamount habitats constitute approximately 4.7% of the ocean floor, whilst knolls cover 16.3%. Regional distribution of these features is examined, and we find a disproportionate number of productive knolls, with a summit depth of o1.5 km, located in the Southern Ocean. Less than 2% of seamounts are within marine protected areas and the majority of these are located within exclusive economic zones with few on the High Seas. The database of seamounts and knolls resulting from this study will be a useful resource for researchers and conservation planners.”

Reference:
Yesson, C., Clark, M. R., Taylor, M. L., & Rogers, A. D. (2011). The global distribution of seamounts based on 30 arc seconds bathymetry data. Deep Sea Research Part I: Oceanographic Research Papers, 58(4), 442-453. doi: 10.1016/j.dsr.2011.02.004

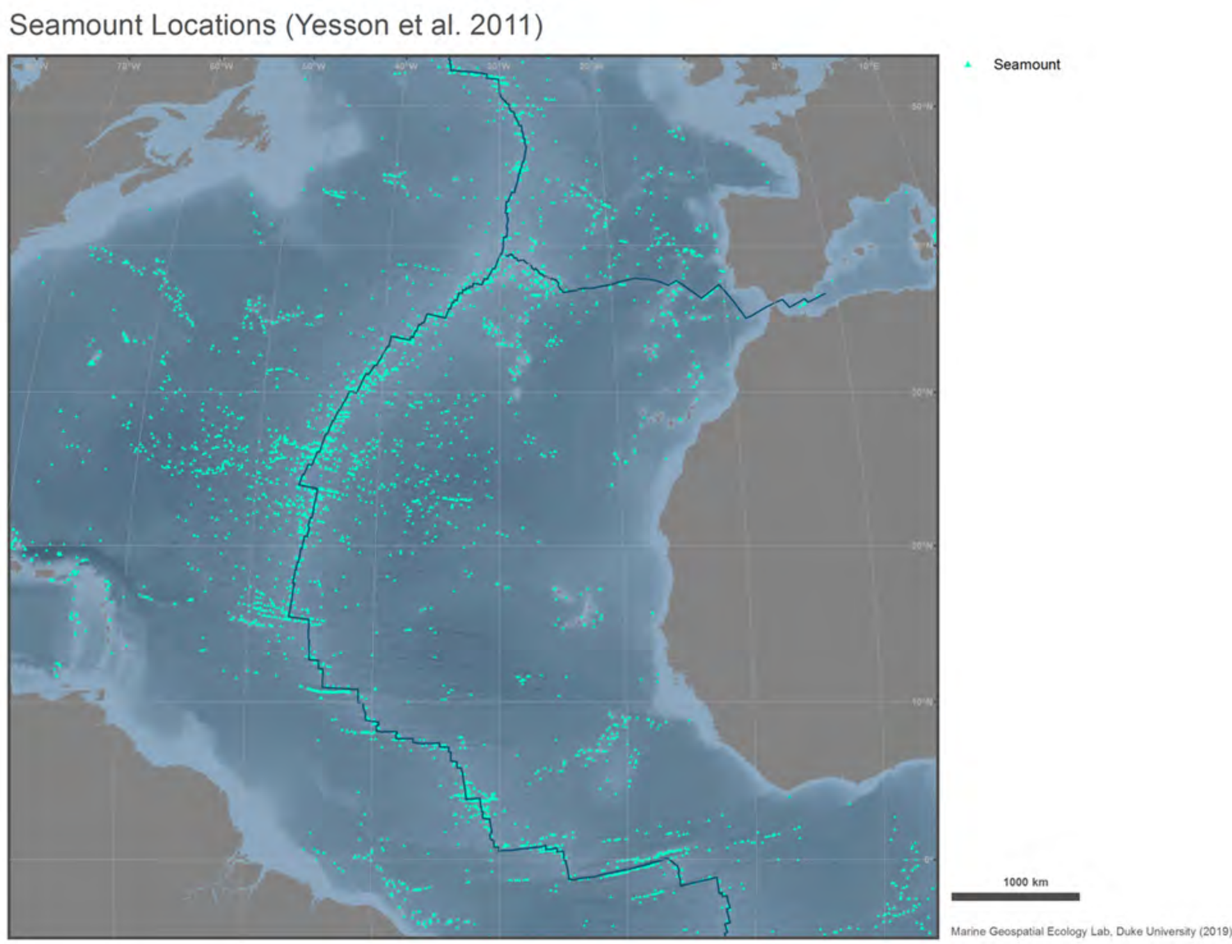

Figure 2.5-1 Seamount locations

2.6 Global Seamount Classification

Abstract (Clark et al. 2011):
"Seamounts are prominent features of the world's seafloor, and are the target of deep-sea commercial fisheries, and of interest for minerals exploitation. They can host vulnerable benthic communities, which can be rapidly and severely impacted by human activities. There have been recent calls to establish networks of marine protected areas on the High Seas, including seamounts. However, there is little biological information on the benthic communities on seamounts, and this has limited the ability of scientists to inform managers about seamounts that should be protected as part of a network. In this paper we present a seamount classification based on "biologically meaningful" physical variables for which global-scale data are available. The approach involves the use of a general biogeographic classification for the bathyal depth zone (near-surface to 3500 m), and then uses four key environmental variables (overlying export production, summit depth, oxygen levels, and seamount proximity) to group seamounts with similar characteristics. This procedure is done in a simple hierarchical manner, which results in 194 seamount classes throughout the world's oceans. The method was

compared against a multivariate approach, and ground-truthed against octocoral data for the North Atlantic. We believe it gives biologically realistic groupings, in a transparent process that can be used to either directly select, or aid selection of, seamounts to be protected.”

Reference:
Clark, Malcolm R., Les Watling, Ashley A. Rowden, John M. Guinotte, and Craig R. Smith. "A global seamount classification to aid the scientific design of marine protected area networks." Ocean & Coastal Management 54, no. 1 (2011): 19-36. doi: 10.1016/j.ocecoaman.2010.10.006

Source: http://seamounts.sdsc.edu/

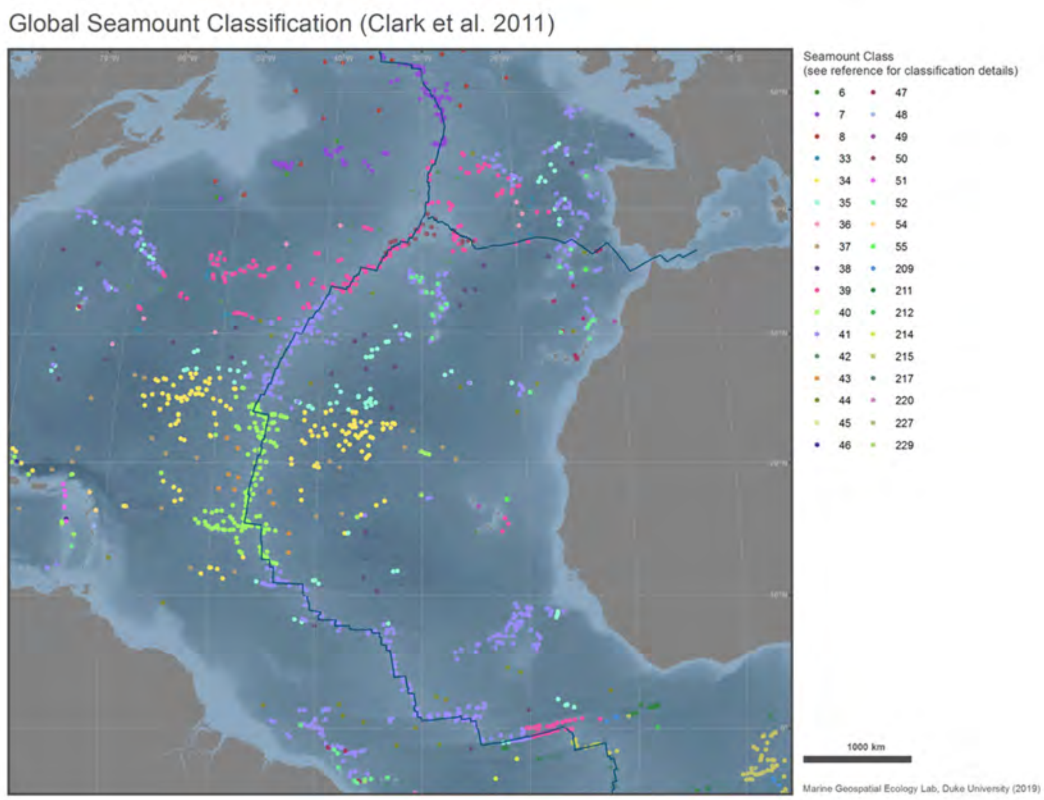

Figure 2.6-1 Global seamount classification

2.7 Total Sediment Thickness of the World’s Oceans & Marginal Seas

“NCEI's global ocean sediment thickness grid of Divins (2003) updated by Whittaker et al. (2013) has been updated again for the NE Atlantic, Arctic, Southern Ocean, and Mediterranean regions. The new global 5-arc-minute total sediment thickness grid, GlobSed, incorporates new data and several regional oceanic sediment thickness maps, which have been compiled and published for the, (1) NE Atlantic (Funck et al., 2017; Hopper et al., 2014), (2) Mediterranean (Molinari & Morelli, 2011), (3) Arctic (Petrov et al., 2016), (4) Weddell Sea (Huang et al., 2014), and (5) the Ross Sea, Amundsen Sea, and Bellingshausen Sea sectors off West Antarctica (Lindeque et al., 2016; Wobbe et al., 2014). This version also includes updates in the White Sea region based on the VSEGEI map of Orlov and Fedorov (2001). GlobSed covers a larger area than NCEI's previous global grids (Divins, 2003; Whittaker et al. 2013), and the new updates results in a 29.7% increase in estimated total oceanic sediment volume."

Source: https://www.ngdc.noaa.gov/mgg/sedthick/

Reference:
Straume, E.O., Gaina, C., Medvedev, S., Hochmuth, K., Gohl, K., Whittaker, J. M., et al. (2019). GlobSed: Updated total sediment thickness in the world's oceans. Geochemistry, Geophysics, Geosystems, 20. DOI: 10.1029/2018GC008115

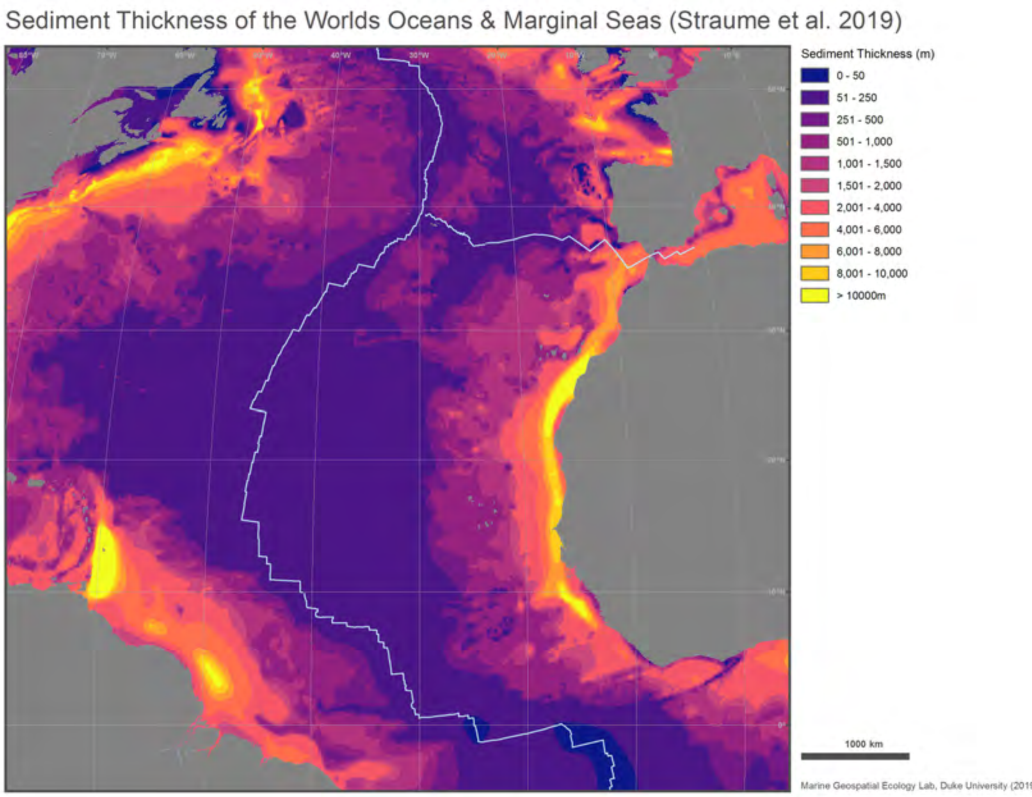

Figure 2.7-1 Sediment thickness

2.8 Seafloor Lithology

Abstract (Dutkiewicz et al. 2015)
"Knowing the patterns of distribution of sediments in the global ocean is critical for understanding biogeochemical cycles and how deep-sea deposits respond to environmental change at the sea surface. We present the first digital map of seafloor lithologies based on descriptions of nearly 14,500 samples from original cruise reports, interpolated using a support

vector machine algorithm. We show that sediment distribution is more complex, with significant deviations from earlier hand-drawn maps, and that major lithologies occur in drastically different proportions globally. By coupling our digital map to oceanographic data sets, we find that the global occurrence of biogenic oozes is strongly linked to specific ranges in sea-surface parameters. In particular, by using recent computations of diatom distributions from pigment-calibrated chlorophyll-*a* satellite data, we show that, contrary to a widely held view, diatom oozes are not a reliable proxy for surface productivity. Their global accumulation is instead strongly dependent on low surface temperature (0.9–5.7 °C) and salinity (33.8–34.0 PSS, Practical Salinity Scale 1978) and high concentrations of nutrients. Under these conditions, diatom oozes will accumulate on the seafloor regardless of surface productivity as long as there is limited competition from biogenous and detrital components, and diatom frustules are not significantly dissolved prior to preservation. Quantifying the link between the seafloor and the sea surface through the use of large digital data sets will ultimately lead to more robust reconstructions and predictions of climate change and its impact on the ocean environment."

Reference:
Dutkiewicz, A., R. Müller, S. O'Callaghan, and H. Jónasson. 2015. "Census of Seafloor Sediments in the World's Ocean." *Geology* 43 (9): 795–98. https://doi.org/10.1130/G36883.1.

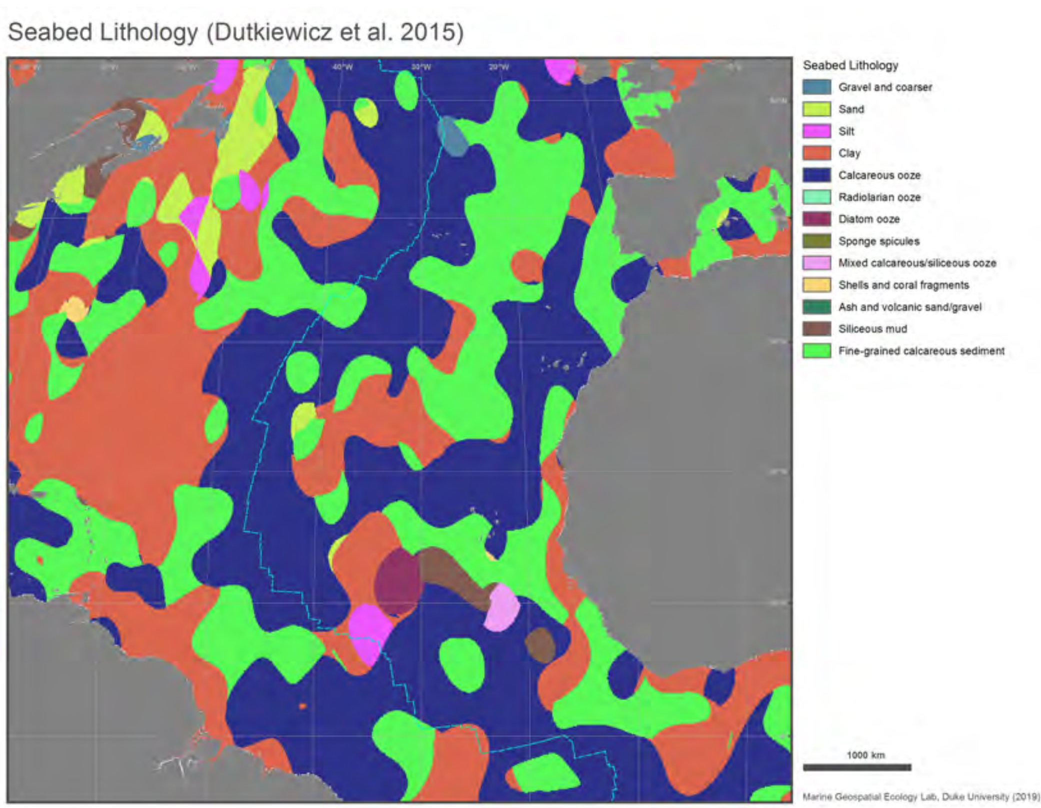

Figure 2.8-1 Global seabed lithology

2.9 Global Seabed Sediment Lithology

Abstract (Garlan et al. 2018):
"Production of a global sedimentological seabed map has been initiated in 1995 to provide the necessary tool for searches of aircraft and boats lost at sea, to give sedimentary information for nautical charts, and to provide input data for acoustic propagation modelling. This original approach had already been initiated one century ago when the French hydrographic service and the University of Nancy had produced maps of the distribution of marine sediments of the French coasts and then sediment maps of the continental shelves of Europe and North America. The current map of the sediment of oceans presented was initiated with a UNESCO's general map of the deep ocean floor. This map was adapted using a unique sediment classification to present all types of sediments: from beaches to the deep seabed and from glacial deposits to tropical sediments. In order to allow good visualization and to be adapted to the different applications, only the granularity of sediments is represented. The published seabed maps are studied, if they present an interest, the nature of the seabed is extracted from them, the sediment classification is transcribed and the resulted map is integrated in the world map. Data come also from interpretations of Multibeam Echo Sounder (MES) imagery of large hydrographic surveys of deep-ocean. These allow a very high-quality mapping of areas that until then were represented as homogeneous. The third and principal source of data comes from the integration of regional maps produced specifically for this project. These regional maps are carried out using all the bathymetric and sedimentary data of a region. This step makes it possible to produce a regional synthesis map, with the realization of generalizations in the case of over-precise data. 86 regional maps of the Atlantic Ocean, the Mediterranean Sea, and the Indian Ocean have been produced and integrated into the world sedimentary map."

Reference:
Garlan, T., Gabelotaud, I., Lucas, S., & Marchès, E. (2018, June). A World Map of Seabed Sediment Based on 50 Years of Knowledge. In Proceedings of the 20th International Research Conference, New York, NY, USA (pp. 3-4).

Source: https://data.shom.fr/

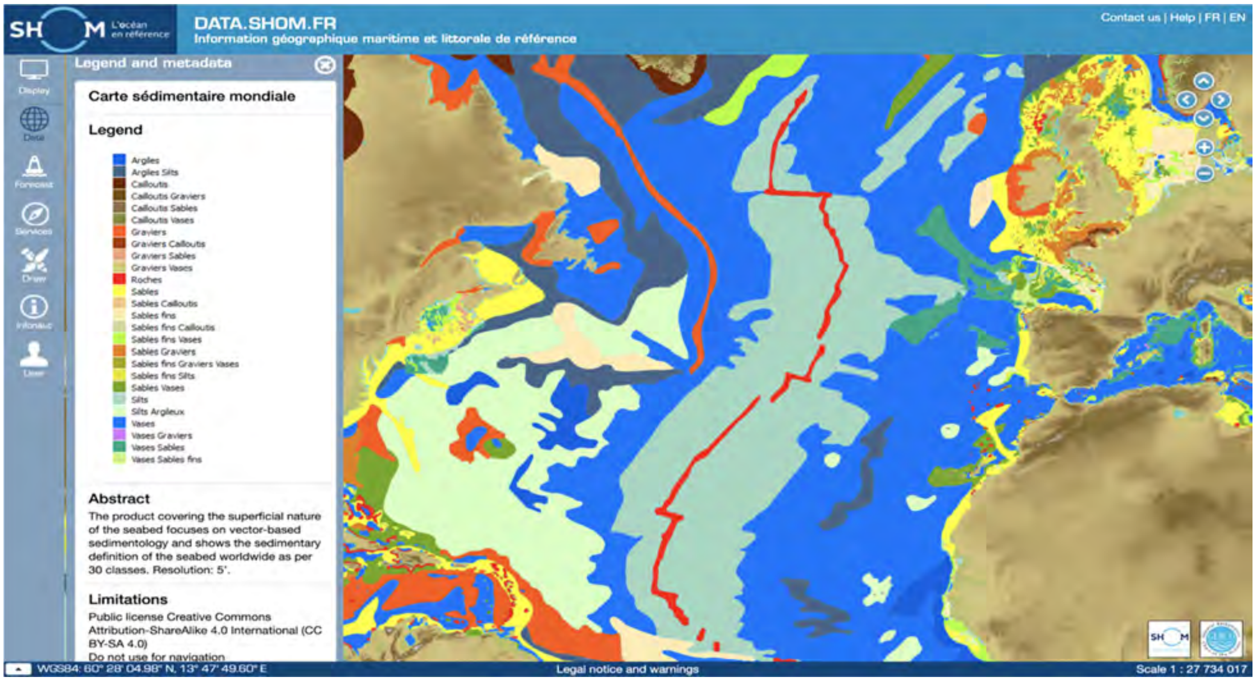

Figure 2.9-1 Global seabed sediment maps

2.10 Multibeam Bathymetric Survey Tracklines

"The Multibeam Bathymetry Database (MBBDB) at NCEI collects and archives multibeam data from the earliest commercial installations (circa 1980) through today's modern high-resolution collections. Data are acquired from both U.S. and international government and academic sources (see individual cruise metadata records for source information) and consist of the raw (as collected) sonar data files. Datasets may also include processed or edited versions of the sonar data, ancillary data (i.e., sound velocity data), derived products (i.e., grids), and/or metadata for the data collection. The MBBDB provides data that span the globe and are discoverable and accessible via map interface or text-only search options. This map service shows ship tracks for multibeam bathymetric surveys archived at NCEI."

Source: https://www.ngdc.noaa.gov/mgg/bathymetry/multibeam.html

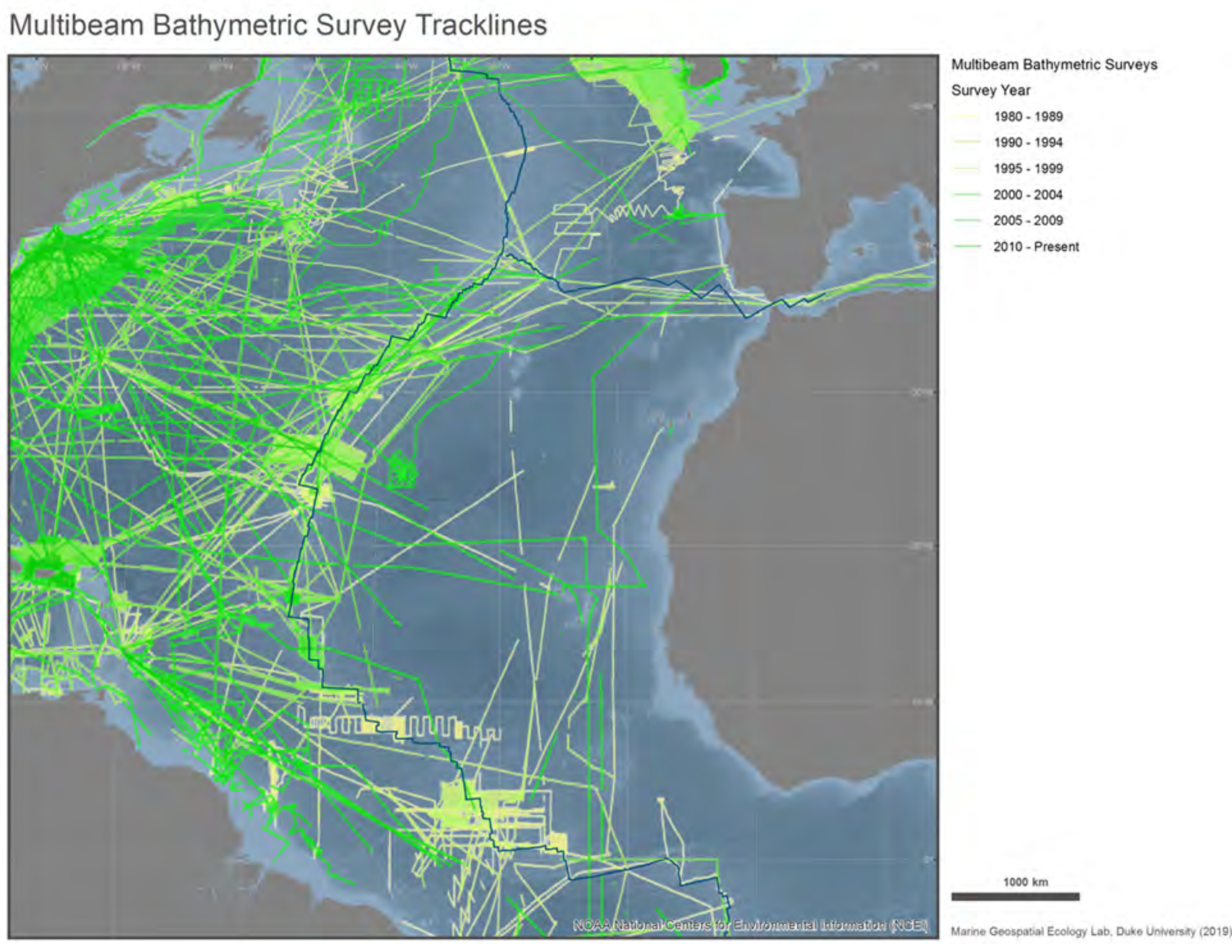

Figure 2.10-1 Multibeam bathymetry survey tracklines

2.11 Physical Oceans Climatologies from CARS

“CARS (Ridgway, et al., 2002; http://www.marine.csiro.au/~dunn/cars2009/) is a digital climatology, or atlas of seasonal ocean water properties. It comprises gridded fields of mean ocean properties over the period of modern ocean measurement, and average seasonal cycles for that period. It is derived from a quality-controlled archive of all available historical subsurface ocean property measurements - primarily research vessel instrument profiles and autonomous profiling buoys. As data availability has enormously increased in recent years, the CARS mean values are inevitably biased towards the recent ocean state. A number of global ocean climatologies are presently available, such as NODC's World Ocean Atlas. CARS is different as it employs extra stages of in-house quality control of input data, and uses an adaptive-lengthscale loess mapper to maximize resolution in data-rich regions, and the mapper's "BAR" algorithm takes account of topographic barriers (Dunn and Ridgway, 2002; Condie and Dunn, 2006). The result is excellent definition of oceanic structures and accuracy of point values.”

Reference:

Ridgway K.R., J.R. Dunn, and J.L. Wilkin, Ocean interpolation by four-dimensional least squares - Application to the waters around Australia, J. Atmos. Ocean. Tech., Vol 19, No 9, 1357-1375, 2002

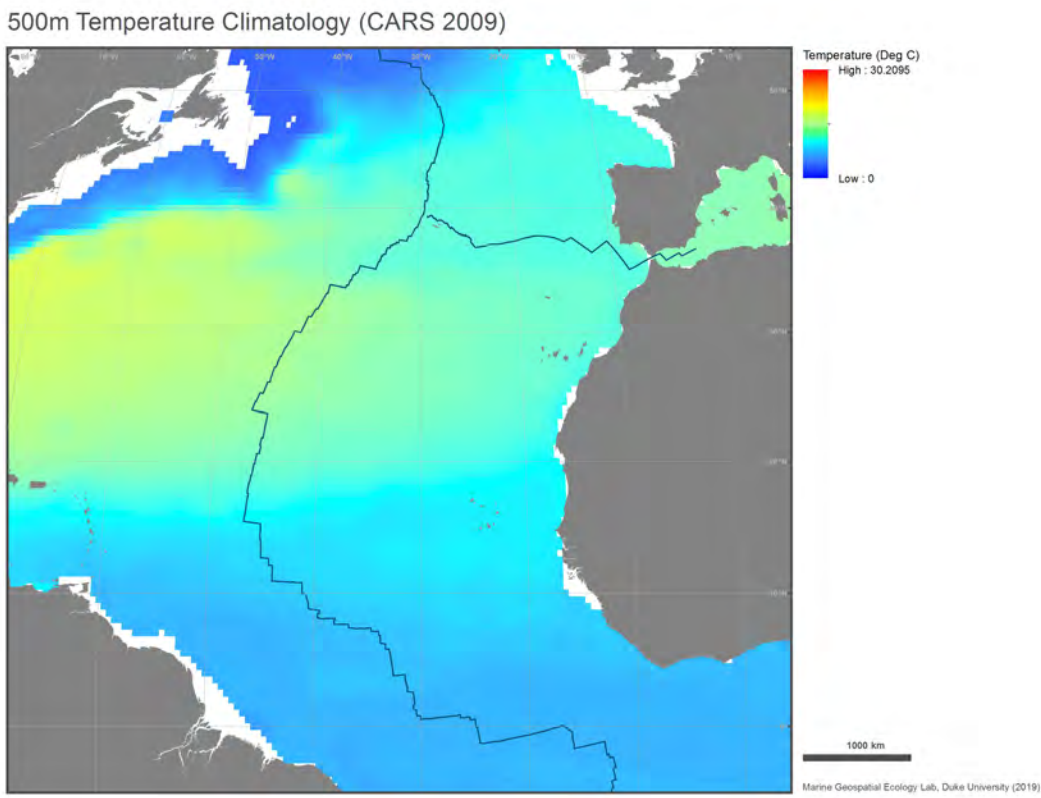

Figure 2.11-1 Temperature, 500 m

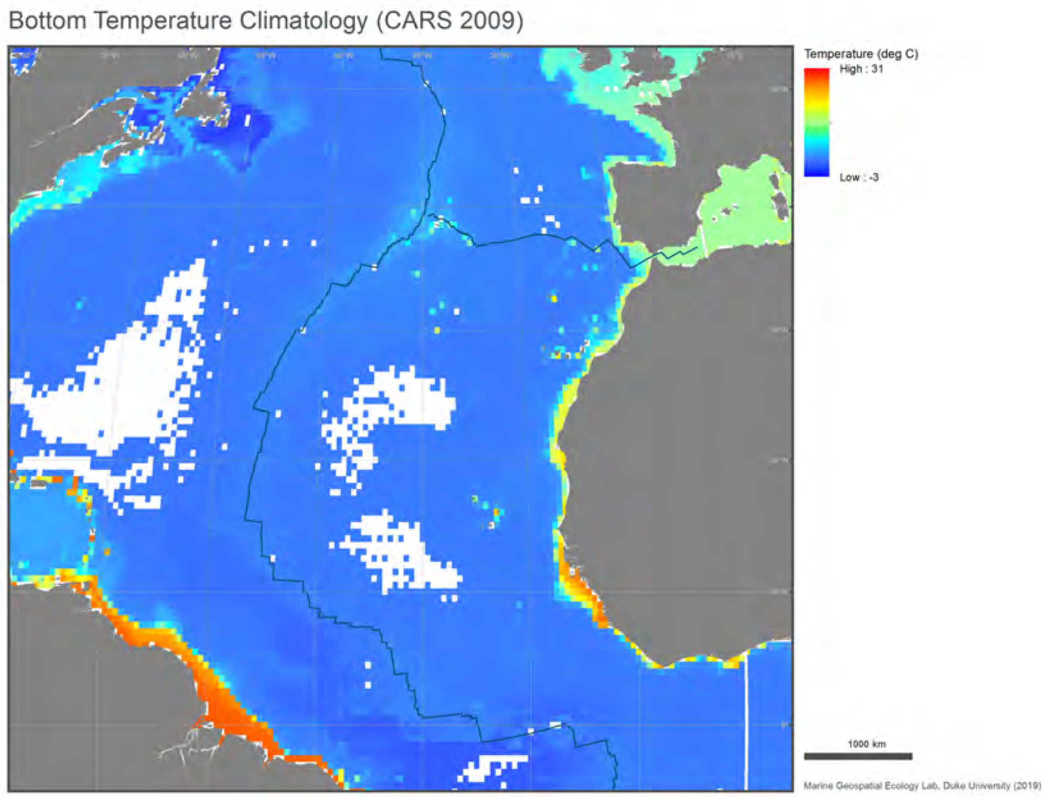

Figure 2.11-2 Bottom temperature

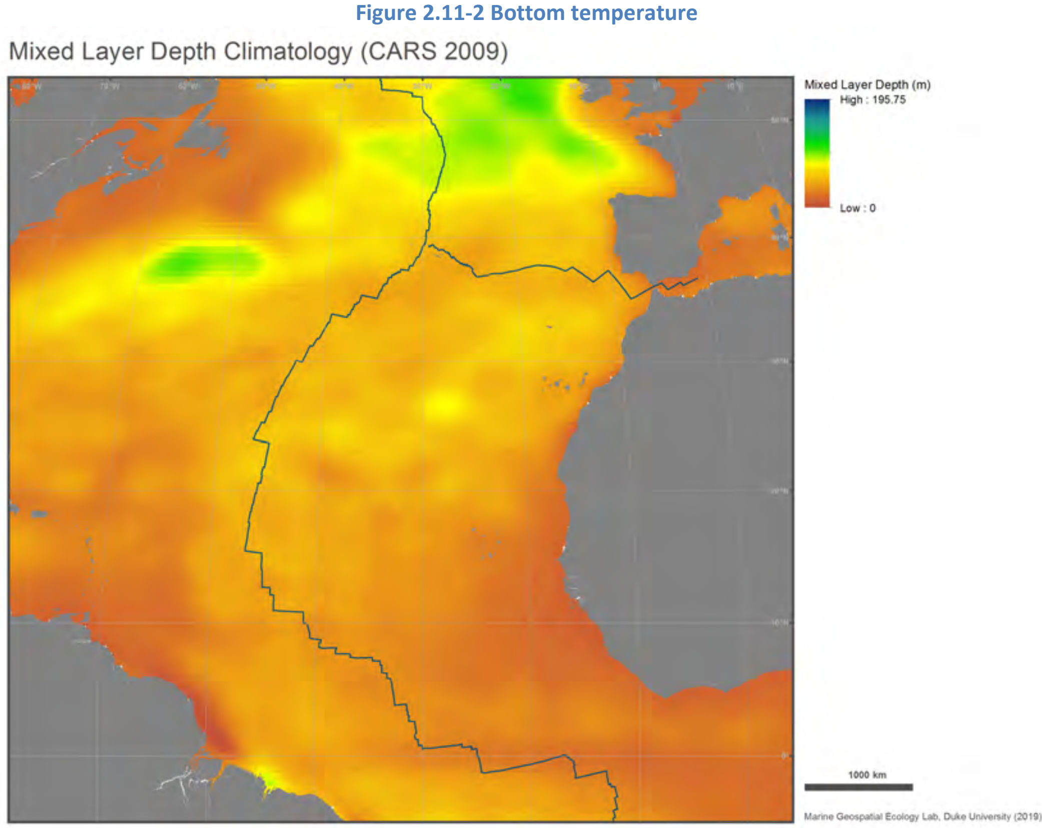

Figure 2.11-3 Mixed layer depth

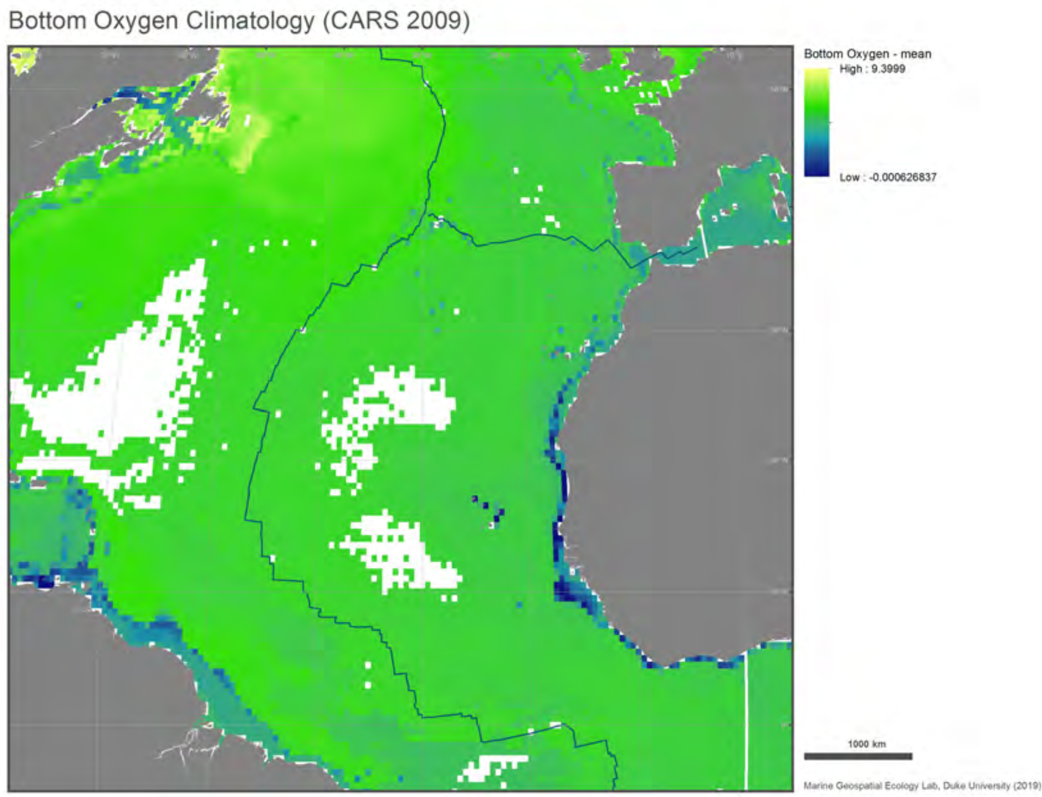

Figure 2.11-4 Bottom Oxygen

2.12 World Ocean Atlas

"The WOA18 updates previous versions of the World Ocean Atlas to include approximately 3 million new oceanographic casts added to the World Ocean Database and renewed quality control. This final version of WOA18 published in July, 2019 is replacing a prereleased version made available in September, 2018. The changes between the versions include:

- For the first time the Animal mounted pinniped temperature profiles (APB) have been added improving coverage in high latitude areas.
- A different Expendable Bathythermograph (XBT) correction (Cheng et al., 2014) has been employed.
- A double XBT correction has been detected in pre-release version and fixed in final version.
- All temperature and salinity climatological fields were re-calculated to account for these adjustments."

Source: https://www.nodc.noaa.gov/OC5/woa18/

Reference:

Locarnini, R. A., A. V. Mishonov, O. K. Baranova, T. P. Boyer, M. M. Zweng, H. E. Garcia, J. R. Reagan, D. Seidov, K. Weathers, C. R. Paver, and I. Smolyar, 2018. *World Ocean Atlas 2018, Volume 1: Temperature.* A. Mishonov Technical Ed.; NOAA Atlas NESDIS 81, 52 pp.

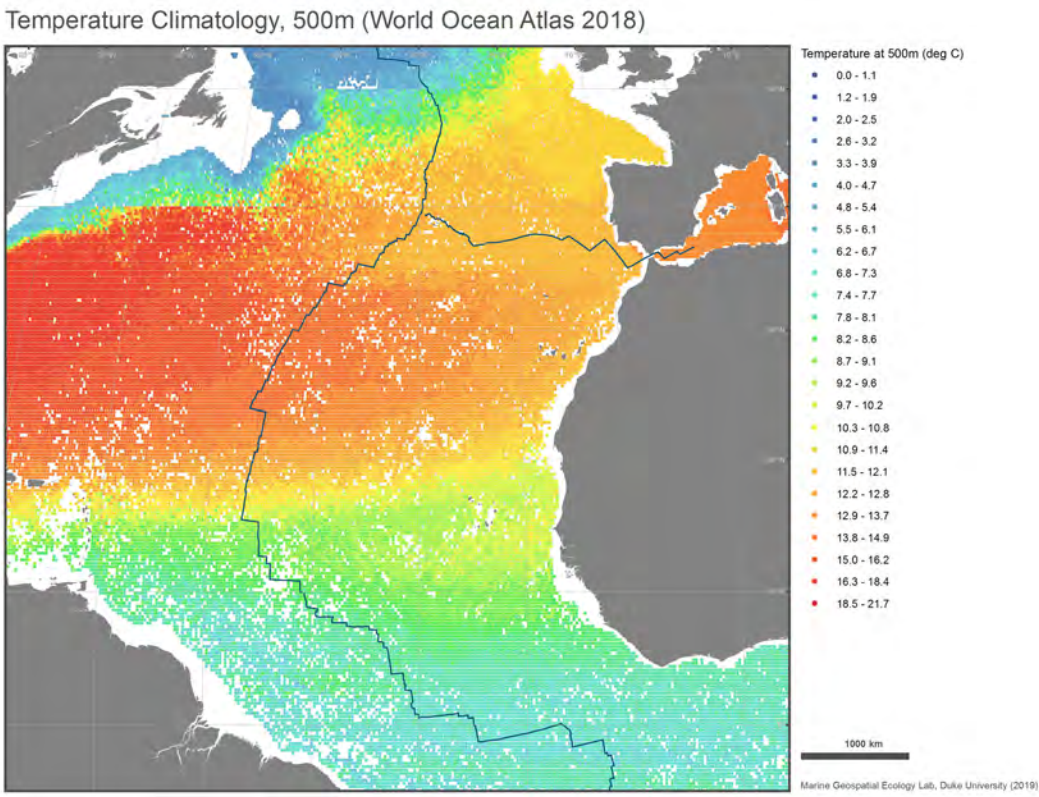

Figure 2.12-1 Temperature, 500m

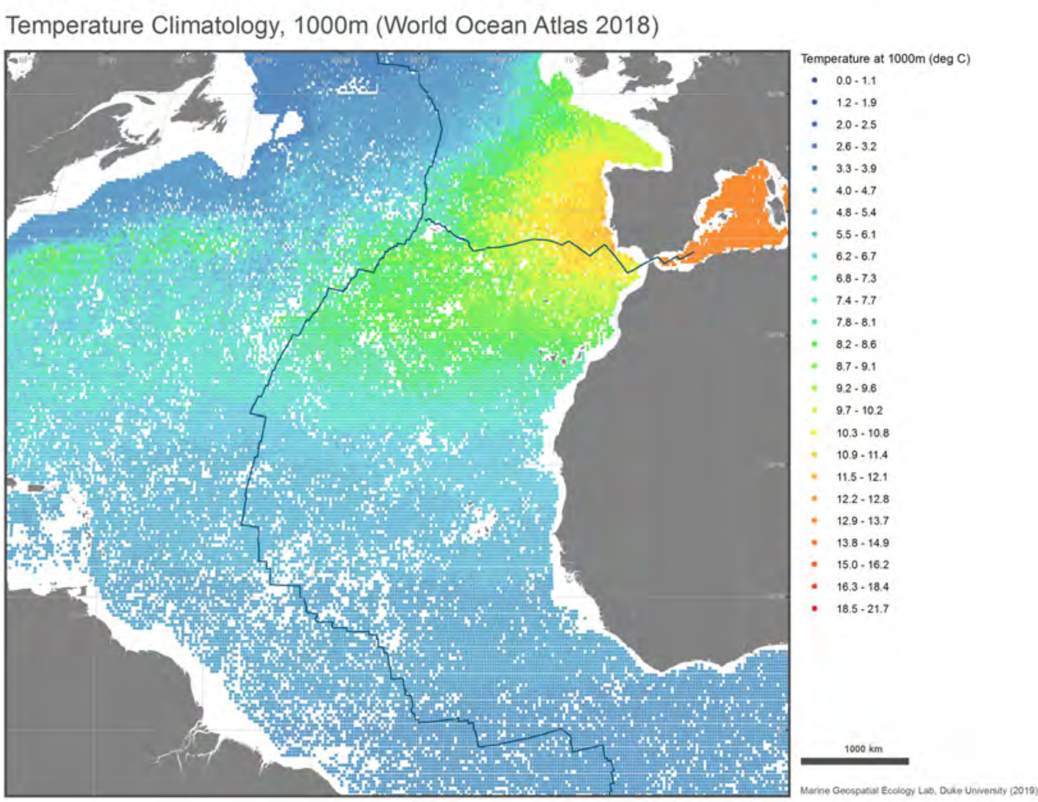

Figure 2.12-2 Temperature, 1000m

2.13 Hybrid Coordinate Ocean Model (HYCOM) Data

The HYCOM consortium (https://hycom.org/about) is a multi-institutional effort sponsored by the National Ocean Partnership Program (NOPP), as part of the U.S. Global Ocean Data Assimilation Experiment (GODAE), to develop and evaluate a data-assimilative hybrid isopycnal-sigma-pressure (generalized) coordinate ocean model (called HYbrid Coordinate Ocean Model or HYCOM).

Here, climatologies of the 500 m current velocity and bottom temperature (Figures 11 and 12) were created using the “Create Climatological Rasters for HYCOM GLBu0.08 4D Variable” tool in the Marine Geospatial Ecology Tools (MGET) for ArcGIS (Roberts et al., 2010). This tool uses data from the Hybrid Coordinate Ocean Model (HYCOM) model GLBu0.08 (Chassignet et al. 2009). This tool produces rasters showing the climatological average value (or other statistic) of a HYCOM GLBu0.08 4D variable. Given a desired variable, a statistic, and a climatological bin definition, this tool downloads daily images for each depth layer of the variable, classifies them into bins, and produces a single raster for each bin. Each cell of the raster is produced by calculating the statistic on the values of that cell extracted from all of the rasters in the bin. This tool accesses a concatenation of several sequential HYCOM + NCODA Global 1/12 Degree "uniform" (GLBu0.08) datasets, treating them as a continuous virtual dataset running from late 1992 to the present day using the OPeNDAP protocol.

Data were summarized for single months in 2018 and can also be summarized into other climatologies as needed.

References:
Chassignet, E. et al. 2009. US GODAE: Global Ocean Prediction with the HYbrid Coordinate Ocean Model (HYCOM). - Oceanog. 22: 64–75.

Roberts, J.J., B.D. Best, D.C. Dunn, E.A. Treml, and P.N. Halpin (2010). Marine Geospatial Ecology Tools: An integrated framework for ecological geoprocessing with ArcGIS, Python, R, MATLAB, and C++. Environmental Modelling & Software 25: 1197-1207.

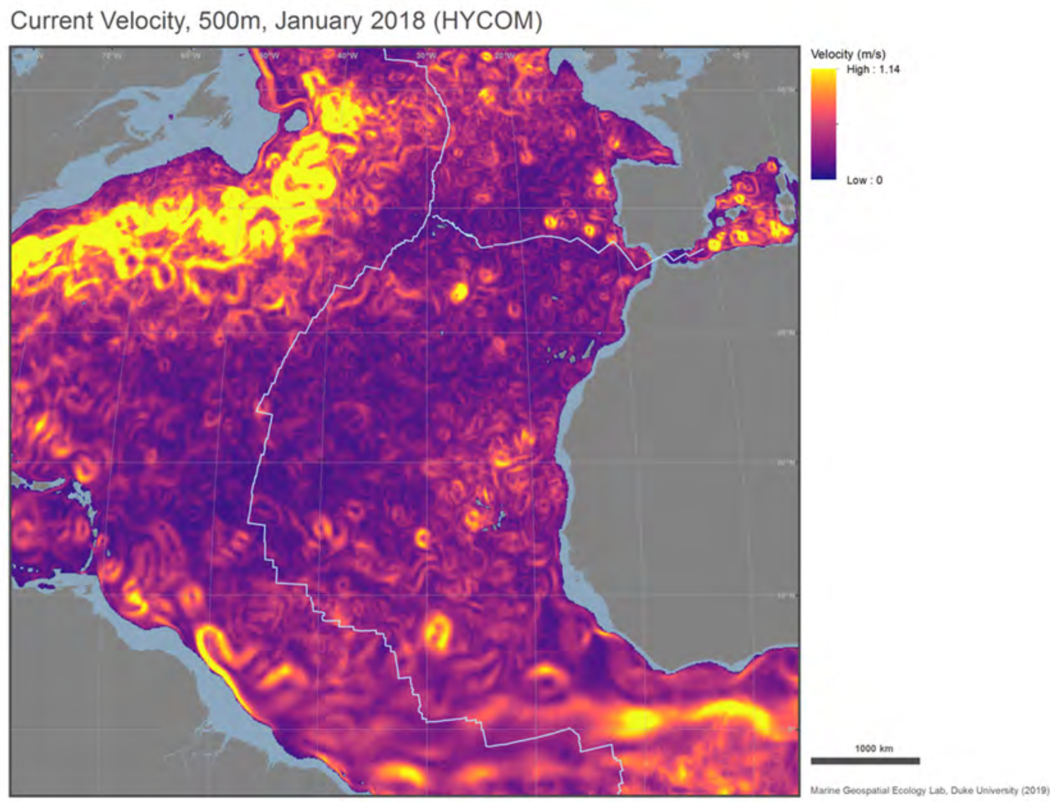

Figure 2.13-1 Current velocity, 500m, January 2018

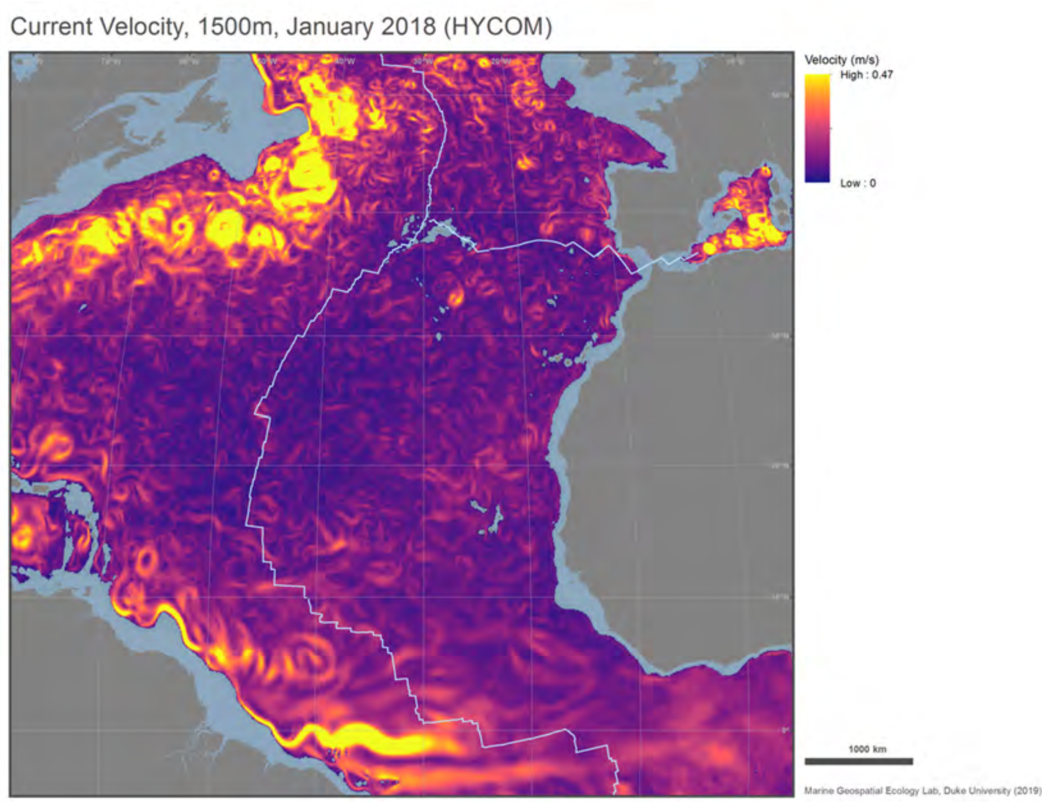

Figure 2.13-2 Current velocity, 1500m, January 2018

Current Velocity, 2500m, January 2018 (HYCOM)

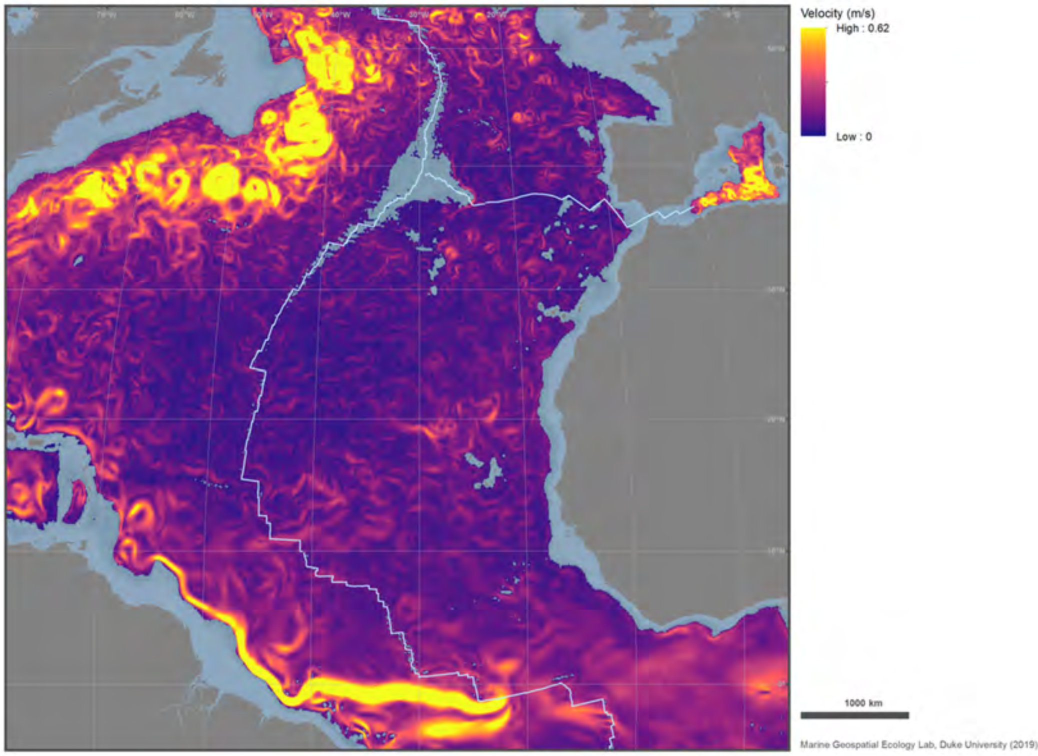

Figure 2.13-3 Current velocity, 2500m, January 2018

Current Velocity, Bottom, January 2018 (HYCOM)

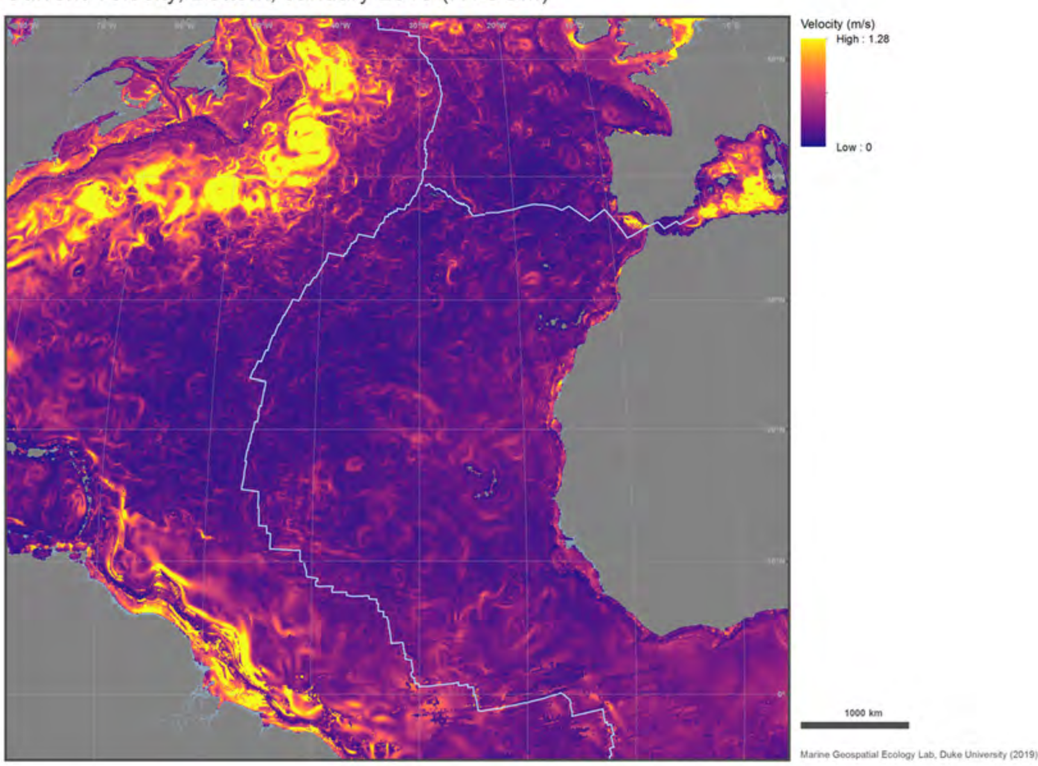

Figure 2.13-4 Current velocity, Bottom, January 2018

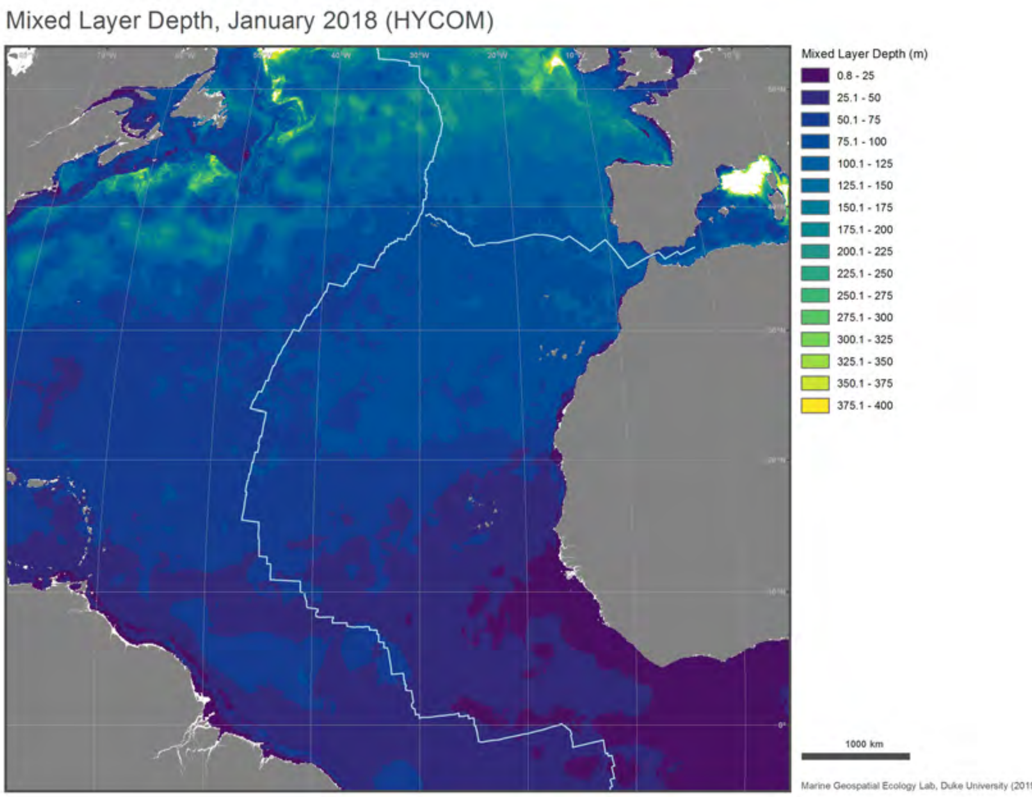

Figure 2.13-5 Mixed layer depth, January 2018

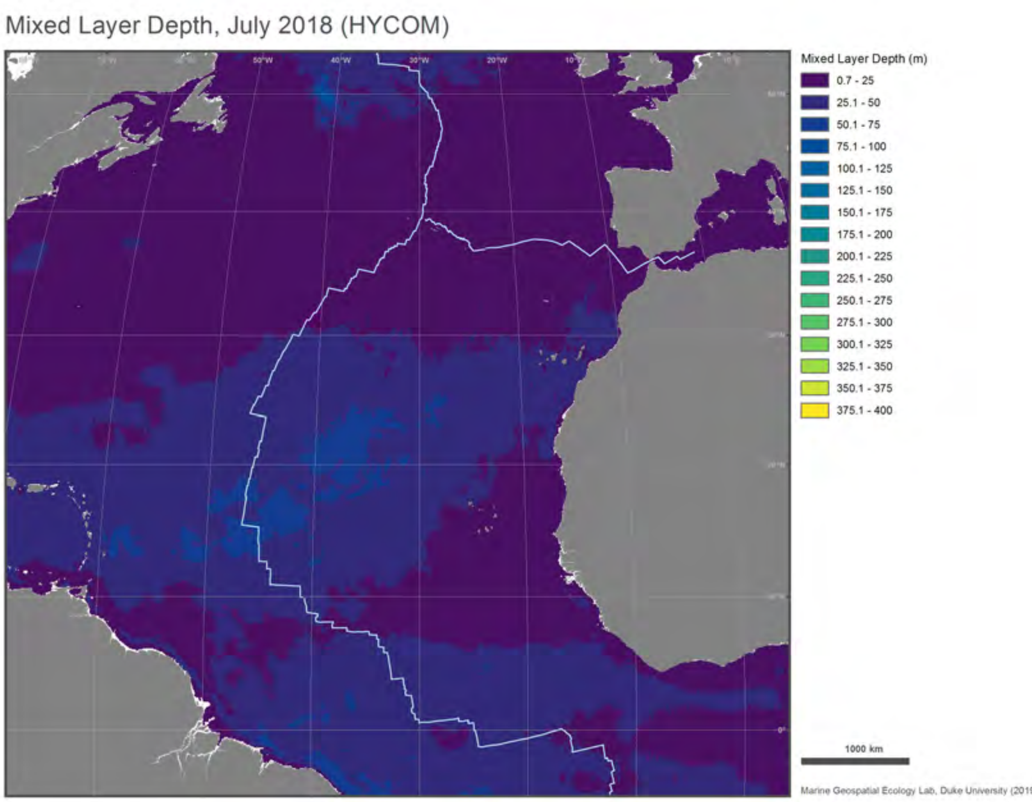

Figure 2.13-6 Mixed layer depth, July 2018

2.14 Seasonal AVHRR thermal front frequency

Reference:
Miller, P. I., Read, J. F., & Dale, A. C. (2013). Thermal front variability along the North Atlantic Current observed using microwave and infrared satellite data. Deep Sea Research Part II: Topical Studies in Oceanography, 98, 244-256.doi: 10.1016/j.dsr2.2013.08.014

2.15 Mesoscale eddy climatology

"The altimeter the Mesoscale Eddy Trajectory Atlas products were produced by SSALTO/DUACS and distributed by AVISO+ (http://www.aviso.altimetry.fr/) with support from CNES, in collaboration with Oregon State University with support from NASA. Eddies detected from the multimission altimetry datasets, with location each day for the whole altimetry period (1993-ongoing, in delayed-time), type (cyclonic/anticyclonic), speed, radius and associated metadata."

Source: Mesoscale Eddy Trajectory Atlas, version 2.0exp, https://www.aviso.altimetry.fr/index.php?id=3280&L=1

Reference:
Mesoscale Eddy Trajectory Atlas Product Handbook, SALP-MU-P-EA-23126, issue 2.0 https://www.aviso.altimetry.fr/fileadmin/documents/data/tools/hdbk_eddytrajectory_2.0exp.pdf

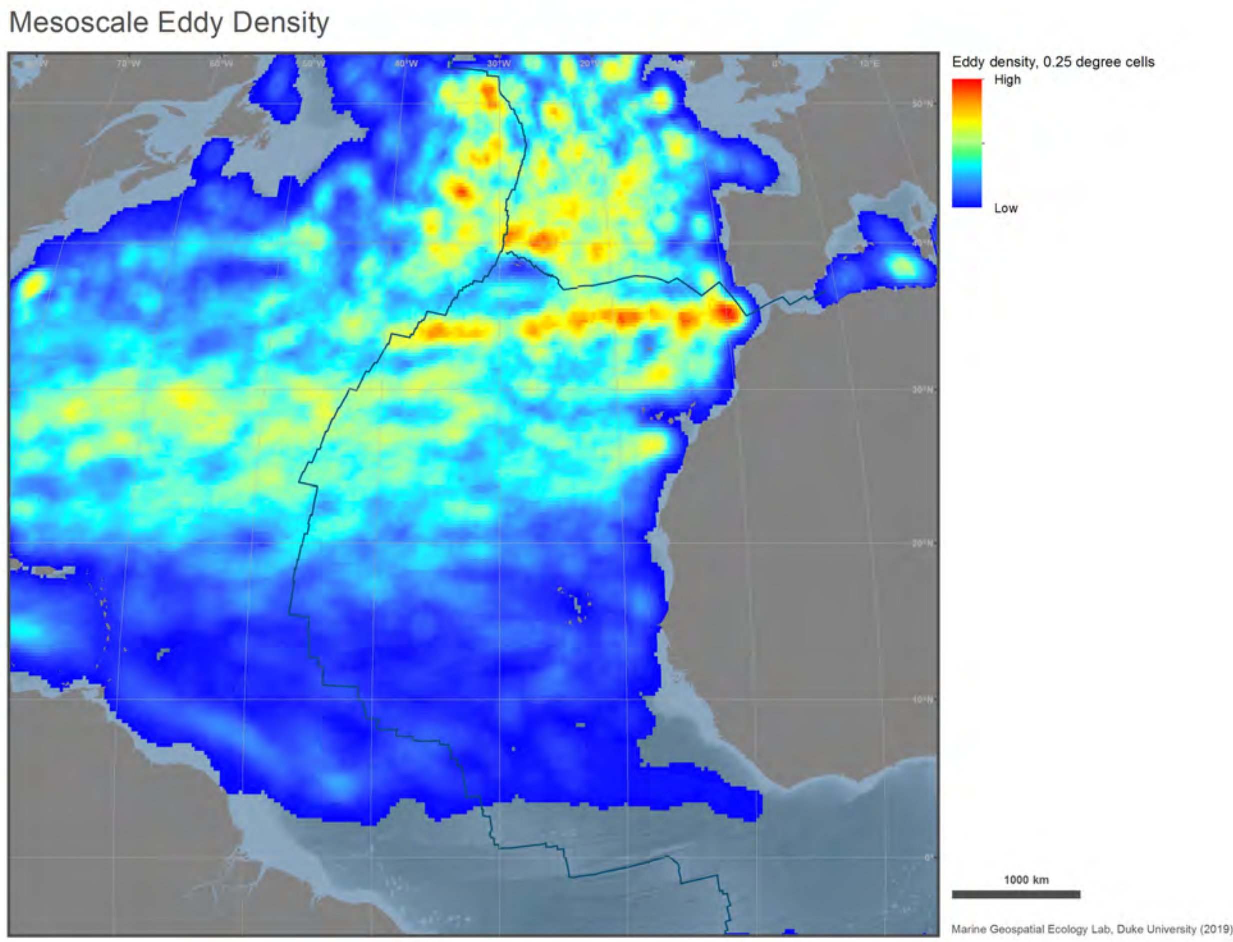

Figure 2.15-1 Mesoscale eddy density

2.16 Drifter Climatology of Near-Surface Currents

Description:
“Satellite-tracked SVP drifting buoys (Sybrandy and Niiler, 1991; Niiler, 2001) provide observations of near-surface circulation at unprecedented resolution. In September 2005, the Global Drifter Array became the first fully realized component of the Global Ocean Observing System when it reached an array size of 1250 drifters. A drifter is composed of a surface float which includes a transmitter to relay data, a thermometer that reads temperature a few centimeters below the air/sea interface, and a submergence sensor used to detect when/if the drogue is lost. The surface float is tethered to a holey sock drogue, centered at 15 m depth. The drifter follows the flow integrated over the drogue depth, although some slip with respect to this motion is associated with direct wind forcing (Niiler and Paduan, 1995). This slip is greatly enhanced in drifters that have lost their drogues (Pazan and Niiler, 2000). Drifter velocities are derived from finite differences of their position fixes. These velocities, and the concurrent SST measurements, are archived at AOML's Drifting Buoy Data Assembly Center, where the data are quality controlled and

interpolated to 1/4-day intervals (Hansen and Herman, 1989; Hansen and Poulain, 1996).”

Source: https://www.aoml.noaa.gov/phod/gdp/mean_velocity.php

Reference:

Laurindo, L. C., Mariano, A. J., & Lumpkin, R. (2017). An improved near-surface velocity climatology for the global ocean from drifter observations. Deep Sea Research Part I: Oceanographic Research Papers, 124, 73-92. doi: 10.1016/j.dsr.2017.04.009

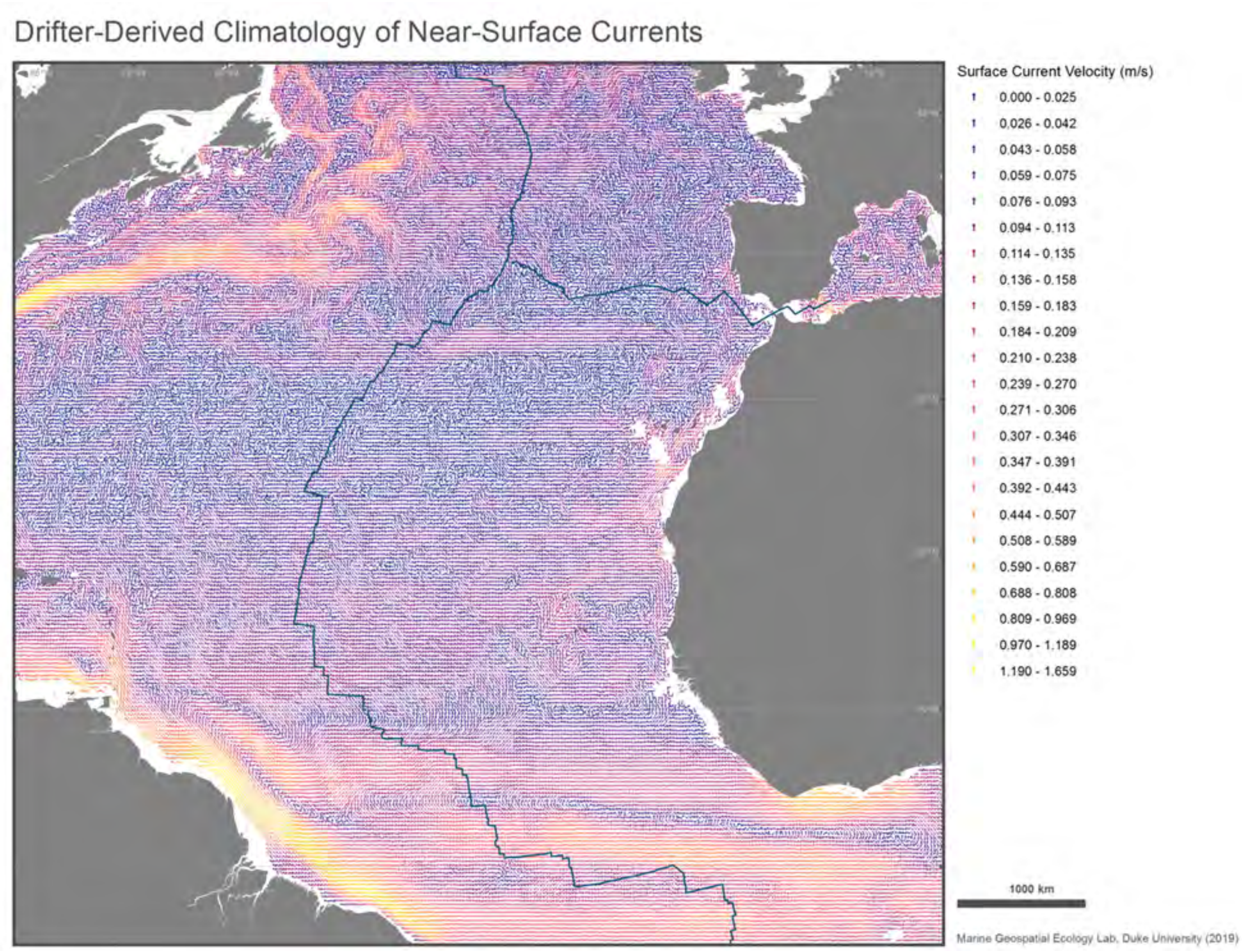

Figure 2.16-1 Drifter-derived climatology of near-surface currents

2.17 Chlorophyll A Seasonal Climatology

Seasonal cumulative chlorophyll A climatologies for 2018 were created using the “Create Climatological Rasters for NASA OceanColor L3 SMI Product” tool in the Marine Geospatial Ecology Tools (MGET) for ArcGIS (Roberts et al., 2010). This tool uses data from the MODIS sensor on the Aqua satellite. One climatology was generated for each quarter: January – March, April – June, July – September, October - December.

Reference:

Roberts, Jason J., Benjamin D. Best, Daniel C. Dunn, Eric A. Treml, and Patrick N. Halpin. 2010. “Marine Geospatial Ecology Tools: An Integrated Framework for Ecological Geoprocessing with ArcGIS, Python, R, MATLAB, and C++.” *Environmental Modelling & Software* 25 (10):1197–1207. https://doi.org/10.1016/j.envsoft.2010.03.029.

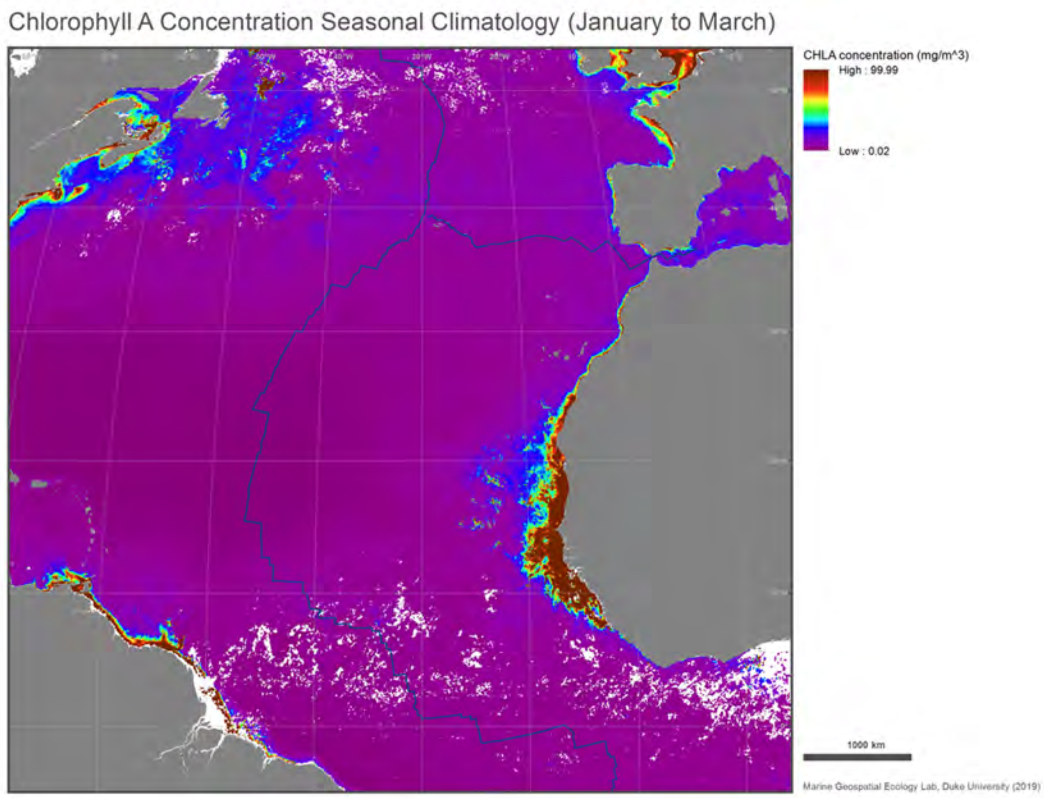

Figure 2.17-1 Chlorophyll A concentration seasonal climatology: January - March

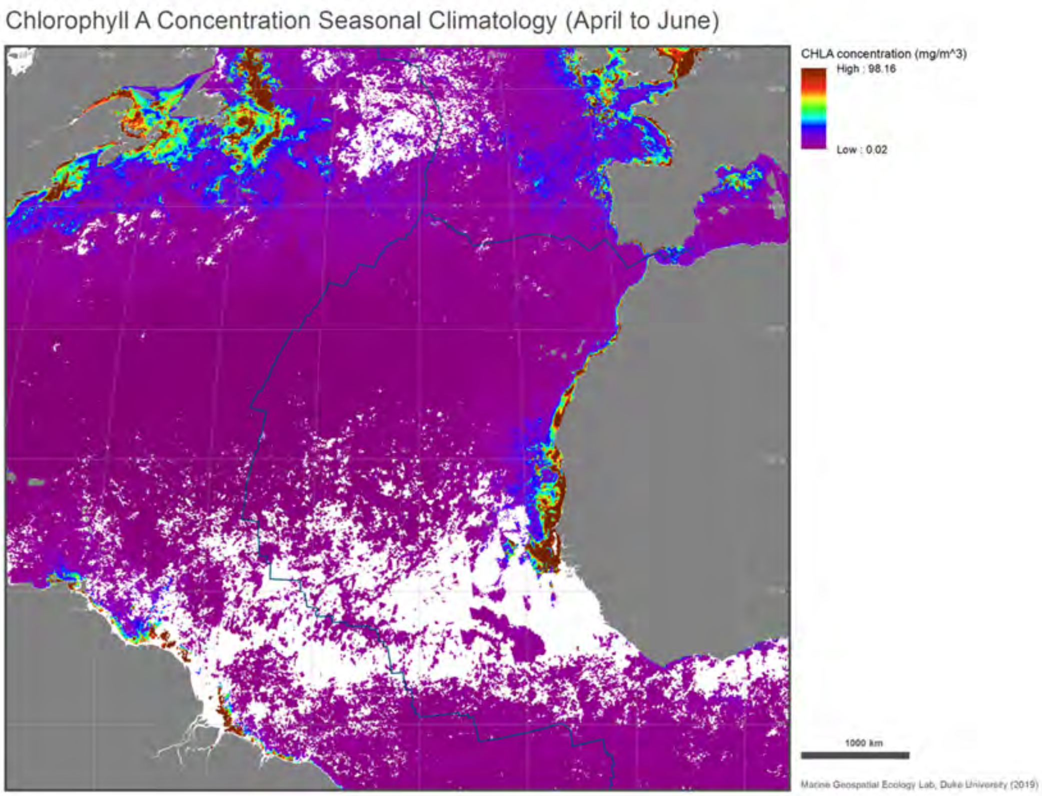

Figure 2.17-2 Chlorophyll A concentration seasonal climatology: April - June

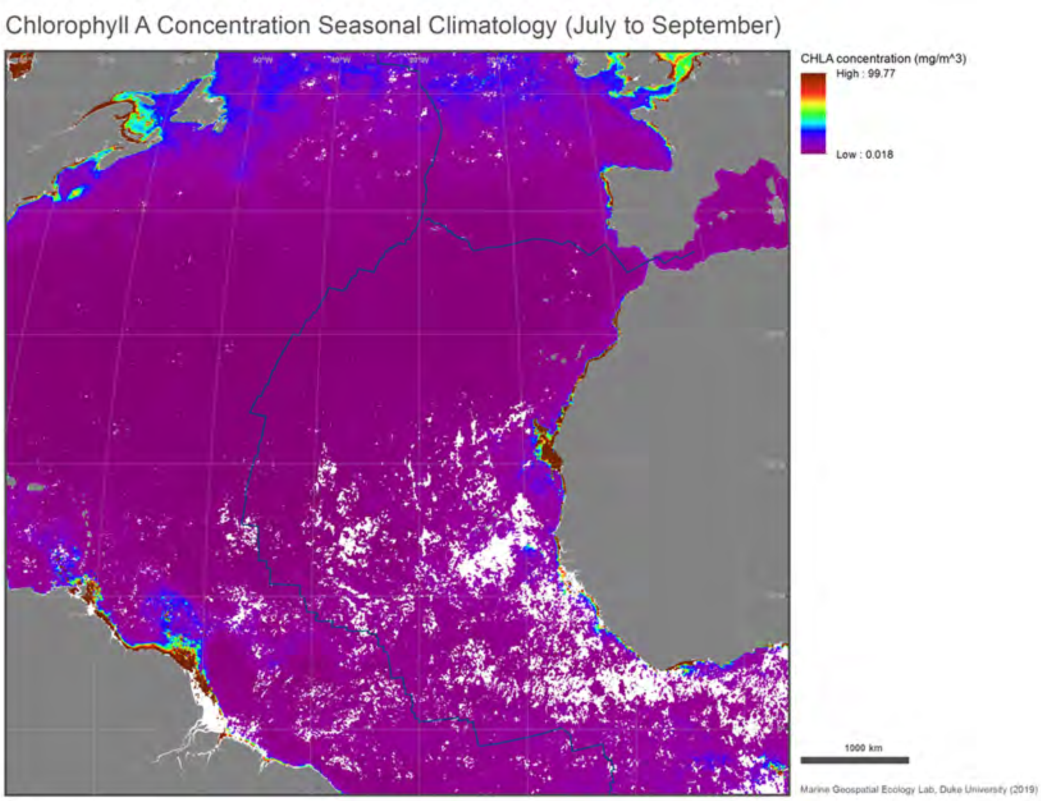

Figure 2.17-3 Chlorophyll A concentration seasonal climatology: July - September

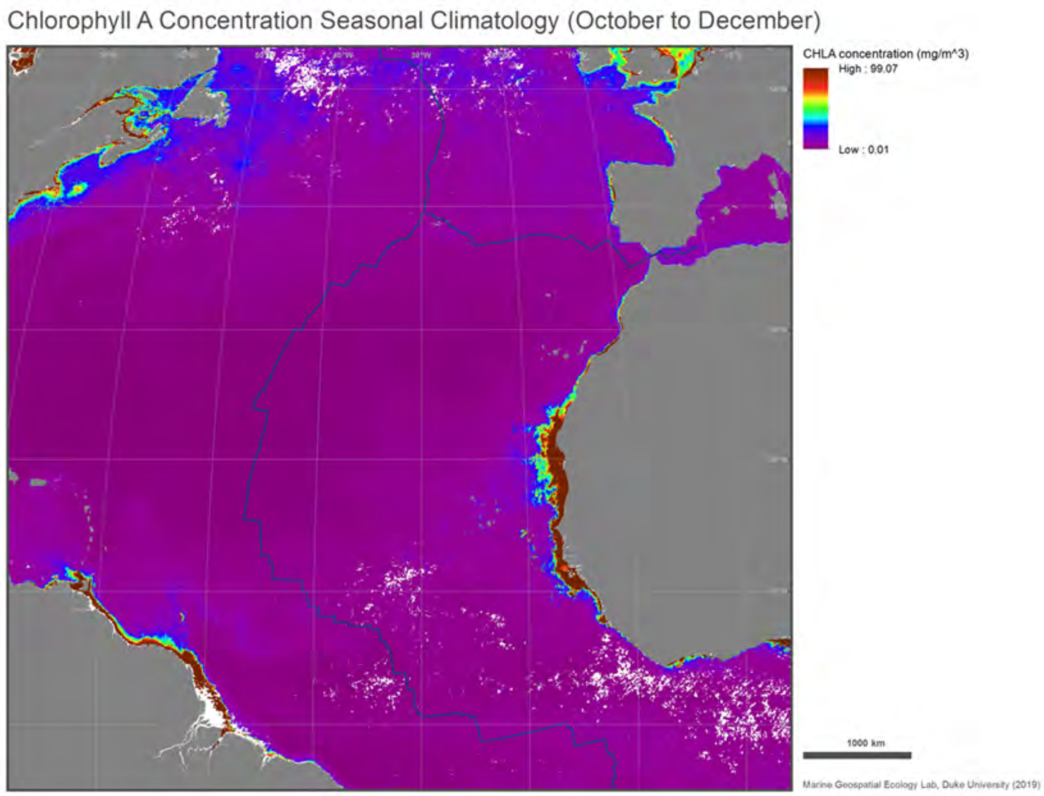

Figure 2.17-4 Chlorophyll A concentration seasonal climatology: October - December

2.18 VGPM Primary Productivity

Standard Ocean Productivity Products are based on the original description of the Vertically Generalized Production Model (VGPM) (Behrenfeld & Falkowski 1997), MODIS surface chlorophyll concentrations (Chl_{sat}), MODIS sea surface temperature data (SST), and MODIS cloud-corrected incident daily photosynthetically active radiation (PAR). Euphotic depths are calculated from Chl_{sat} following Morel and Berthon (1989). For this effort, a cumulative climatology was created from Standard VGPM data derived from MODIS AQUA data from 2003-2007.

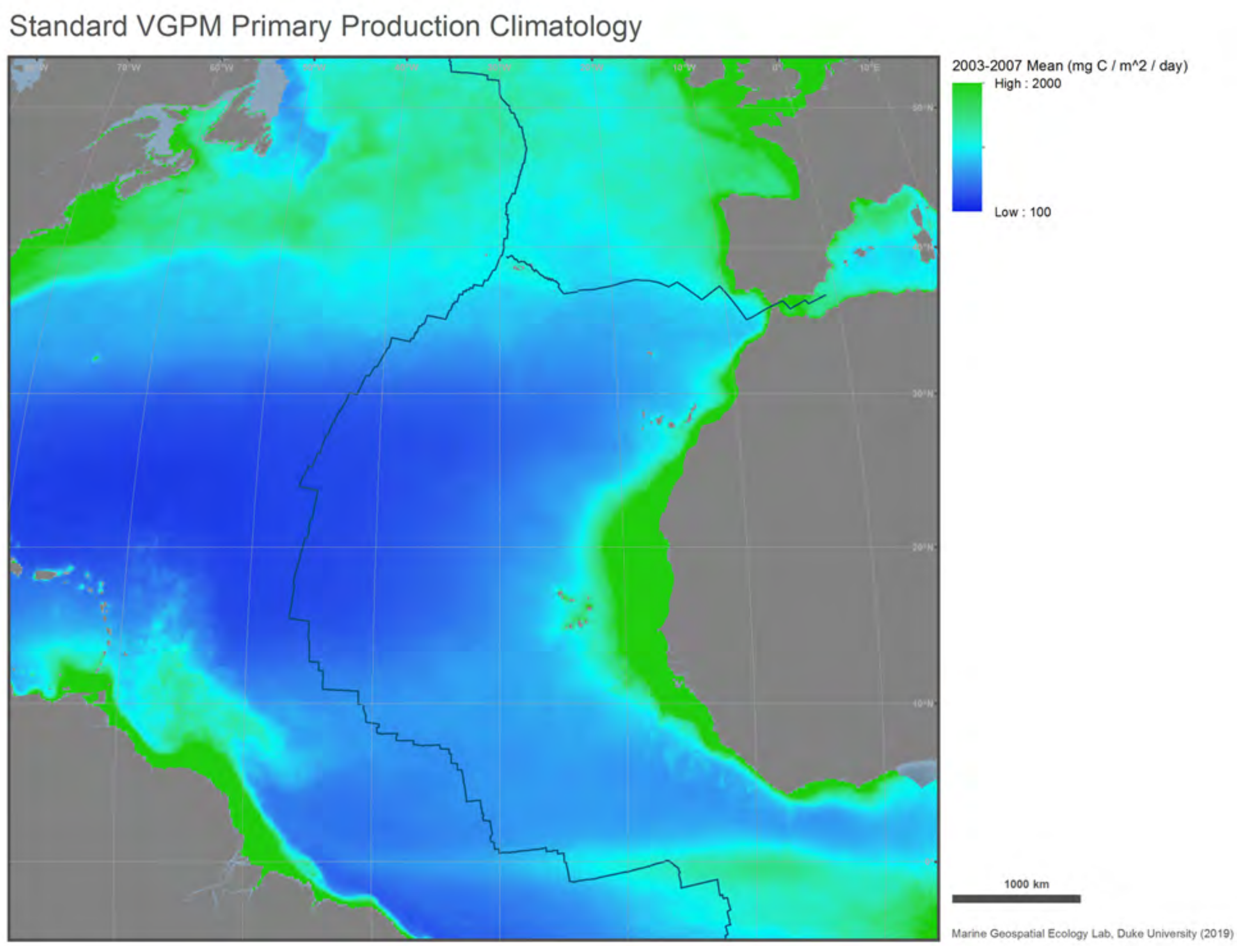

Figure 2.18-1 VGPM primary productivity climatology

2.19 Net Primary Productivity - Operational Mercator Ocean Biogeochemical Global Ocean Analysis and Forecast System

Description:
"The Operational Mercator Ocean biogeochemical global ocean analysis and forecast system at 1/4 degree is providing 10 days of 3D global ocean forecasts updated weekly. The time series is aggregated in time, in order to reach a two full year's time series sliding window. This product includes daily and monthly mean files of biogeochemical parameters (chlorophyll, nitrate, phosphate, silicate, dissolved oxygen, dissolved iron, primary production, phytoplankton, PH, and surface partial pressure of carbon dioxyde) over the global ocean. The global ocean output files are displayed with a 1/4 degree horizontal resolution with regular longitude/latitude equirectangular projection. 50 vertical levels are ranging from 0 to 5700 meters."

Source: http://marine.copernicus.eu/services-portfolio/access-to-products/?option=com_csw&view=details&product_id=GLOBAL_ANALYSIS_FORECAST_BIO_001_028

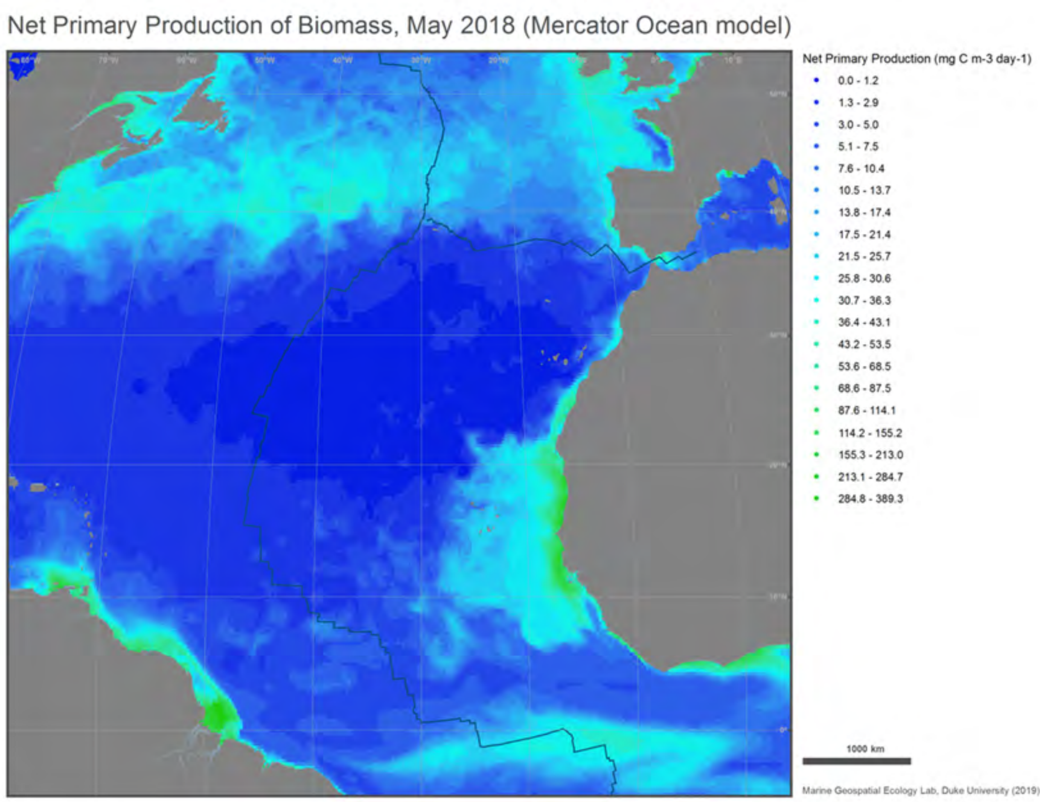

Figure 2.19-1 Net primary production of biomass, May 2018

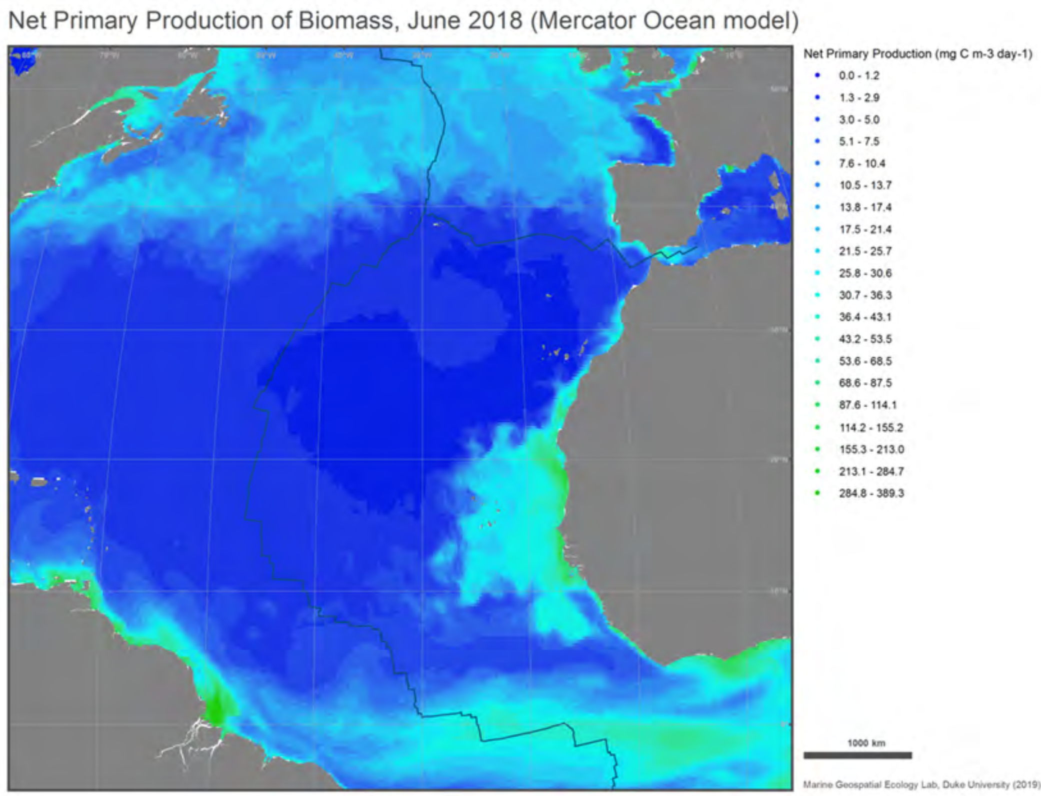

Figure 2.19-2 Net primary production of biomass, June 2018

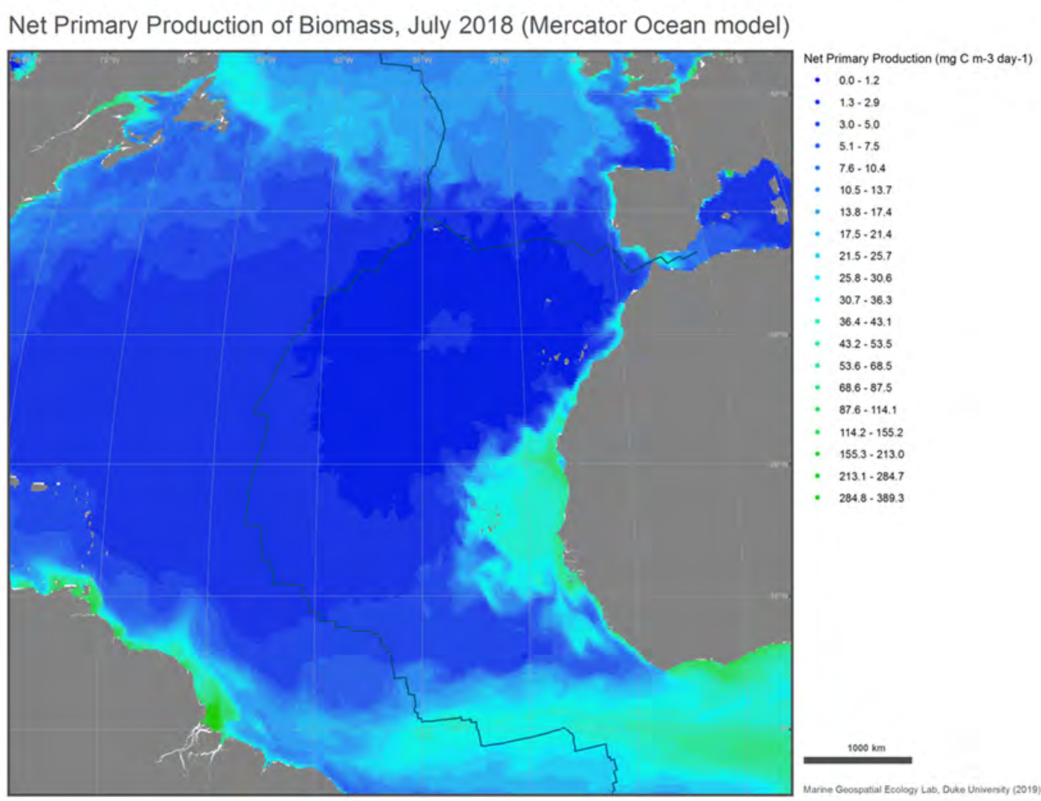

Figure 2.19-3 Net primary production of biomass, July 2018

2.20 Global Ocean Low and Mid Trophic Levels Biomass Hindcast

Description:
"The low and mid-trophic levels (LMTL) reanalysis for global ocean is produced at (https://www.cls.fr) (Toulouse, France). It provides 2D fields of zooplankton biomass and six groups of micronekton biomass for the time period 1998-2016 at 1/4 degree and weekly time resolution. It uses the LMTL component of dynamical population model (http://www.seapodym.eu/). No data assimilation in this product.

- Latest SEAPODYM LMTL version (2.1.03) http://www.seapodym.eu/

Forcings:

- Ocean currents and ocean temperature from FREEGLORYS2V4 ocean physics produced at Mercator-Ocean
- Net Primary Production (NPP) computed from chlorophyll, Sea Surface Temperature (SST) and Photosynthetically Active Radiation (PAR) satellite observation and model
- daily SST from NOAA NCEI AVHRR-only (Reynolds (https://www.ncdc.noaa.gov/oisst)) and PAR from https://apps.ecmwf.int/datasets/data/interim-full-daily/levtype=sfc"

Source: http://marine.copernicus.eu/services-portfolio/access-to-products/?option=com_csw&view=details&product_id=GLOBAL_REANALYSIS_BIO_001_033

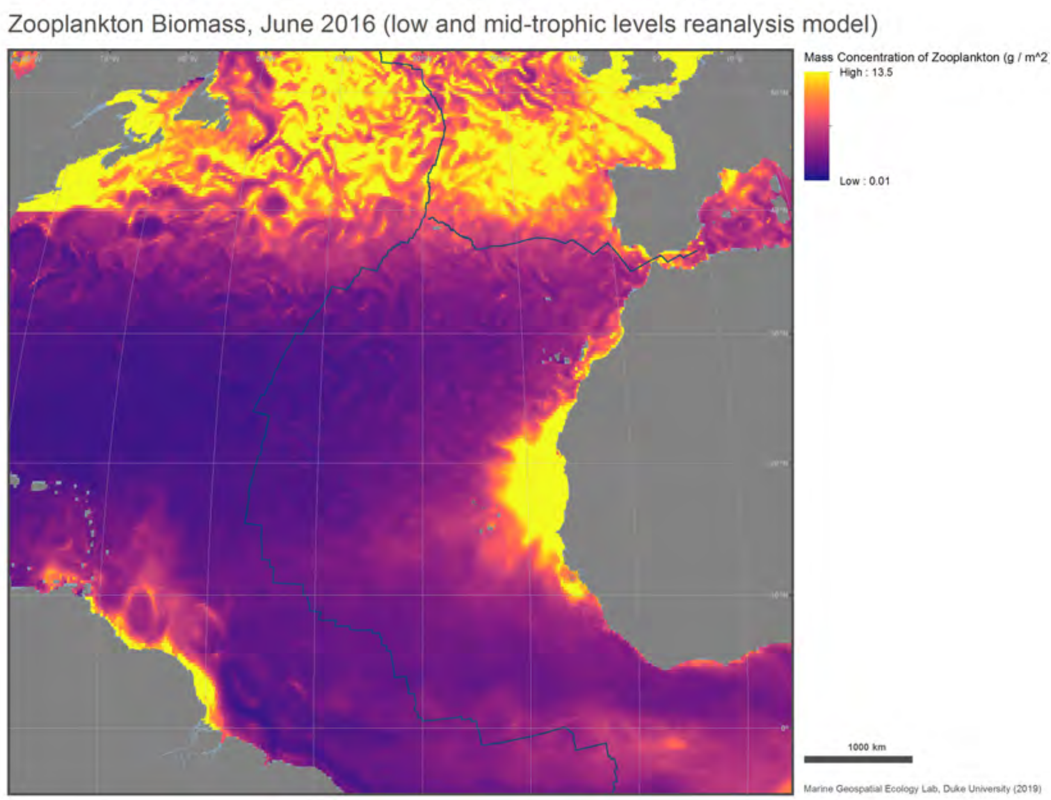

Figure 2.20-1 Zooplankton biomass, June 2016

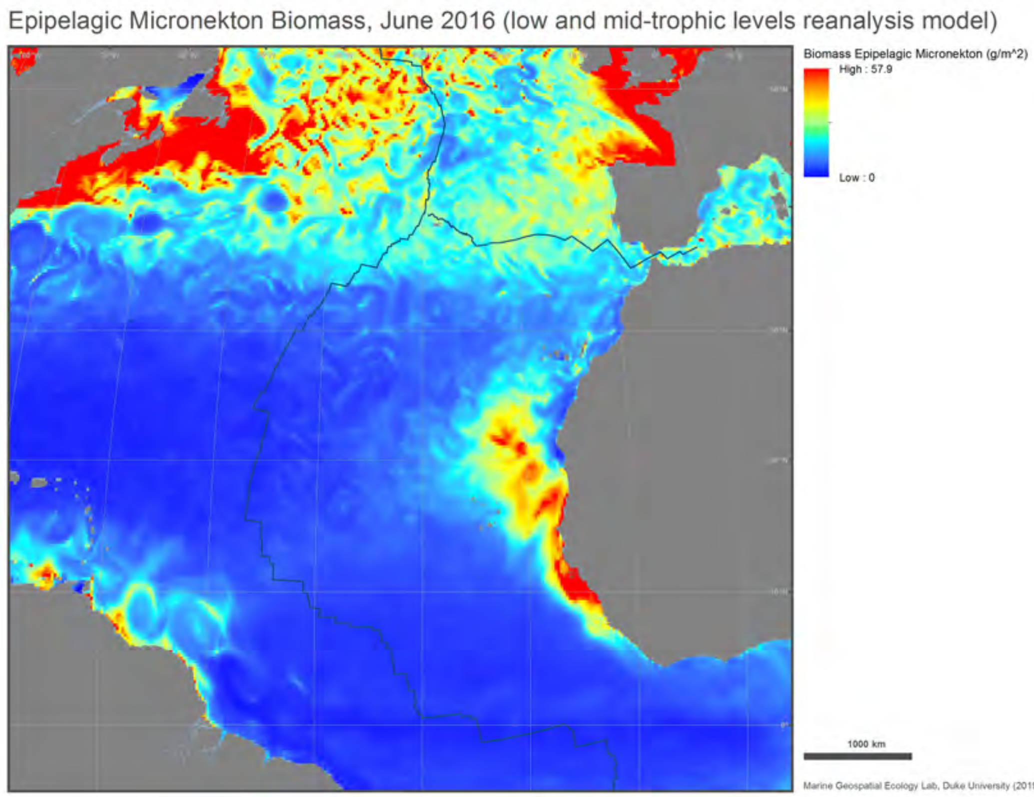

Figure 2.20-2 Epipelagic micronekton biomass, June 2018

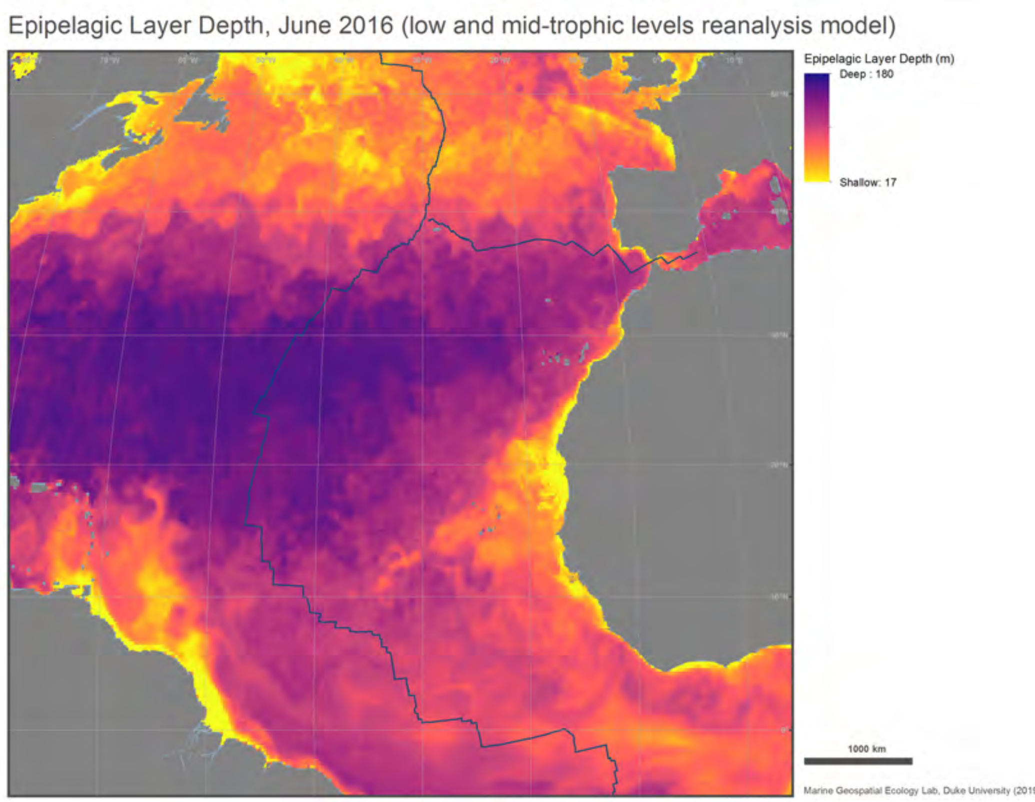

Figure 2.20-3 Epipelagic layer depth, June 2018

2.21 Seafloor POC Flux

Abstract (Lutz et al. 2007):
"We investigate the functioning of the ocean's biological pump by analyzing the vertical transfer efficiency of particulate organic carbon (POC). Data evaluated include globally distributed time series of sediment trap POC flux, and remotely sensed estimates of net primary production (NPP) and sea surface temperature (SST). Mathematical techniques are developed to compare these temporally discordant time series using NPP and POC flux climatologies. The seasonal variation of NPP is mapped and shows regional- and basin-scale biogeographic patterns reflecting solar, climatic, and oceanographic controls. Patterns of flux are similar, with more high-frequency variability and a subtropical-subpolar pattern of maximum flux delayed by about 5 days per degree latitude increase, coherent across multiple sediment trap time series. Seasonal production-to-flux analyses indicate during intervals of bloom production, the sinking fraction of NPP is typically half that of other seasons. This globally synchronous pattern may result from seasonally varying biodegradability or multiseasonal retention of POC. The relationship between NPP variability and flux variability reverses with latitude, and may reflect dominance by the large-amplitude seasonal NPP signal at higher latitudes. We construct algorithms describing labile and refractory flux components as a function of remotely sensed NPP rates, NPP variability, and SST, which predict POC flux with accuracies greater than equations typically employed by global climate models. Globally mapped predictions of POC export, flux to depth, and sedimentation are supplied. Results indicate improved ocean carbon cycle forecasts may be obtained by combining satellite-based observations and more mechanistic representations taking into account factors such as mineral ballasting and ecosystem structure."

Reference:
Lutz, M. J., Caldeira, K., Dunbar, R. B., & Behrenfeld, M. J. (2007). Seasonal rhythms of net primary production and particulate organic carbon flux to depth describe the efficiency of biological pump in the global ocean. Journal of Geophysical Research: Oceans, 112(C10). doi:10.1029/2006JC003706.

Particulate Organic Carbon Flux to the Seafloor (Lutz et al. 2007)

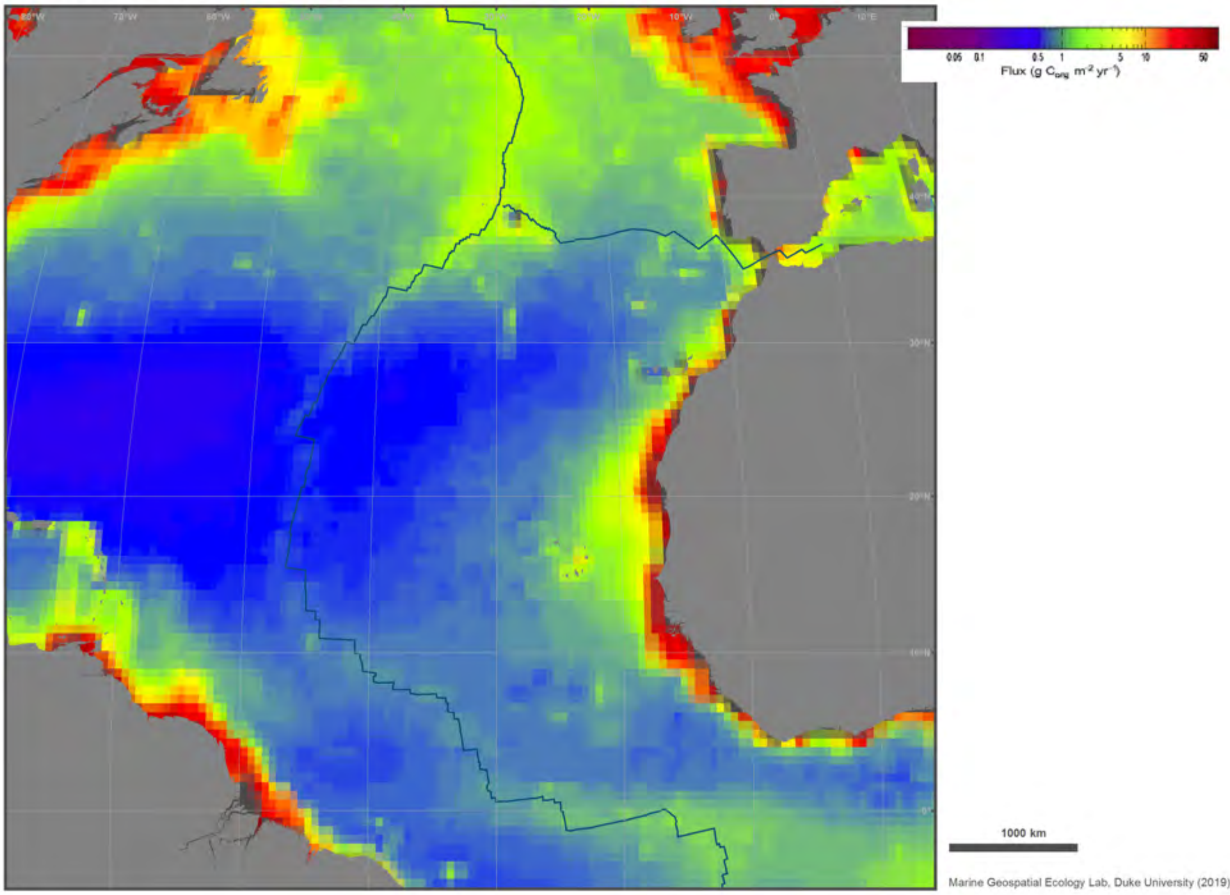

Figure 2.21-1 Particulate organic carbon flux to the seafloor

Original Caption: Figure 14, "Annual average particulate organic carbon (d) flux to the seafloor (g Corg m−2 yr−1)"

2.22 Internal Tides

Abstract (Tuerena et al. 2019):
"Diapycnal mixing of nutrients from the thermocline to the surface sunlit ocean is thought to be relatively weak in the world's subtropical gyres as energy inputs from winds are generally low. The interaction of internal tides with rough topography enhances diapycnal mixing, yet the role of tidally induced diapycnal mixing in sustaining nutrient supply to the surface subtropical ocean remains relatively unexplored. During a field campaign in the North Atlantic subtropical gyre, we tested whether tidal interactions with topography enhance diapycnal nitrate fluxes in the upper ocean. We measured an order of magnitude increase in diapycnal nitrate fluxes to the deep chlorophyll maximum (DCM) over the Mid-Atlantic Ridge compared to the adjacent deep ocean. Internal tides drive this enhancement, with diapycnal nitrate supply to the DCM increasing by a factor of 8 between neap and spring tides. Using a global tidal dissipation

database, we find that this spring-neap enhancement in diapycnal nitrate fluxes is widespread over ridges and seamounts. Mid-ocean ridges therefore play an important role in sustaining the nutrient supply to the DCM, and these findings may have important implications in a warming global ocean."

Reference:
Tuerena, R. E., Williams, R. G., Mahaffey, C., Vic, C., Green, J. M., Naveira-Garabato, A., ... & Sharples, J. (2019). Internal tides drive nutrient fluxes into the deep chlorophyll maximum over mid-ocean ridges. Global Biogeochemical Cycles, 33(8), 995-1009. doi:10.1029/2019GB006214

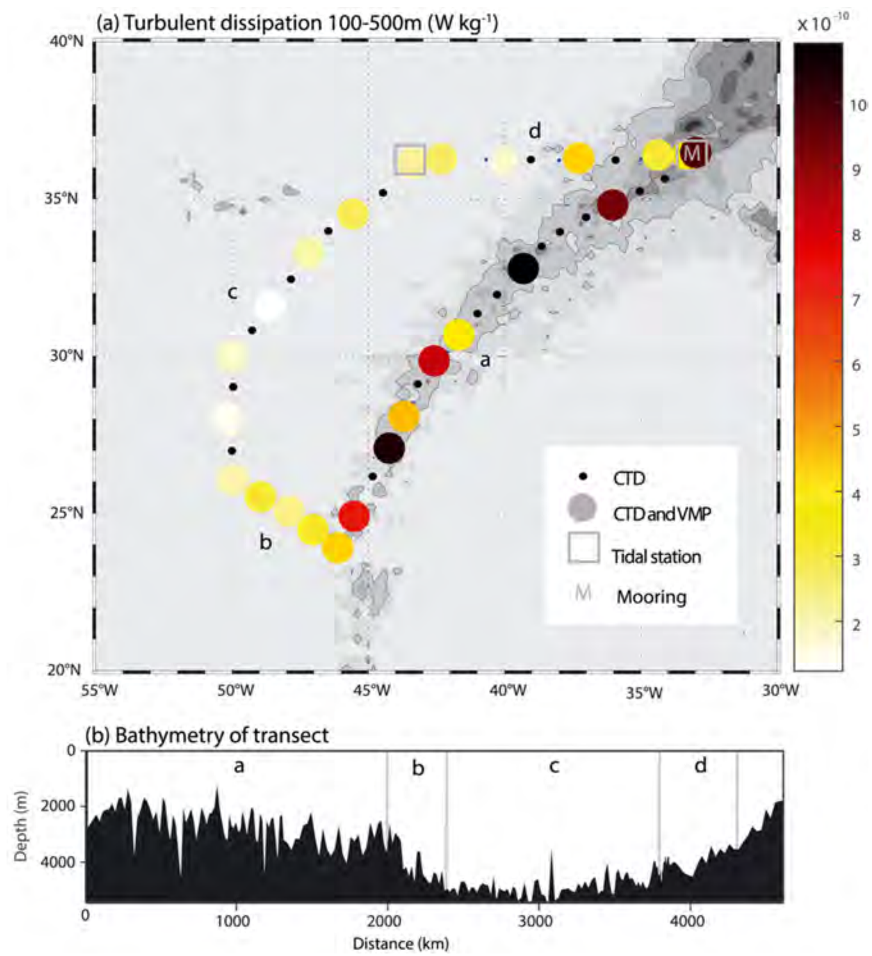

Figure 2.22-1 Figure 1 from Tuerena et al. (2019)

Original Caption: Fig 1. (a) Map of study area displaying locations of full water column CTD (conductivity, temperature, depth) and Vertical Microstructure Profiler sampling over the Mid-Atlantic Ridge and in the adjacent abyssal ocean. Filled circles indicate the average water column turbulent kinetic energy dissipation between 100 and 500 m, which are enhanced along the ridge (eastern transect). The on- and off-ridge tidal stations and mooring are highlighted in the northern transect. (b) The changing bathymetry plotted against distance along the cruise track, the on-ridge, a; off-ridge, d; and cross ridge, b, d, sections are highlighted. VMP = Vertical Microstructure Profiler.

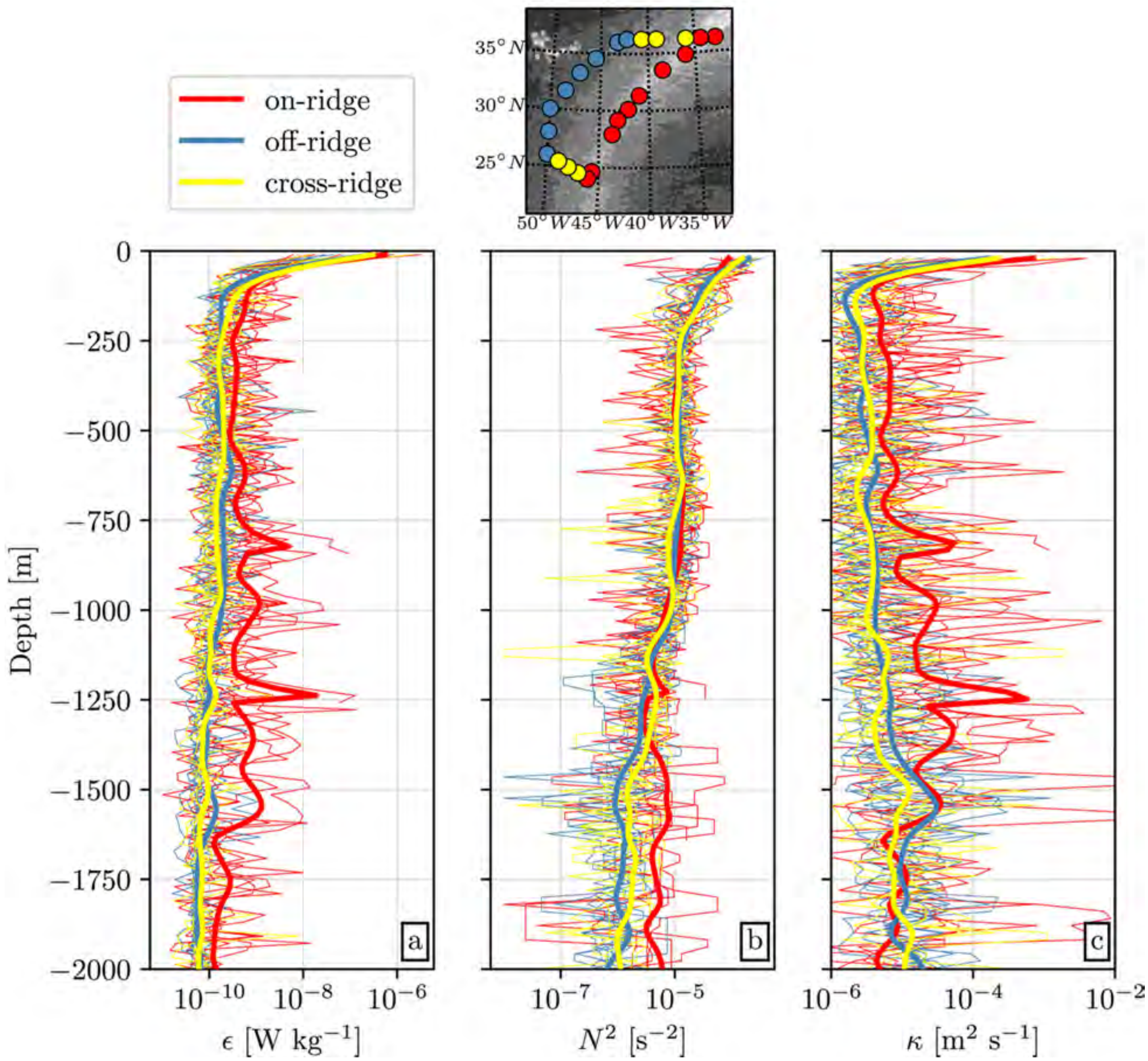

Figure 2.22-2 Figure 2 from Tuerena et al. (2019)

Original Caption: Fig 2. Depth profiles of (a) turbulent dissipation (W/Kg), (b) N2 (s−2), and (c) turbulent diffusivity (m2/s) in the upper 2,000 m across our study site. Stations are defined as on ridge (red), cross ridge (yellow), and off ridge (blue).

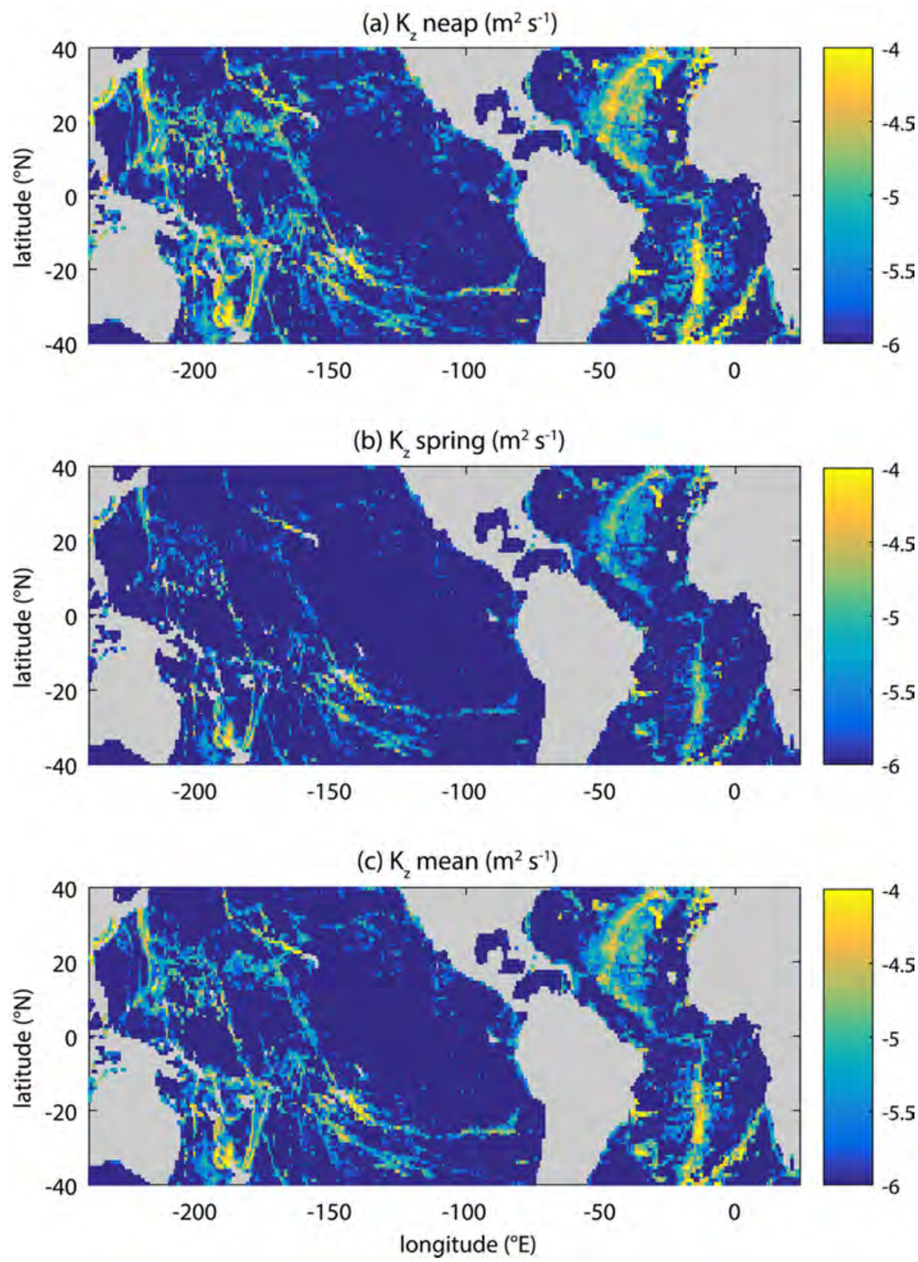

Figure 2.22-3 Figure 7 from Tuerena et al. (2019)

Original Caption: Fig. 7. Spring and neap tidal variations in upper ocean diapycnal diffusivity Kz (100–500 m). Upper ocean Kz (log10 m2/s) is calculated at spring and neap tides over the low-latitude ocean, (a) Kz over neap tides, (b) Kz over spring tides, and (c) tidally averaged Kz.

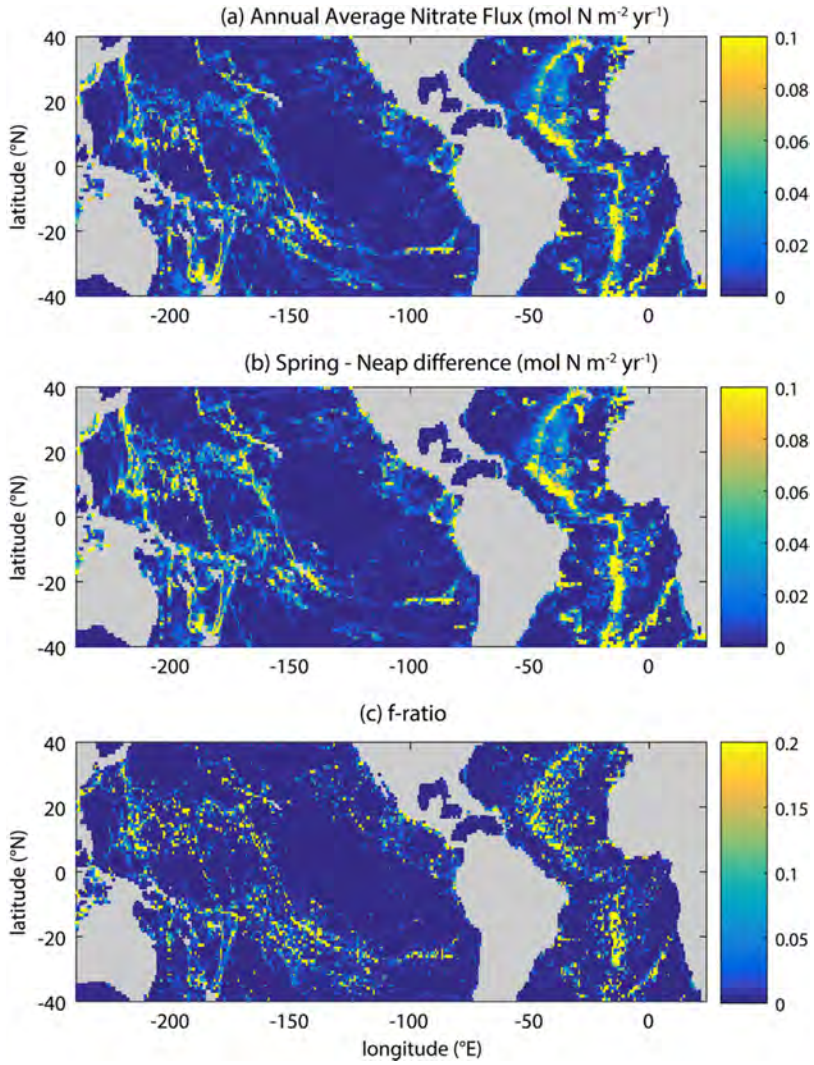

Figure 2.22-4 Figure 8 from Tuerena et al. (2019)

Original Caption: Fig 8. Estimated tidal variation in diapycnal nitrate fluxes over the Atlantic and Pacific basins between 40°S and 40°N. Nutrient gradients were estimated using the maximum gradient in the upper 500 m from WOA climatology. Diapycnal diffusivity was calculated using dissipation from the TPOX8 database assuming that the energy redistributed in the vertical is directly proportional to the buoyancy frequency. (a) Annual average diapycnal nitrate flux in mole of nitrogen per square meter per year. (b) Tidal variability (spring tide minus neap tide) in mole of nitrogen per square meter per year. (c) Estimated f-ratio at the deep chlorophyll maximum. Calculated by assuming that the nitrate flux is converted to carbon fixation following Redfield stoichiometry (C:N = 106:16) and the calculated f-ratio = [Redfield C fixed by internal tidal supply of N] / [annual net primary production from satellite]; annual net primary production is calculated using published methods (Behrenfeld et al., 2006).

2.23 Deep Ocean Circulation in the north Mid Atlantic Ridge

Abstract (Lahaye et al. 2019)

"Over mid-ocean ridges, the interaction between the currents and the topography gives rise to complex flows, which drive the transport properties of biogeochemical constituents, and especially those associated with hydrothermal vents, thus impacting associated ecosystems. This paper describes the circulation in the rift valley along the Azores sector of the North Mid-Atlantic Ridge, using a combination of in-situ data from several surveys and realistic high-resolution modeling. It confirms the presence of a mean deep current with an up-valley branch intensified along the right inner flank of the valley (looking downstream), and a weaker down-valley branch flowing at shallower depth along the opposite flank. The hydrographic properties of the rift-valley water, and in particular the along-valley density gradient that results from a combination of the topographic isolation, the deep flow and the related mixing, are quantified. We also show that the deep currents exhibit significant variability and can be locally intense, with typical values greater than 10 cm/s. Finally, insights on the dynamical forcings of the deep currents and their variability are provided using numerical simulations, showing that tidal forcing of the mean circulation is important and that the overlying mesoscale turbulence triggers most of the variability."

Reference:

Lahaye, N., Gula, J., Thurnherr, A. M., Reverdin, G., Bouruet-Aubertot, P., & Roullet, G. (2019). Deep currents in the rift valley of the North Mid-Atlantic Ridge. Frontiers in Marine Science, 6, 597.doi: 10.3389/fmars.2019.00597

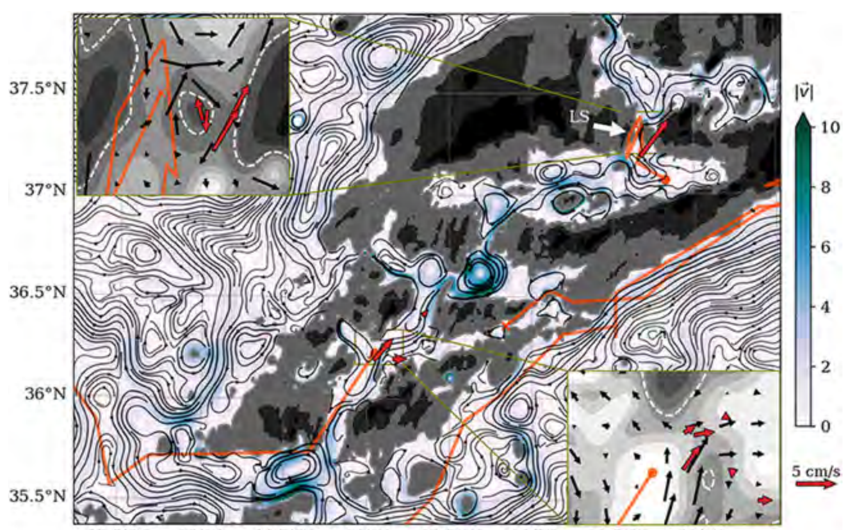

Figure 2.23-1 Figure 2 from Lahaye et al. (2019)

Original Caption: Figure 2. Rift valley circulation at 2,000 m. The mean flow from numerical modeling is shown in black ("streamplot" with the line thickness proportional to the speed amplitude) and colors further indicate its magnitude. Superimposed are two ARGO float tracks near 1,990 m inside the rift valley and two other ones near 1,500 m flowing southward along *the eastern flank of the ridge (orange, with the location of the release and last record indicated by a plain circle and a cross, respectively). Red arrows represent the mean velocity from selected moorings near the Rainbow vent field (2,100 m deep) and in the East canyon at Lucky Strike (1,875 m, LS label). Insets show zooms over these regions, representing the mean flow with black arrows. Black shading indicates bathymetry (using the same convention as in Figure 1) and white dashed contours in the insets indicate the depth at which the mean velocity is computed from the simulation (2,100 m at Rainbow, 1,800 m at Lucky-Strike, to match most of the available observations). At Rainbow, all 6 moorings available in the region are plotted. At Lucky-Strike, moorings are taken from (going west to east): Momar (1,700 m), DIVA (1,680 m), and Graviluck (1,930 and 1,874 m).*

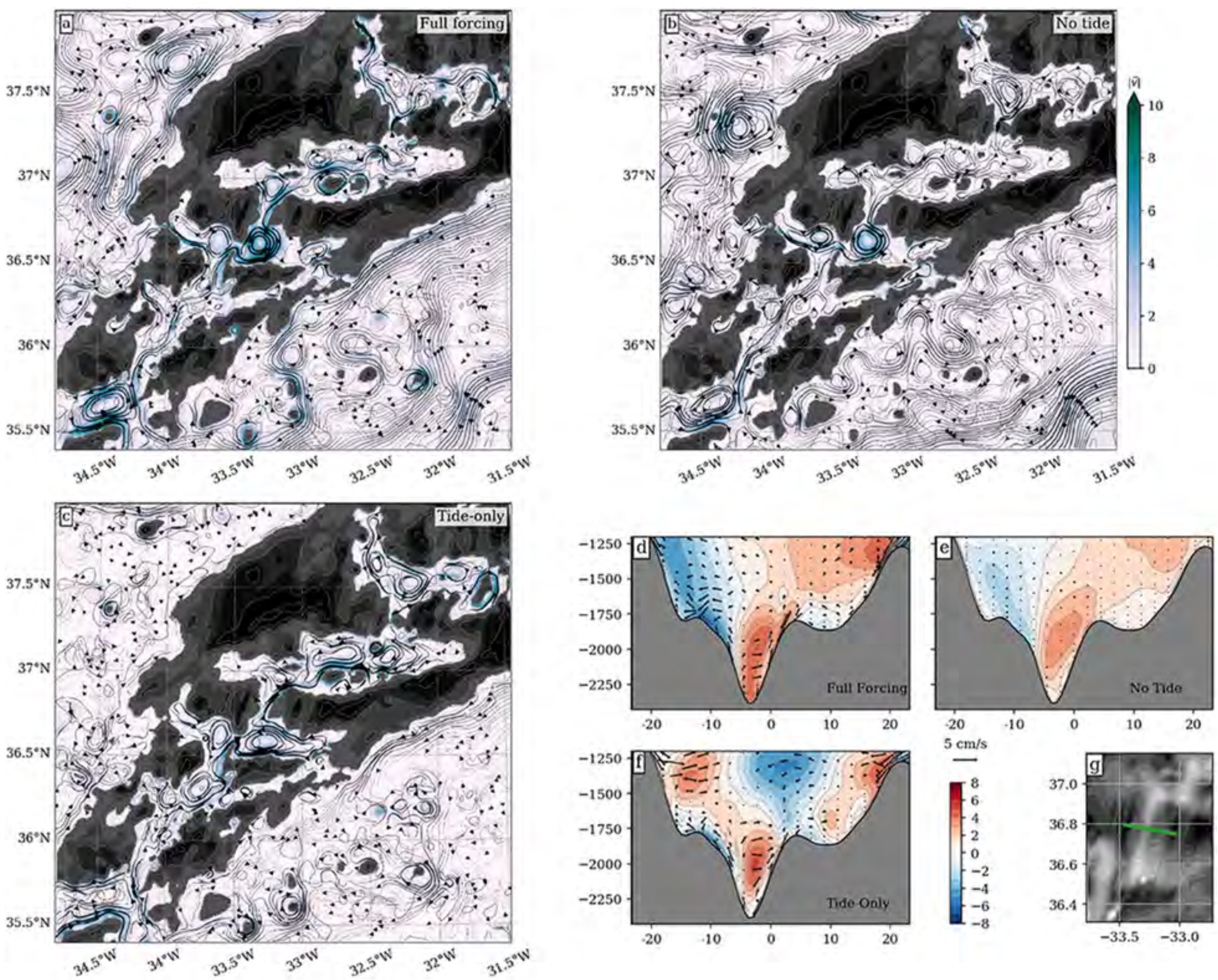

Figure 2.23-2 Figure 9 from Lahaye et al. (2019)

Original Caption: Figure 9. Comparison of different simulations with different forcing, as seen from the mean horizontal current at 2,000 m (a–c—same convention as in Figure 2) and the vertical structure across a section in the Famous segment (d–f, and localization of the section in g—same convention as in Figure 3). The different configurations correspond to full forcing (a,d), no tide (b,e), and tide-only (c,f).

2.24 Ocean Biogeochemistry

Reference:
Mora, Camilo, Abby G. Frazier, Ryan J. Longman, Rachel S. Dacks, Maya M. Walton, Eric J. Tong, Joseph J. Sanchez et al. "The projected timing of climate departure from recent variability." Nature 502, no. 7470 (2013): 183. Doi: 10.1038/nature12540

2.25 NOAA Climate Change Portal

“A key approach for examining climate, especially how it will change in the future, uses complex computer models of the climate system that includes atmosphere, ocean, sea ice and land components. Some models also include additional aspects of the earth system, including chemistry and biology. The Climate Change Portal is a web interface developed by the NOAA ESRL Physical Sciences Division to access and display the immense volumes of climate and earth system model output that informed the Intergovernmental Panel on Climate Change (IPCC) Fifth Assessment Report (AR5). The webtool makes climate change information more accessible to natural resource managers, decision makers and educators.”

Link: https://www.esrl.noaa.gov/psd/ipcc/ocn/

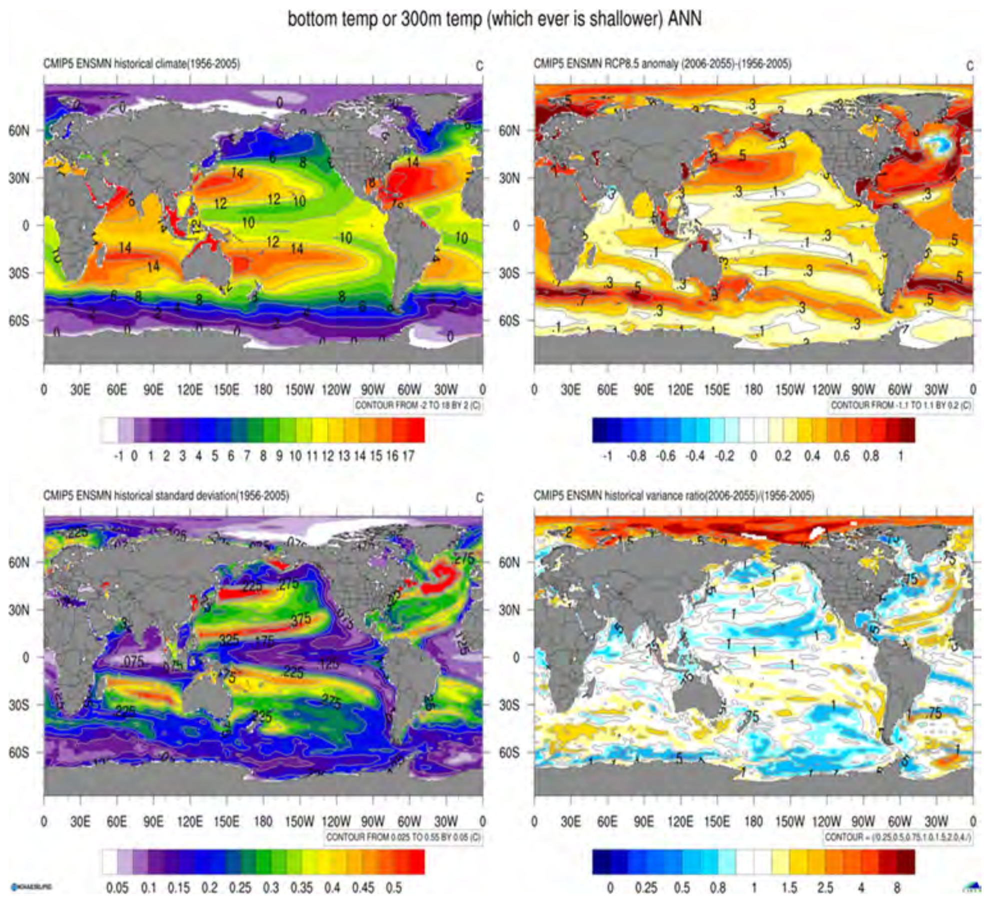

Figure 2.25-1 Climate change variables from CMIP5 data

2.26 Hydrothermally extinct seafloor massive sulphide (eSMS) in Mid-Atlantic Ridge

Abstract (Murton et al. 2019):

"Deep-sea mineral deposits potentially represent vast metal resources that could make a major contribution to future global raw material supply. Increasing demand for these metals, many of which are required to enable a low-carbon and high-technology society and to relieve pressure on land-based resources, may result in deep sea mining within the next decade. Seafloor massive sulphide (SMS) deposits, containing abundant copper, zinc, gold and silver, have been the subject of recent and ongoing commercial interest. Although many seafloor hydrothermally systems have been studied, inactive SMS deposits are likely more accessible to future mining and far more abundant, but are often obscured by pelagic sediment and hence difficult to locate. Furthermore, SMS deposits are three dimensional. Yet, to date, very few have been explored or sampled below the seafloor. Here, we describe the most comprehensive study to date of hydrothermally extinct seafloor massive sulphide (eSMS) deposits formed at a slow spreading ridge. Our approach involved two research cruises in the summer of 2016 to the Trans-Atlantic Geotraverse (TAG) hydrothermal field at 26°N on the Mid-Atlantic Ridge. These expeditions mapped a number of hydrothermally extinct SMS deposits using an autonomous underwater vehicle and remotely operated vehicle, acquired a combination of geophysical data including sub-seafloor seismic reflection and refraction data from 25 ocean bottom instruments, and recovered core using a robotic lander-type seafloor drilling rig. Together, these results that have allowed us to construct a new generic model for extinct seafloor massive sulphide deposits indicate the presence of up to five times more massive sulphide at and below the seafloor than was previously thought."

Reference:

Murton, B.J., Lehrmann, B., Dutrieux, A.M., Martins, S., de la Iglesia, A.G., Stobbs, I.J., Barriga, F.J., Bialas, J., Dannowski, A., Vardy, M.E, North, L.J.,Yeo, I A.L.M., Lusty, P. A.J., Petersen, S., (2019). Geological fate of seafloor massive sulphides at the TAG hydrothermal field (Mid-Atlantic Ridge). Ore Geology Reviews. doi: 10.1016/j.oregeorev.2019.03.005

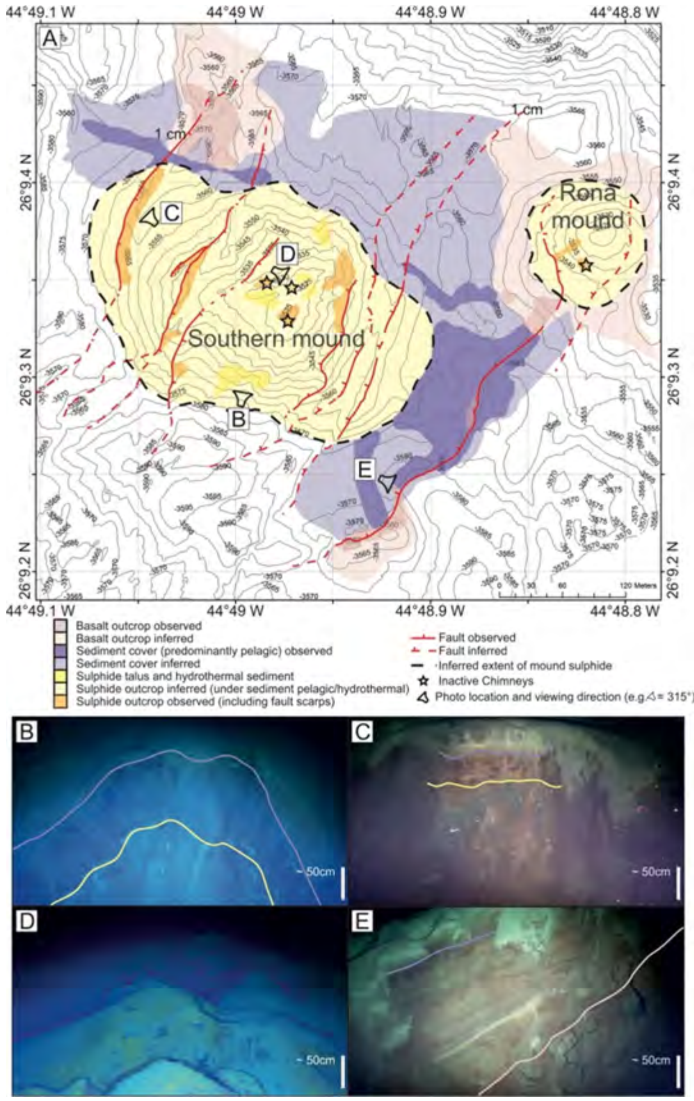

Figure 2.26-1 Figure 5 from Murton et al. (2019)

Original Caption: Fig. 5. (A) Geological map of Southern Mound and Rona Mound, interpreted from the high-resolution bathymetry, surface samples and video surveys. Note, the white areas are unmapped and trapezoidal-shaped symbol is the viewing direction for the photographs. (B) Slump scarp on the SW side of Southern Mound; coloured lines indicate separation between the pelagic carbonate sediment cover (upper magenta line) and oxidised iron-rich sediments and sulphide rubble (lower yellow line). (C): The western most fault scarp on Southern Mound showing transition from pelagic carbonate to iron-rich sediments (upper magenta line) to underlying sulphide rubble (lower yellow line). (D): blocks of sulphide (dark objects) with yellow coloured jarosite staining on the summit of Southern Mound surrounded by pelagic carbonate sediment. (E): layered sulphide material, deposited by mass-wasting, overlying brecciated basalt at the edge of the flank of Southern Mound (magenta lines delineate boundaries with pelagic carbonate ooze and sulphide-rich sediments and the pink line marks the contact with underlying basaltic breccia. Images: National Oceanography Centre.

3 Biological Data

3.1 Ocean Biogeographic Information System (OBIS) Data

"The Ocean Biogeographic Information System (OBIS) seeks to absorb, integrate, and assess isolated datasets into a larger, more comprehensive picture of life in our oceans. The system hopes to stimulate research about our oceans to generate new hypotheses concerning evolutionary processes, species distributions, and roles of organisms in marine systems on a global scale. OBIS generate maps that contribute to the 'big picture' of our oceans: a comprehensive, collaborative, worldwide view of our oceans.

OBIS (http://www.iobis.org/about/index) provides a portal or gateway to many datasets containing information on where and when marine species have been recorded. The datasets are integrated so you can search them all seamlessly by species name, higher taxonomic level, geographic area, depth, and time; and then map and find environmental data related to the locations."

The maps provided in this report are based on available OBIS records for the Atlantic Ocean. Data gaps do exist in OBIS and thus these summaries are not exhaustive.

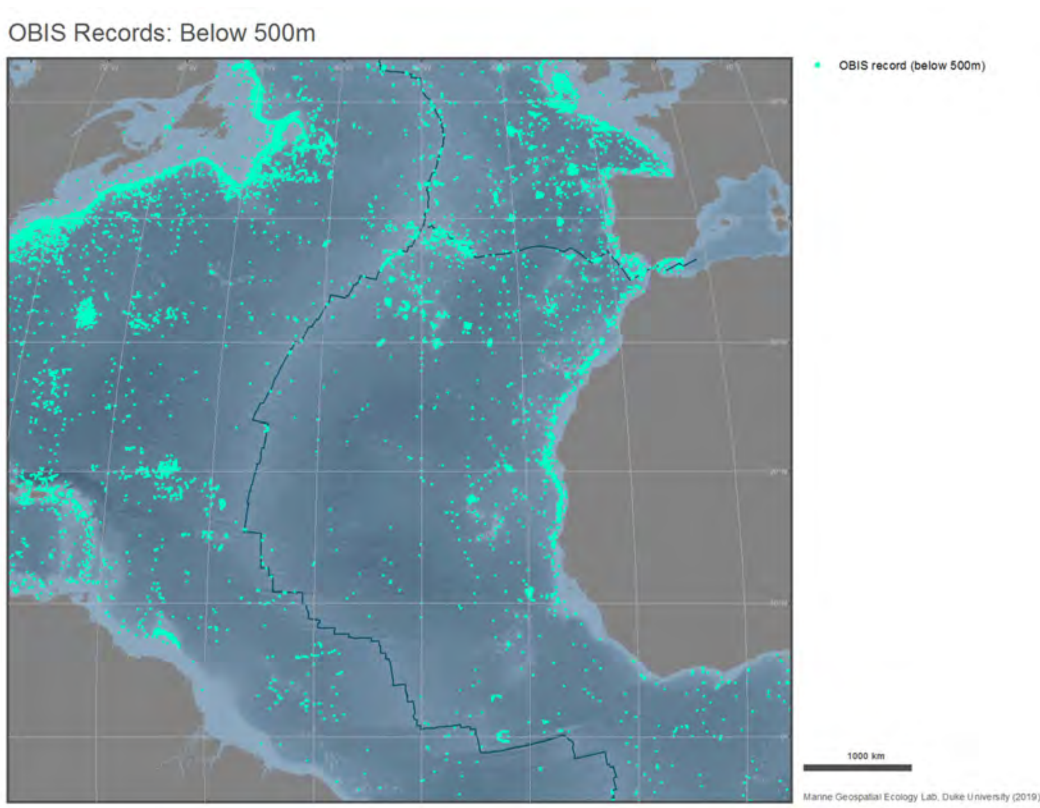

Figure 3.1-1 All OBIS records below 500 m

3.2 OBIS Vulnerable Marine Ecosystems (VMEs) Indicator Taxa

The Food and Agriculture Organization (FAO) of the United Nations International Guidelines for the Management of Deep-sea Fisheries in the High Seas (FAO, 2009) provide general tools and considerations for the identification of vulnerable marine ecosystems (VMEs). They include a set of criteria that should be used, individually or in combination, for the identification process. Specifically: Uniqueness or rareness, Functional significance of the habitat, Fragility, Life-history of species make recovery difficult, and Structural complexity.

VME Indicator taxa

Common name	Scientific name	Taxonomical level
Stony coral	Scleractinia	Order
Sponge	Porifera	Phylum
Black coral	Antipatharia	Order
Lace coral	Stylasteridae	Family
Gorgonian	Alcyonacea	Order
Sea-pen	Pennatulacea	Order
Blue coral	Helioporacea	Order

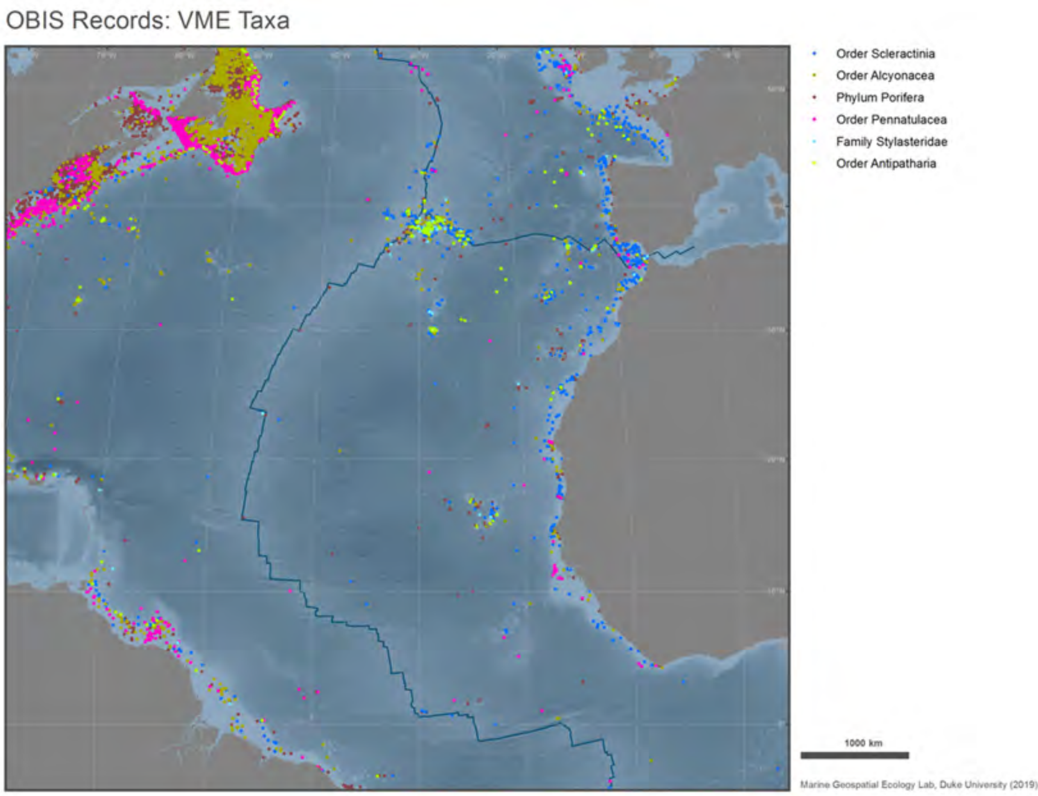

Figure 3.2-1 OBIS records for all VME taxa

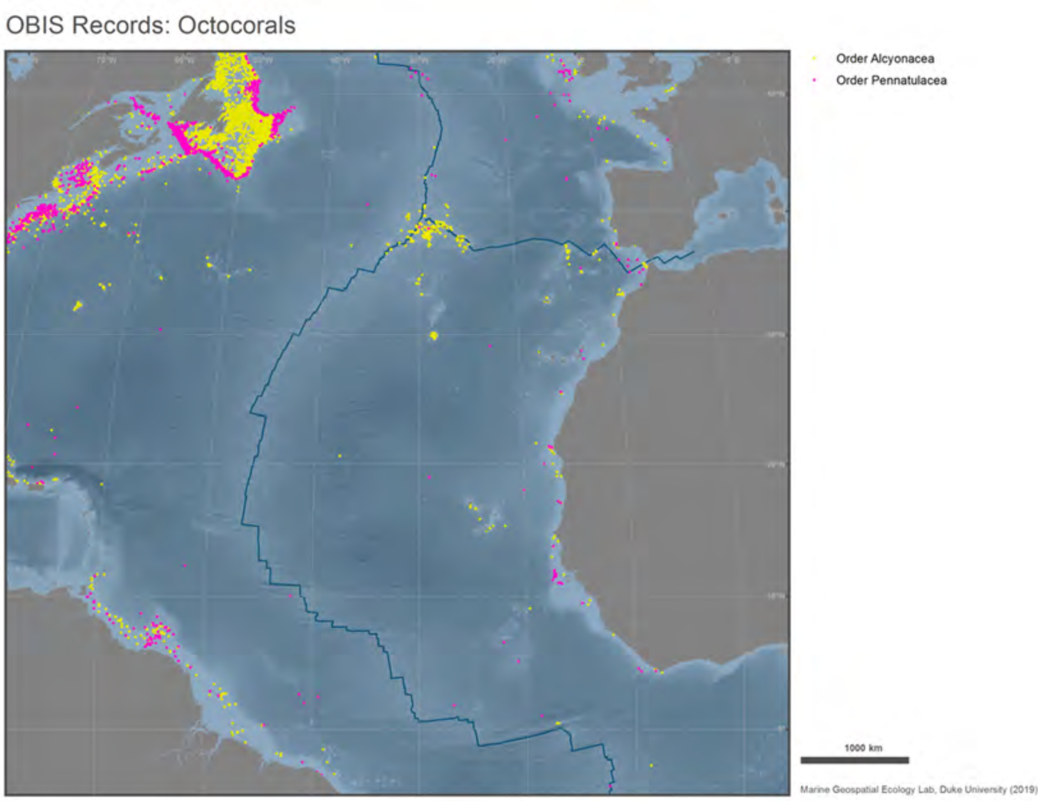

Figure 3.2-2 OBIS records of Octocorals

OBIS Records: Order Scleractinia

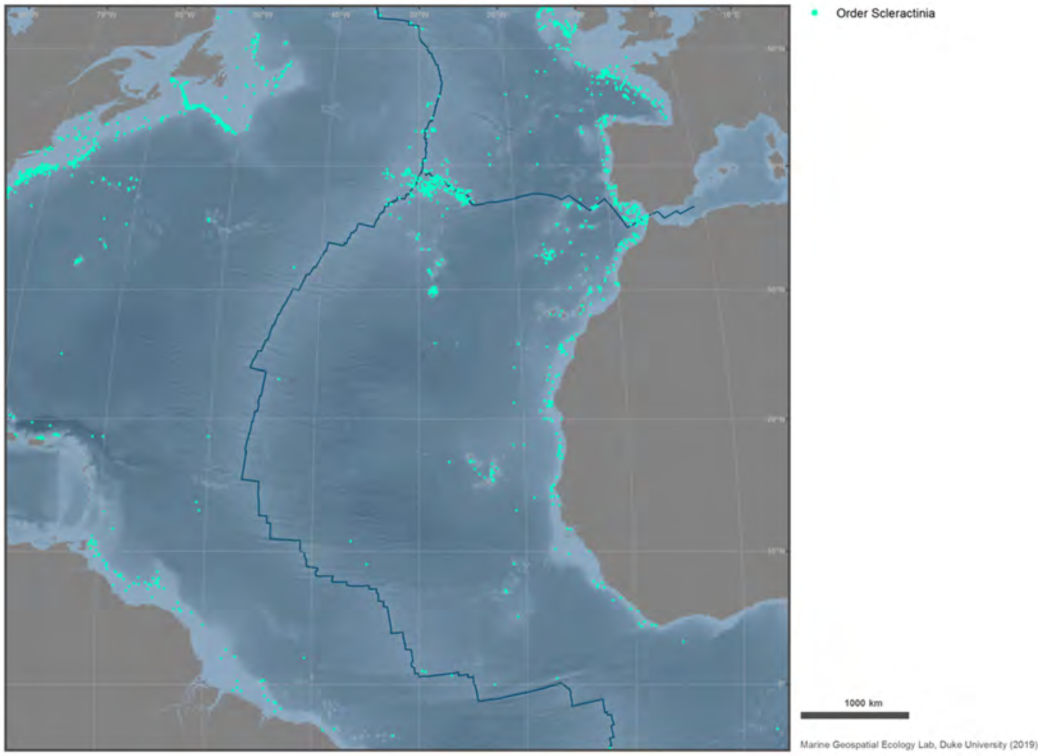

Figure 3.2-3 OBIS records of Scleractinia

OBIS Records: Sponges

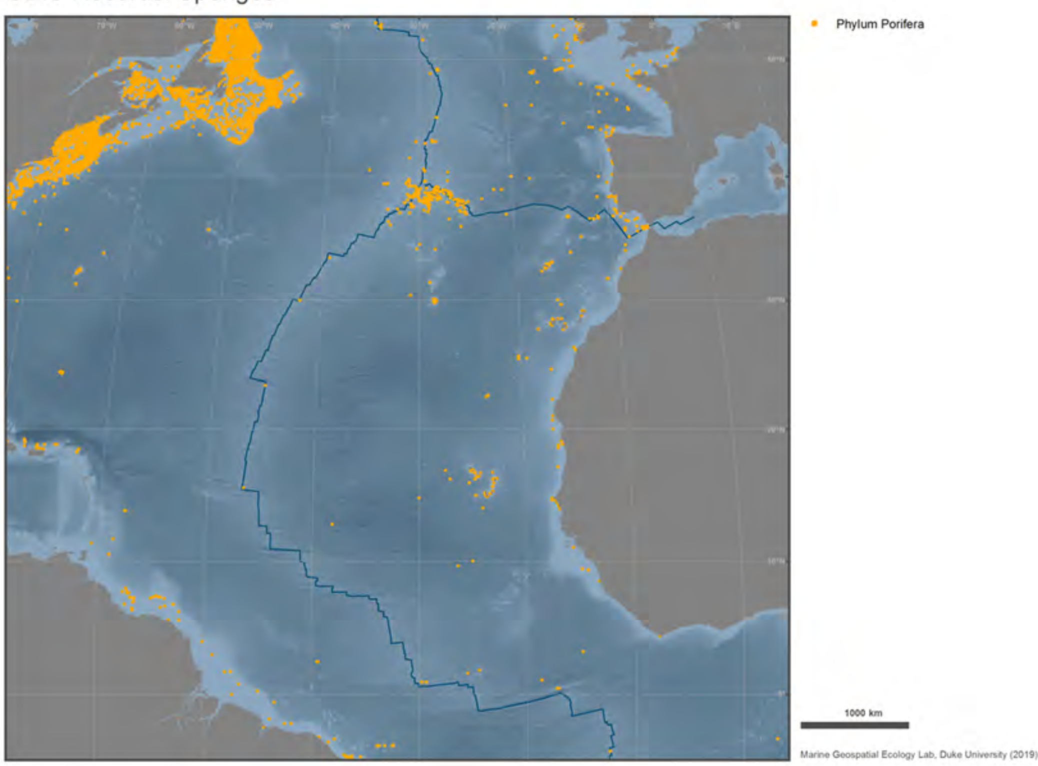

Figure 3.2-4 OBIS records of Sponges

3.3 Vulnerable Marine Ecosystem (VME) identification method

Abstract (Morato et al. 2018):
"In international fisheries management, scientific advice on the presence of "vulnerable marine ecosystems" (VMEs) per United Nations resolutions, has generally used qualitative assessments based on expert judgment of the occurrence of indicator taxa such as cold-water corals and sponges. Use of expert judgment alone can be criticized for inconsistency and sometimes a lack of transparency; therefore, development of robust and repeatable numeric methods to detect the presence of VMEs would be advantageous. Here, we present a multi-criteria assessment (MCA) method to evaluate how likely a given area of seafloor represents a VME. The MCA is a taxa-dependent spatial method that accounts for both the quantity and data quality available. This was applied to a database of records of VMEs built, held and compiled by the International Council for the Exploration of the Sea (ICES). A VME index was generated which ranged from 1.51 to 4.52, with 5.0 being reserved for confirmed VME habitats. An index of confidence was also computed that ranged from 0.0 to 0.75, with 1 being reserved for those confirmed VME habitats. Overall the MCA captured the important elements of the ICES VME database and provided a simplified, spatially aggregated, and weighted estimate of how likely a given area is to contain VMEs. The associated estimate of confidence gave an indication of how uncertain that assessment was for the same given area. This methodology provides a more systematic and standardized approach for assessing the likelihood of presence of VMEs in the North-East Atlantic."

Reference:
Morato, T., Pham, C. K., Pinto, C., Golding, N., Ardron, J. A., Muñoz, P. D., & Neat, F. (2018). A multi criteria assessment method for identifying Vulnerable Marine Ecosystems in the North-East Atlantic. Frontiers in Marine Science, 5(DEC). doi: 10.3389/fmars.2018.00460

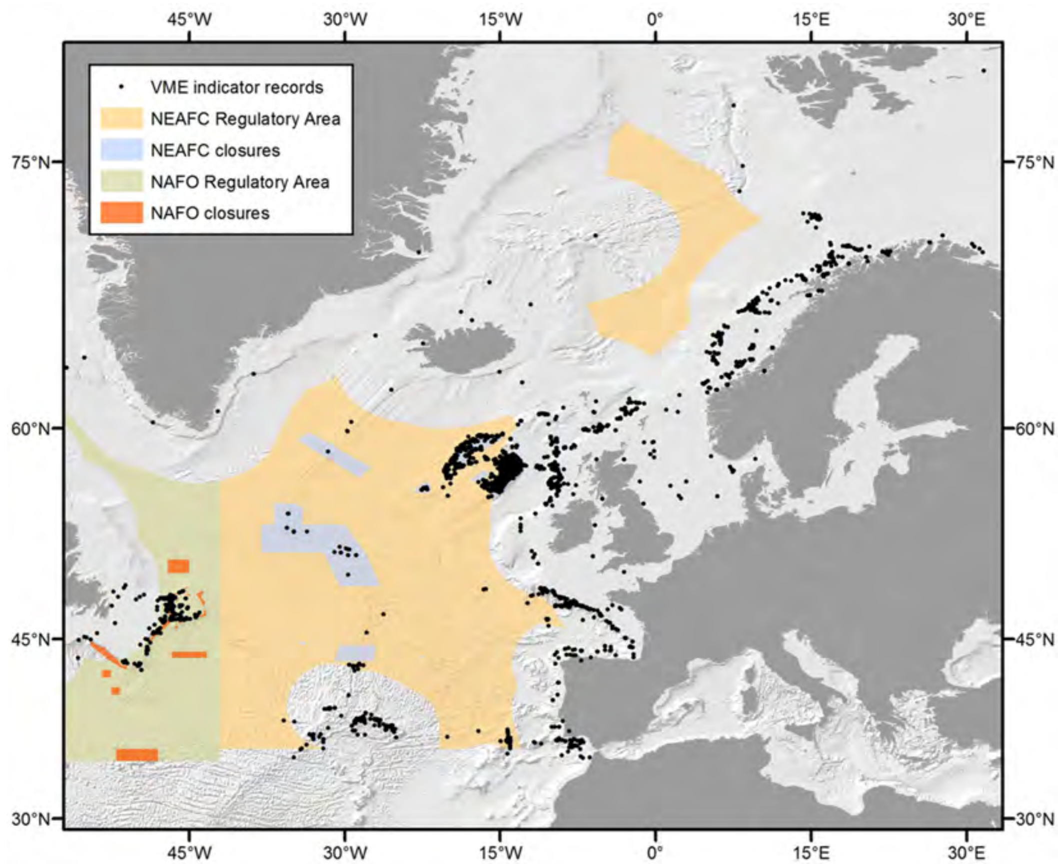

Figure 3.3-1 Figure 1 from Morato et al. (2018)

Original Caption: Figure 1. The distribution of VME indicator records throughout the North Atlantic contained within the ICES VME database (ICES, 2016a)

3.4 Global Distribution of Deep-Water Antipatharia Habitat

Abstract (Yesson et al. 2017)
"Antipatharia are a diverse group of corals with many species found in deep water. Many Antipatharia are habitat for associates, have extreme longevity and some species can occur beyond 8500 m depth. As they are major constituents of 'coral gardens', which are Vulnerable Marine Ecosystems (VMEs), knowledge of their distribution and environmental requirements is an important pre-requisite for informed conservation planning particularly where the expense and difficulty of deep-sea sampling prohibits comprehensive surveys.

This study uses a global database of Antipatharia distribution data to perform habitat suitability modelling using the Maxent methodology to estimate the global extent of black coral habitat suitability. The model of habitat suitability is driven by temperature but there is notable influence from other variables of topography, surface productivity and oxygen levels.

This model can be used to predict areas of suitable habitat, which can be useful for conservation planning. The global distribution of Antipatharia habitat suitability shows a marked contrast with the distribution of specimen observations, indicating that many potentially suitable areas have not been sampled, and that sampling effort has been disproportionate to shallow, accessible areas inside marine protected areas (MPAs). Although 25% of Antipatharia observations are located in MPAs, only 7-8% of predicted suitable habitat is protected, which is short of the Convention on Biological Diversity target to protect 10% of ocean habitats by 2020."

Reference:
Yesson, C., F. Bedford, A. Rogers, and M. Taylor. 2017. "The Global Distribution of Deep-Water Antipatharia Habitat." *Deep Sea Research Part II: Topical Studies in Oceanography*, Towards ecosystem based management and monitoring of the deep Mediterranean, North-East Atlantic and Beyond, 145 (November): 79–86. https://doi.org/10.1016/j.dsr2.2015.12.004.

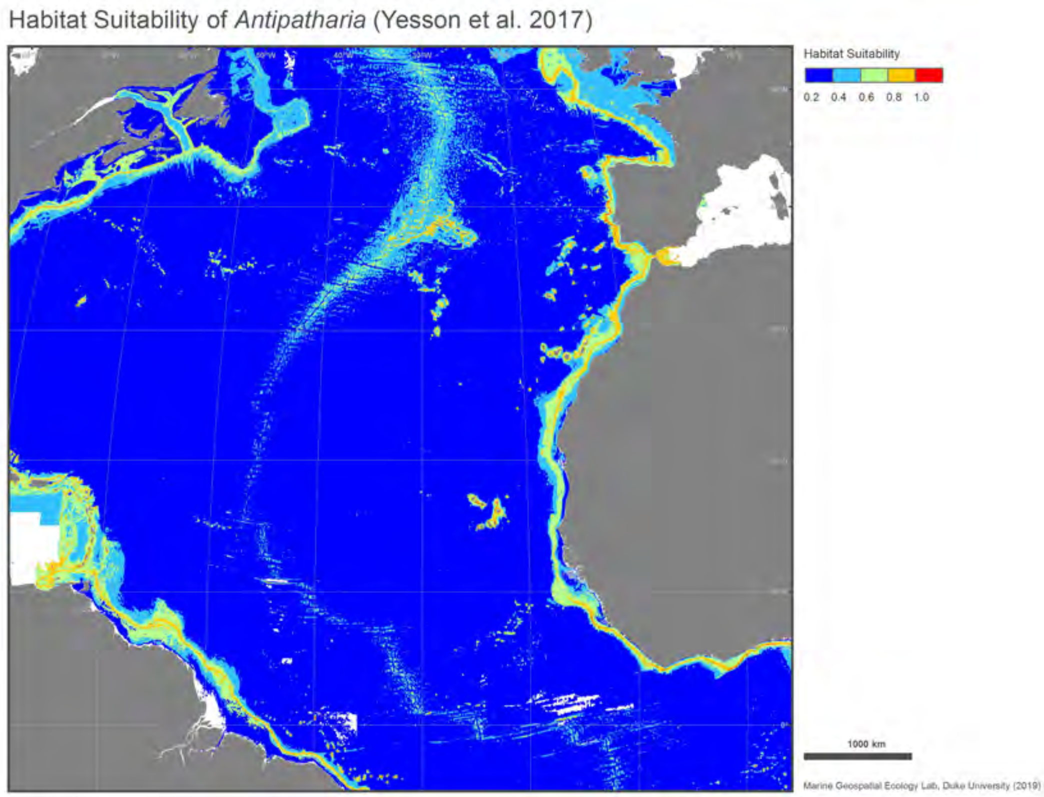

Figure 3.4-1 Deep-Water Antipatharia Habitat

3.5 Predictions of Habitat Suitability for Cold-Water Octocorals

Abstract (Yesson et al. 2012):
"Three-quarters of Octocorallia species are found in deep waters. These cold- water octocoral colonies can form a major constituent of structurally complex habitats. The global distribution and the habitat requirements of deep-sea octocorals are poorly understood given the expense and difficulties of sampling at depth. Habitat suitability models are useful tools to extrapolate distributions and provide an understanding of ecological requirements. Here, we present global habitat suitability models and distribution maps for seven suborders of Octocorallia: Alcyoniina, Calcaxonia, Holaxonia, Scleraxonia, Sessiliflorae, Stolonifera and Subselliflorae."

Reference:
Yesson C, Taylor ML, Tittensor DP, Davies AJ, Guinotte J, Baco A, Black J, Hall-Spencer JM, Rogers AD (2012) Global habitat suitability of cold-water octocorals. Journal of Biogeography 39:1278–1292. Doi: 10.1111/j.1365-2699.2011.02681.x

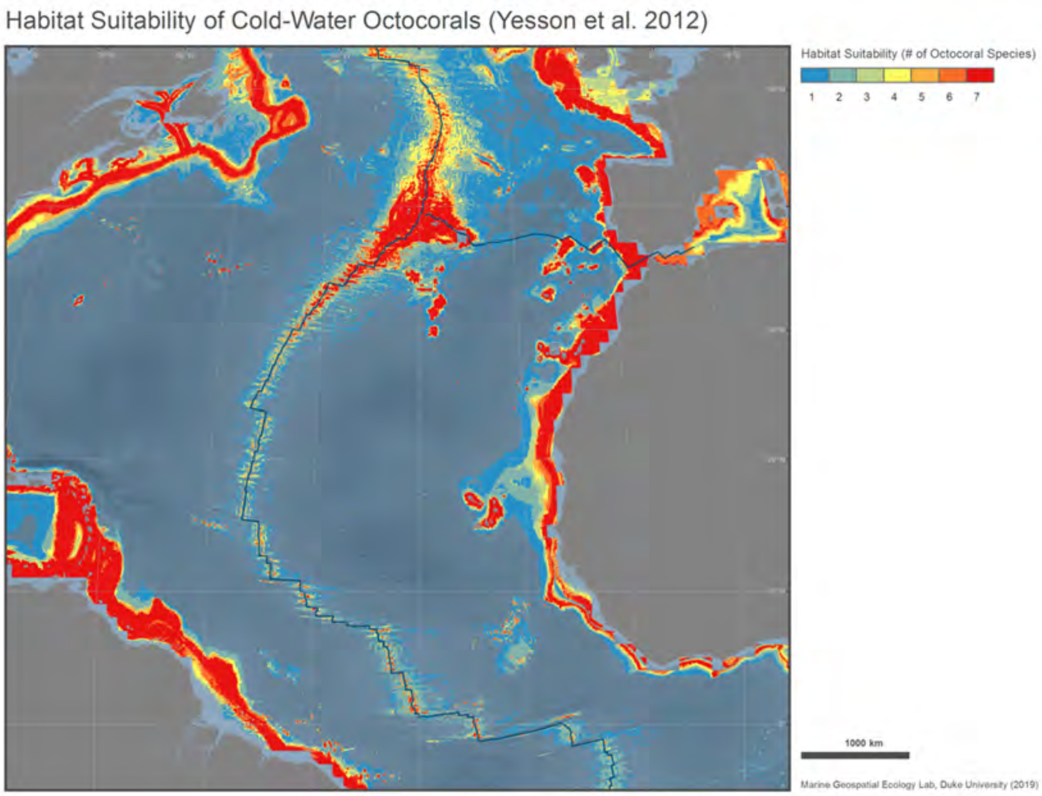

Figure 3.5-1 Deep-Sea Octocoral habitat suitability – consensus

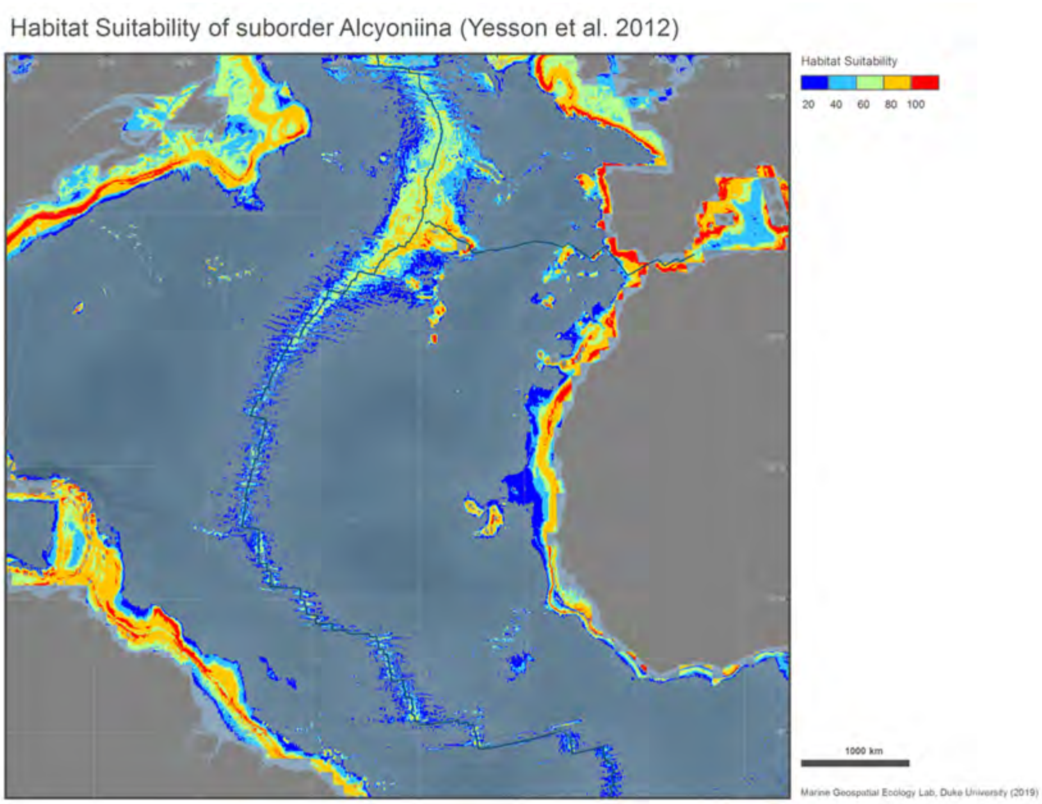

Figure 3.5-2 Deep-Sea Octocoral habitat suitability - Alcyoniina

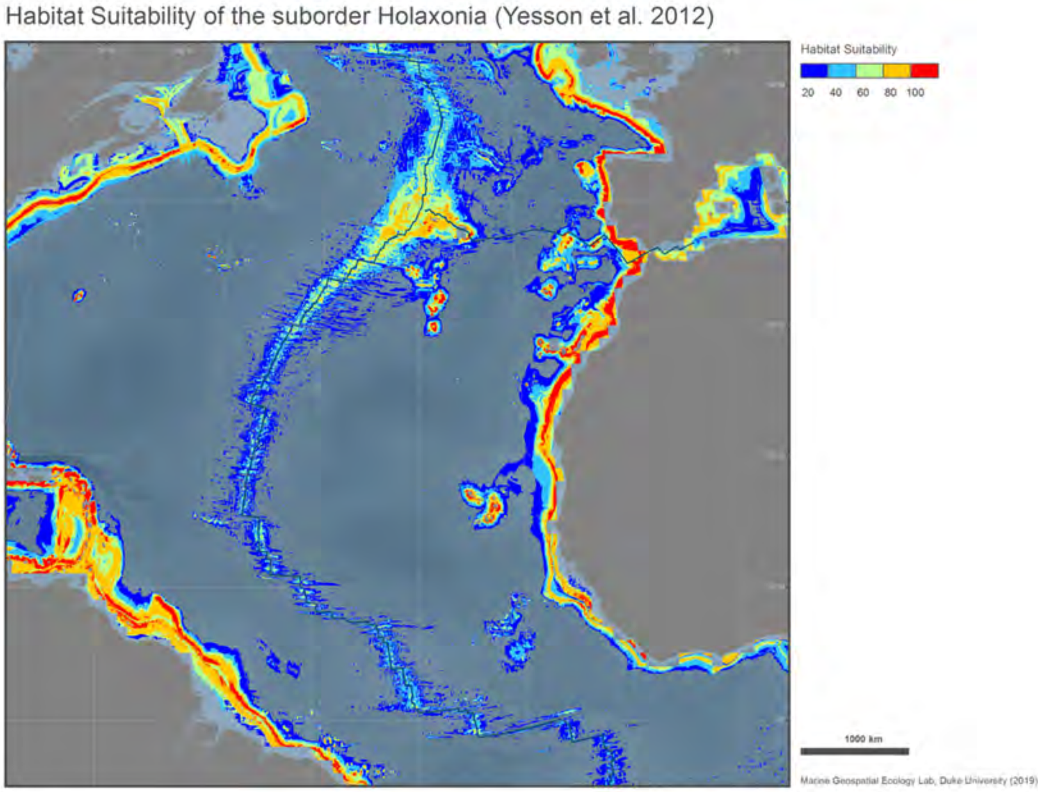

Figure 3.5-3 Deep-Sea Octocoral habitat suitability - Holaxonia

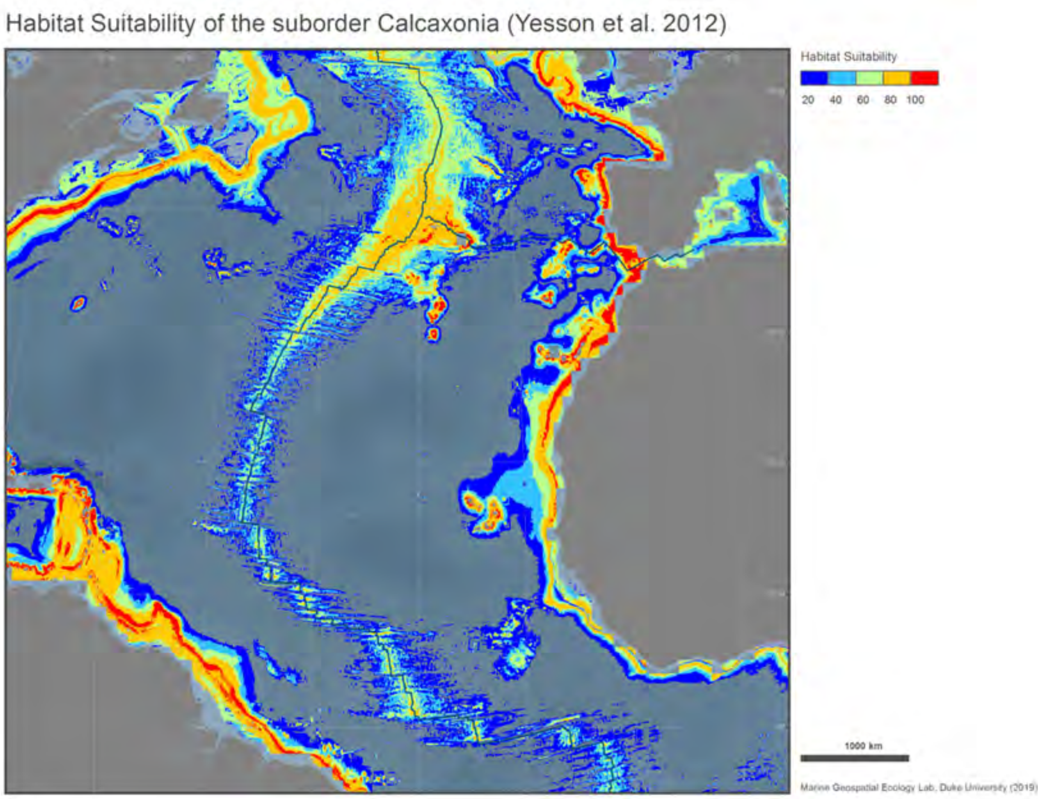

Figure 3.5-4 Deep-Sea Octocoral habitat suitability - Calcaxonia

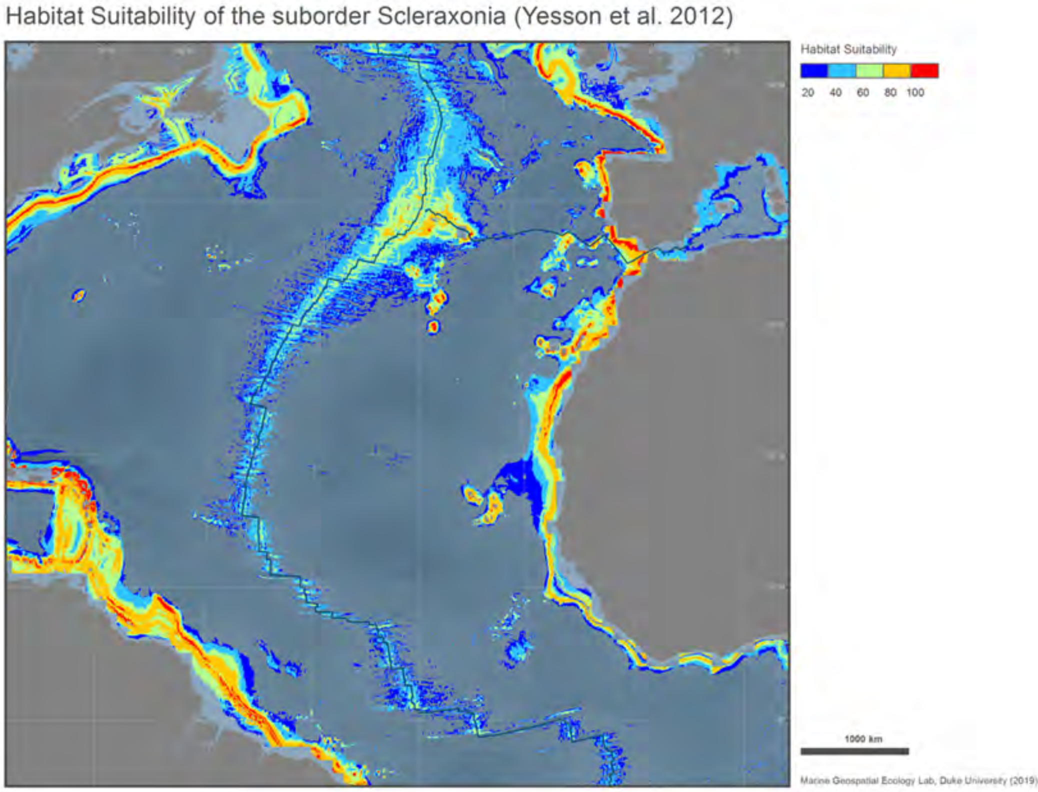

Figure 3.5-5 Deep-Sea Octocoral habitat suitability - Scleraxonia

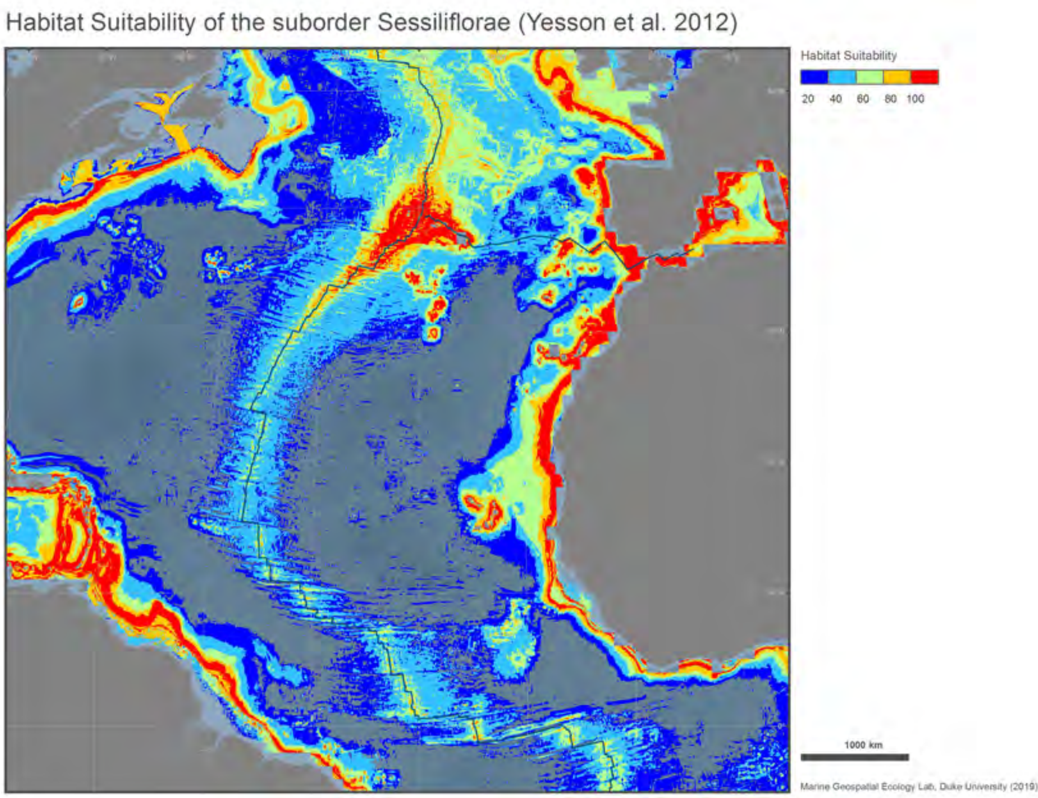

Figure 3.5-6 Deep-Sea Octocoral habitat suitability - Sessiliflorae

Habitat Suitability of the suborder Stolonifera (Yesson et al. 2012)

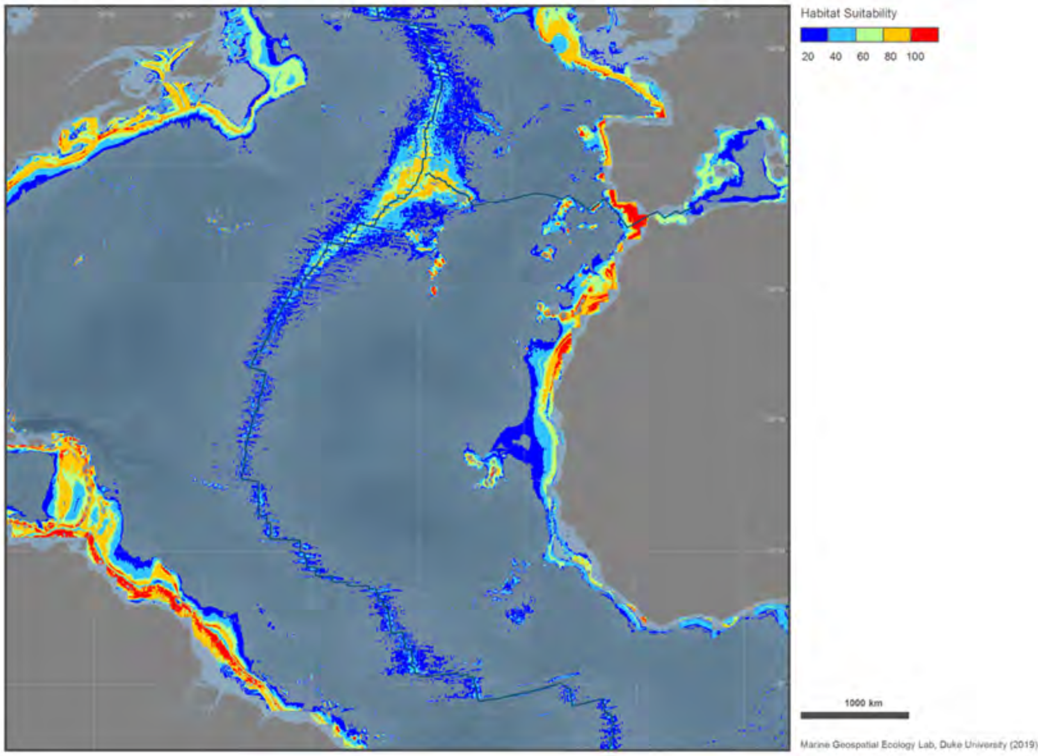

Figure 3.5-7 Deep-Sea Octocoral habitat suitability - Stolonifera

Habitat Suitability of the suborder Subselliflorae (Yesson et al. 2012)

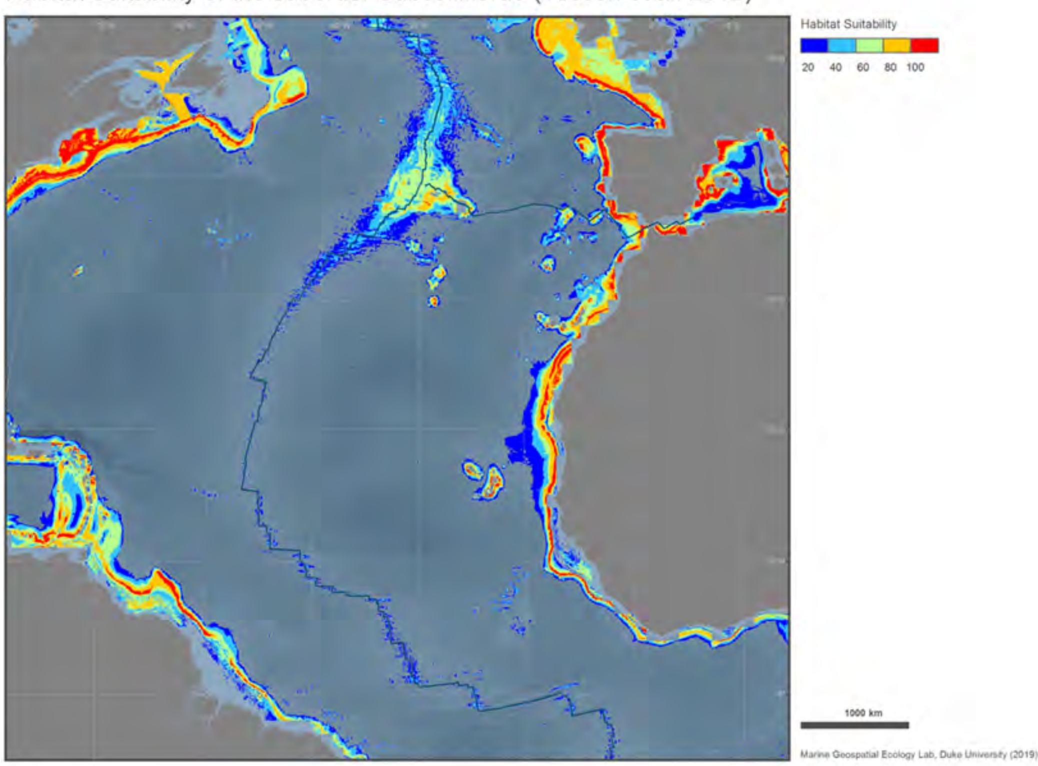

Figure 3.5-8 Deep-Sea Octocoral habitat suitability - Subselliflorae

3.6 Predictions of Habitat Suitability for Framework-Forming Scleractinian Corals

Abstract (Davies & Guinotte 2011):
"Predictive habitat models are increasingly being used by conservationists, researchers and governmental bodies to identify vulnerable ecosystems and species' distributions in areas that have not been sampled. However, in the deep sea, several limitations have restricted the widespread utilisation of this approach. These range from issues with the accuracy of species presences, the lack of reliable absence data and the limited spatial resolution of environmental factors known or thought to control deep-sea species' distributions. To address these problems, global habitat suitability models have been generated for five species of framework-forming scleractinian corals by taking the best available data and using a novel approach to generate high resolution maps of seafloor conditions. High-resolution global bathymetry was used to resample gridded data from sources such as World Ocean Atlas to produce continuous 30-arc second (1 km^2) global grids for environmental, chemical and physical data of the world's oceans. The increased area and resolution of the environmental variables resulted in a greater number of coral presence records being incorporated into habitat models and higher accuracy of model predictions. The most important factors in determining cold-water coral habitat suitability were depth, temperature, aragonite saturation state and salinity. Model outputs indicated the majority of suitable coral habitat is likely to occur on the continental shelves and slopes of the Atlantic, South Pacific and Indian Oceans. The North Pacific has very little suitable scleractinian coral habitat. Numerous small scale features (i.e., seamounts), which have not been sampled or identified as having a high probability of supporting cold-water coral habitat were identified in all ocean basins. Field validation of newly identified areas is needed to determine the accuracy of model results, assess the utility of modeling efforts to identify vulnerable marine ecosystems for inclusion in future marine protected areas and reduce coral bycatch by commercial fisheries."

Reference:
Davies AJ, Guinotte JM (2011) Global Habitat Suitability for Framework-Forming Cold-Water Corals. PLoS ONE 6(4): e18483. doi:10.1371/journal.pone.0018483

Habitat Suitability of Scleractinia (Davies and Guinotte 2011)

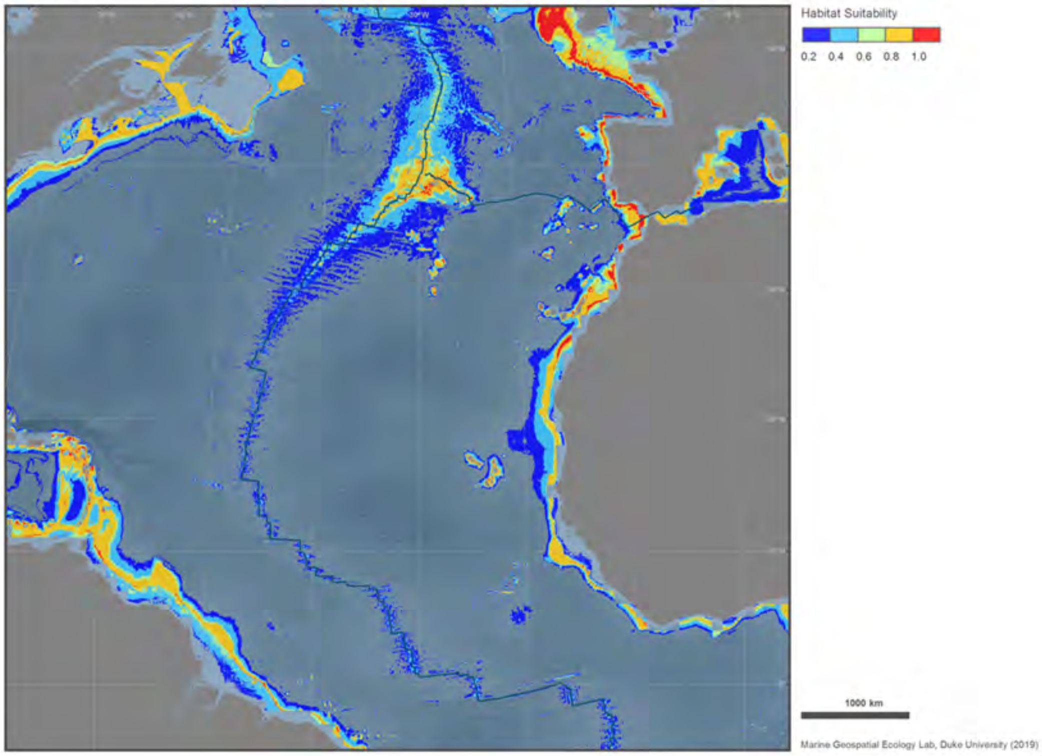

Figure 3.6-1 Deep-Sea Scleractinia habitat suitability – all five framework forming species

Habitat Suitability of Lophelia pertusa (Davies & Guinotte 2011)

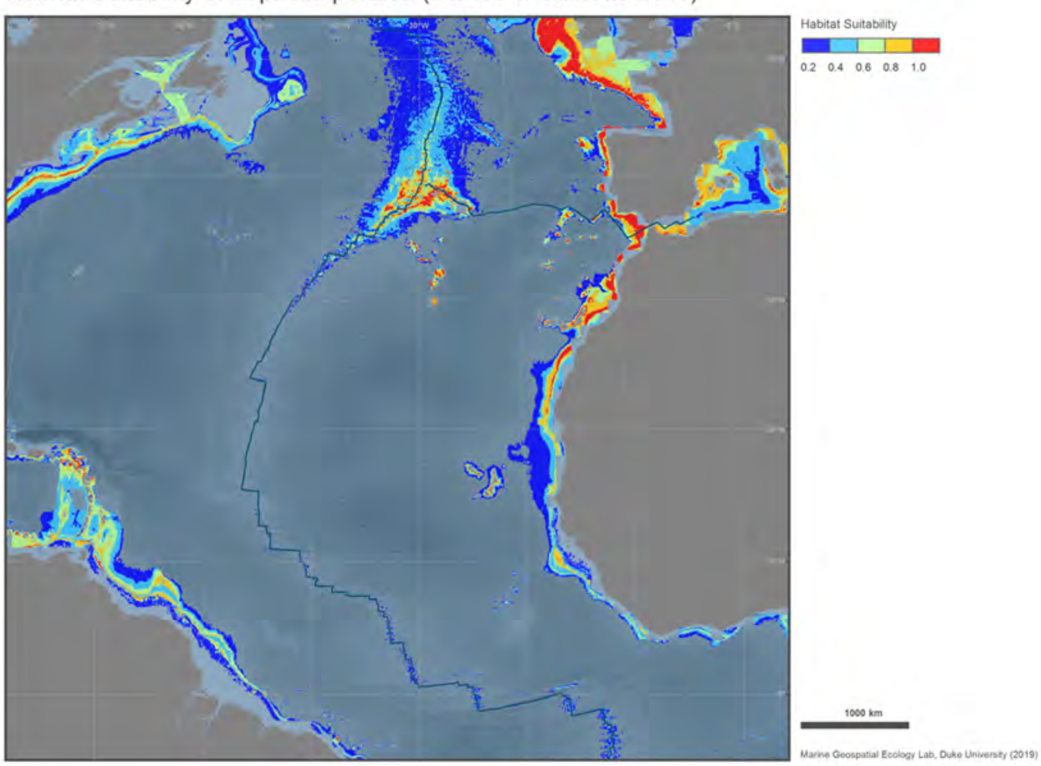

Figure 3.6-2 Deep-Sea Scleractinia habitat suitability – *Lophelia pertusa*

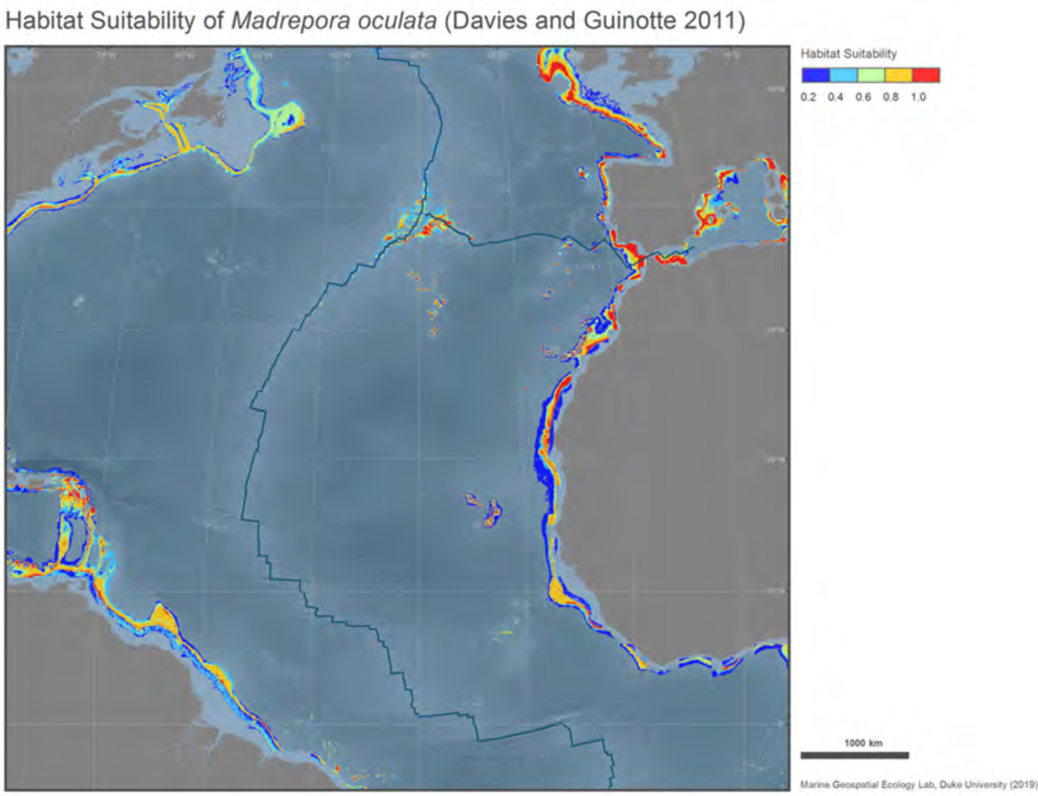

Figure 3.6-3 Deep-Sea Scleractinia habitat suitability – *Madrepora oculata*

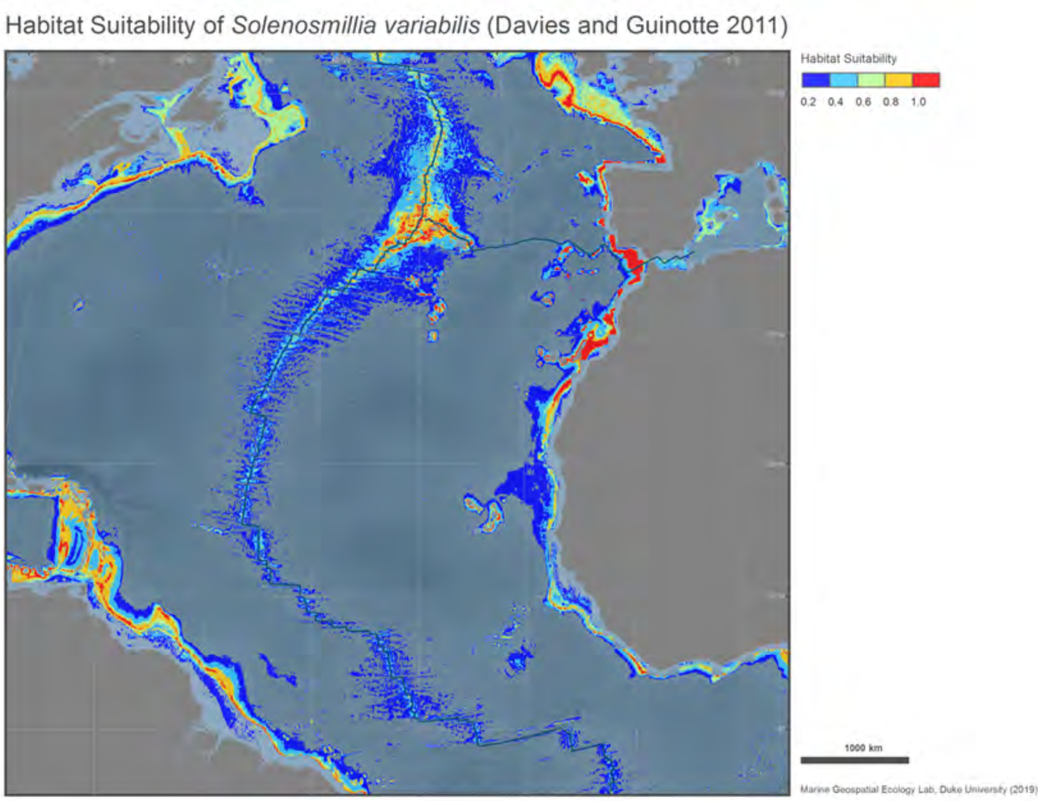

Figure 3.6-4 Deep-Sea Scleractinia habitat suitability – *Solenosmilia variabilis*

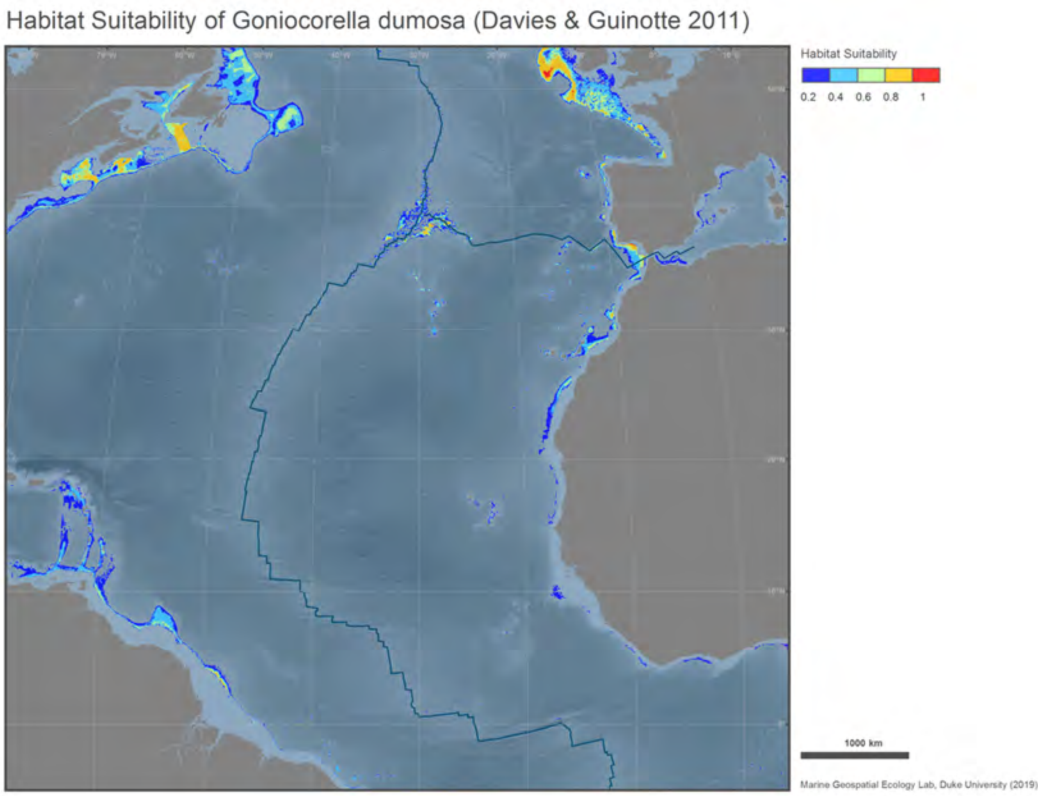

Figure 3.6-5 Deep-Sea Scleractinia habitat suitability – *Goniocorella dumosa*

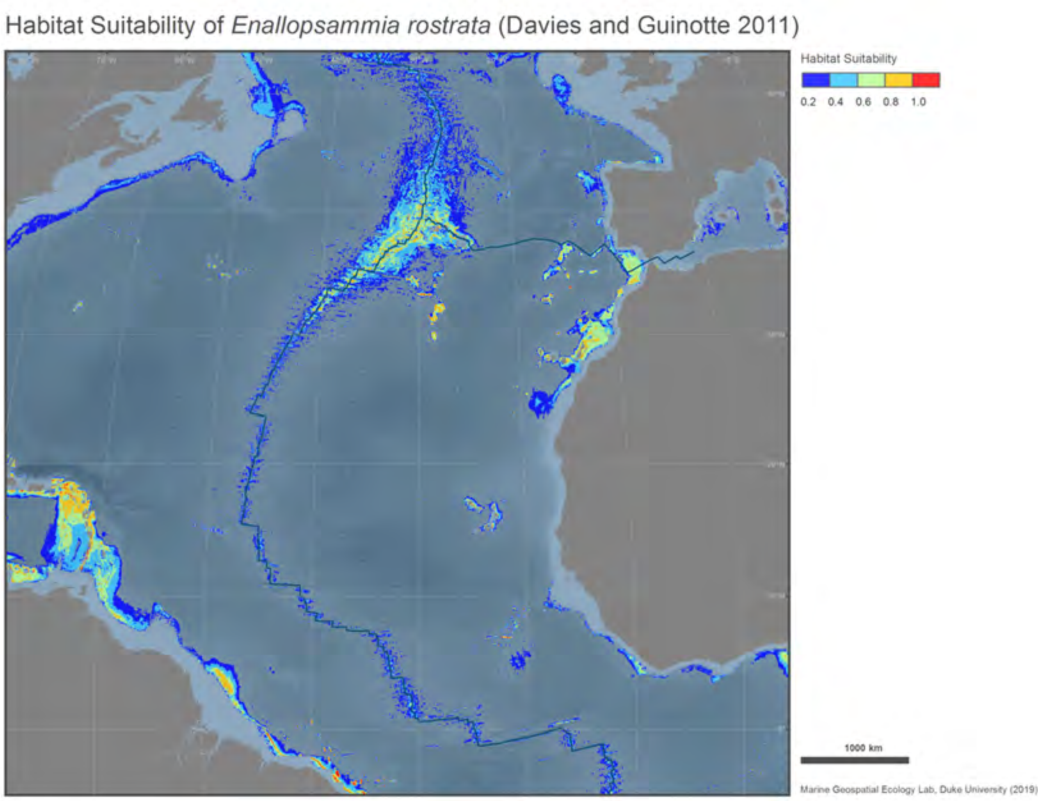

Figure 3.6-6 Deep-Sea Scleractinia habitat suitability – *Enallopsammia rostrata*

3.7 International Seabed Authority Deep Data Portal

“The newly developed “ISA Deep Seabed and Ocean Database” (*DeepData*) was launched in July 2019 at the Authority's 25th Session. This database has been designed to serve as a spatial, internet-based data management system. Its main function is to host all deep-seabed activities related data and in particular, data collected by the contractors on their exploration activities as well as any other relevant environmental and resources related data for the Area.

DeepData contains information on mineral resource assessment (geological data) and environmental baseline/assessment data. However, only the environmental data are accessible to the public. This include biological, physical and geochemical parameters of the marine ecosystems from the seafloor to the ocean surface.

The Geographical Information System (GIS) is part of *DeepData* functionalities. As such, it allows visualization of contract areas, reserved areas and designated areas of particular environmental interest (APEIs). GIS information accessible through *DeepData* also include sampling locations containing biological, physical and/or geochemical parameters of the seabed sediments and water column.”

Deep Data Portal: https://data.isa.org.jm/isa/map/

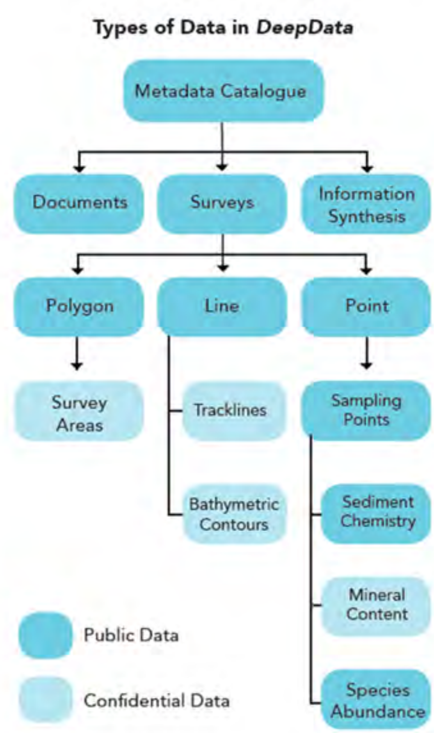

Figure 3.7-1 Chart of data types in Deep Data

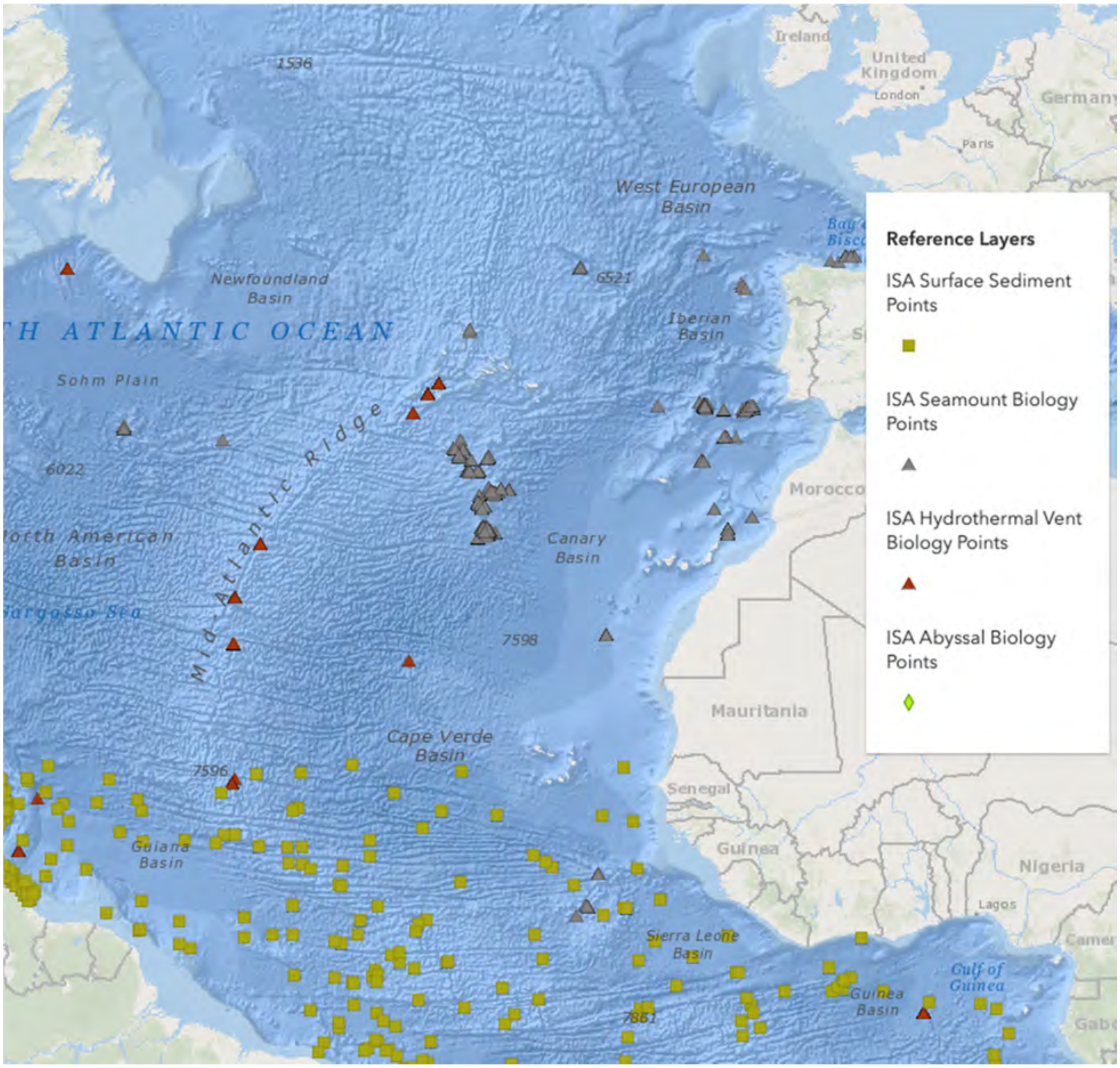

Figure 3.7-2 ISA Deep Data portal sampling points

3.8 Bathyal benthic megafauna from the Mid-Atlantic Ridge in the region of the Charlie-Gibbs fracture zone

Abstract (Alt et al. 2019):
“Mid-ocean ridges are important geological features that cover around 33% of the global ocean floor, increase environmental heterogeneity on a regional scale and influence benthic community ecology. Benthic communities at the Mid-Atlantic Ridge (MAR) were studied at four contrasting sites, located east and west of the ridge, which were further separated into northern (54°N) and southern (48°N) sites by the Charlie-Gibbs Fracture Zone (CGFZ) and the Sub-Polar Front (SPF). The MAR in the CCFZ region area had flat areas surrounded by gentle slopes between rocky cliffs. A total of 32 remotely operated vehicle video transects (32,000 m2 of seafloor) were surveyed on the flat areas and sedimented slopes (10°). In total, 154 distinct taxonomic units were identified (from 9 phyla) across all sites. The sediments of the flat and sloping sites were generally similar, but differences were seen in the community composition and faunal abundance (~ 4 times higher in the flat sites, except at the northwestern site). Significant differences in abundance were observed between sites (highest in the northern sites). The two northern sites had distinct community compositions, while the two southern sites were similar. This suggests that the MAR acts as a stronger barrier between communities north of the CGFZ than it does to the south. There was high heterogeneity between transects and it was not possible to identify general drivers for the benthic megafauna at the MAR. Our results emphasize the limited knowledge of this vast system with its unique benthic megafauna”

Reference:
Alt, C. H., Kremenetskaia, A., Gebruk, A. V., Gooday, A. J., & Jones, D. O. (2019). Bathyal benthic megafauna from the Mid-Atlantic Ridge in the region of the Charlie-Gibbs fracture zone based on remotely operated vehicle observations. Deep Sea Research Part I: Oceanographic Research Papers, 145, 1-12.doi: 10.1016/j.dsr.2018.12.006

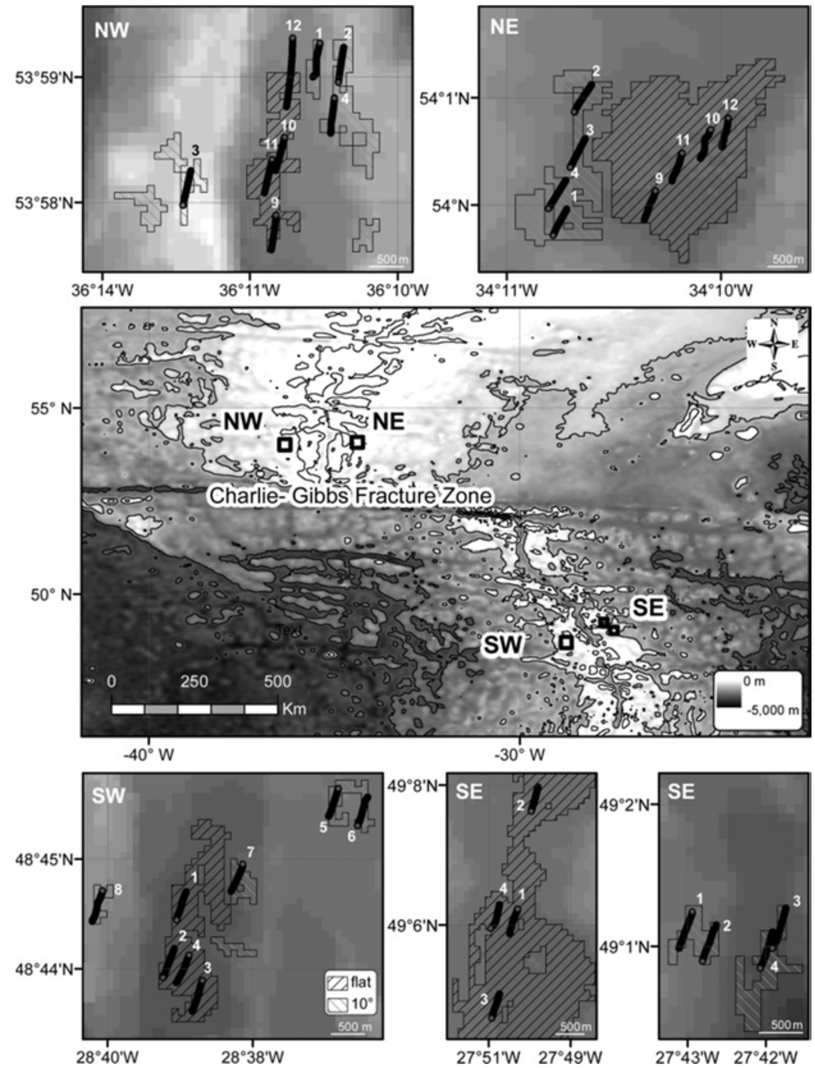

Figure 3.8-1 Figure 1 from Alt et al. (2019)

Original Caption: Fig. 1. Survey Map: The central map shows the general sample area around the Charlie-Gibbs Fracture Zone, highlighting the four sample sites and the bathymetry of the area. The individual sites are shown in their relative positions, indicating the habitat type and the individual transects that were analysed, together with the respective transect number.

3.9 New records of *Heteropathes Opresko*

Reference:
Molodtsova, T. N. (2017). New records of Heteropathes Opresko, 2011 (Anthozoa: Antipatharia) from the Mid-Atlantic Ridge. Marine Biodiversity, 47(1), 179-186. doi:10.1007/s12526-016-0460-y

3.10 Data on benthic and fish communities from the Mid-Atlantic Ridge

Reference:
Molodtsova, T. N., Galkin, S. V., Kobyliansky, S. G., Simakova, U. V., Vedenin, A. A., Dobretsova, I. G., & Gebruk, A. V. (2017). First data on benthic and fish communities from the Mid-Atlantic Ridge, 16° 40′− 17° 14′ N. Deep Sea Research Part II: Topical Studies in Oceanography, 137, 69-77. doi: 10.1016/j.dsr2.2016.10.006

3.11 Hyperspectral imaging in the Trans-Atlantic Geotraverse hydrothermal field

Abstract (Dumke et al. 2018):
“Underwater hyperspectral imaging is a relatively new method for characterizing seafloor composition. To date, it has been deployed from moving underwater vehicles, such as remotely operated vehicles and autonomous underwater vehicles. While moving vehicles allow relatively rapid surveying of several 10-1000 m2, they are subjected to short-term variations in vehicle attitude that often compromise image acquisition and quality. In this study, we tested a stationary platform that was landed on the seabed and used an underwater hyperspectral imager (UHI) on a vertical swinging bracket. The imaged seafloor areas have dimensions of 2.3 m × 1 m and are characterized by very stable UHI data of high spatial resolution. The study area was the Trans-Atlantic Geotraverse hydrothermal field at the Mid-Atlantic Ridge (26° N) in water depths of 3530-3660 m. UHI data were acquired at 12 stations on an active and an inactive hydrothermal sulfide mound. Based on supervised classification, 24 spectrally different seafloor materials were detected, including hydrothermal and non-hydrothermal materials, and benthic fauna. The results show that the UHI data are able to spectrally distinguish different types of surface materials and benthic fauna in hydrothermal areas, and may therefore represent a promising tool for high-resolution seafloor exploration in potential future deep-sea mining areas.”

Reference:
Dumke, I., Ludvigsen, M., Ellefmo, S. L., Søreide, F., Johnsen, G., & Murton, B. J. (2018). Underwater hyperspectral imaging using a stationary platform in the Trans-Atlantic

Geotraverse hydrothermal field. IEEE Transactions on Geoscience and Remote Sensing, 57(5), 2947-2962. Doi: 10.1109/TGRS.2018.2878923

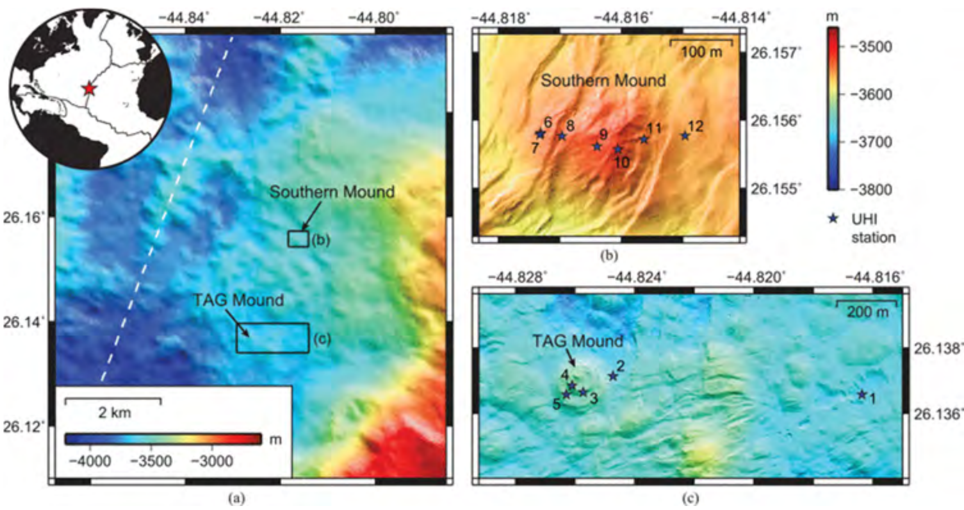

Figure 3.11-1 Figure 1 from Dumke et al. (2018)

Original Caption: Fig. 1 - Overview of the study area. (a) Ship-based bathymetry (30 m resolution) showing the TAG hydrothermal field (location marked in the inset) with the study areas TAG Mound and Southern Mound. The white dashed line indicates the ridge center. Plate boundaries are from [51]. (b) UHI stations at Southern Mound (second survey). (c) UHI stations at and around TAG Mound (first survey). The high-resolution bathymetry (0.5–2 m resolution) shown in (b) and (c) was collected by the AUV Abyss (GEOMAR) during RV Meteor cruise M127 in 2016 [54]. Note that the color scale in (a) differs from that in (b) and (c).

3.12 Gene flow between Atlantic and Pacific Ocean basins in three lineages of deep-sea clams

Reference:
LaBella, A. L., Van Dover, C. L., Jollivet, D., & Cunningham, C. W. (2017). Gene flow between Atlantic and Pacific Ocean basins in three lineages of deep-sea clams (Bivalvia: Vesicomyidae: Pliocardiinae) and subsequent limited gene flow within the Atlantic. Deep Sea Research Part II: Topical Studies in Oceanography, 137, 307-317. Doi: 10.1016/j.dsr2.2016.08.013

3.13 Sensitivity of marine protected area network connectivity to atmospheric variability

Abstract (Fox et al. 2016):
“International efforts are underway to establish well-connected systems of marine protected areas (MPAs) covering at least 10% of the ocean by 2020. But the nature and dynamics of ocean ecosystem connectivity are poorly understood, with unresolved effects of climate variability. We used 40-year runs of a particle tracking model to examine the sensitivity of an MPA network for habitat-forming cold-water corals in the northeast Atlantic to changes in larval dispersal driven by atmospheric cycles and larval behaviour. Trajectories of Lophelia pertusa larvae were strongly correlated to the North Atlantic Oscillation (NAO), the dominant pattern of interannual atmospheric circulation variability over the northeast Atlantic. Variability in trajectories significantly altered network connectivity and source–sink dynamics, with positive phase NAO conditions producing a well-connected but asymmetrical network connected from west to east. Negative phase NAO produced reduced connectivity, but notably some larvae tracked westward-flowing currents towards coral populations on the mid-Atlantic ridge. Graph theoretical metrics demonstrate critical roles played by seamounts and offshore banks in larval supply and maintaining connectivity across the network. Larval longevity and behaviour mediated dispersal and connectivity, with shorter lived and passive larvae associated with reduced connectivity. We conclude that the existing MPA network is vulnerable to atmospheric-driven changes in ocean circulation.”

Reference:

Fox, A. D., Henry, L. A., Corne, D. W., & Roberts, J. M. (2016). Sensitivity of marine protected area network connectivity to atmospheric variability. Royal Society open science, 3(11), 160494.doi: 10.1098/rsos.160494

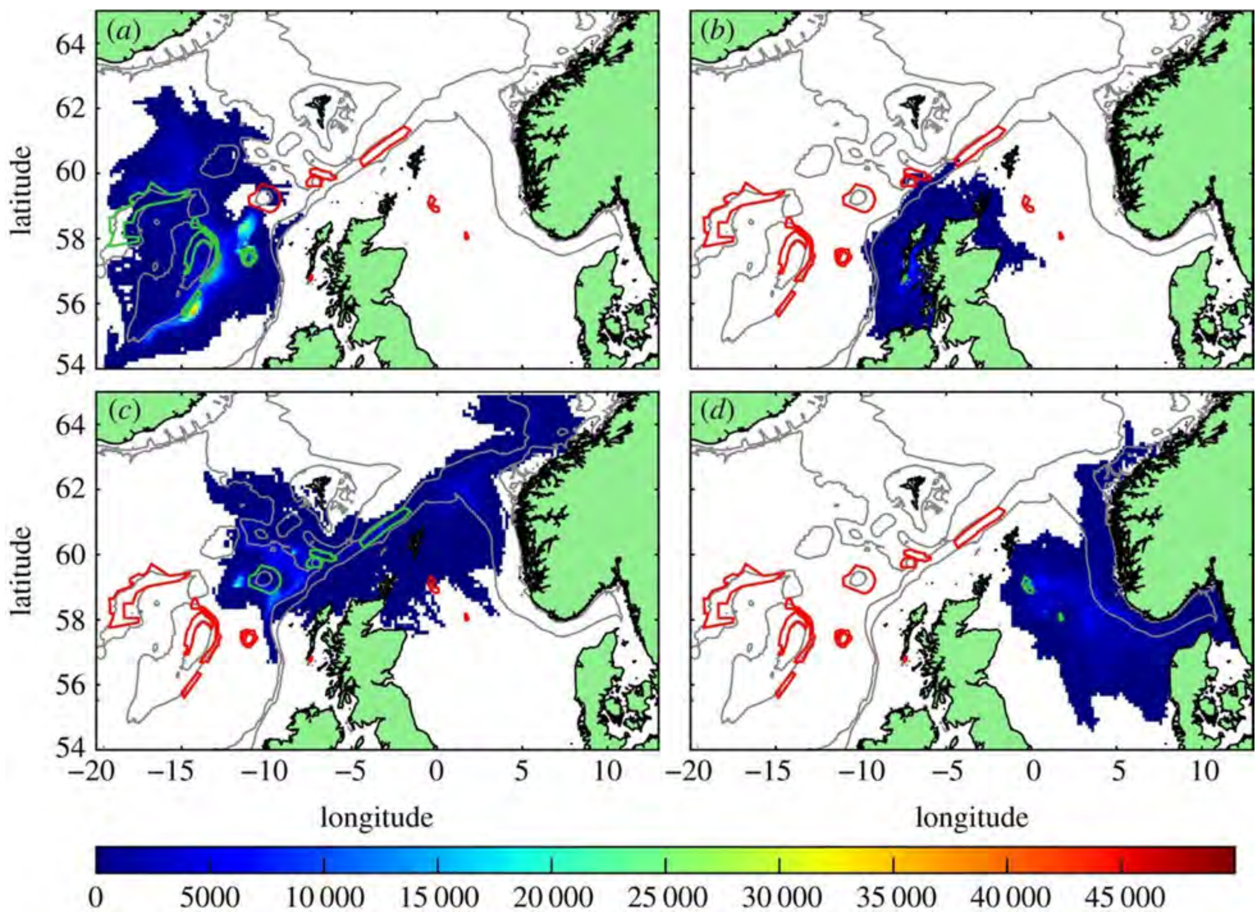

Figure 3.13-1 Figure 3 from Fox et al. (2016)

Original Caption: Figure 3. Standard run. Distribution of competent larvae, ready to settle, plotted by source MPAs (shown in green outline, other MPAs red outline). Larval source: (a) western MPAs, (b) East Mingulay, (c) northern MPAs and (d) North Sea sites. Colour scale is the number of larval days recorded in the model grid square. Each model day the positions of the larvae are examined and each competent larva in a grid-box counts 1. A figure of 20 000 could, for example, be 20 000 larvae in the grid square for one day each, or 400 larvae for 50 days each, etc.

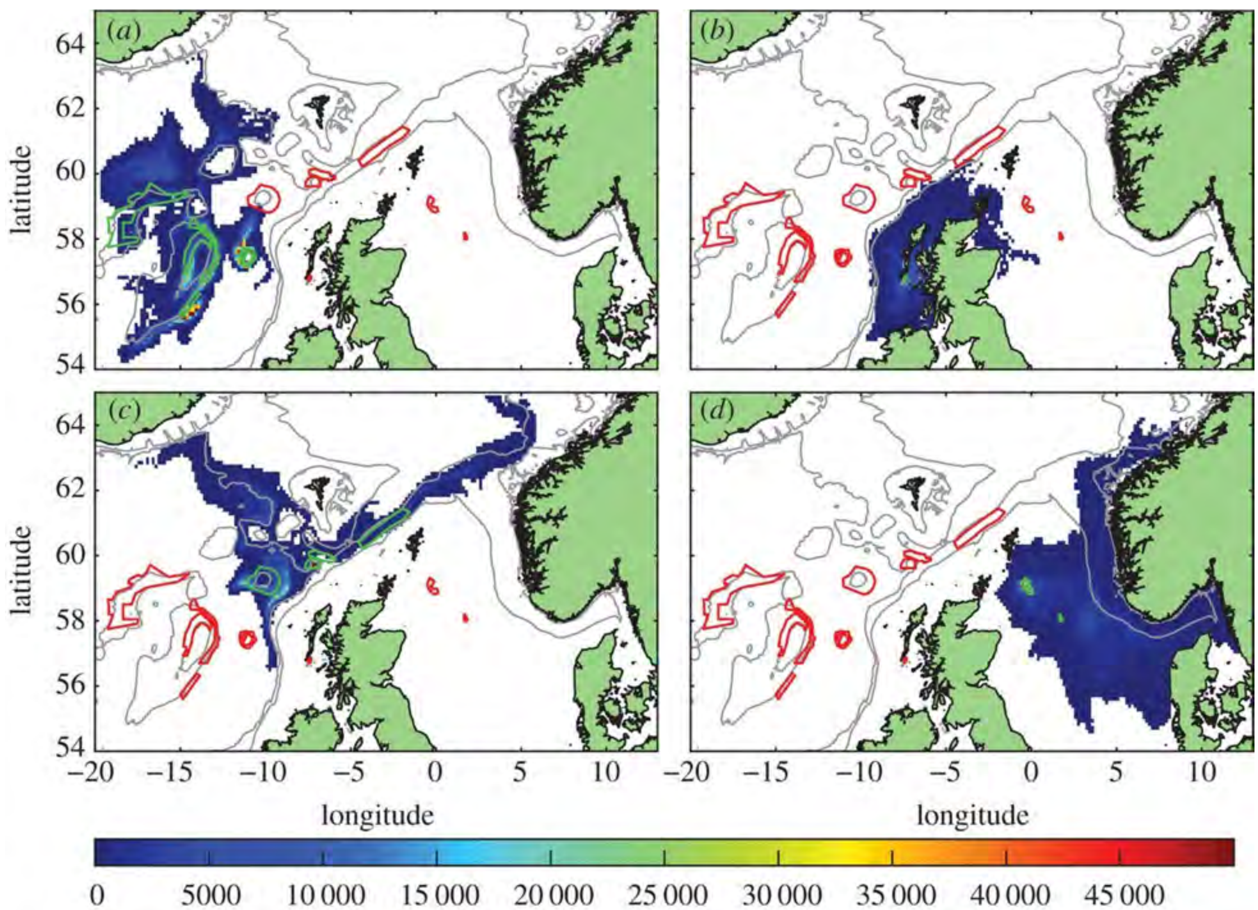

Figure 3.13-2 Figure 4 from Fox et al. (2016)

Original Caption: Figure 4. Distribution of competent larvae, ready to settle, in the passive run. Plotted by source MPAs (shown in green outline, other MPAs red outline). Larval source: (a) western MPAs, (b) East Mingulay, (c) northern MPAs and (d) North Sea MPAs. Colour scale is the number of larval days recorded in the model grid square.

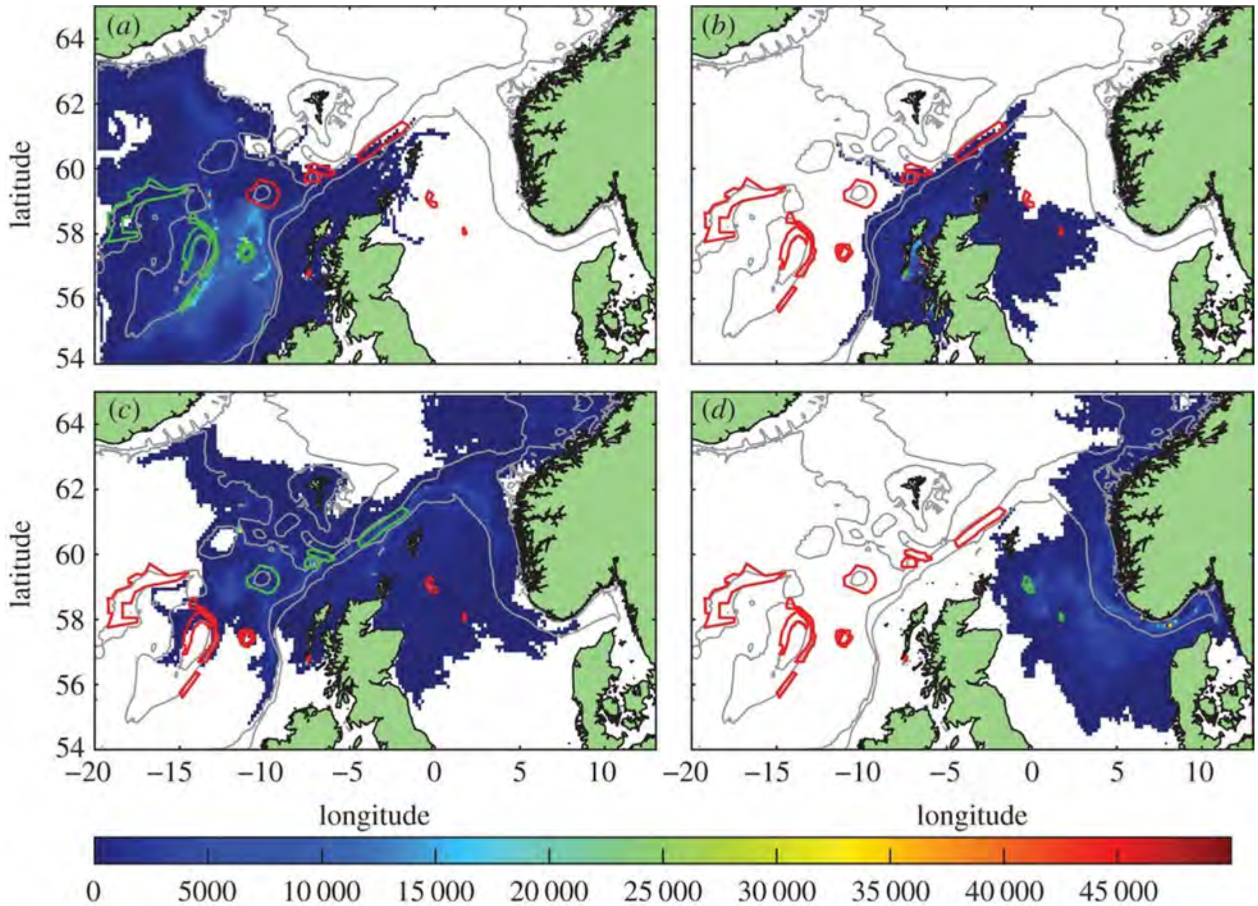

Figure 3.13-3 Figure 5 from Fox et al. (2016)

Original Caption: Figure 5. Distribution of competent larvae, ready to settle, in the long-lived run. Plotted by source MPAs (shown in green outline, other MPAs red outline). Larval source: (a) western MPAs, (b) East Mingulay, (c) northern MPAs and (d) North Sea MPAs. Colour scale is the number of larval days recorded in the model grid square.

3.14 Dispersion of deep-sea hydrothermal vent effluents and larvae by submesoscale and tidal currents

Reference:

Vic, C., Gula, J., Roullet, G., & Pradillon, F. (2018). Dispersion of deep-sea hydrothermal vent effluents and larvae by submesoscale and tidal currents. Deep Sea Research Part I: Oceanographic Research Papers, 133, 1-18. doi: 10.1016/j.dsr.2018.01.001

3.15 Genetic Connectivity of vent mussel *Bathymodiolus spp.*. Evidence of stepping stone habitat along the Mid Atlantic Ridge

Reference:

Breusing, C., Biastoch, A., Drews, A., Metaxas, A., Jollivet, D., Vrijenhoek, R. C., ... & Dubilier, N. (2016). Biophysical and population genetic models predict the presence of “phantom” stepping stones connecting Mid-Atlantic Ridge vent ecosystems. Current Biology, 26(17), 2257-2267.doi: 10.1016/j.cub.2016.06.062

3.16 Limpets population connectivity in the Mid Atlantic Ridge

Reference:

Yahagi, T., Fukumori, H., Warén, A., & Kano, Y. (2017). Population connectivity of hydrothermal-vent limpets along the northern Mid-Atlantic Ridge (Gastropoda: Neritimorpha: Phenacolepadidae). Journal of the Marine Biological Association of the United Kingdom, 1-7. doi: 10.1017/S0025315417001898

3.17 Predicted faunal assemblage with 3D high resolution data

Abstract (Gerdes et al. 2019):

“Active hydrothermal vent fields are complex, small-scale habitats hosting endemic fauna that changes at scales of centimeters, influenced by topographical variables. In previous studies, it has been shown that the distance to hydrothermal fluids is also a major structuring factor. Imagery analysis based on two dimensional photo stitching revealed insights to the vent field zonation around fluid exits and a basic knowledge of faunal assemblages within hydrothermal vent fields. However, complex three dimensional surfaces could not be adequately replicated in those studies, and the assemblage structure, as well as their relation to abiotic terrain variables, is often only descriptive. In this study we use ROV video imagery of a hydrothermal vent field on the southeastern Indian Ridge in the Indian Ocean. Structure from Motion photogrammetry was applied to build a high resolution 3D reconstruction model of one side of a newly discovered active hydrothermal chimney complex, allowing for the quantification of abundances. Likewise, the reconstruction was used to infer terrain variables at a scale important for megabenthic specimens, which were related to the abundances of the faunal assemblages. Based on the terrain variables, applied random forest model predicted the faunal assemblage distribution with an accuracy of 84.97 %. The most important structuring variables were the distances to diffuse- and black fluid exits, as well as the height of the chimney complex. This novel approach enabled us to classify quantified abundances of megabenthic taxa to distinct faunal assemblages and relate terrain variables to their distribution. The successful prediction of faunal assemblage occurrences further supports the importance of abiotic terrain variables as key structuring factors in hydrothermal systems and offers the possibility to detect suitable areas for Marine Protected areas on larger spatial scales. This technique works for any kind of video imagery, regardless of its initial purpose and can be implemented in marine monitoring and management."

Reference:

Gerdes, K., Martinez Arbizu, P., Schwarz-Schampera, U., Schwentner, M., & Kihara, T. C. (2019). Detailed Mapping of Hydrothermal Vent Fauna: A 3D Reconstruction Approach Based on Video Imagery. Frontiers in Marine Science, 6, 96.doi: 10.3389/fmars.2019.00096

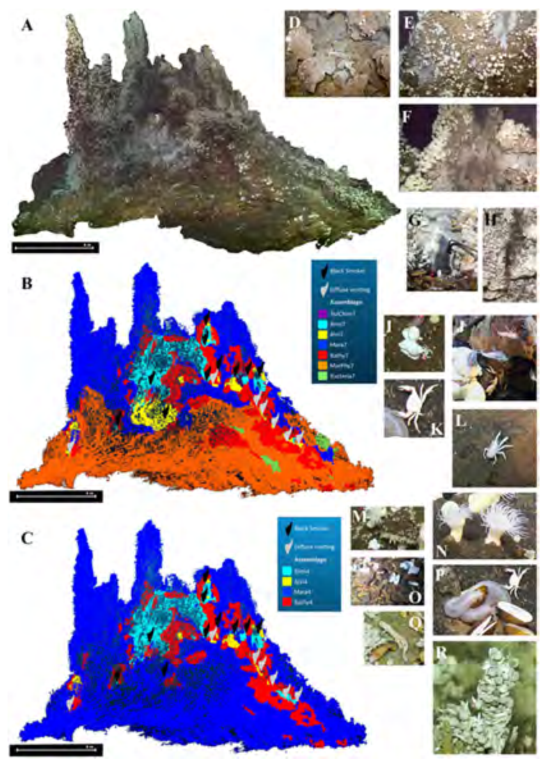

Figure 3.17-1 Figure 4 from Gerdes et al. (2019)

Original Caption: FIGURE 4 | South side structure from motion textured mesh of the 3D chimney reconstruction, detail of the textured surface and manually assigned faunal assemblages. (A) Textured reconstructed chimney. (B) Faunal assemblage distribution assigned by dominant taxa. (C) Faunal assemblage distribution based on k-medoid clustering. (D) Sulfide blocks of the chimney complex. (E) Overview of mussel and shrimp aggregations. (F) Overview of shrimp and anemone aggregations. (G) Diffuse fluid exit. (H) Black fluid exit. (I) Phymorhynchus spp.. (J) Rimicaris kairei. (K) Austinograea rodriguezensis. (L) Munidopsis pallida. (M) Neolepas marisindica. (N) Maractis sp.. (O) Bathymodiolus septemdierum. (P) Chiridota sp.. (Q) Zoarcidae gen. sp.. (R) Alviniconcha marisindica.

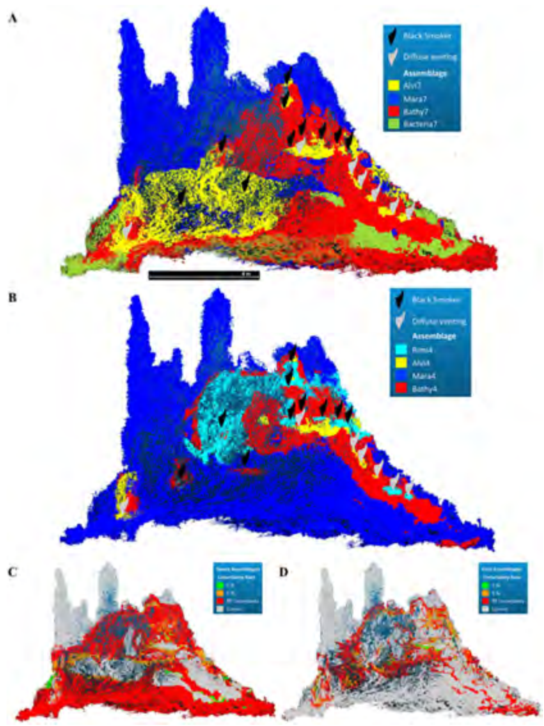

Figure 3.17-2 Figure 7 from Gerdes et al. (2019)

Original Caption: FIGURE 7 | Predicted faunal assemblage occurrence across the reconstructed chimney complex based on random forest modeling. (A) Occurrence of the seven faunal assemblages based on the winning classes of the predicted random forest model (Accuracy = 0.4405). (B) Occurrence of the four faunal assemblages based on the winning classes of the predicted random forest model (Accuracy = 0.8497). (C,D) False positive uncertainty rate at 1%, 5% and the random forest prediction uncertainty for both assemblages.

3.18 Global Patterns in Benthic Biomass

Abstract (Yool et al. 2017):
"Deep-water benthic communities in the ocean are almost wholly dependent on near-surface pelagic ecosystems for their supply of energy and material resources. Primary production in sunlit surface waters is channelled through complex food webs that extensively recycle organic material, but lose a fraction as particulate organic carbon (POC) that sinks into the ocean interior. This exported production is further rarefied by microbial breakdown in the abyssal ocean, but a residual ultimately drives diverse assemblages of seafloor heterotrophs. Advances have led to an understanding of the importance of size (body mass) in structuring these communities. Here we force a size-resolved benthic biomass model, BORIS, using seafloor POC flux from a coupled ocean-biogeochemistry model, NEMO-MEDUSA, to investigate global patterns in benthic biomass. BORIS resolves 16 size classes of metazoans, successively doubling in mass from approximately 1 µg to 28 mg. Simulations find a wide range of seasonal responses

to differing patterns of POC forcing, with both a decline in seasonal variability, and an increase in peak lag times with increasing body size. However, the dominant factor for modelled benthic communities is the integrated magnitude of POC reaching the seafloor rather than its seasonal pattern. Scenarios of POC forcing under climate change and ocean acidification are then applied to investigate how benthic communities may change under different future conditions. Against a backdrop of falling surface primary production (-6.1%), and driven by changes in pelagic remineralization with depth, results show that while benthic communities in shallow seas generally show higher biomass in a warmed world (+3.2%), deep-sea communities experience a substantial decline (-32%) under a high greenhouse gas emissions scenario. Our results underscore the importance for benthic ecology of reducing uncertainty in the magnitude and seasonality of seafloor POC fluxes, as well as the importance of studying a broader range of seafloor environments for future model development."

Reference:

Yool, Andrew, Adrian P. Martin, Thomas R. Anderson, Brian J. Bett, Daniel OB Jones, and Henry A. Ruhl. "Big in the benthos: Future change of seafloor community biomass in a global, body size-resolved model." Global change biology 23, no. 9 (2017): 3554-3566.doi: 10.1111/gcb.13680

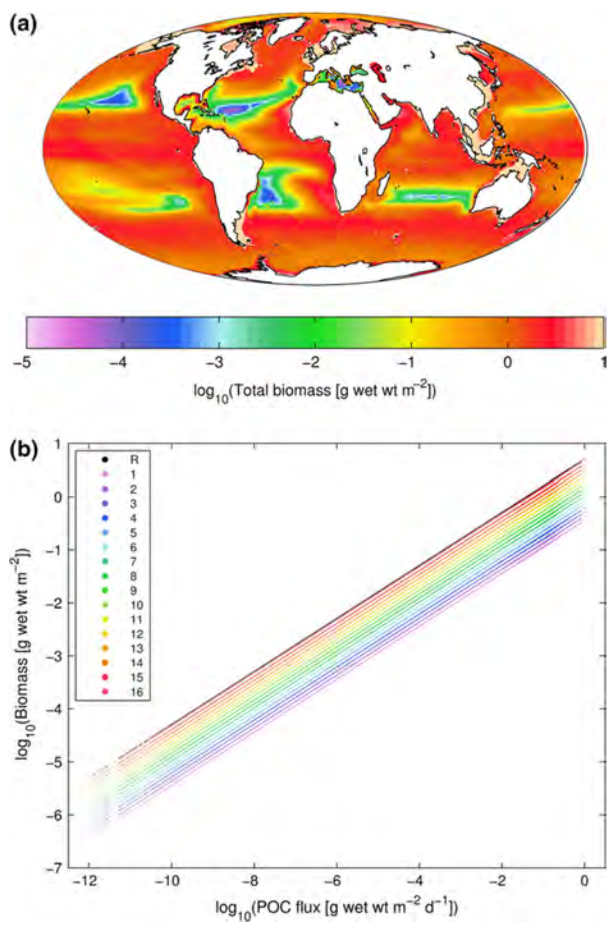

Figure 3.18-1 Mean annual field of total modelled seafloor biomass

3.19 Geo-Referenced Library

A Geo-Referenced Library (GRL) of peer-reviewed articles about the MAR assigned to 1x1 degree cells based on the location of their sampling sites was created to support the SEMPIA workshop process (Morato et al, 2015). Each article was classified into different categories: realm (benthic, benthopelagic, bathypelagic, or pelagic); main taxonomic group; indicator of vulnerable marine ecosystem.

Reference:

Morato, T., J. Cleary, G.H. Taranto, F. Vandeperre, C.K. Pham, D. Dunn, A. Colaço, P.N. Halpin (2015) Data report: Towards development of a strategic Environmental Management Plan for deep seabed mineral exploitation in the Atlantic basin. IMAR & MGEL, Horta, Portugal. 103 pp.

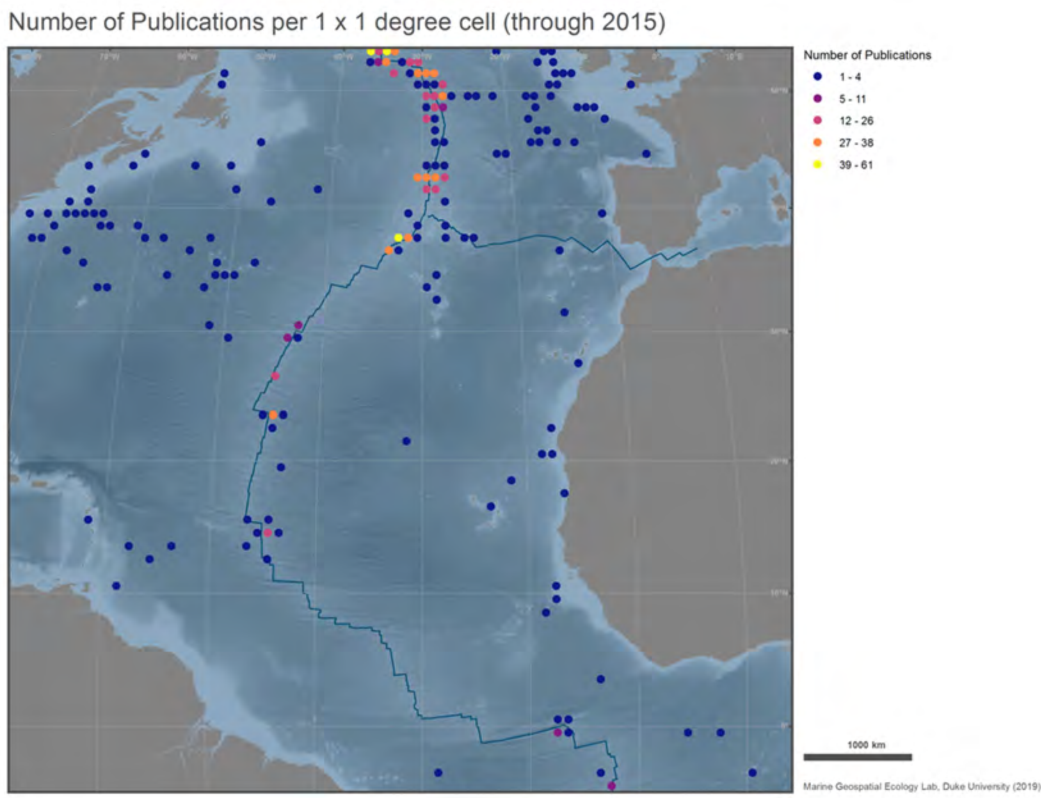

Figure 3.19-1 Total number of publications assigned to 1x1 degree cells based on the location of their sampling sites

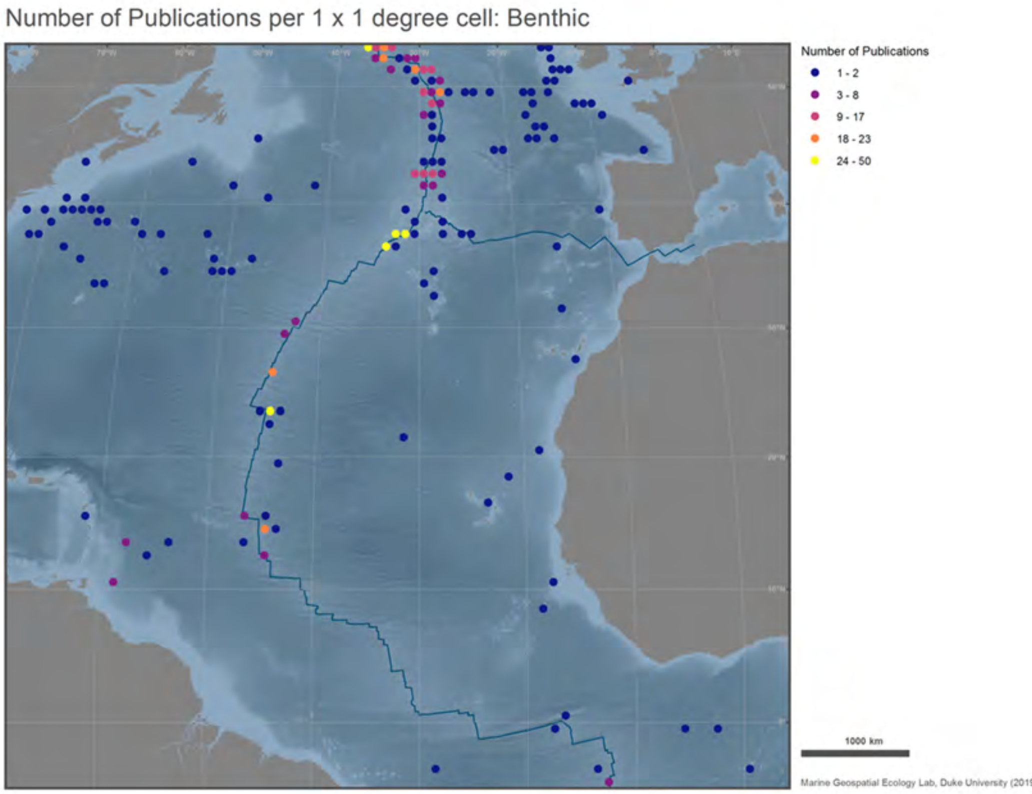

Figure 3.19-2 Total number of publications – benthic

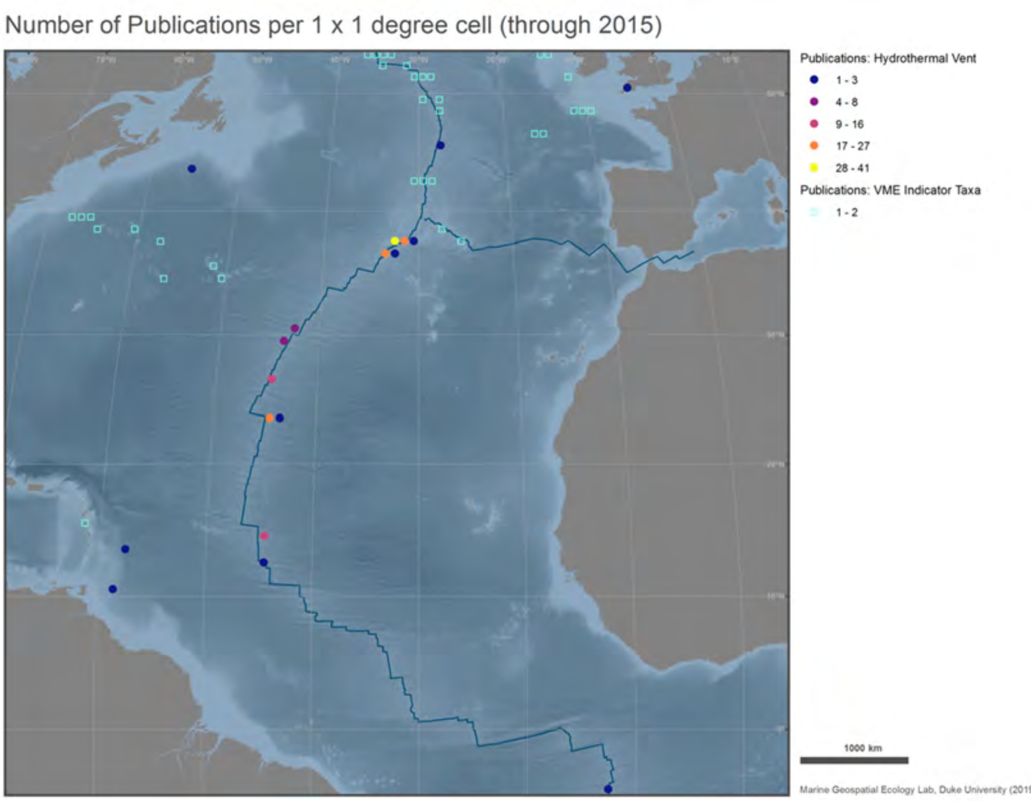

Figure 3.19-3 Total number of publications – VME indicator taxa and hydrothermal vents

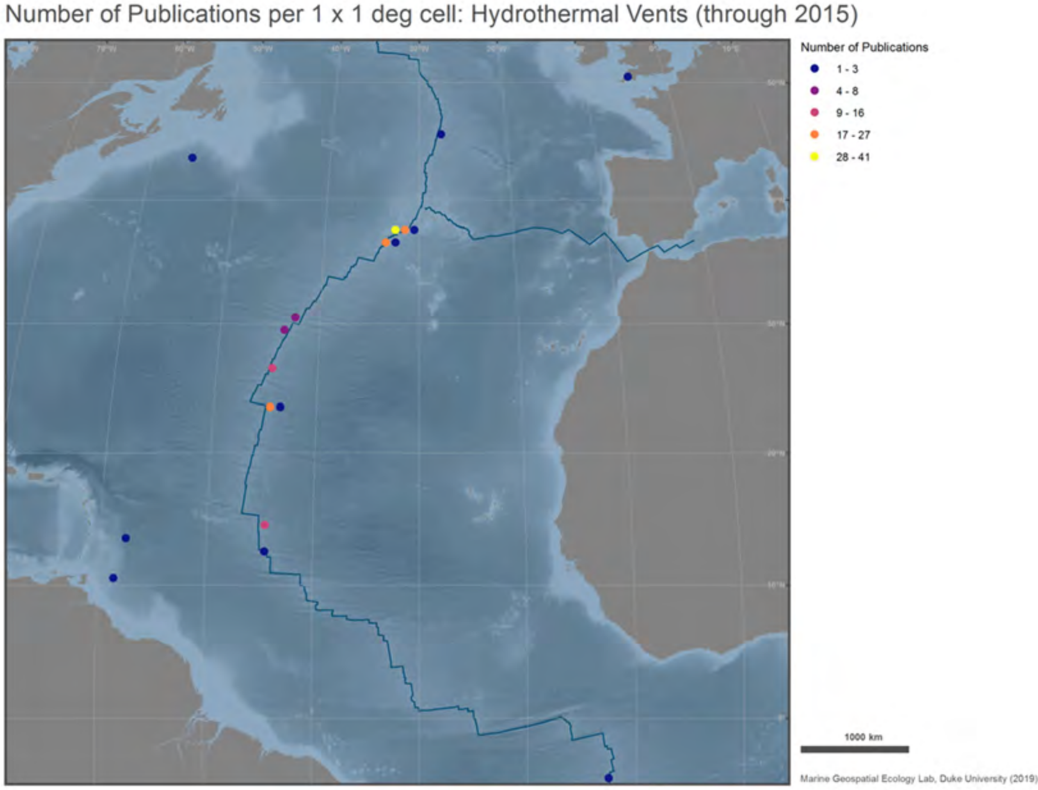

Figure 3.19-4 Total number of publications – hydrothermal vents and cold seeps type

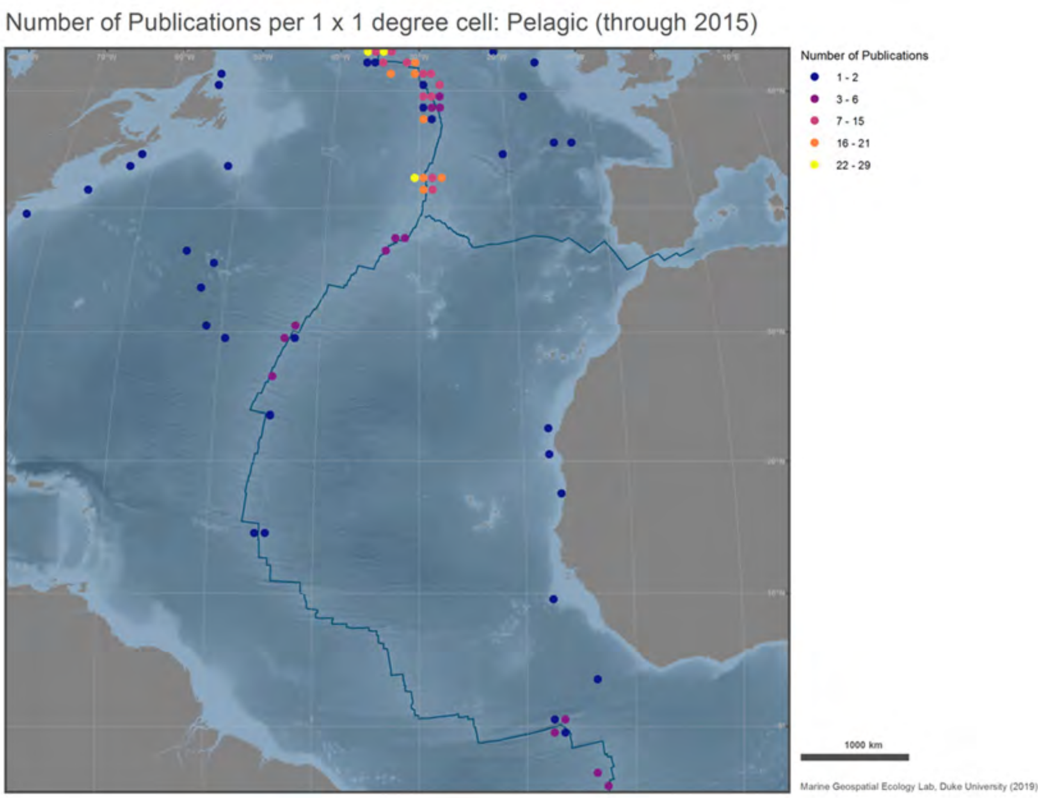

Figure 3.19-5 Total number of publications – pelagic

3.20 Landings of pelagic commercial species

The landings of commercial tuna and swordfish presented here were obtained from the CATDIS (https://www.iccat.int/en/accesingdb.htm) database made available by the International Commission for the Conservation of Atlantic Tunas (ICCAT). CATDIS is basically an estimate of Task-1 nominal catches (T1NC) for the nine major tuna and tuna like species of ICCAT, stratified in time (trimester) and space (5x5 degree squares). It assumes that, time/space distribution of Task II partial catch data (obtained from catch and effort reports) is representative of T1NC overall annual catches dispersion in time and space. The catches for the main pelagic sharks were obtained from Task II Catch and Effort (T2CE) database from the International Commission for the Conservation of Atlantic Tunas (ICCAT). T2CE are basically data obtained from sampling a portion of the individual fishing operations of a given fishery in a specified period of time.

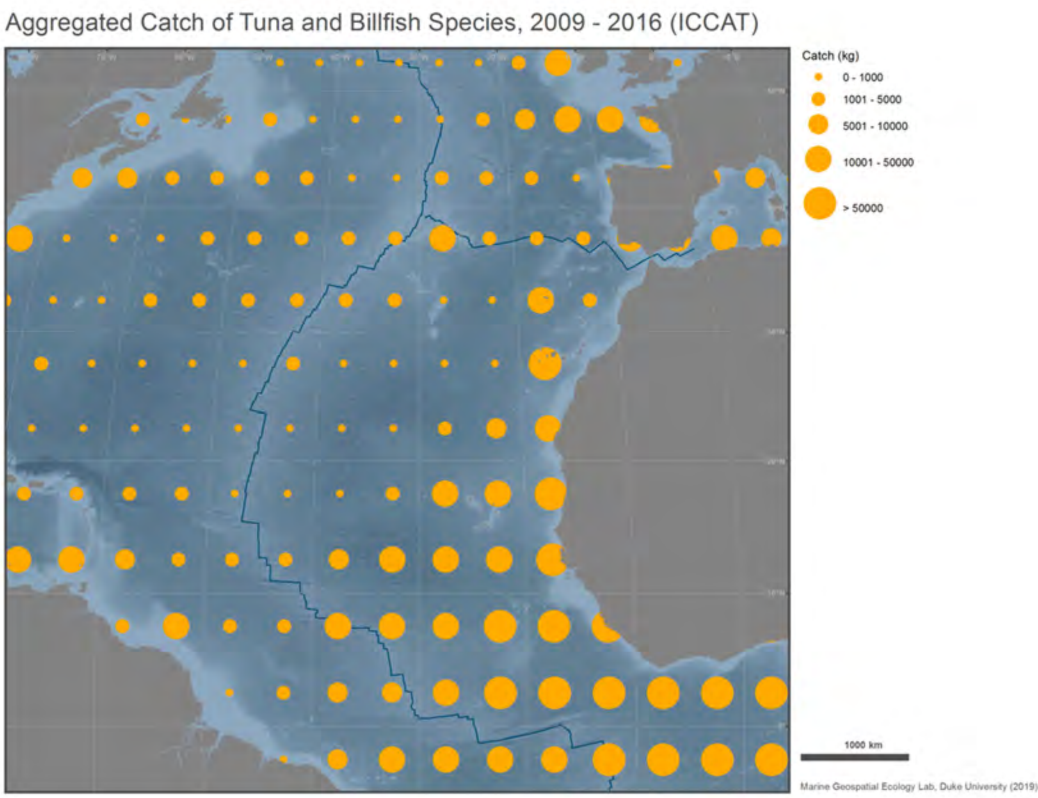

Figure 3.20-1 Aggregated landings for the five main tuna species (Atlantic bluefin tuna, yellowfin tuna, albacore, bigeye tuna and skipjack tuna) and billfish (Atlantic sailfish, Atlantic blue marlin, Atlantic white marlin, Swordfish)

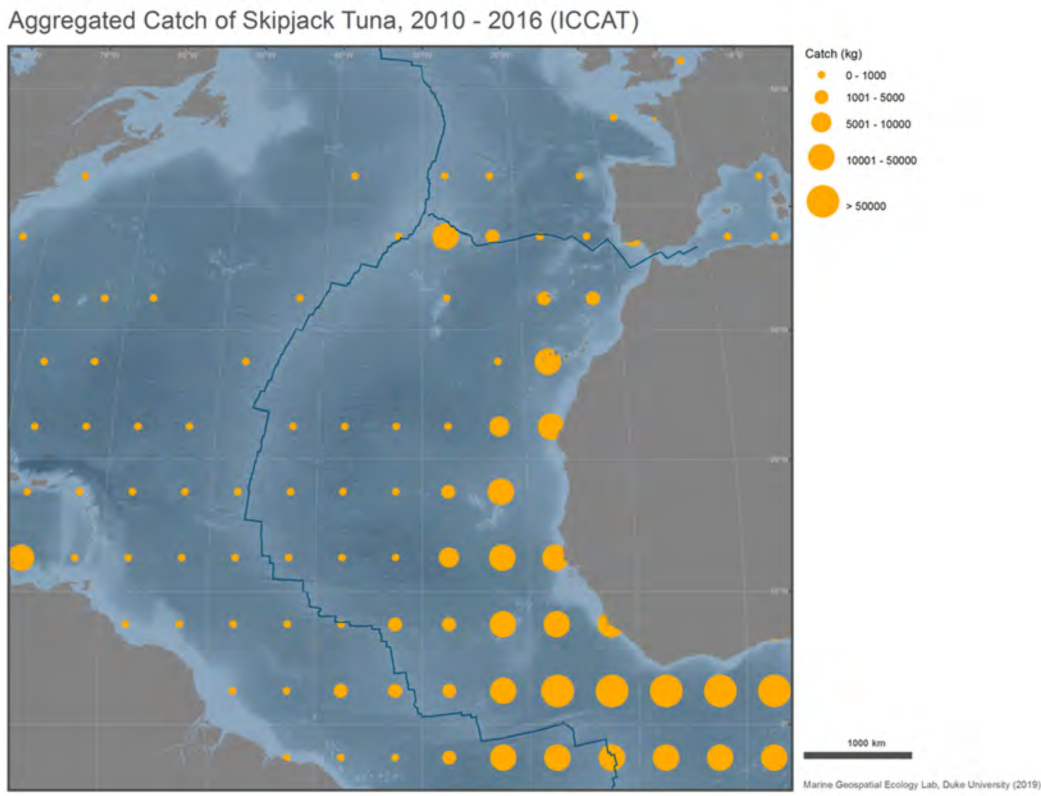

Figure 3.20-2 Aggregated landings for skipjack tuna

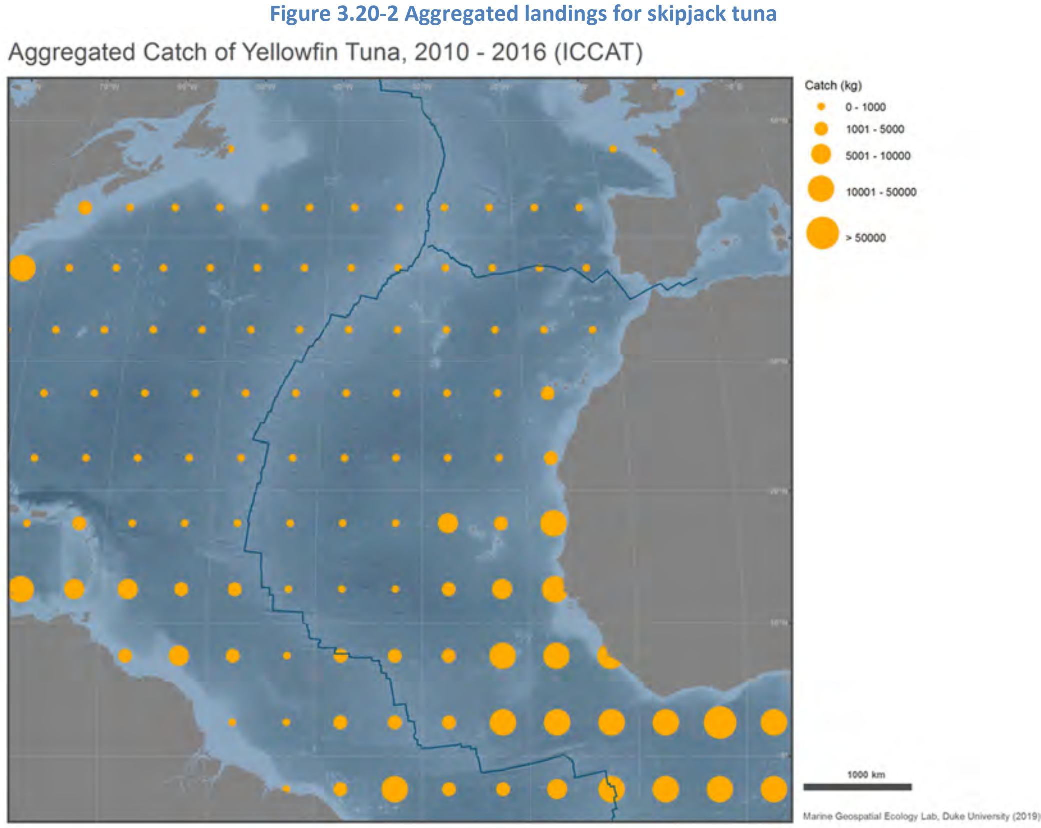

Figure 3.20-3 Aggregated landings for yellowfin tuna

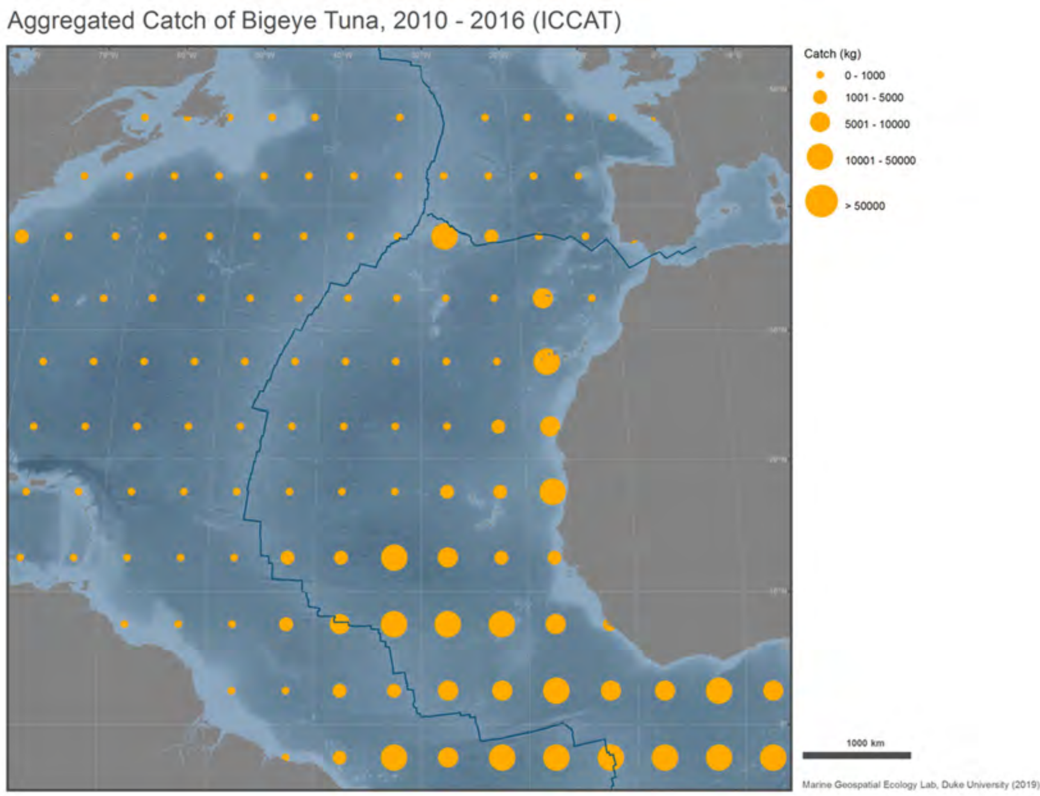

Figure 3.20-4 Aggregated landings for bigeye tuna

3.21 Turtle tagging data aggregated by OBIS-SEAMAP

OBIS-SEAMAP (http://seamap.env.duke.edu/), Ocean Biogeographic Information System Spatial Ecological Analysis of Megavertebrate Populations, is a spatially referenced online database, aggregating marine mammal, seabird and sea turtle observation data from across the globe. Data from several turtle tracking efforts were extracted from OBIS-SEAMAP data center for the study area and displayed on a per species basis.

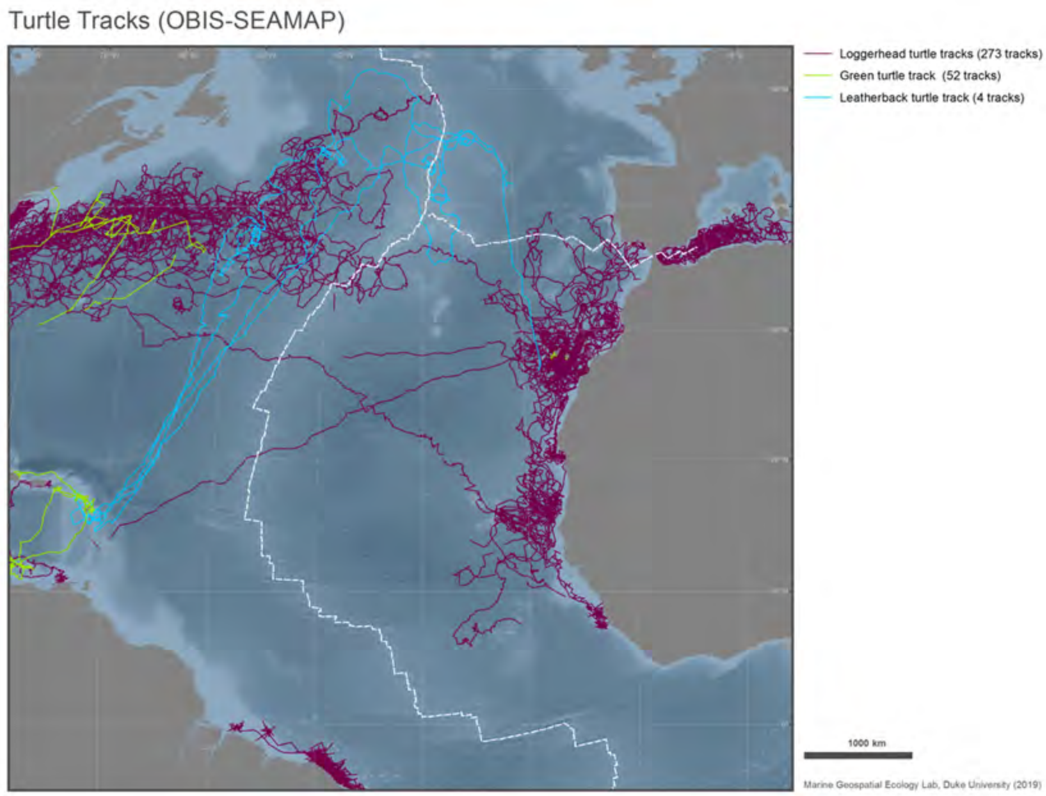

Figure 3.21-1 Turtle telemetry

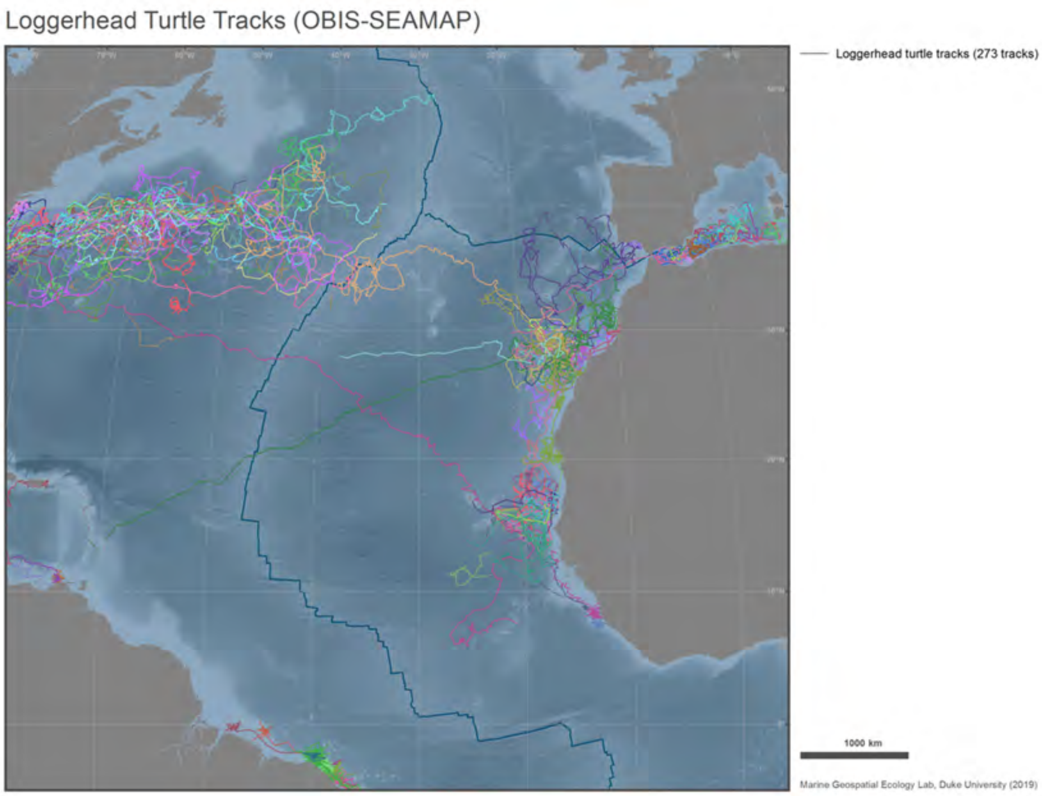

Figure 3.21-2 Loggerhead turtle telemetry

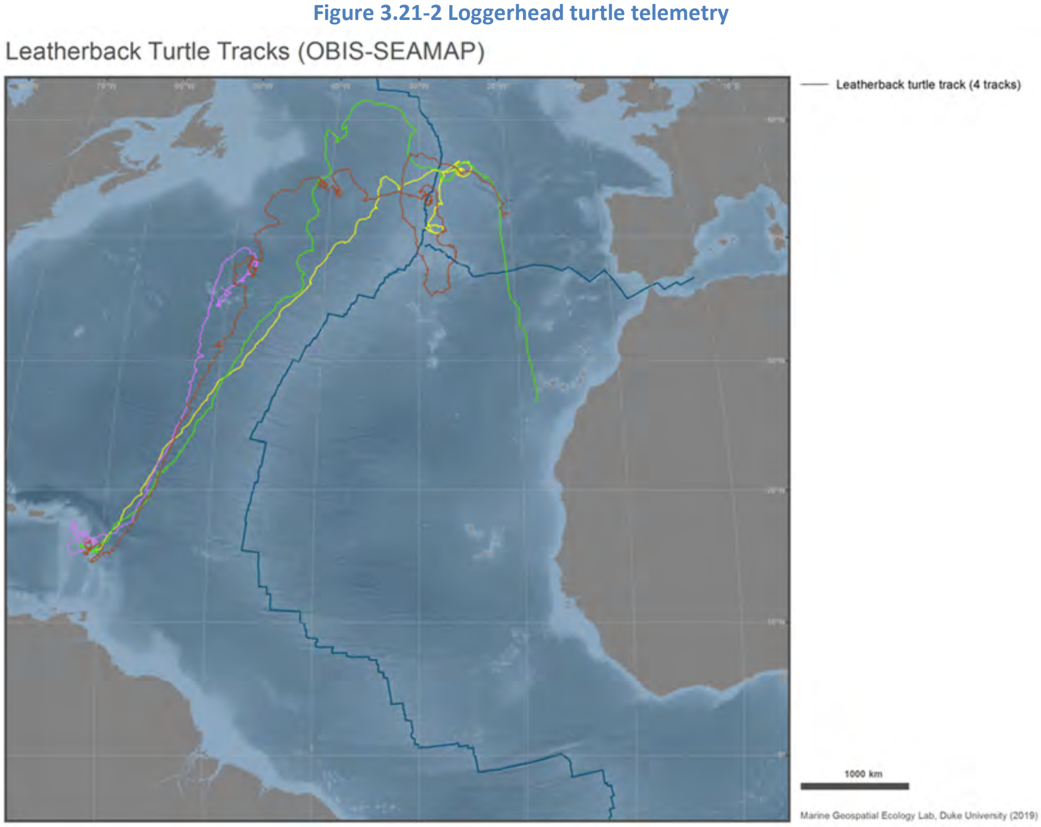

Figure 3.21-3 Leatherback turtle telemetry

3.22 Leatherback Turtle Telemetry and Density

Abstract (Fossette et al. 2014):
"Large oceanic migrants play important roles in ecosystems, yet many species are of conservation concern as a result of anthropogenic threats, of which incidental capture by fisheries is frequently identified. The last large populations of the leatherback turtle, Dermochelys coriacea, occur in the Atlantic Ocean, but interactions with industrial fisheries could jeopardize recent positive population trends, making bycatch mitigation a priority. Here, we perform the first pan-Atlantic analysis of spatio-temporal distribution of the leatherback turtle and ascertain overlap with longline fishing effort. Data suggest that the Atlantic probably consists of two regional management units: northern and southern (the latter including turtles breeding in South Africa). Although turtles and fisheries show highly diverse distributions, we highlight nine areas of high susceptibility to potential bycatch (four in the northern Atlantic and five in the southern/equatorial Atlantic) that are worthy of further targeted investigation and mitigation. These are reinforced by reports of leatherback bycatch at eight of these sites. International collaborative efforts are needed, especially from nations hosting regions where susceptibility to bycatch is likely to be high within their exclusive economic zone (northern Atlantic: Cape Verde, Gambia, Guinea Bissau, Mauritania, Senegal, Spain, USA and Western Sahara; southern Atlantic: Angola, Brazil, Namibia and UK) and from nations fishing in these high-susceptibility areas, including those located in international waters."

Reference:
Fossette, S., Witt, M.J., Miller, P., Nalovic, M. a, Albareda, D., Almeida, a P., Broderick, a C., Chacón-Chaverri, D., Coyne, M.S., Domingo, A., Eckert, S., Evans, D., Fallabrino, A., Ferraroli, S., Formia, A., Giffoni, B., Hays, G.C., Hughes, G., Kelle, L., Leslie, A., López-Mendilaharsu, M., Luschi, P., Prosdocimi, L., Rodriguez-Heredia, S., Turny, A., Verhage, S. & Godley, B.J. (2014) Pan-atlantic analysis of the overlap of a highly migratory species, the leatherback turtle, with pelagic longline fisheries. Proc R Soc B, 281, 20133065.doi: 10.1098/rspb.2013.3065

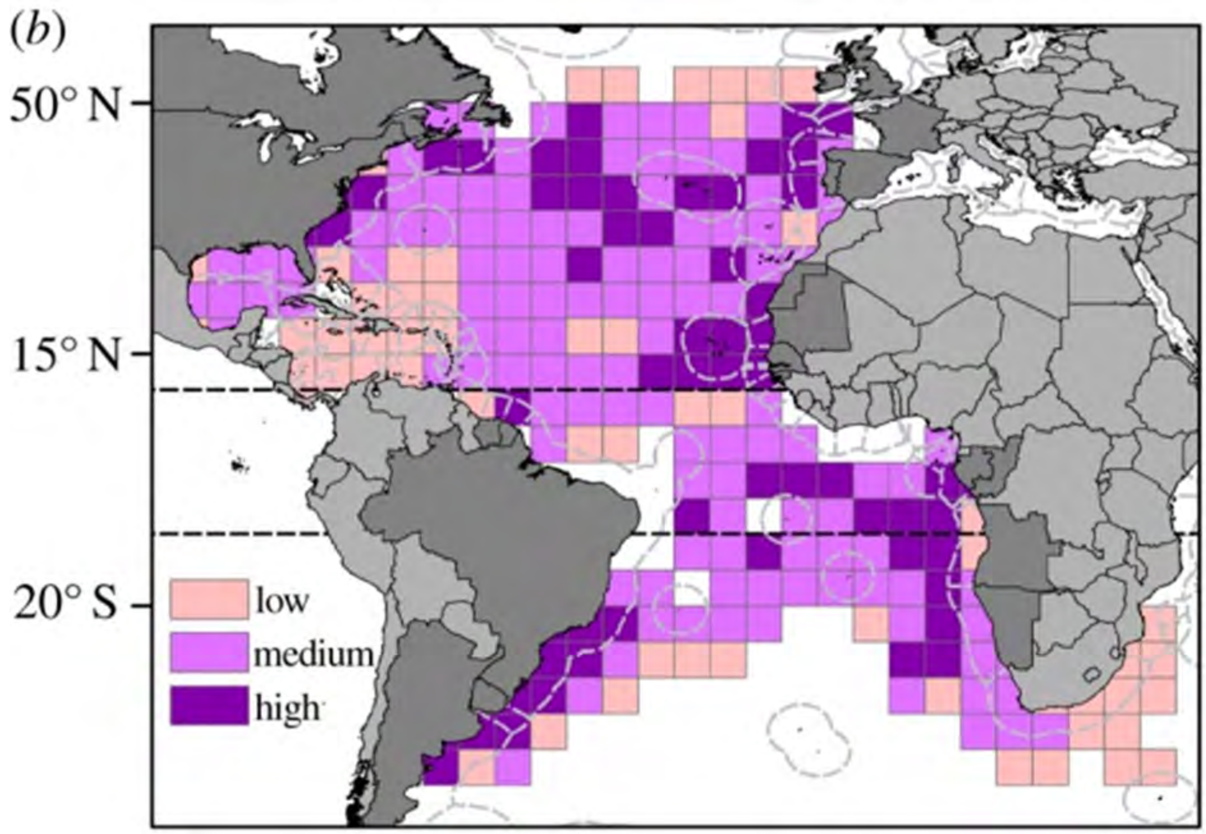

Figure 3.22-1 Density distribution of satellite-tracked leatherbacks in the Atlantic Ocean.

Original Caption: Figure 1b from Fossette et al. (2014): Density of leatherback daily locations (locations were time-weighted and population-size normalized). Three density classes were defined: low, medium and high use. White pixels represent areas from which tracking data were not received. High-use areas occurred both in international waters and within the EEZs of 20 countries (in dark grey) fringing the northern Atlantic (Canada, Cape Verde, Gambia, Guinea Bissau, France/French Guiana, Mauritania, Portugal/Azores, Senegal, Spain/Canaries, Suriname, United States of America, Western Sahara) or the southern Atlantic (Angola, Argentina, Brazil, Congo, Gabon, Namibia, United Kingdom/Ascension Island and Uruguay). Dashed grey lines represent the limits of national EEZs.

3.23 Global patterns of marine turtle bycatch

Abstract (Wallace et al. 2010):
"Fisheries bycatch is a primary driver of population declines in several species of marine megafauna (e.g., elasmobranchs, mammals, seabirds, turtles). Characterizing the global bycatch seascape using data on bycatch rates across fisheries is essential for highlighting conservation priorities. We compiled a comprehensive database of reported data on marine turtle bycatch in gillnet, longline, and trawl fisheries worldwide from 1990 to 2008. The total reported global marine turtle bycatch was ~85,000 turtles, but due to the small percentage of fishing effort

observed and reported (typically <1% of total fleets), and to a global lack of bycatch information from small-scale fisheries, this likely underestimates the true total by at least two orders of magnitude. Our synthesis also highlights an apparently universal pattern across fishing gears and regions where high bycatch rates were associated with low observed effort, which emphasizes the need for strategic bycatch data collection and reporting. This study provides the first global perspective of fisheries bycatch for marine turtles and highlights region–gear combinations that warrant urgent conservation action (e.g., gillnets, longlines, and trawls in the Mediterranean Sea and eastern Pacific Ocean) and region–gear combinations in need of enhanced observation and reporting efforts (e.g., eastern Indian Ocean gillnets, West African trawls)."

Reference:

Wallace, B.P., Lewison, R.L., Mcdonald, S.L., Mcdonald, R.K., Kot, C.Y., Kelez, S., Bjorkland, R.K., Finkbeiner, E.M., Helmbrecht, S. & Crowder, L.B. (2010) Global patterns of marine turtle bycatch. Conservation Letters, 3, 131–142.doi: 10.1111/j.1755-263X.2010.00105.x

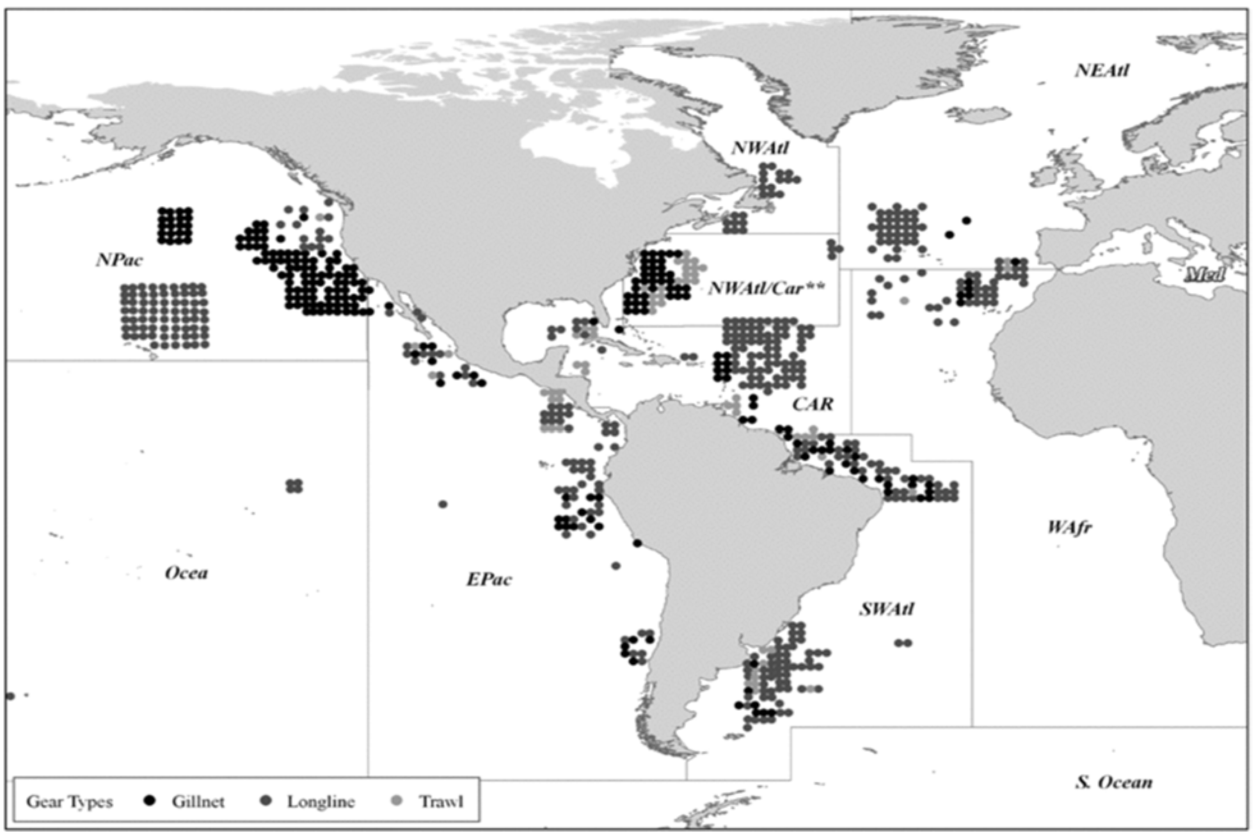

Figure 3.23-1 Overview of sea turtle bycatch data

Original Caption: Geographic delineation of regions and putative distribution of marine turtle bycatch records for gillnets, longlines, and trawls. Points represent all records we compiled in our database (n= 993), including those we used in analyses (n= 700). Locations were plotted according to reported geographic coordinates, or when coordinates were not available, based on region-specific descriptions of each fishing gear.

3.24 Sharks caught by the Brazilian tuna longline fleet

Reference:

Frédou, F.L., Tolotti, M.T., Frédou, T., Carvalho, F., Hazin, H., Burgess, G., Coelho, R., Waters, J.D., Travassos, P. & Hazin, F.H.V. (2015) Sharks caught by the Brazilian tuna longline fleet: an overview. Reviews in Fish Biology and Fisheries, 25, 365–377. doi: 10.1007/s11160-014-9380-8

3.25 Blue shark telemetry

Abstract (Vandeperre et al. 2014):

“Spatial structuring and segregation by sex and size is considered to be an intrinsic attribute of shark populations. These spatial patterns remain poorly understood, particularly for oceanic species such as blue shark (*Prionace glauca*), despite its importance for the management and conservation of this highly migratory species. This study presents the results of a long-term electronic tagging experiment to investigate the migratory patterns of blue shark, to elucidate how these patterns change across its life history and to assess the existence of a nursery area in the central North Atlantic. Blue sharks belonging to different life stages (n = 34) were tracked for periods up to 952 days during which they moved extensively (up to an estimated 28.139 km), occupying large parts of the oceanic basin. Notwithstanding a large individual variability, there were pronounced differences in movements and space use across the species' life history. The study provides strong evidence for the existence of a discrete central North Atlantic nursery, where juveniles can reside for up to at least 2 years. In contrast with previously described nurseries of coastal and semi-pelagic sharks, this oceanic nursery is comparatively vast and open suggesting that shelter from predators is not its main function. Subsequently, male and female blue sharks spatially segregate. Females engage in seasonal latitudinal migrations until approaching maturity, when they undergo an ontogenic habitat shift towards tropical latitudes. In contrast, juvenile males generally expanded their range southward and apparently displayed a higher degree of behavioural polymorphism. These results provide important insights into the spatial ecology of pelagic sharks, with implications for the sustainable management of this heavily exploited shark, especially in the central North Atlantic where the presence of a nursery and the seasonal overlap and alternation of different life stages coincides with a high fishing mortality.”

Reference:

Vandeperre, F., Aires-da-Silva, A., Fontes, J., Santos, M., Santos, R. S., & Afonso, P. (2014). Movements of blue sharks (Prionace glauca) across their life history. PLoS One, 9(8), e103538.doi: 10.1371/journal.pone.0103538

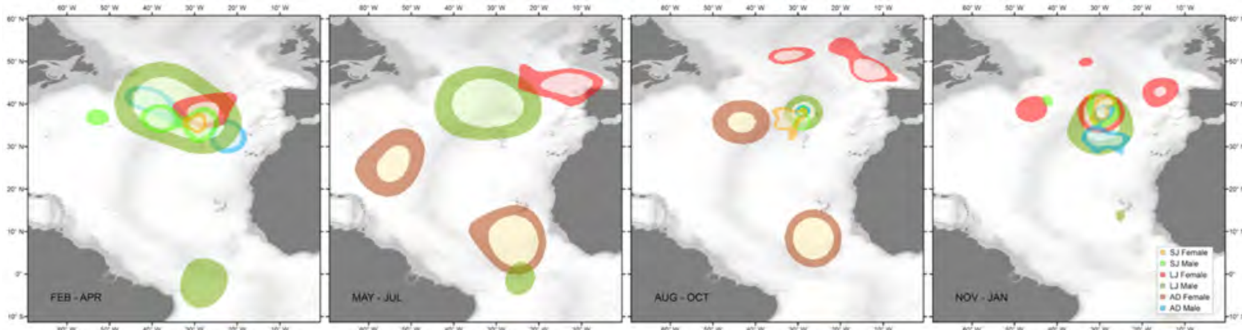

Figure 3.25-1 Quarterly 25% and 50% Kernel Utilisation Distributions (KUD) for the different life stages of blue sharks tagged in the Azores. Figure 8 from Vandeperre et al. (2014)

3.26 Pelagic sharks tracking overlap with longline fishing hotspots

Abstract (Queiroz et al. 2016):
"Overfishing is arguably the greatest ecological threat facing the oceans, yet catches of many highly migratory fishes including oceanic sharks remain largely unregulated with poor monitoring and data reporting. Oceanic shark conservation is hampered by basic knowledge gaps about where sharks aggregate across population ranges and precisely where they overlap with fishers. Using satellite tracking data from six shark species across the North Atlantic, we show that pelagic sharks occupy predictable habitat hotspots of high space use. Movement modeling showed sharks preferred habitats characterized by strong sea surface-temperature gradients (fronts) over other available habitats. However, simultaneous Global Positioning System (GPS) tracking of the entire Spanish and Portuguese longline-vessel fishing fleets show an 80% overlap of fished areas with hotspots, potentially increasing shark susceptibility to fishing exploitation. Regions of high overlap between oceanic tagged sharks and longliners included the North Atlantic Current/Labrador Current convergence zone and the Mid-Atlantic Ridge southwest of the Azores. In these main regions, and subareas within them, shark/vessel co-occurrence was spatially and temporally persistent between years, highlighting how broadly the fishing exploitation efficiently "tracks" oceanic sharks within their space-use hotspots year-round. Given this intense focus of longliners on shark hotspots, our study argues the need for international catch limits for pelagic sharks and identifies a future role of combining fine-scale fish and vessel telemetry to inform the ocean-scale management of fisheries."

Reference:
Queiroz, N., Humphries, N.E., Mucientes, G., Hammerschlag, N., Lima, F.P., Scales, K.L., Miller, P.I., Sousa, L.L., Seabra, R. and Sims, D.W., (2016). Ocean-wide tracking of pelagic sharks reveals extent of overlap with longline fishing hotspots. Proceedings of the National Academy of Sciences, 113(6), pp.1582-1587.doi: 10.1073/pnas.1510090113

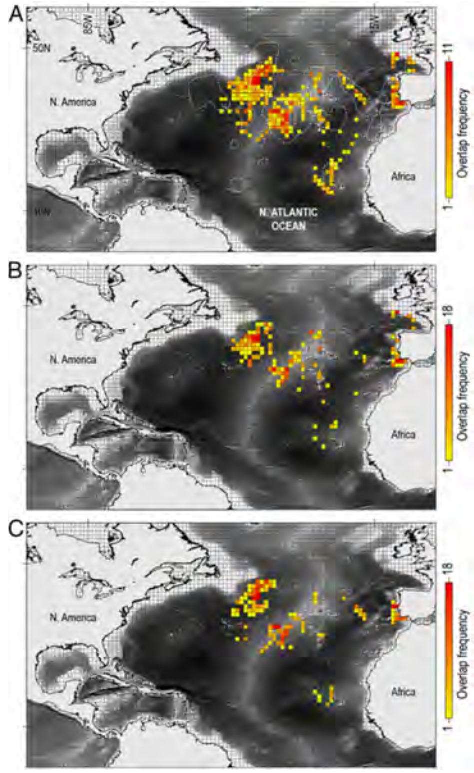

Figure 3.26-1 Oceanic shark spatial and temporal overlap with longline vessels

Original Caption: Fig. 4. Oceanic shark spatial and temporal overlap with longline vessels. (A) Distribution of the temporal co occurrence (shared grid cell) between satellite-tracked oceanic sharks and Spanish and Portuguese pelagic longliners. Dotted white lines denote edges of space-use hotspots in Fig. 1D. Temporal persistence across years of the cooccurrence of tracked oceanic sharks and longliners: 2005 (B) and 2009 (C).

3.27 Blue and fin whale telemetry

Abstract (Silva et al. 2013):
"The need to balance energy reserves during migration is a critical factor for most long-distance migrants and an important determinant of migratory strategies in birds, insects and land mammals. Large baleen whales migrate annually between foraging and breeding sites, crossing vast ocean areas where food is seldom abundant. How whales respond to the demands and constraints of such long migrations remains unknown. We applied a behaviour discriminating hierarchical state-space model to the satellite tracking data of 12 fin whales and 3 blue whales tagged off the Azores, to investigate their movements, behaviour (transiting and area-restricted search, ARS) and daily activity cycles during the spring migration. Fin and blue whales remained at middle latitudes for prolonged periods, spending most of their time there in ARS behaviour.

While near the Azores, fin whale ARS behaviour occurred within a restricted area, with a high degree of overlap among whales. There were noticeable behavioural differences along the migratory pathway of fin whales tracked to higher latitudes: ARS occurred only in the Azores and north of 56°N, whereas in between these areas whales travelled at higher overall speeds while maintaining a nearly direct trajectory. This suggests fin whales may alternate periods of active migration with periods of extended use of specific habitats along the migratory route. ARS behaviour in blue whales occurred over a much wider area as whales slowly progressed northwards. The tracks of these whales terminated still at middle latitudes, before any behavioural switch was detected. Fin whales exhibited behavioural-specific diel rhythms in swimming speed but these varied significantly between geographic areas, possibly due to differences in the day-night cycle across areas. Finally, we show a link between fin whales seen in the Azores and those summering in eastern Greenland-western Iceland along a migratory corridor located in central Atlantic waters."

Reference:
Silva, M.A., Prieto, R., Jonsen, I., Baumgartner, M.F. & Santos, R.S. (2013) North Atlantic Blue and Fin Whales Suspend Their Spring Migration to Forage in Middle Latitudes: Building up Energy Reserves for the Journey? PLoS ONE, 8, e76507. Doi: 10.1371/journal.pone.0076507

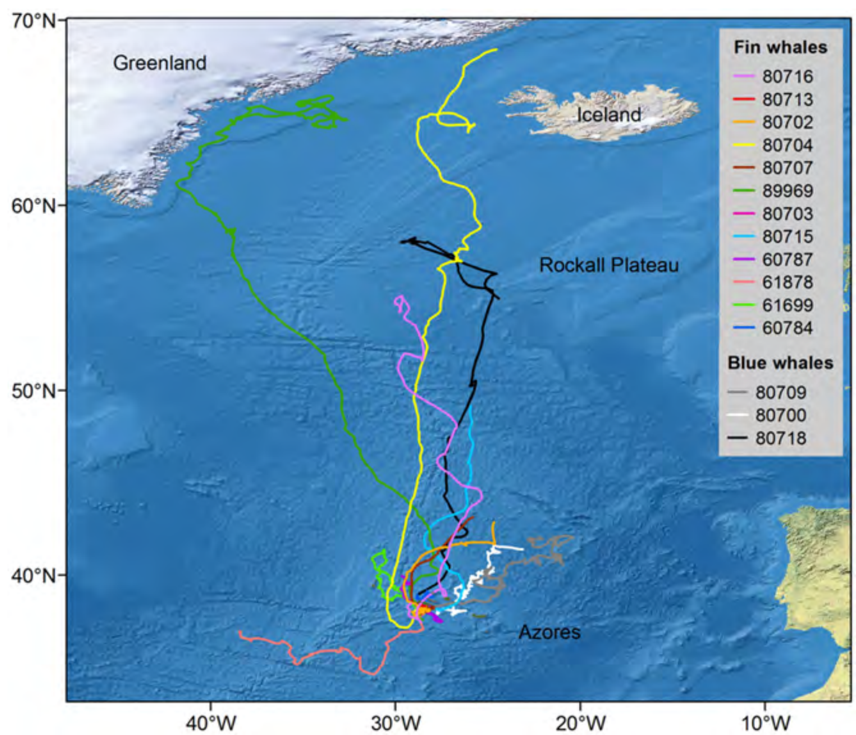

Figure 3.27-1 Blue and fin whale telemetry

Original Caption: Figure 1 Hierarchical switching state-space model derived tracks of 12 fin whales and 3 blue whales.

3.28 Important Bird Areas (IBAs)

BirdLife Important Bird Areas (IBAs) have been identified using several data sources: 1) terrestrial seabird breeding sites are shown with point locality and species that qualifies at the IBA (http://www.birdlife.org/datazone/site/search), 2) marine areas around breeding colonies have been identified based on literature review where possible to guide the distance required by each species; where literature is sparse or lacking, extensions have been applied on a precautionary basis (http://seabird.wikispaces.com/), and 3) sites identified by satellite tracking data via kernel density analysis, first passage time analysis and bootstrapping approaches (www.seabirdtracking.org). Together these IBAs form a network of sites of importance to coastal, pelagic, resident and or migratory species.

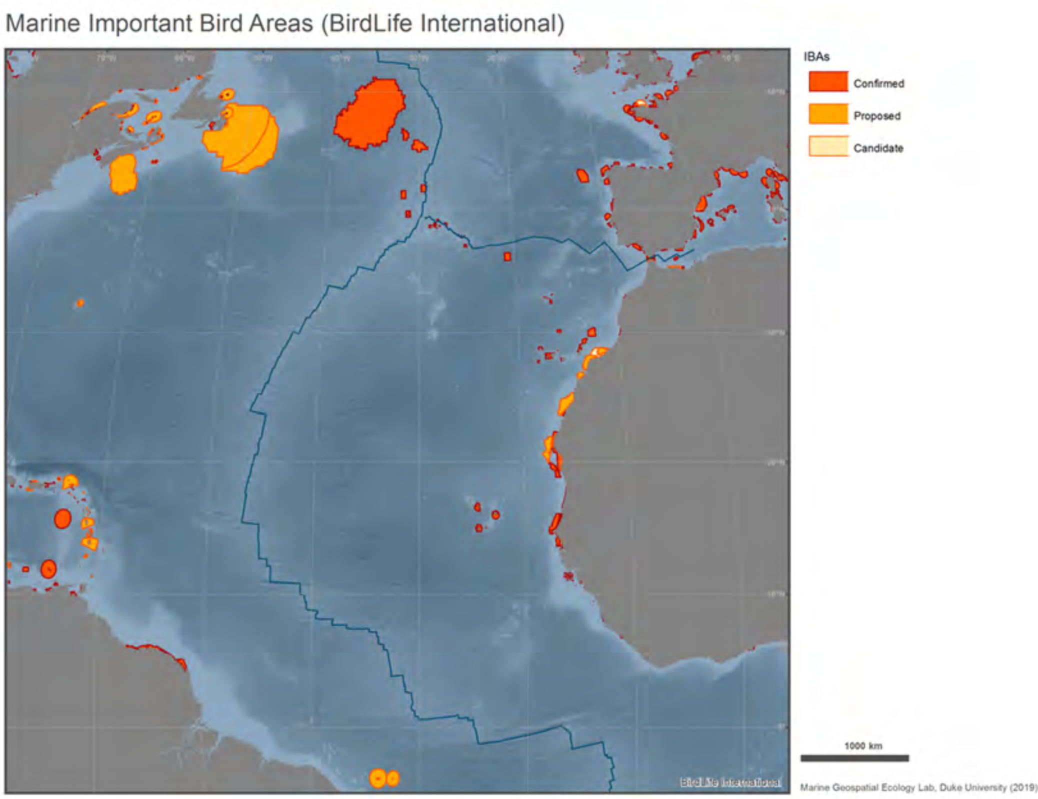

Figure 3.28-1 Important Bird Areas (BirdLife)

3.29 Seabirds in the central North Atlantic

Abstract (Boertmann 2011):
"From 12 to 17 September 2006 a "snapshot" of seabird densities in the northern Atlantic between Greenland and the Azores was obtained using the strip-transect method. Relatively high densities of seabirds in the Greenland shelf and subpolar waters as well as very low densities in the oceanic subtropical waters, described by early authors, were confirmed. Highest oceanic densities (average 21 individuals/km2 per subtransect) were observed on 15 September approximately 200 km south of the subpolar front at about 50°N and approximately 600 km west of the Mid-Atlantic Ridge. Most numerous in this area were Leach's Storm-Petrel (552 on-transect), Great Shearwater (317 on-transect) and Cory's Shearwater (125 on-transect), and noteworthy were small numbers of Arctic Terns and Long-tailed Skuas. This high-density site was located in the centre of the stopover site/foraging area recently discovered by tracking Arctic Terns, Long-tailed Skuas, Sooty Shearwaters and Cory's Shearwaters. This combined aggregation area seems to be associated with the subpolar front between the Grand Banks and the Charlie–Gibbs fracture zone."

Reference:

Boertmann, D. (2011) Seabirds in the central north Atlantic, September 2006: Further evidence for an oceanic seabird aggregation area. *Marine Ornithology*, **39**, 183–188.

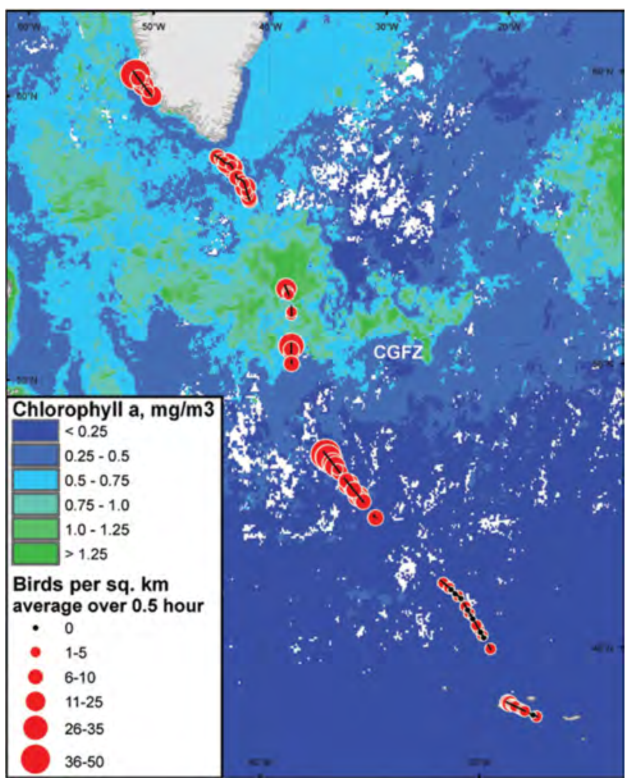

Figure 3.29-1 Densities of seabirds (all species on-transect combined) along the transect in September 2006. Figure 2 from Boertmann (2011)

3.30 Migratory Connectivity in the Ocean; Seabird and Sea Turtle Area Use

Abstract (Dunn et al 2019):
"The distributions of migratory species in the ocean span local, national and international jurisdictions. Across these ecologically interconnected regions, migratory marine species interact with anthropogenic stressors throughout their lives. Migratory connectivity, the geographical linking of individuals and populations throughout their migratory cycles, influences how spatial and temporal dynamics of stressors affect migratory animals and scale up to influence population abundance, distribution and species persistence. Population declines of many migratory marine species have led to calls for connectivity knowledge, especially insights from animal tracking studies, to be more systematically and synthetically incorporated into decision-making. Inclusion of migratory connectivity in the design of conservation and management measures is critical to ensure they are appropriate for the level of risk associated with various degrees of connectivity. Three mechanisms exist to incorporate migratory connectivity into international marine policy which guides conservation implementation: site-selection criteria, network design criteria and policy recommendations. Here, we review the concept of migratory connectivity and its use in international policy, and describe the Migratory Connectivity in the Ocean system, a migratory connectivity evidence-base for the ocean. We propose that without such collaboration focused on migratory connectivity, efforts to effectively conserve these critical species across jurisdictions will have limited effect."

References:

Dunn, D. C., Harrison, A-L et al. 2019. The importance of migratory connectivity for global ocean policy. Proceedings of the Royal Society B: Biological Sciences 286:20191472.

Migratory Connectivity in the Ocean (MiCO). Highly migratory marine species nodes and corridors, developed with data contributed to MiCO. Available from the MiCO System Version 1.0. MiCO. https://mico.eco. Accessed 10/23/2019.

MiCO Data Providers:
Cory's Shearwater: Maria Ana Dias, Paulo Catry, Jose Pedro Granadeiro

Loggerhead: Annette Broderick, Brendan Godley, Lucy Hawkes, Catherine McClellan, Andrew Read, Nuria Varo-Cruz, Luis Felipe Lopez-Jurado, Daniel Cejudo, Juan Antonio Bermejo, Antonio Machado

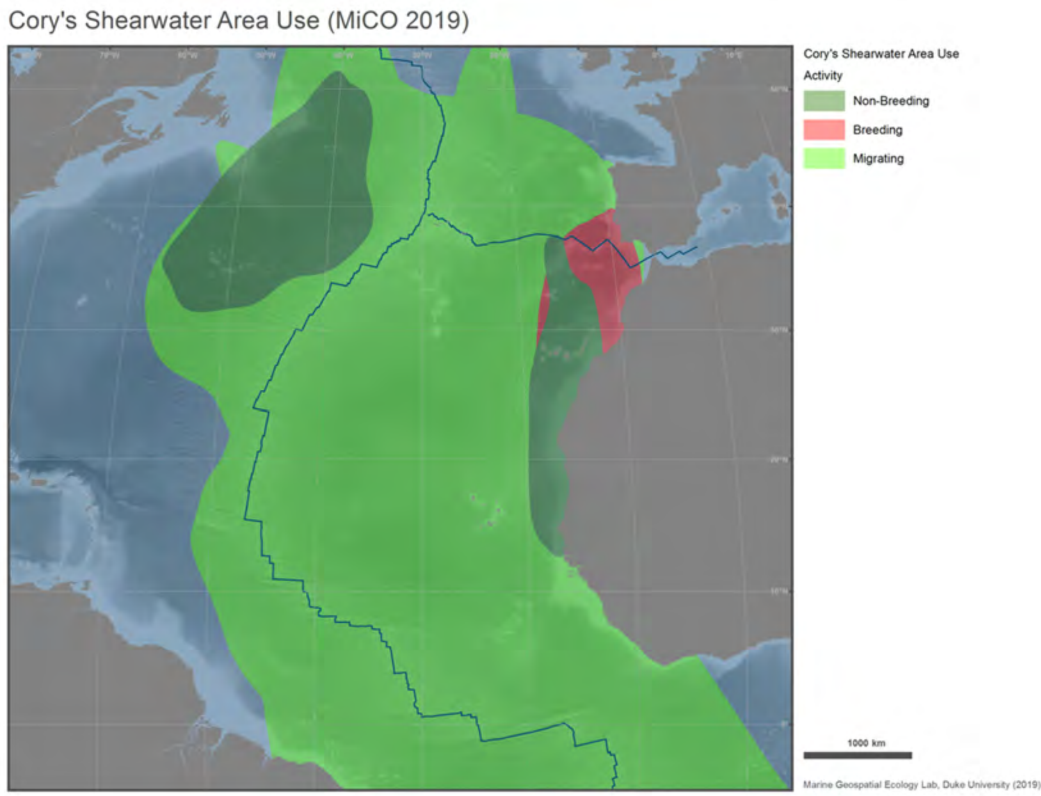

Figure 3.30-1 Cory's Shearwater area use

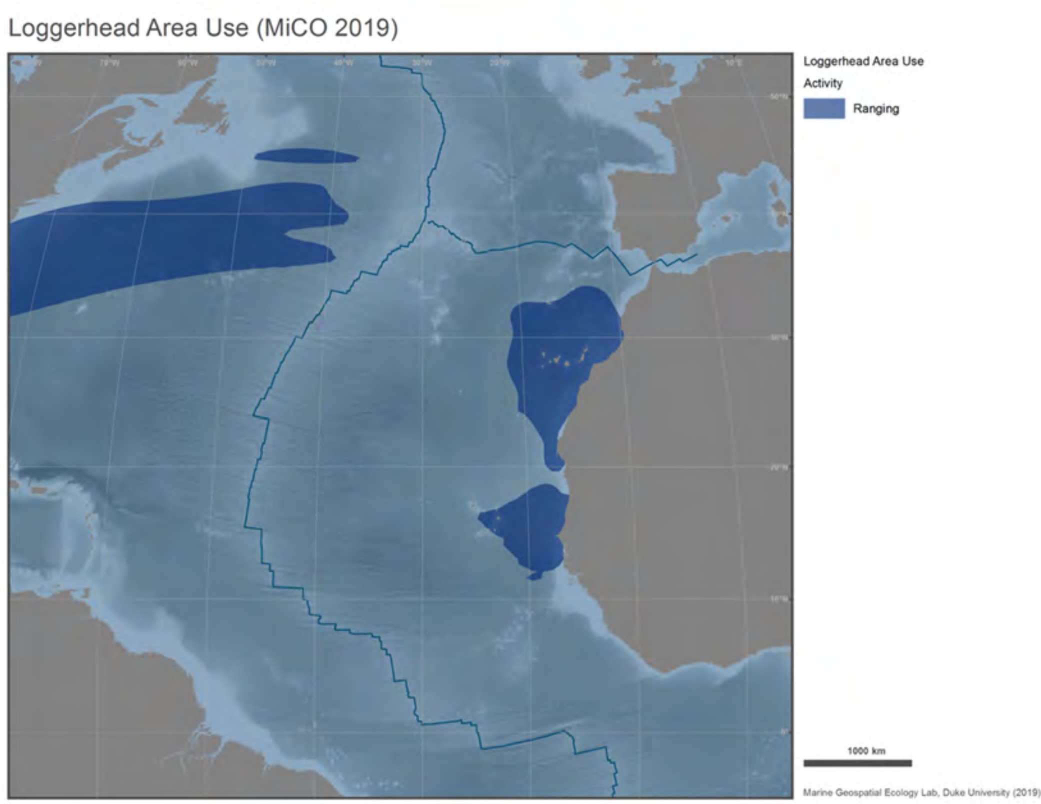

Figure 3.30-2 Loggerhead turtle area use

4 Biogeographic Classification

4.1 Global Open Ocean and Deep Seabed (GOODS) biogeographic classification

"GOODS is the first attempt at comprehensively classifying the open-ocean and deep seafloor into distinct biogeographic regions (UNESCO, 2009). The classification was produced by an international and multidisciplinary group of experts under the auspices of a number of international and intergovernmental organizations as well as governments, and under the ultimate umbrella of the United Nations Educational, Scientific and Cultural Organization (UNESCO) and its Intergovernmental Oceanographic Commission (IOC). The maps shown below include the updates made by Watling et al. (2013).

The biogeographic classification classifies specific ocean regions using environmental features and – to the extent data are available – their species composition. GOODS is hypothesis-driven and still preliminary, and will thus require further refinement and peer review in the future. However, parts of it have already been published (e.g. pelagic provinces; Spalding et al. 2012). Watling et al. (2013) tried to refine the GOODS bathyal and abyssal provinces including some new variables. Physical and chemical proxies thought to be good predictors of the distributions of organisms at the deep-sea floor, and thus used for the definition of biogeographic provinces, were: depth, temperature (T), salinity (S), dissolved oxygen (O), and particulate organic carbon flux (POC) to the seafloor.

The major open ocean pelagic and deep sea benthic zones presented by the GOODS report and by Watling et al. (2013) are considered by their authors a reasonable basis for advancing efforts towards the conservation and sustainable use of biodiversity in marine areas beyond the limits of national jurisdiction in line with a precautionary approach."

References:

UNESCO. 2009. Global Open Oceans and Deep Seabed (GOODS) – Biogeographic Classification. Paris, UNESCO-IOC. (IOC Technical Series, 84.)

Watling, L., Guinotte, J., Clark, M. R., and Smith, C. R. (2013) A proposed biogeography of the deep ocean floor. Progress in Oceanography, 11, 91-112.

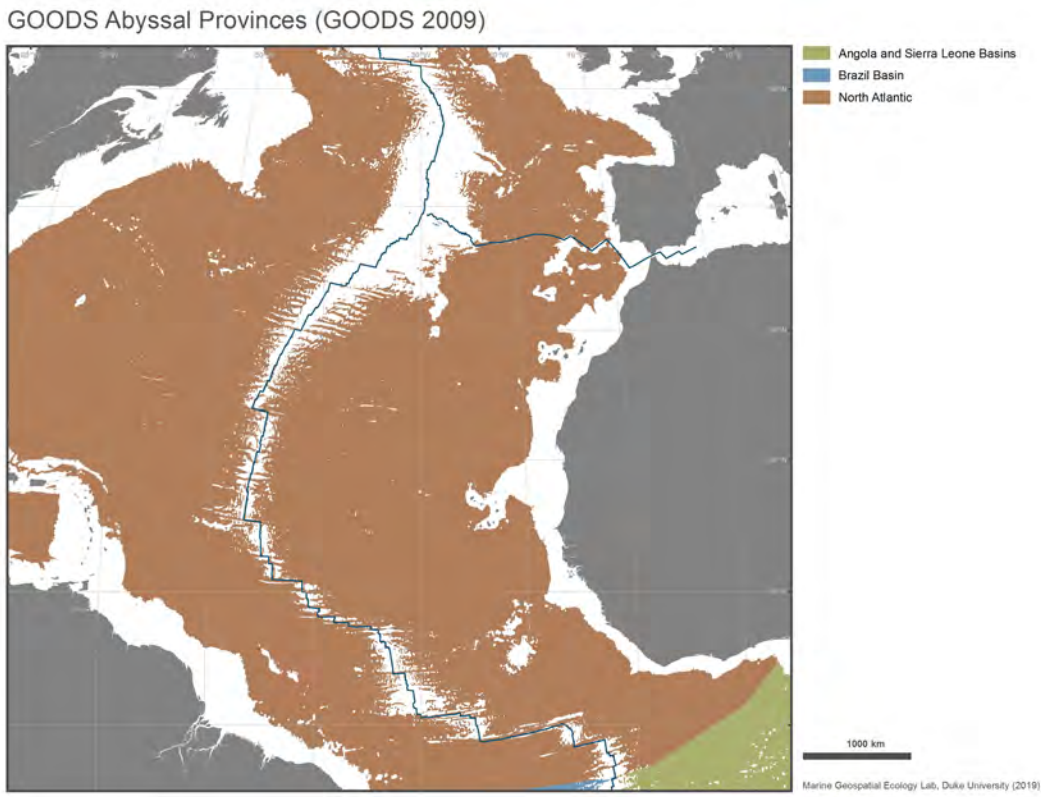

Figure 4.1-1 GOODS abyssal provinces

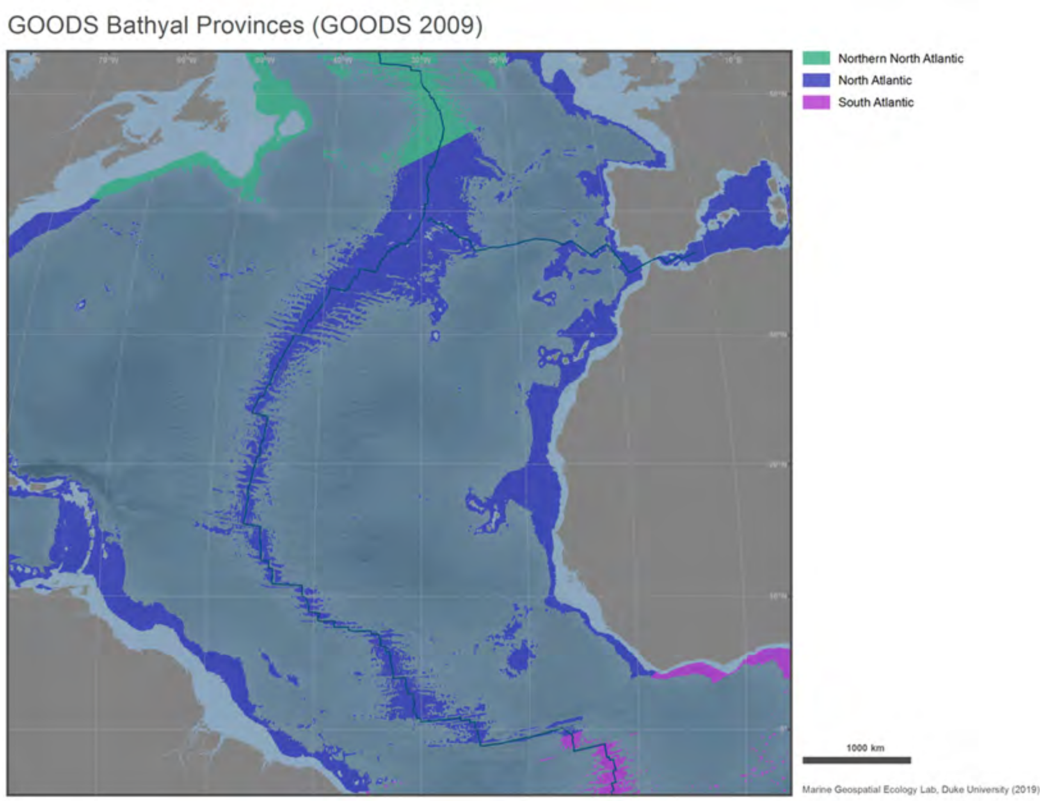

Figure 4.1-2 GOODS bathyal provinces

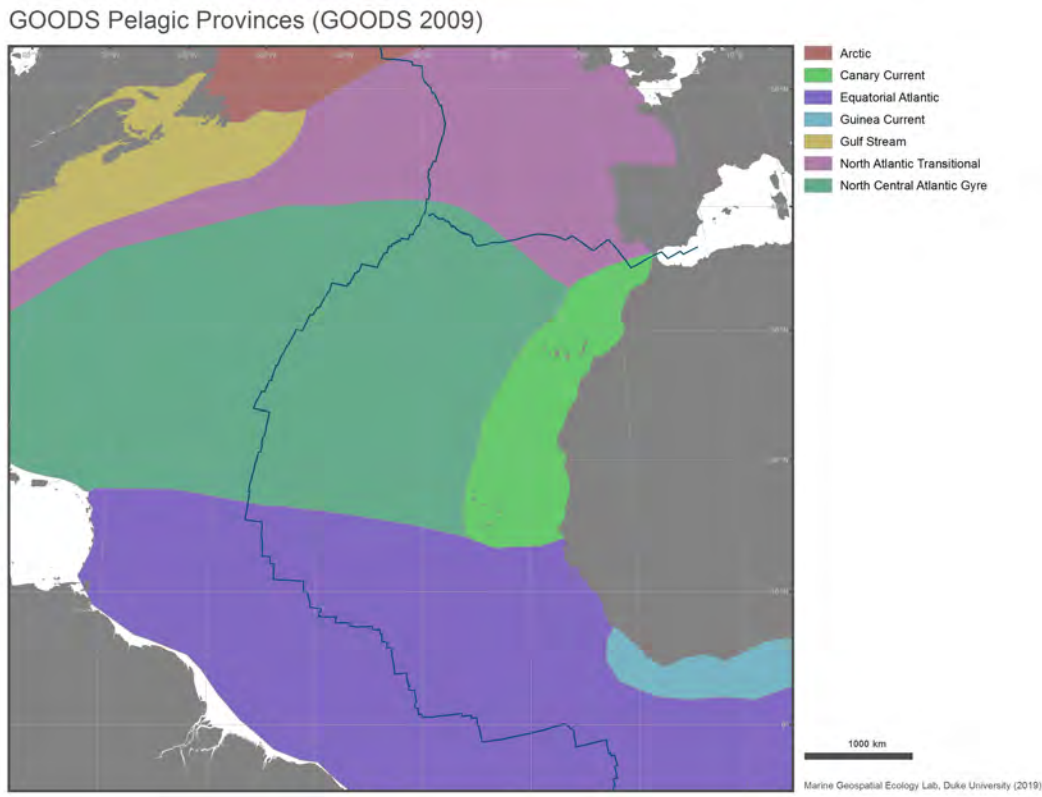

Figure 4.1-3 GOODS pelagic provinces

4.2 Global Mesopelagic Biogeography

Abstract (Sutton et al. 2017):
"We have developed a global biogeographic classification of the mesopelagic zone to reflect the regional scales over which the ocean interior varies in terms of biodiversity and function. An integrated approach was neces- sary, as global gaps in information and variable sampling methods preclude strictly statistical approaches. A panel combining expertise in oceanography, geospatial mapping, and deep-sea biology convened to collate expert opinion on the distributional patterns of pelagic fauna relative to environmental proxies (temperature, salinity, and dissolved oxygen at mesopelagic depths). An iterative Delphi Method integrating additional bio- logical and physical data was used to classify biogeographic ecoregions and to identify the location of ecoregion boundaries or inter-regions gradients. We define 33 global mesopelagic ecoregions. Of these, 20 are oceanic while 13 are 'distant neritic.' While each is driven by a complex of controlling factors, the putative primary driver of each ecoregion was identified. While work remains to be done to produce a comprehensive and robust mesopelagic biogeography (i.e., reflecting temporal variation), we believe that the classification set forth in this study will prove to be a useful and timely input to policy planning and management for conservation of deep- pelagic marine resources. In particular, it gives an indication of the spatial

scale at which faunal communities are expected to be broadly similar in composition, and hence can inform application of ecosystem-based management approaches, marine spatial planning and the distribution and spacing of network of representative protected areas.”

Reference:

Sutton, T.T., Clark, M.R., Dunn, D.C., Halpin, P.N., Rogers, A.D., Guinotte, J., Bograd, S.J., Angel, M.V., Perez, J.A.A., Wishner, K. and Haedrich, R.L., (2017). A global biogeographic classification of the mesopelagic zone. Deep Sea Research Part I: Oceanographic Research Papers, 126, pp.85-102.

Dataset downloaded from Marine Regions (August 2019)
http://www.marineregions.org/gazetteer.php?p=details&id=50384

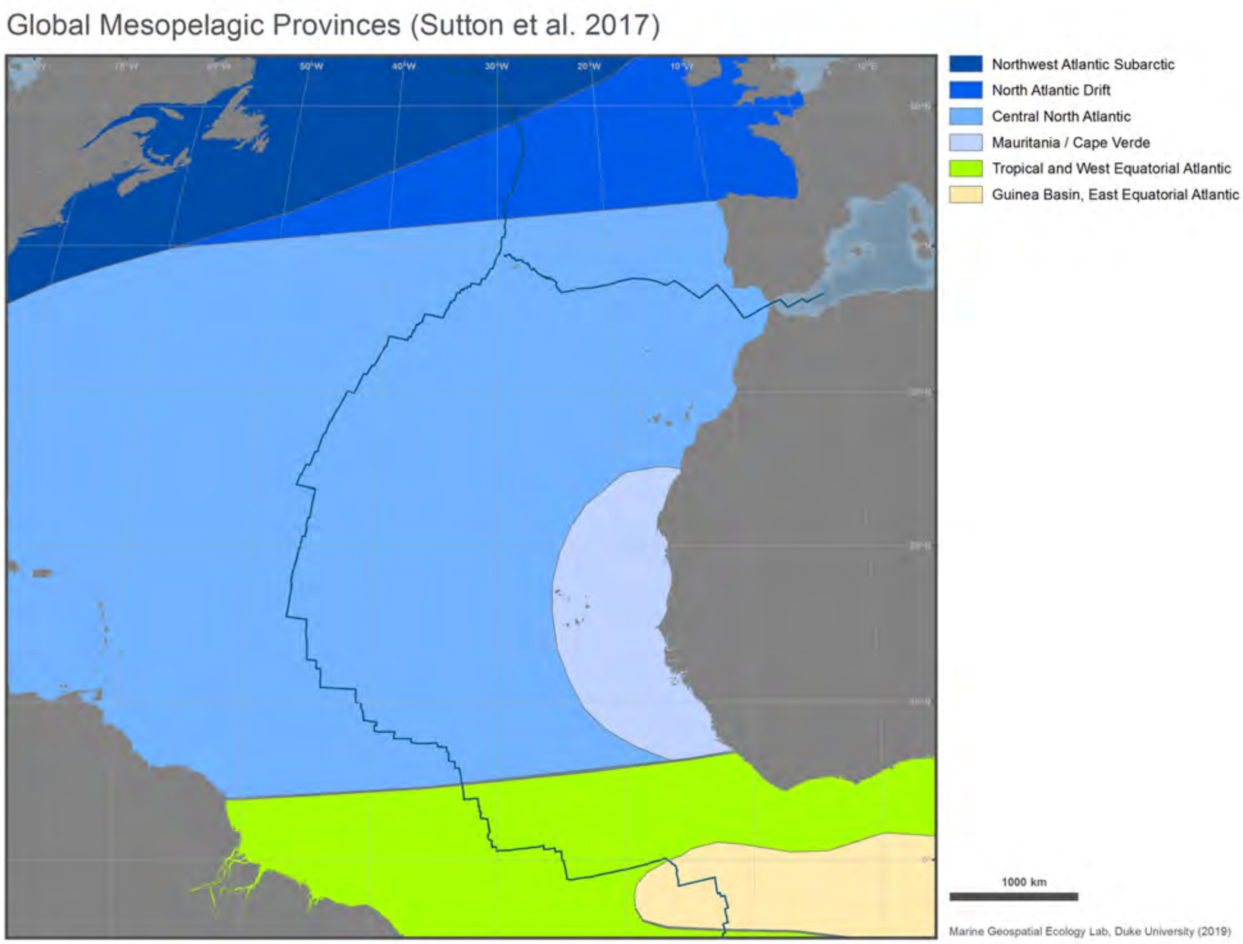

Figure 4.2-1 Mesopelagic provinces

4.3 Longhurst Marine Provinces

Abstract (Longhurst 2006):
"This dataset represents a partition of the world oceans into provinces as defined by Longhurst (1995; 1998; 2006), and are based on the prevailing role of physical forcing as a regulator of phytoplankton distribution. The dataset represents the initial static boundaries developed at the Bedford Institute of Oceanography, Canada. Note that the boundaries of these provinces are not fixed in time and space, but are dynamic and move under seasonal and interannual changes in physical forcing. At the first level of reduction, Longhurst recognized four principal biomes (also referred to as domains in earlier publications): the Polar Biome, the Westerlies Biome, the Trade-Winds Biome, and the Coastal Boundary Zone Biome. These four Biomes are recognizable in every major ocean basin. At the next level of reduction, the ocean basins are partitioned into provinces, roughly ten for each basin. These partitions provide a template for data analysis or for making parameter assignments on a global scale."

Source: VLIZ (2009). Longhurst Biogeographical Provinces. Available online at http://www.marineregions.org/. Consulted on 2013-01-14.

Reference:
Longhurst, A.R. (2006). Ecological Geography of the Sea. 2nd Edition. Academic Press, San Diego, 560p.

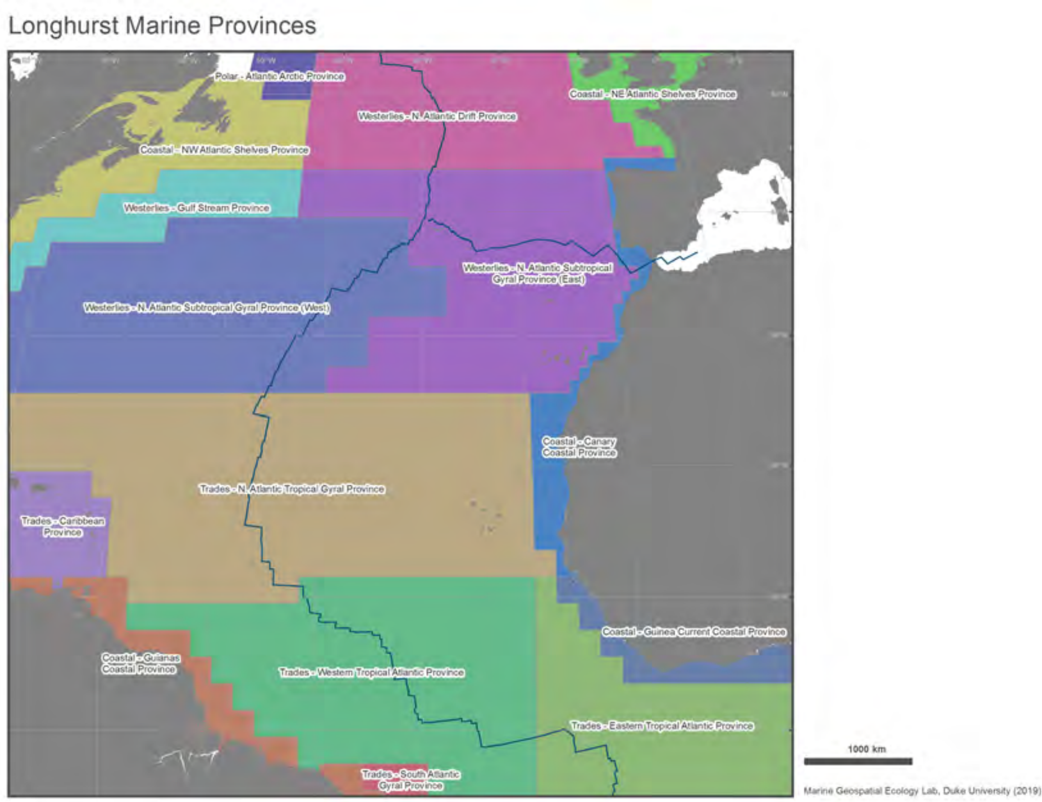

Figure 4.3-1 Longhurst marine provinces

4.4 An ecological partition of the Atlantic Ocean and its adjacent seas

Reference:

Beaugrand, G., Edwards, M. & Hélaouët, P. (2019) An ecological partition of the Atlantic Ocean and its adjacent seas. *Progress in Oceanography* **173**, 86–102.

4.5 Global Seascapes

Abstract (Harris & Whiteway 2009):

"Designing a representative network of high seas marine protected areas (MPAs) requires an acceptable scheme to classify the benthic (as well as the pelagic) bioregions of the oceans. Given the lack of sufficient biological information to accomplish this task, we used a multivariate statistical method with 6 biophysical variables (depth, seabed slope, sediment thickness, primary production, bottom water dissolved oxygen and bottom temperature) to objectively classify the ocean floor into 53,713 separate polygons comprising 11 different categories, that we have termed seascapes. A cross-check of the seascape classification was carried out by comparing the seascapes with existing maps of seafloor geomorphology and seabed sediment type and by GIS analysis of the number of separate polygons, polygon area and perimeter/area ratio. We conclude that seascapes, derived using a multivariate statistical approach, are biophysically meaningful subdivisions of the ocean floor and can be expected to contain different biological associations, in as much as different geomorphological units do the same. Less than 20% of some seascapes occur in the high seas while other seascapes are largely confined to the high seas, indicating specific types of environment whose protection and conservation will require international cooperation. Our study illustrates how the identification of potential sites for high seas marine protected areas can be accomplished by a simple GIS analysis of seafloor geomorphic and seascape classification maps. Using this approach, maps of seascape and geomorphic heterogeneity were generated in which heterogeneity hotspots identify themselves as MPA candidates. The use of computer aided mapping tools removes subjectivity in the MPA design process and provides greater confidence to stakeholders that an unbiased result has been achieved."

Reference:

Harris, P.T. & Whiteway, T. (2009) High seas marine protected areas: Benthic environmental conservation priorities from a GIS analysis of global ocean biophysical data. *Ocean and Coastal Management*, **52**, 22–38.

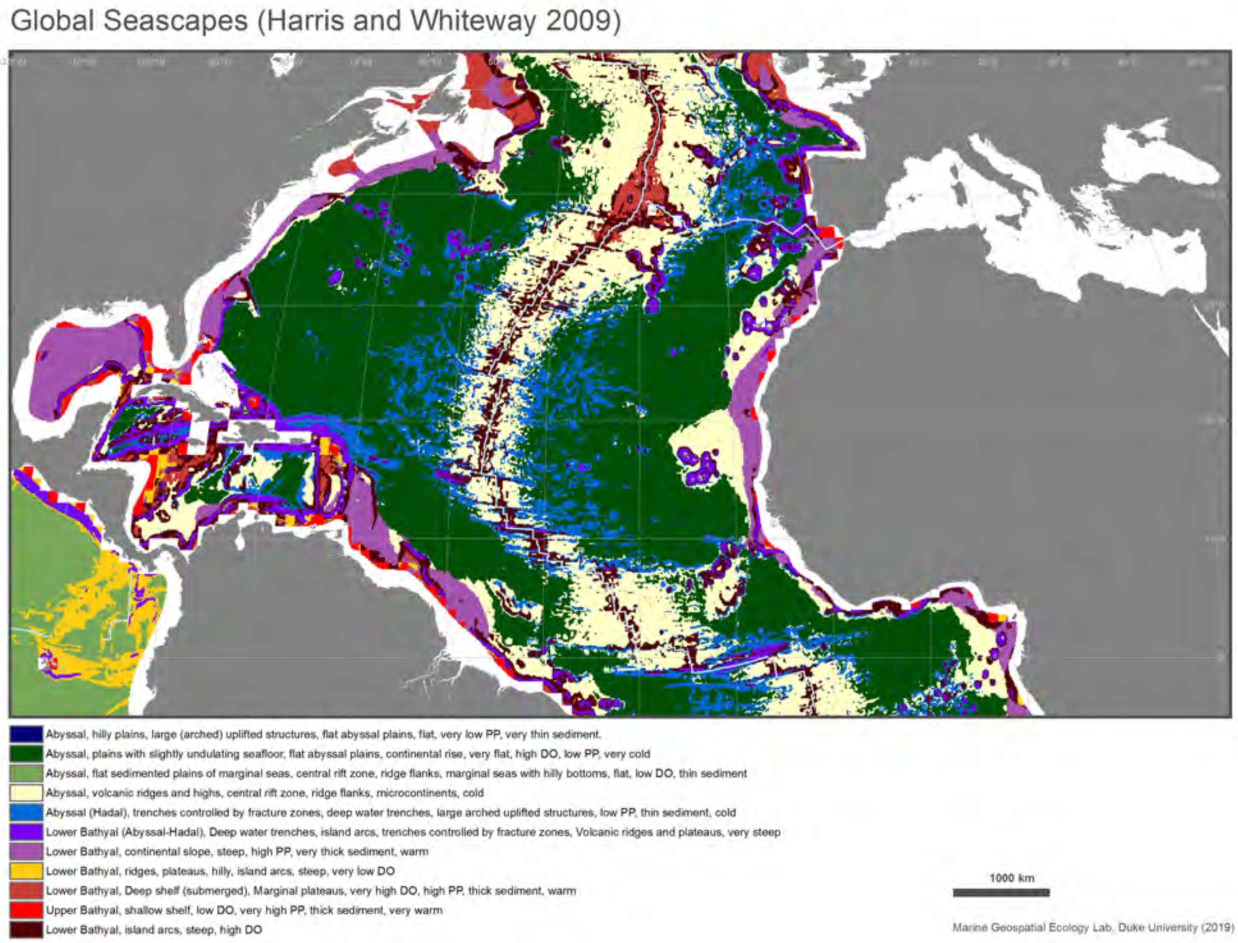

Figure 4.5-1 Global seascapes

4.6 Global Hydrothermal Vents Biogeography

Abstract (Rogers et al. 2012):
"Since the first discovery of deep-sea hydrothermal vents along the Gala´pagos Rift in 1977, numerous vent sites and endemic faunal assemblages have been found along mid-ocean ridges and back-arc basins at low to mid latitudes. These discoveries have suggested the existence of separate biogeographic provinces in the Atlantic and the North West Pacific, the existence of a province including the South West Pacific and Indian Ocean, and a separation of the North East Pacific, North East Pacific Rise, and South East Pacific Rise. The Southern Ocean is known to be a region of high deep-sea species diversity and centre of origin for the global deep-sea fauna. It has also been proposed as a gateway connecting hydrothermal vents in different oceans but is little explored because of extreme conditions. Since 2009 we have explored two segments of the East Scotia Ridge (ESR) in the Southern Ocean using a remotely operated vehicle. In each segment we located deep-sea hydrothermal vents hosting high-temperature black smokers up to 382.8uC and diffuse venting. The chemosynthetic ecosystems hosted by these vents are dominated by a new yeti crab (Kiwa n. sp.), stalked barnacles, limpets, peltospiroid gastropods, anemones, and a predatory sea star. Taxa abundant in vent ecosystems in other oceans, including polychaete worms (Siboglinidae), bathymodiolid mussels, and alvinocaridid shrimps, are absent from the ESR vents. These groups, except the Siboglinidae, possess planktotrophic larvae, rare in Antarctic marine invertebrates, suggesting that the environmental conditions of the Southern Ocean may act as a dispersal filter for vent taxa. Evidence from the distinctive fauna, the unique community structure, and multivariate analyses suggest that the Antarctic vent ecosystems represent a new vent biogeographic province. However, multivariate analyses of species present at the ESR and at other deep-sea hydrothermal vents globally indicate that vent biogeography is more complex than previously recognised."

Reference:
Rogers, A.D., Tyler, P.A., Connelly, D.P., Copley, J.T., James, R., Larter, R.D., Linse, K., Mills, R.A., Garabato, A.N., Pancost, R.D. and Pearce, D.A., (2012). The discovery of new deep-sea hydrothermal vent communities in the Southern Ocean and implications for biogeography. PLoS Biology, 10(1), p.e1001234. Doi: 10.1371/journal.pbio.1001234

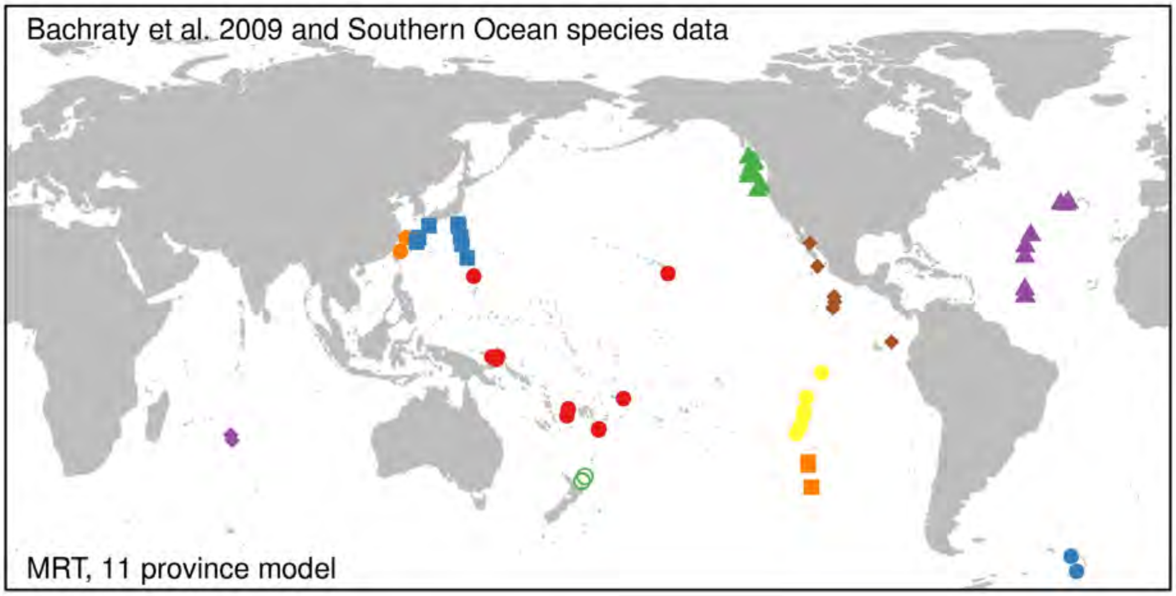

Figure 4.6-1 Results of geographically constrained clustering using multivariate regression trees. Figure 6 from Rogers et al. (2012)

4.7 A biogeographic network reveals evolutionary links between deep-sea hydrothermal vent and methane seep faunas

Reference:
Kiel, S. (2016). A biogeographic network reveals evolutionary links between deep-sea hydrothermal vent and methane seep faunas. Proceedings of the Royal Society B: Biological Sciences, 283(1844), 20162337.doi:10.1098/rspb.2016.2337

5 Human Uses

5.1 Bottom Fisheries Footprint

Bottom fishing areas are portions of Regional Fisheries Management Organisations (RFMO) convention areas where bottom fishing has historically occurred, even though their exact definition might somewhat vary. (http://www.fao.org/in-action/vulnerable-marine-ecosystems/definitions/en/).

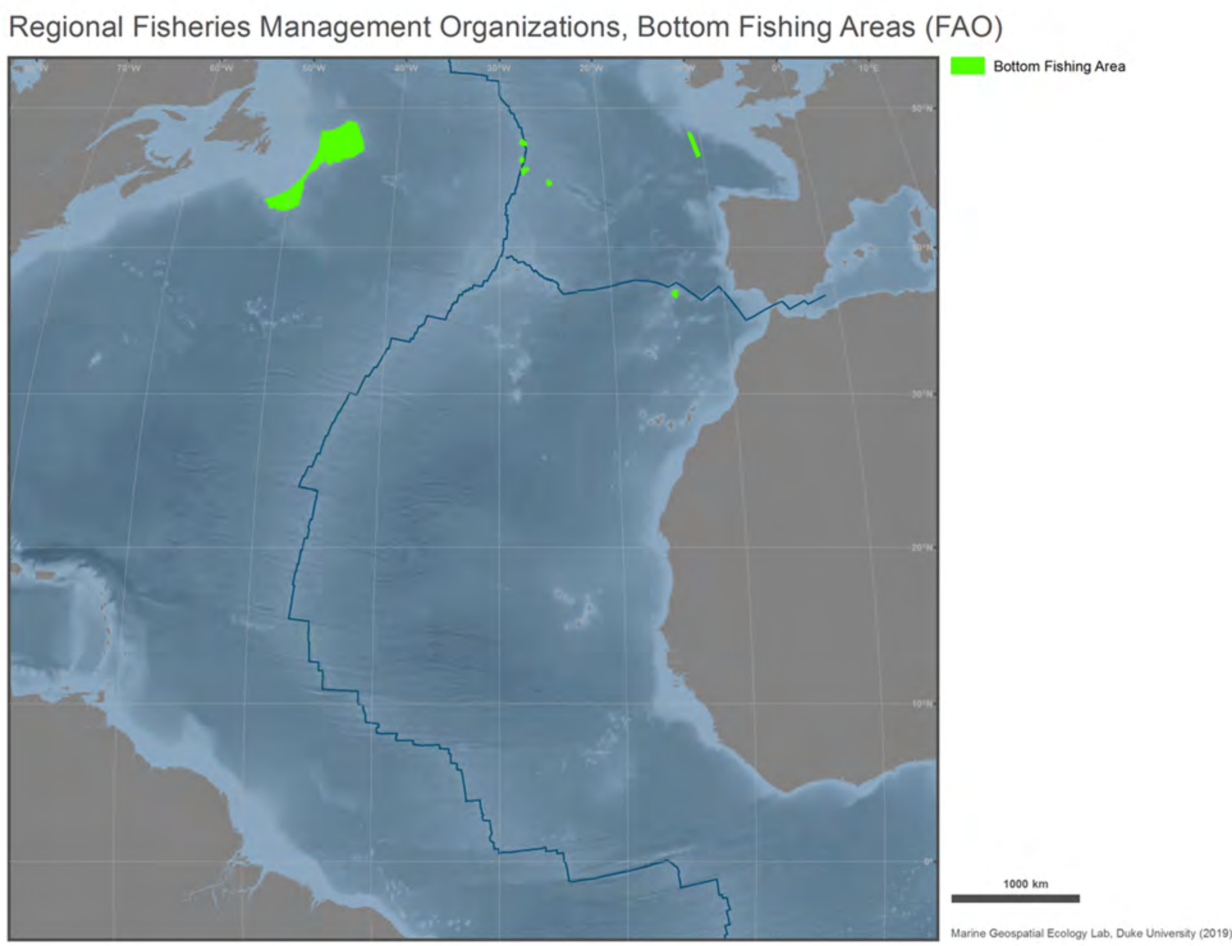

Figure 5.1-1 Bottom fishing areas for RFMOs

5.2 Demersal Destructive Fishing

Here we include a map of demersal destructive fishing from Halpern et al. (2015). These data were created as an input for an analysis of the global impact of human uses on the marine ecosystem.

Reference:
Halpern, B. S. et al. 2015. Spatial and temporal changes in cumulative human impacts on the world's ocean. - Nat Commun 6: 1–7.

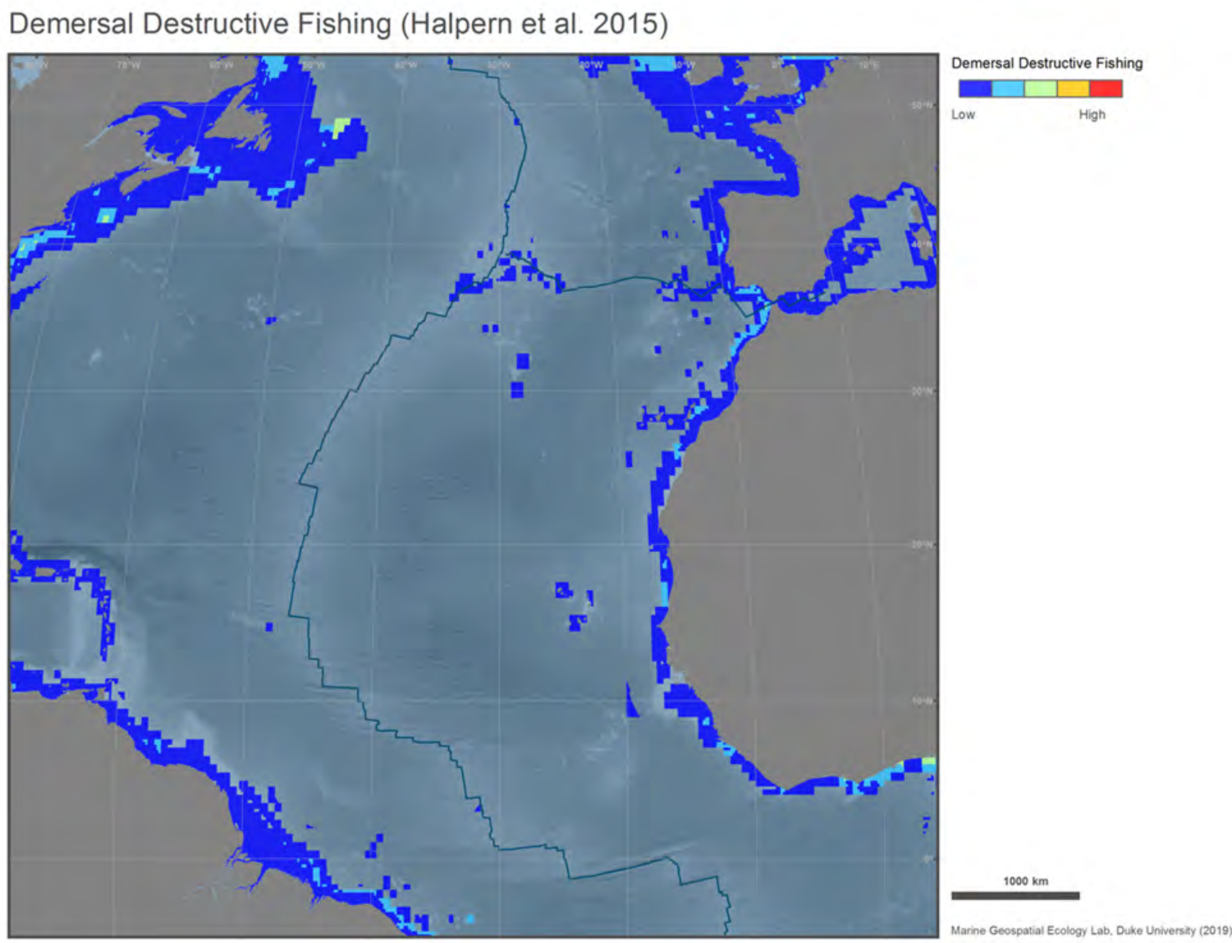

Figure 5.2-1 Demersal destructive bottom fishing

5.3 Longline Fishing Effort

This data product provided by ICCAT is an estimation of the total longline fishing effort (number of hooks), distributed by major flag, month and 5 by 5 degree squares, between 1950 and 2007 for the entire ICCAT convention area (Palma and Gallego, 2010; de Bruyn et al., 2014). The nine major ICCAT tuna and tuna-like species were used to obtain Task I global nominal catches (in weight) and CPUEs from partial catch and effort (Task II) statistics. The model basic assumption considers that catch rates are equivalent at the partial and global level.

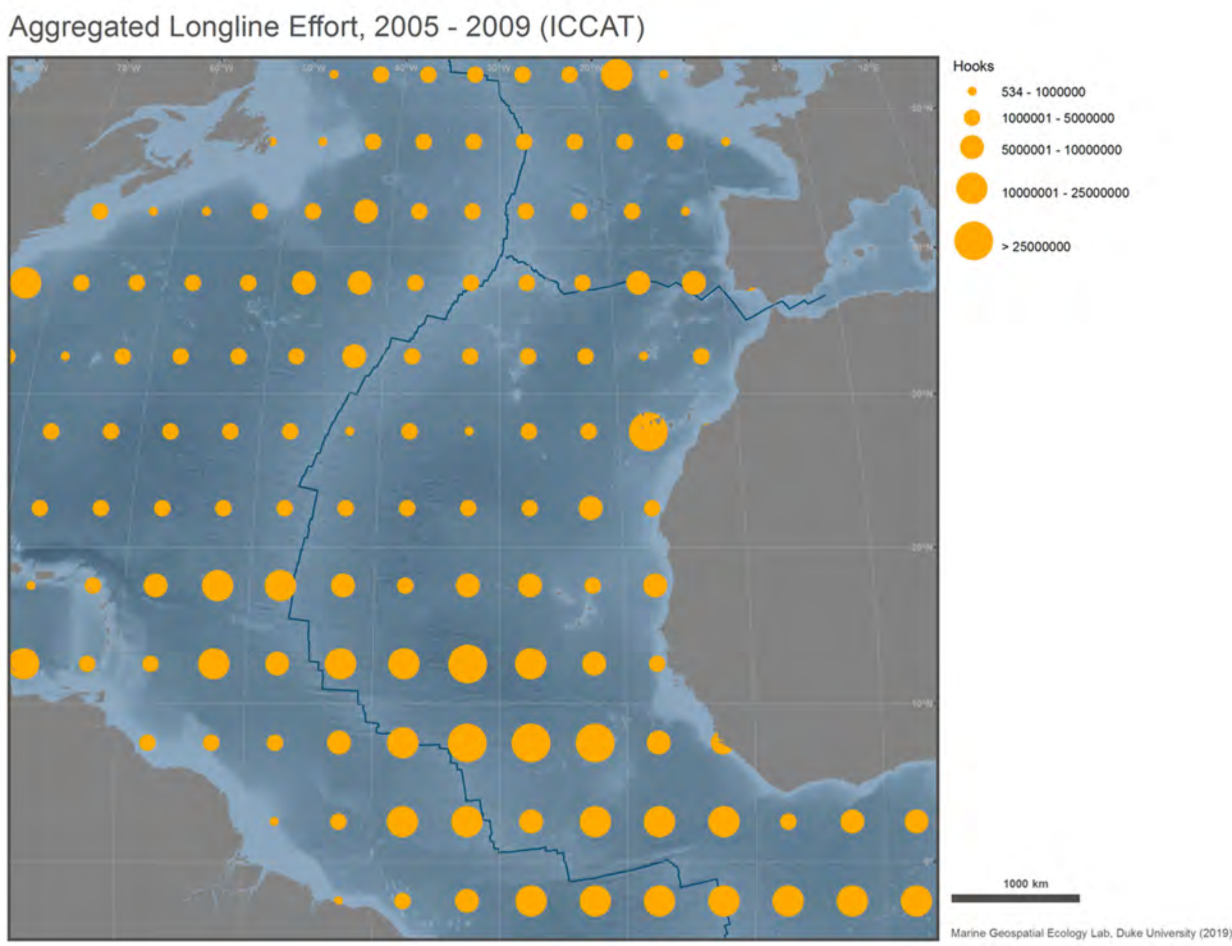

Figure 5.3-1 Aggregated longline fishing effort for all flags

5.4 Areas of Purse Seine Fishing

Here areas by 5 x 5 degrees cells are shown where purse seine fishing occurred during the period 2005-2009, irrespective of the flag, as reported to the Task II Catch and Effort (T2CE) database from the International Commission for the Conservation of Atlantic Tunas (ICCAT). T2CE are basically data obtained from sampling a portion of the individual fishing operations of a given fishery in a specified period of time. This approach was chosen as no universal measure of effort is adopted for this fishery for reporting to ICCAT.

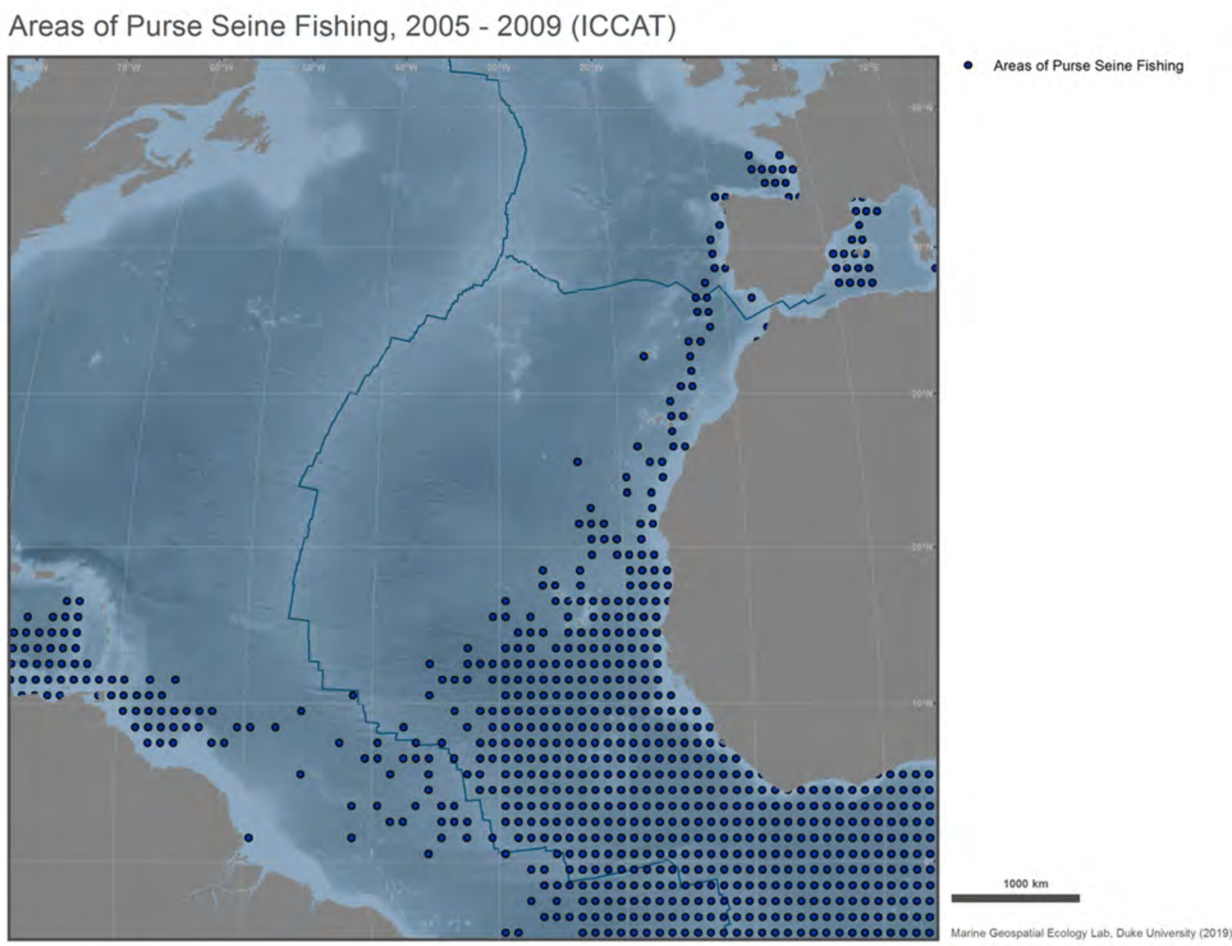

Figure 5.4-1 Occurrence of purse seine fishing for all flags

5.5 Commercial Shipping

Here we include a map of commercial shipping from Halpern et al. (2008) that was created as an input for an analysis of the global impact of human uses on the marine ecosystem.

Supplementary Material:
"Ships from many countries voluntarily participate in collecting meteorological data globally, and therefore also report the location of the ship. We used data collected from 12 months beginning October 2004 (collected as part of the World Meteorological Organization Voluntary Observing Ships Scheme; http://www.vos.noaa.gov/vos_scheme.shtml) as this year had the most ships with vetted protocols and so provides the most representative estimate of global ship locations. The data include unique identifier codes for ships (mobile or a single datum) and stationary buoys and oil platforms (multiple data at a fixed location); we removed all stationary and single point ship data, leaving 1,189,127 mobile ship data points from a total of 3,374 commercial and research vessels, representing roughly 11% of the 30,851 merchant ships >1000 gross tonnage at sea in 2005 (S*14*). We then connected all mobile ship data to create ship tracks, under the assumption that ships travel in straight lines (a reasonable assumption since ships minimize travel distance in an effort to minimize fuel costs). Finally, we removed any tracks that crossed land (e.g. a single ship that records its location in the Atlantic and the Pacific would have a track connected across North America), buffered the remaining 799,853 line segments to be 1km wide to account for the width of shipping lanes, summed all buffered line segments to account for overlapping ship tracks, and converted summed ship tracks to raster data. This produced 1 km2 raster cells with values ranging from 0 to 1,158, the maximum number of ship tracks recorded in a single 1 km2 cell. Because the VOS program is voluntary, much commercial shipping traffic is not captured by these data. Therefore our estimates of the impact of shipping are biased (in an unknown way) to locations and types of ships engaged in the program. In particular, high traffic locations may be strongly underestimated, although the relative impact on these areas versus low-traffic areas appears to be well-captured by the available data, and areas identified as without shipping may actually have low levels of ship traffic. Furthermore, because ships report their location with varying distance between signals, ship tracks are estimates of the actual shipping route taken."

Reference:
Halpern, B. S. et al. 2008. A Global Map of Human Impact on Marine Ecosystems. - Science 319: 948–952.

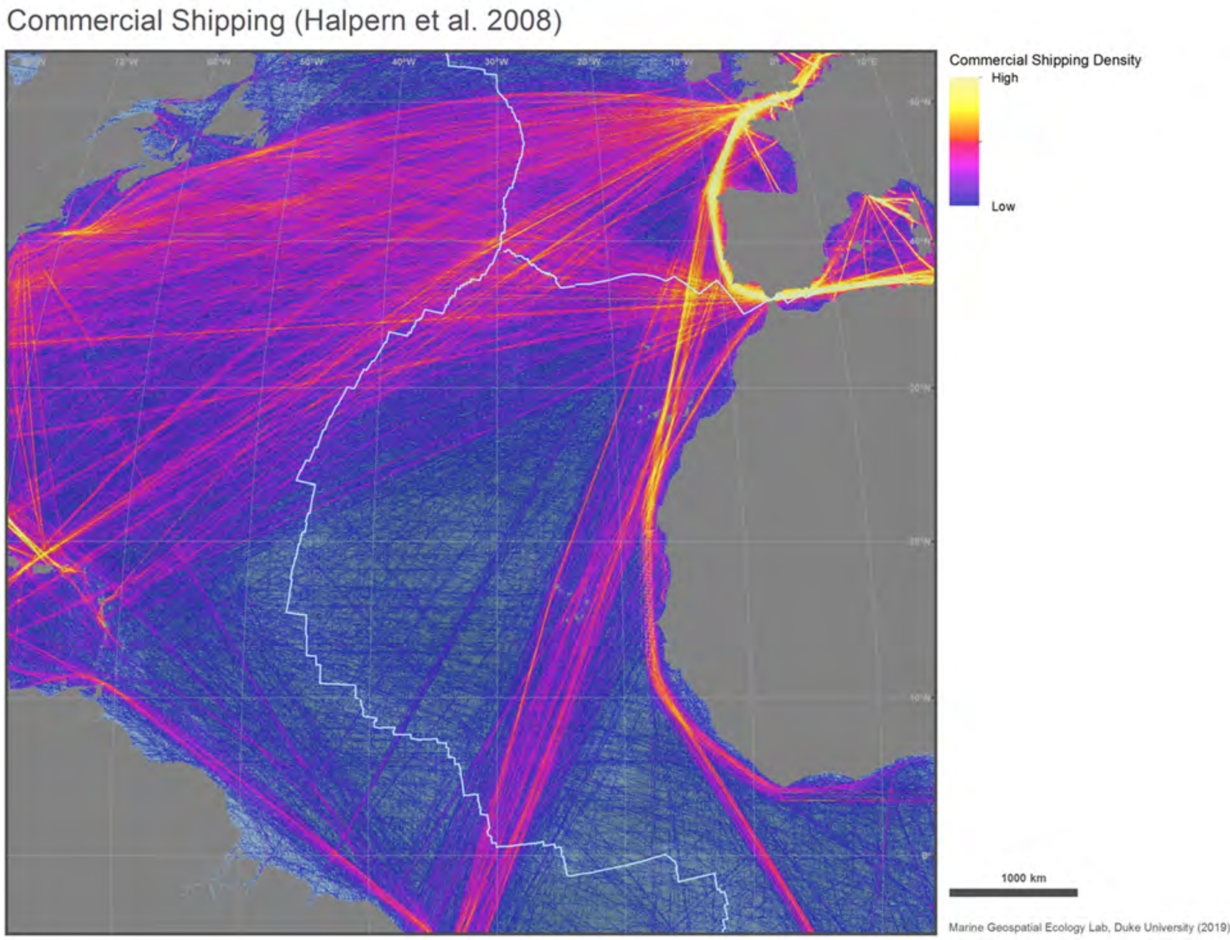

Figure 5.5-1 Commercial shipping

5.6 Vessel Density

Vessels equipped with AIS transponders are now being monitored from satellite by Global Fishing Watch (https://globalfishingwatch.org/). Vessel density was calculated for 0.25 degree grid cells for all AIS-equipped vessels for 2018.

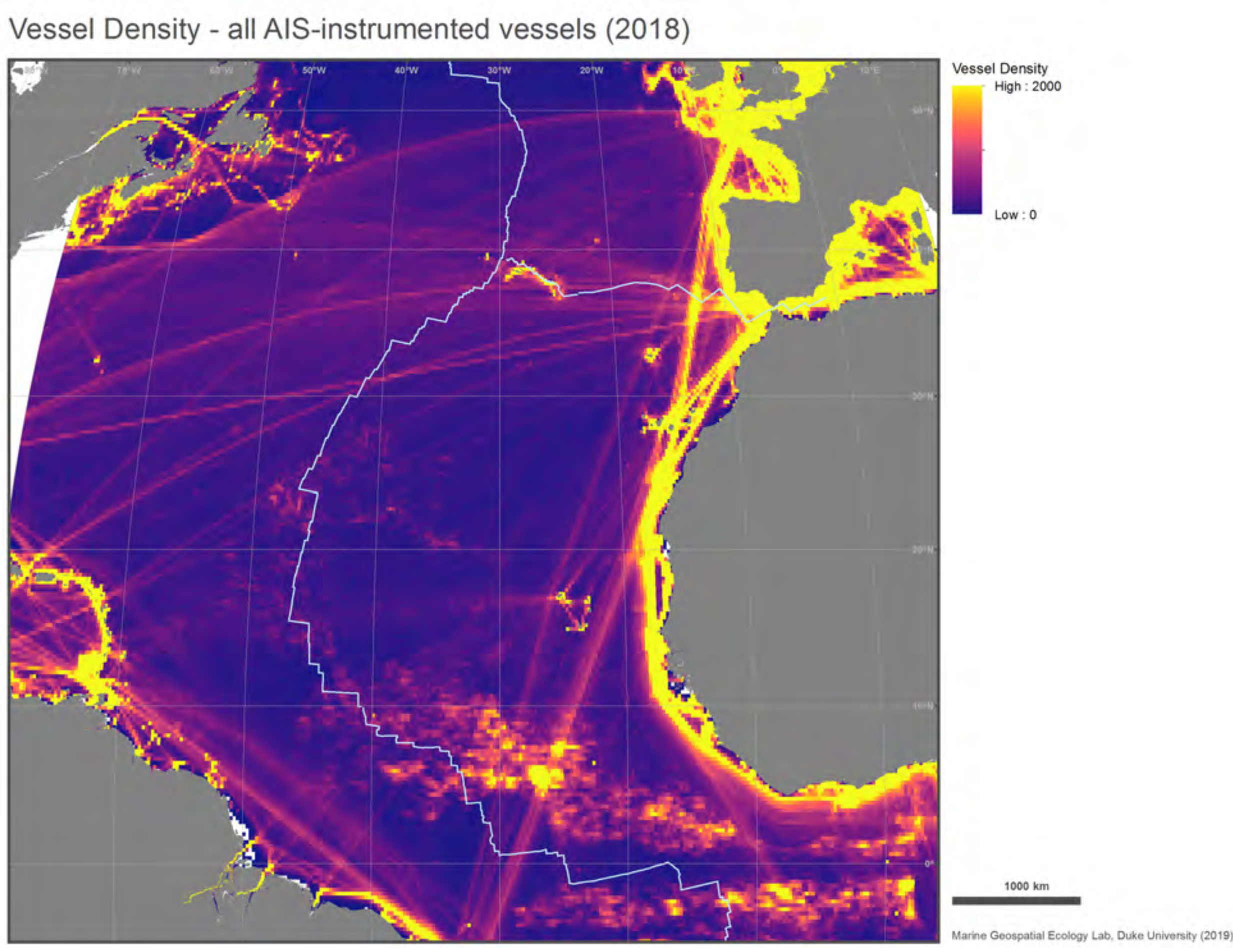

Figure 5.6-1 Vessel density for 2018

5.7 Deep-sea Mining Exploration Areas

The International Seabed Authority (ISA; https://www.isa.org.jm/) provides the localization of all potential mineral resources (polymetallic nodules, polymetallic sulphides and cobalt-rich ferromanganese crusts) across the world's oceans.

The International Seabed Authority has entered into 15-year contracts for exploration for polymetallic nodules (18 contracts), polymetallic sulphides (7 contracts) and cobalt-rich ferromanganese crusts (5 contracts) in the deep seabed.

Eighteen of these contracts are for exploration for polymetallic nodules in the Clarion-Clipperton Fracture Zone (16), Central Indian Ocean Basin (1) and North-west Pacific (1). There are seven contracts for exploration for polymetallic sulphides in the South West Indian Ridge, Central Indian Ridge and the Mid-Atlantic Ridge and five contracts for exploration for cobalt-rich crusts in the North-west Pacific.

The current areas of exploration are as per the following maps and data provided by the Authority: https://www.isa.org.jm/maps

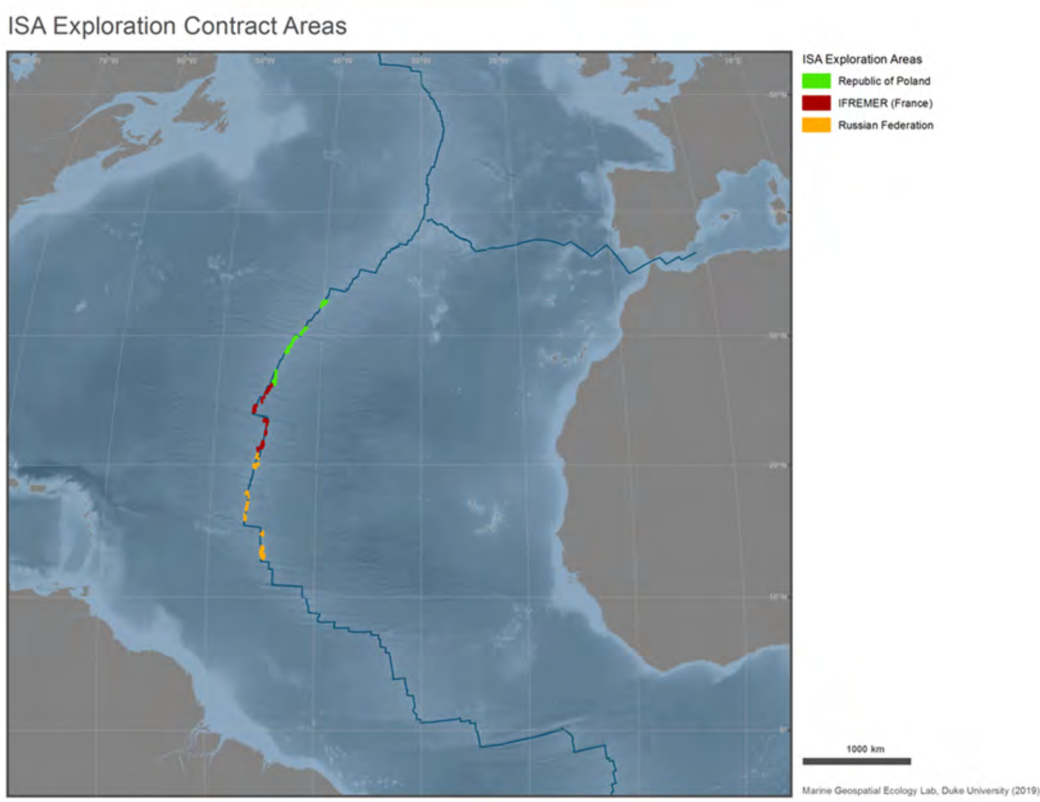

Figure 5.7-1 ISA exploration contract areas for polymetallic sulphides along the Mid-Atlantic Ridge

Republic of Poland Exploration Contract Areas

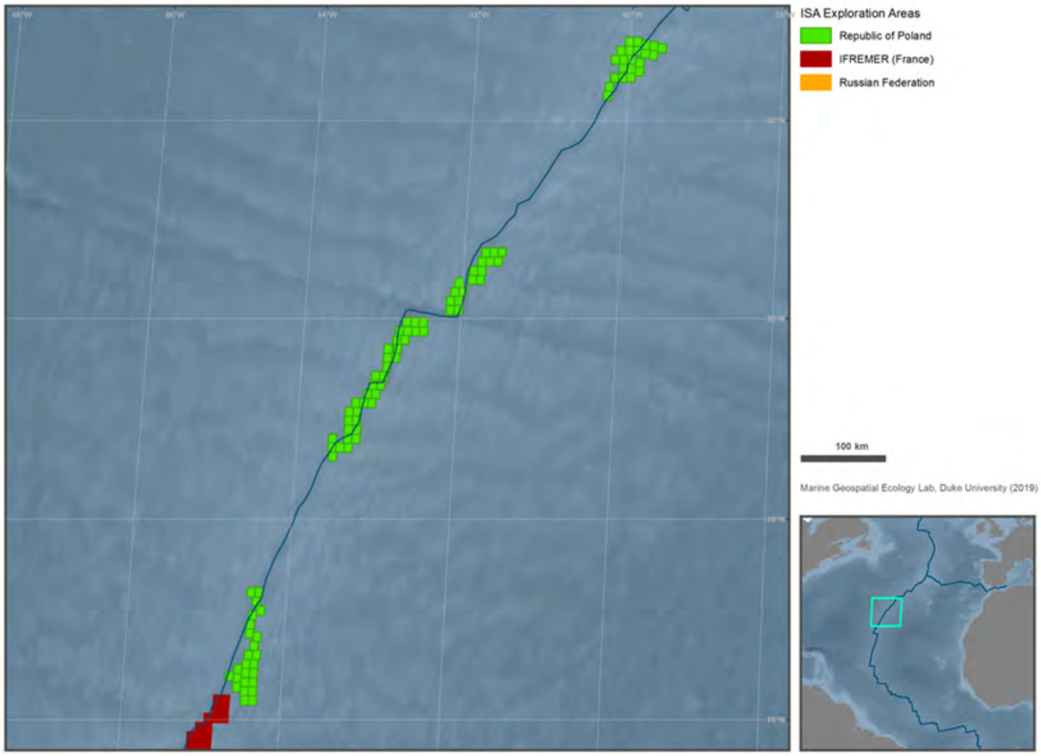

Figure 5.7-2 ISA exploration contract areas, Poland

IFREMER (FR) Exploration Contract Areas

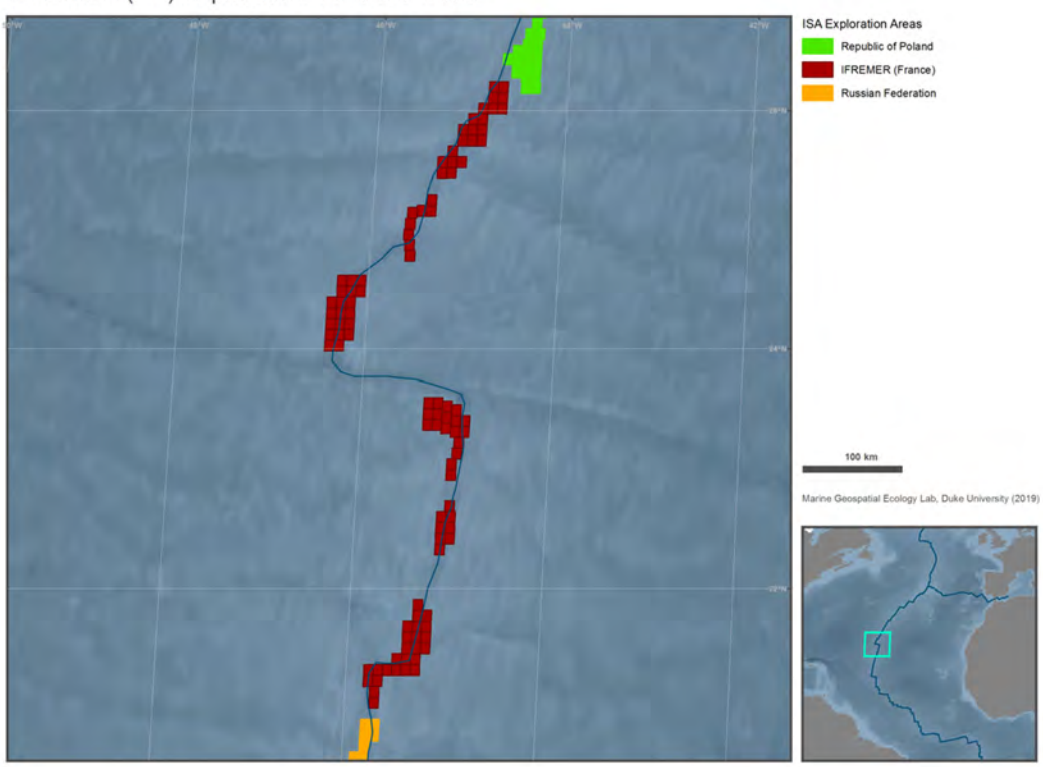

Figure 5.7-3 ISA exploration contract areas, France

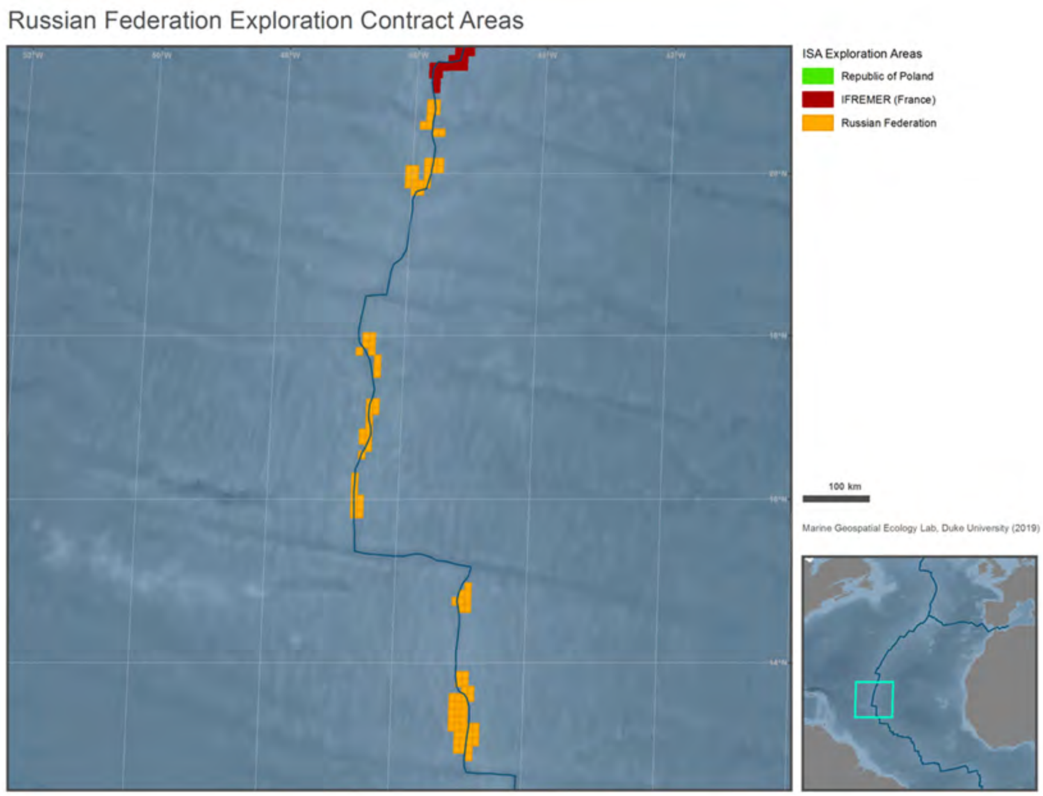

Figure 5.7-4 ISA exploration contract areas, Russian Federation

5.8 Undersea Telecommunications Cables

“This dataset is an attempt to consolidate all the available information about the undersea communications infrastructure. The initial data was harvested from Wikipedia, and further information was gathered by simply googling and transcribing as much data as possible into a useful format, namely a rich geocoded format.”

Source:
https://koordinates.com/layer/3722-undersea-telecommunication-cables/

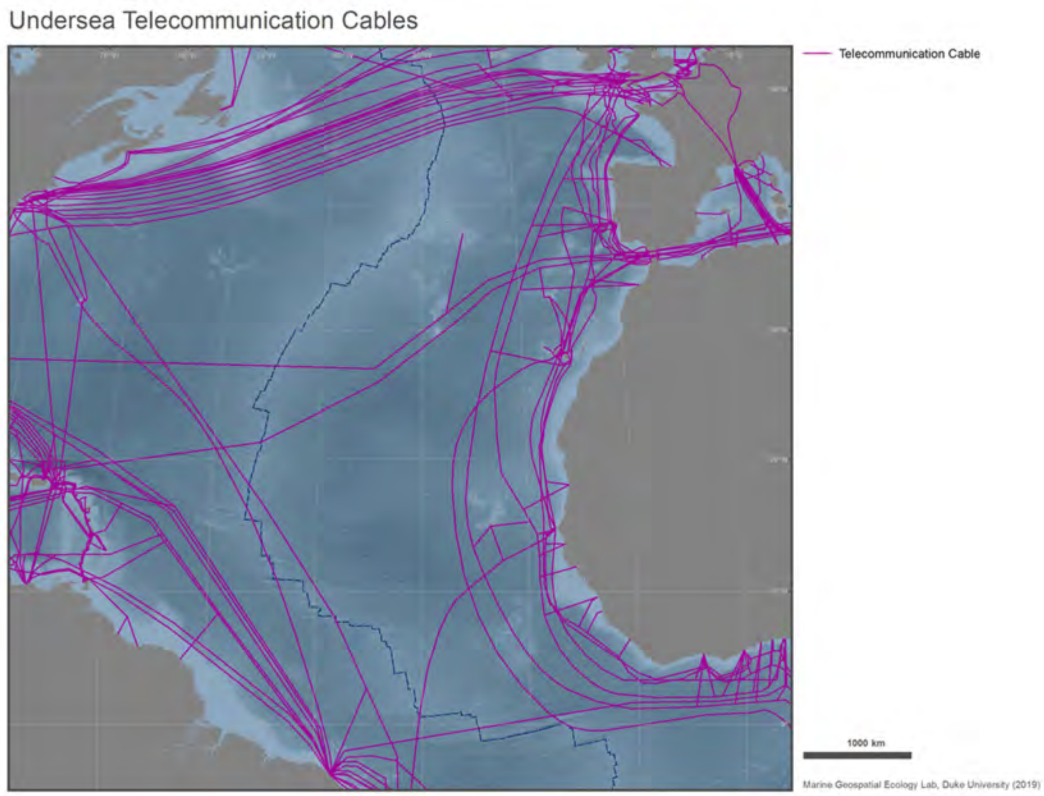

Figure 5.8-1 Undersea telecommunications cables

5.9 Cumulative Human Impacts on the World's Ocean

Abstract (Halpern 2015):
"Human pressures on the ocean are thought to be increasing globally, yet we know little about their patterns of cumulative change, which pressures are most responsible for change, and which places are experiencing the greatest increases. Managers and policymakers require such information to make strategic decisions and monitor progress towards management objectives. Here we calculate and map recent change over 5 years in cumulative impacts to marine ecosystems globally from fishing, climate change, and ocean- and land-based stressors. Nearly 66% of the ocean and 77% of national jurisdictions show increased human impact, driven mostly by climate change pressures. Five percent of the ocean is heavily impacted with increasing pressures, requiring management attention. Ten percent has very low impact with decreasing pressures. Our results provide large-scale guidance about where to prioritize management efforts and affirm the importance of addressing climate change to maintain and improve the condition of marine ecosystems."

Reference:

Halpern, B. S. et al. 2015. Spatial and temporal changes in cumulative human impacts on the world's ocean. - Nat Commun 6: 1–7.doi:10.1038/ncomms8615

Cumulative Human Impact (Halpern et al. 2015)

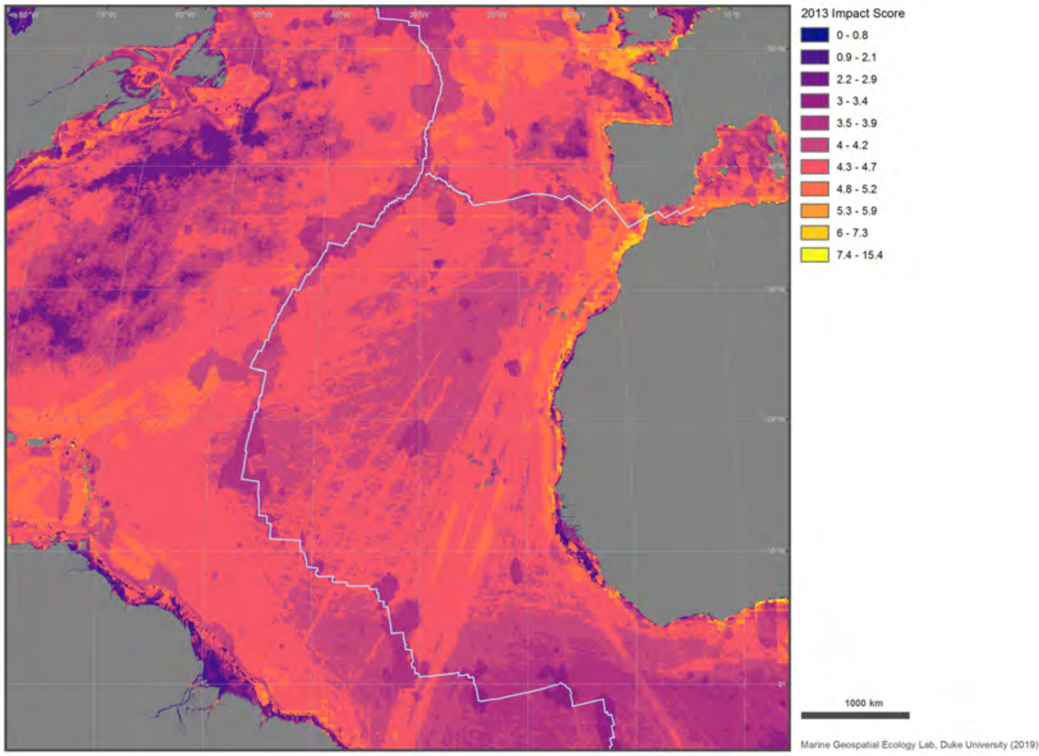

Figure 5.9-1 Cumulative human impact, 2013

Cumulative Human Impact Change, 2008 to 2013 (Halpern et al. 2015)

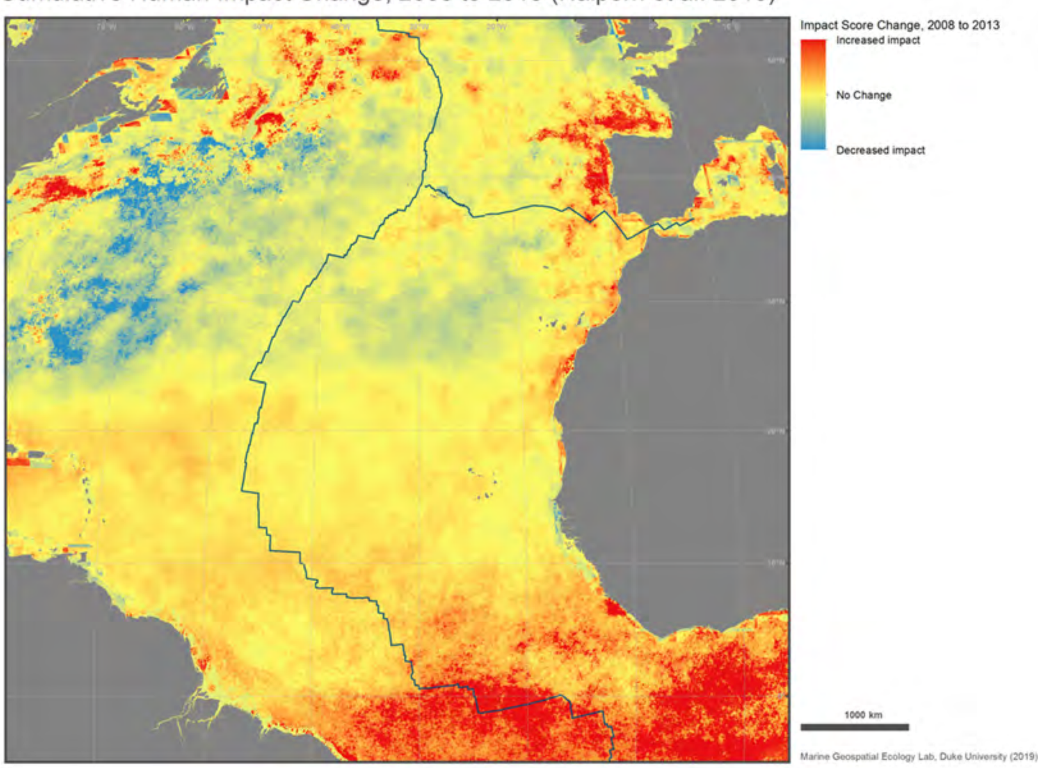

Figure 5.9-2 Change in cumulative human impact, 2008 to 2013

6 Areas Defined for Management and/or Conservation Objectives

6.1 Regional Fisheries Management Organizations (RFMO)

Regional Fishery Bodies (RFBs) are a mechanism through which States or organizations that are parties to an international fishery agreement or arrangement work together towards the conservation, management and/or development of fisheries (http://www.fao.org/fishery/topic/16800/en). The mandates of RFBs vary. Some RFBs have an advisory mandate, and provide advice, decisions or coordinating mechanisms that are not binding on their members. Some RFBs have a management mandate – these are called Regional Fisheries Management Organizations (RFMOs). They adopt fisheries conservation and management measures that are binding on their members. The RFMOs include the North Atlantic Fisheries Organisation (NAFO), North East Atlantic Fisheries Commission (NEAFC), the South East Atlantic Fisheries Organisation (SEAFO).

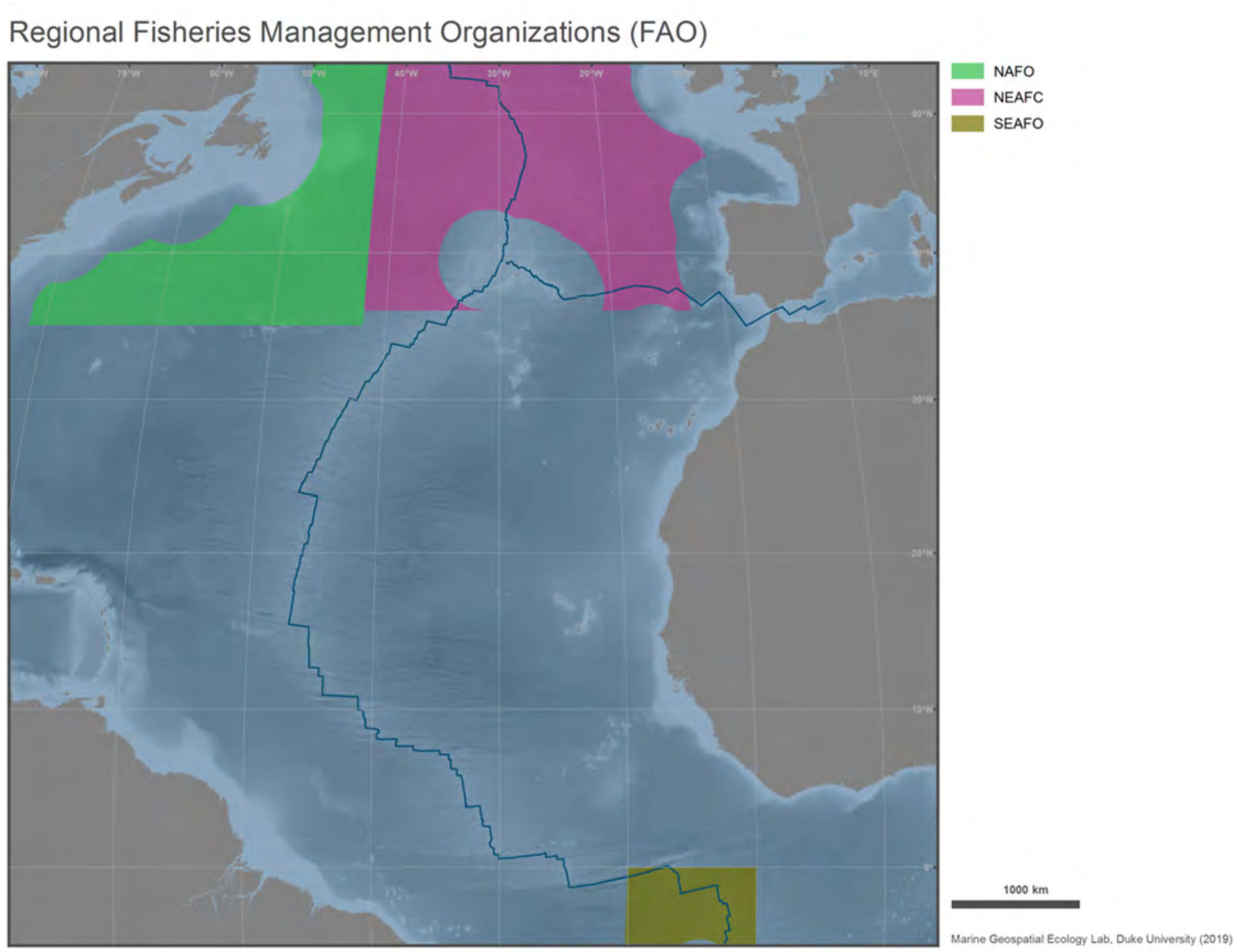

Figure 6.1-1 RFMOs in the North Atlantic Ocean

6.2 VME Closed Areas to Bottom Fishing Activities

NAFO, NEAFC and SEAFO have closed areas to bottom fishing activities (NAFP, 2010; SEAFO, 2010; NEAFC, 2014). Although the exact definition for such protection zones varies between RFMOs, they have been implemented to ensure the protection of VMEs.

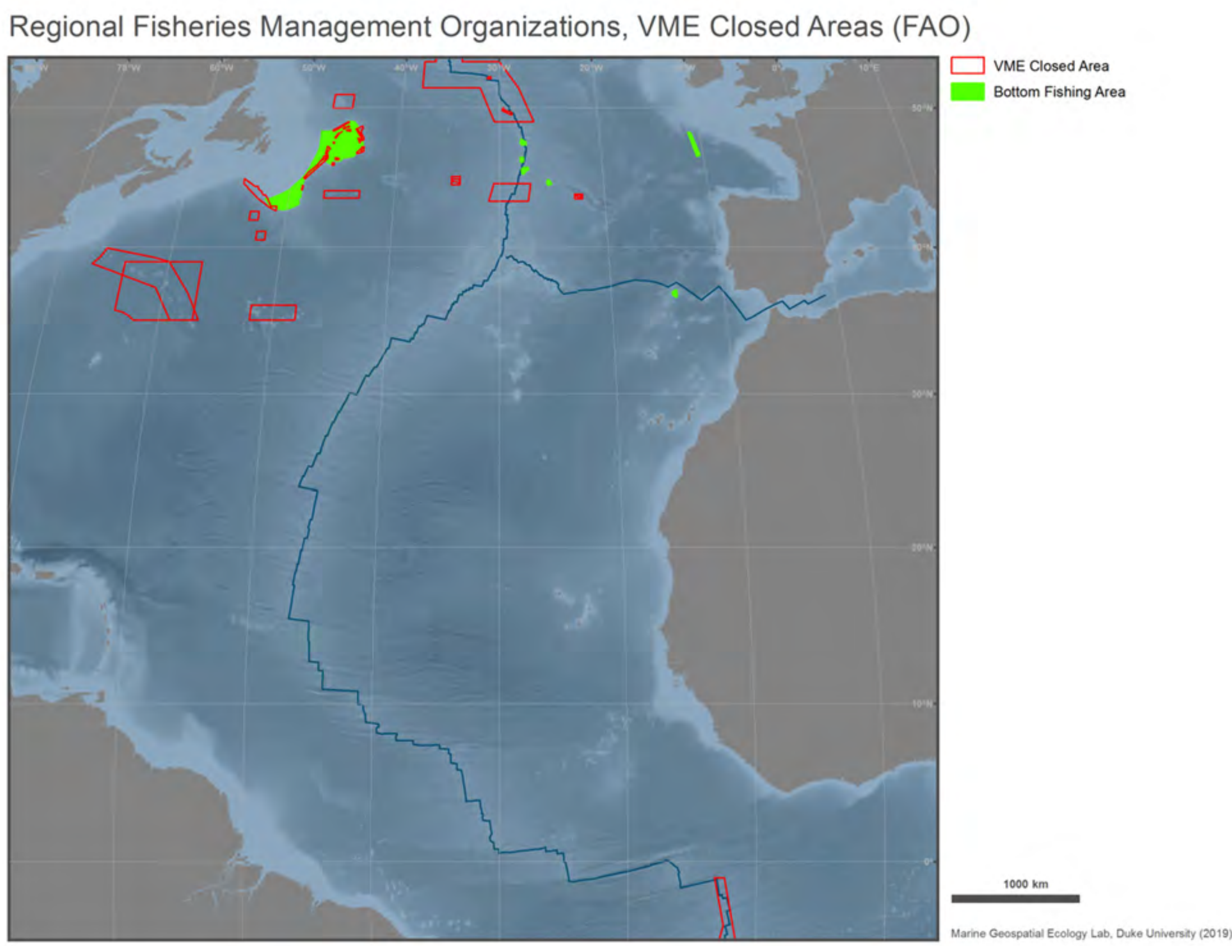

Figure 6.2-1 VME closed areas

6.3 Marine Protected Areas

“Protected Planet is the most up to date and complete source of information on protected areas, updated monthly with submissions from governments, non-governmental organizations, landowners and communities. It is managed by the United Nations Environment Programme's World Conservation Monitoring Centre (UNEP-WCMC) with support from IUCN and its World Commission on Protected Areas (WCPA).
It is a publicly available online platform where users can discover terrestrial and marine protected areas, access related statistics and download data from the World Database on Protected Areas (WDPA).”

Source: https://www.protectedplanet.net/c/world-database-on-protected-areas

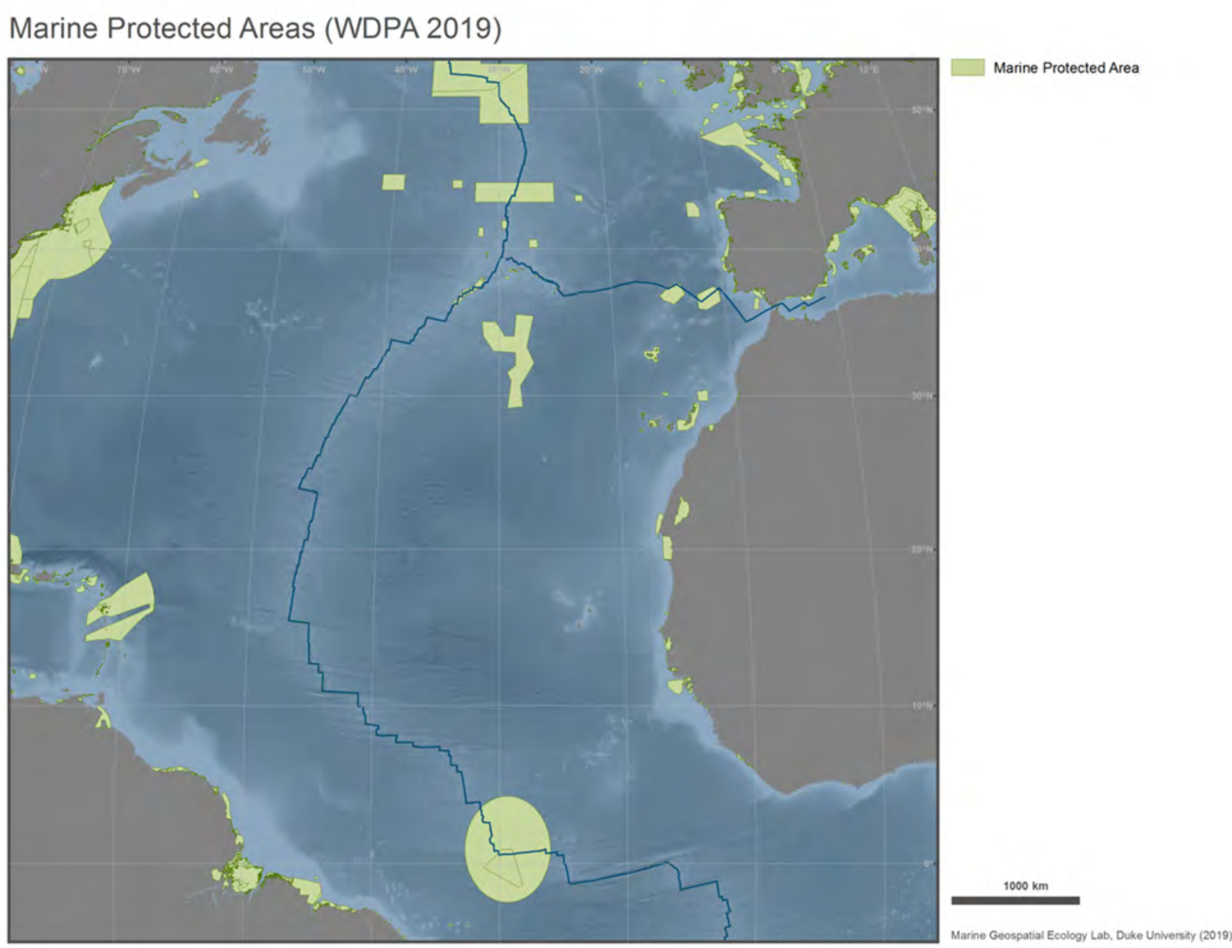

Figure 6.3-1 Marine protected areas

6.4 Convention on Biological Diversity Ecologically or Biologically Significant Areas (EBSAs)

In 2008, the ninth meeting of the Conference of the Parties to the Convention on Biological Diversity (COP 9) adopted the following scientific criteria for identifying ecologically or biologically significant marine areas (EBSAs) in need of protection in open-ocean waters and deep-sea habitats. For more details on the EBSA criteria, please see: wwww.cbd.int/doc/meetings/mar/ebsaws-2014-01/other/ebsaws-2014-01-azores-brochure-en.pdf. CBD scientific criteria for ecologically or biologically significant areas (EBSAs) (annex I, decision IX/20) includes: Uniqueness or Rarity, Special importance for life history stages of species, Importance for threatened, endangered or declining species and/or habitats, Vulnerability, Fragility, Sensitivity, or Slow recovery, Biological Productivity, Biological Diversity, Naturalness. From 2011 to 2019, the CBD convened regional workshops that identified over 300 areas meeting the internationally agreed criteria for Ecologically and Biologically Significant Areas (EBSAs).

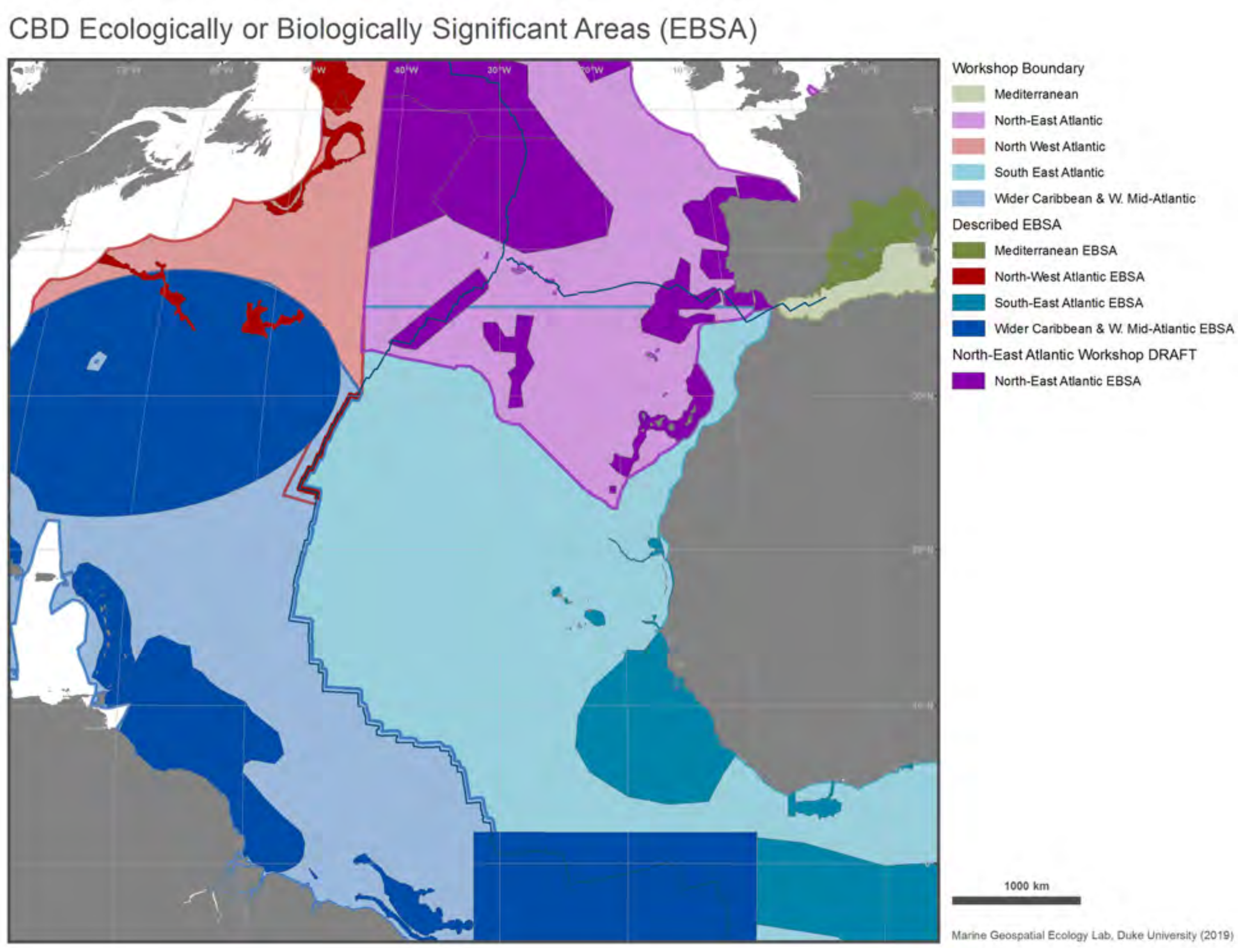

Figure 6.4-1 Convention on Biological Diversity's Ecologically or Biologically Significant Areas (EBSAs)

6.5 Systematic conservation planning for the North-Atlantic deep sea

Abstract (Magali & Sandrine 2019):
"Selection frequency of planning units in final scenarios of the ATLAS-EU basin-scale systematic conservation planning exercise, aiming to identify conservation priority areas for the deep-sea biodiversity. The selection frequency reflects how often the 25km * 25km units were selected within the 30 solutions of the scenario, from 0 for units that were never selected, to 30 for systematically selected units. This basin-scale systematic conservation planning in aimed to inform Marine Spatial Planning and conservation initiatives for the deep sea of the North Atlantic, by identifying conservation priority areas for the Vulnerable Marine Ecosystems (VMEs) and deep fish species and discussing the efficiency of the current spatial management context relatively to conservation stakes. This work is exposed in ATLAS-EU Deliverable 3.4: "Conservation Management Issues in ATLAS. Basin-scale systematic conservation planning: identifying suitable networks for VMEs protection".

Reference:
Combes Magali, Vaz Sandrine (2019). Systematic conservation planning for the North-Atlantic deep sea. SEANOE. https://doi.org/10.17882/62541

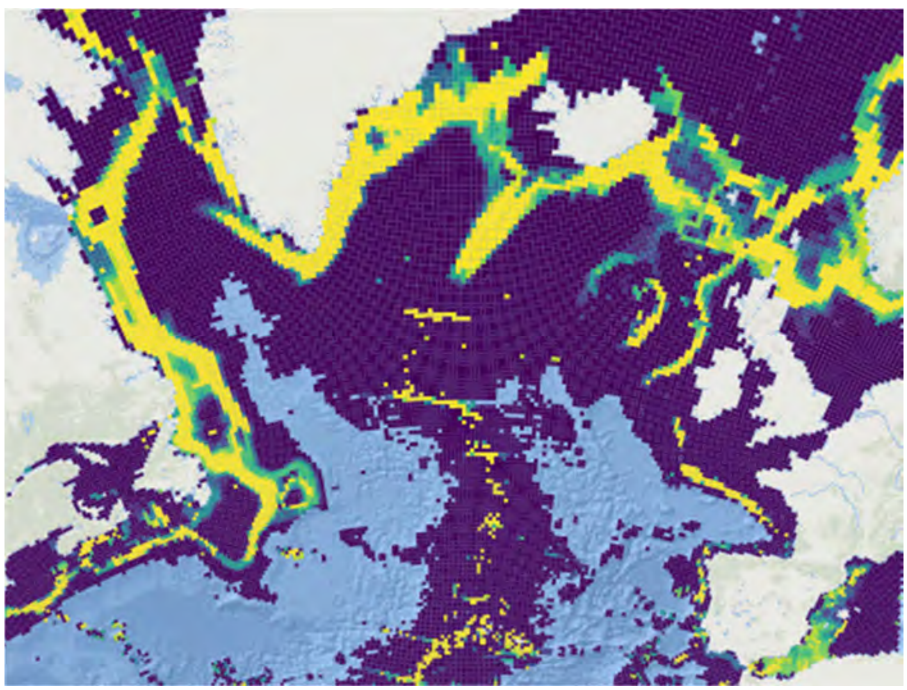

Figure 6.5-1 Spatial prioritization output, cell selection frequency

6.6 Prediction of climate change impact on deep sea MPAs

Abstract (Johnson et al. 2018):
“In the North Atlantic, Area-Based Management Tools (ABMTs), including Marine Protected Areas (MPAs) and areas describing the inherent value of marine biodiversity, have been created in Areas Beyond National Jurisdiction (ABNJ). This deep-sea area (> 200 m) supports vitally important ecosystem services. Dealing with the multiple and increasing pressures placed on the deep sea requires adequate governance and management systems, and a thorough evaluation of cumulative impacts grounded on sound science. Notwithstanding the different objectives of various types of ABMTs, at an ocean scale it makes good sense to consider MPAs, Ecologically or Biologically Significant Areas (EBSAs) and other effective conservation measures, such as areas closed to protect Vulnerable Marine Ecosystems (VMEs), collectively to inform future systematic conservation planning. This paper focuses on climate change pressures likely to affect these areas and the need to evaluate implications for the state of biodiversity features for which they have been established. In a 20–50 year timeframe, virtually all North Atlantic deep-water and open ocean ABMTs will likely be affected. More precise and detailed oceanographic data are needed to determine possible refugia, and more research on adaptation and resilience in the deep sea is needed to predict ecosystem response times. Until such analyses can be made, a more precautionary approach is advocated, potentially setting aside more extensive areas and strictly limiting human uses and/or adopting high protection thresholds before any additional human use impacts are allowed.”

Reference:
Johnson, D., Ferreira, M. A., & Kenchington, E. (2018). Climate change is likely to severely limit the effectiveness of deep-sea ABMTs in the North Atlantic. Marine Policy, 87, 111-122.10.1016/j.marpol.2017.09.034

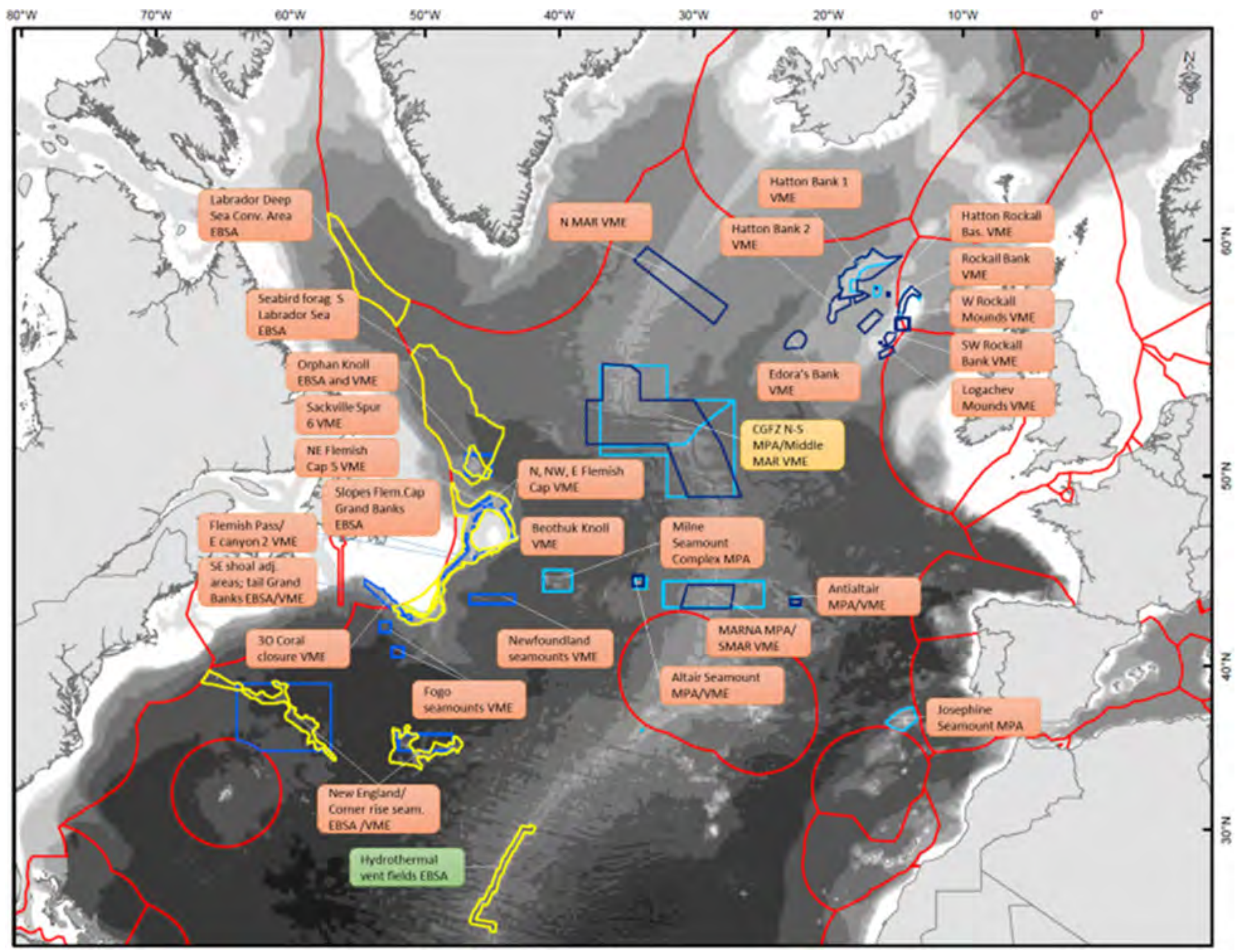

Figure 6.6-1 Expected effect of changing environmental variables on main taxa listed in the conservation objectives for each North Atlantic ABMT in ABNJ

Original Caption: Fig. 2. Expected effect of changing environmental variables on main taxa listed in the conservation objectives for each North Atlantic ABMT in ABNJ. Green: no expected impact; Yellow: low expected impact; Orange: impacted. (For interpretation of the references to color in this figure legend, the reader is referred to the web version of this article.)

7 Acknowledgments

The data collection team gratefully acknowledge contributions from:

Ward Appletans, Pieter Provoost - Ocean Biogeographic Information System

Cindy Van Dover - Duke University

Daniel C. Dunn - University of Queensland, Duke University

Jihyun Lee, Luciana De Melo Santos Genio, Sheldon Carter, Wanfei Qiu, Kioshi Mishiro - ISA Secretariat

Phil Weaver, Rachel Boschen-Rose - Seascape Consultants

Telmo Morato, Gerald H. Taranto, Frederic Vandeperre, Christopher K. Pham, Daniel C. Dunn, Ana Colaço - SEMPIA workshop data collection team